

ЖУРНАЛ
ПРИКЛАДНОЙ ХИМИИ

Vol. 31 No. 1

January 1958

JOURNAL OF
APPLIED CHEMISTRY
OF THE USSR

(ZHURNAL PRIKLADNOI KHIMII)

IN ENGLISH TRANSLATION



CONSULTANTS BUREAU, INC.

Physical Chemistry

PHYSICAL CHEMISTRY Section
of the
PROCEEDINGS OF THE ACADEMY OF SCIENCES
OF THE USSR (DOKLADY)

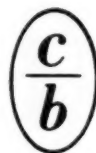
including all reports on:

Chemical Kinetics
Interface Phenomena
Electrochemistry
Absorption Spectra
and related subjects

As in all sections of the Proceedings, the papers are by leading Soviet scientists. Represents a comprehensive survey of the most advanced Soviet research in physical chemistry. The 36 issues will be published in 6 issues annually. Translation began with the 1957 volume. Translation by Consultants Bureau bilingual chemists, in the convenient C. B. format.

Annual subscription	\$160.00
Single issues	35.00
Individual articles	5.00

Cover-to-cover translation, scientifically accurate. Includes all diagrammatic and tabular material integral with the text; clearly reproduced by multilith process; staple bound.



CONSULTANTS BUREAU, INC.
227 W. 17th St., NEW YORK 11, N. Y.

Vol. 31 No. 1

January 1958

JOURNAL OF
APPLIED CHEMISTRY
OF THE USSR

(ZHURNAL PRIKLADNOI KHIMII)

A publication of the Academy of Sciences of the USSR

IN ENGLISH TRANSLATION

Year and issue of first translation:

vol. 23, no. 1 January 1950

	U. S. and Canada	Foreign
<i>Annual subscription</i>	\$60.00	\$65.00
<i>Annual subscription for libraries of non-profit academic institutions</i>	20.00	25.00
<i>Single issue</i>	7.50	7.50

Copyright 1959

CONSULTANTS BUREAU INC.

227 W. 17th ST., NEW YORK 11, N. Y.

Editorial Board
(ZHURNAL PRIKLADNOI KHIMII)

P.P. Budnikov, S.I. Vol'fkovich, A.F. Dobrianskii,
O.E. Zviagintsev, N.I. Nikitin (Editor in Chief),
G.V. Pigulevskii, M.E. Pozin, L.K. Simonova
(Secretary), S.N. Ushakov, N.P. Fedot'ev

NOTE: The sale of photostatic copies of any portion of this
copyright translation is expressly prohibited by the copyright
owners.

Printed in the United States

CONTENTS

	PAGE	RUSS. PAGE
Vladimir Vil'gel'movich Stender	1	3
Production of Pure Xenon. <u>V. G. Fastovskii, A. E. Rovinskii and Iu. V. Petrovskii</u>	3	5
Effect of Additions of Certain Cations and Buffer Solutions on the Regeneration of Arsenical Soda Liquors. <u>N. I. Brodskaiia, M. I. Gerber and S. S. Iordan</u>	10	13
The Hardening of Magnesium Oxychloride Cements. <u>A. G. Bergman and I. P. Vyrodov.</u> ..	16	19
Chromium Boride and Its Use in Hard Facing Alloys. <u>I. I. Iskol'dkii and S. L. Cherkinskaia</u>	22	25
Production of Aluminum and Chromium Phosphate Films on Aluminum and Its Alloys. <u>I. V. Krotov, V. V. Grinina and N. A. Zapol'skaia</u>	29	33
Nature of the Oxide Film Formed on Iron in Alkaline Solutions of Oxidizing Agents. <u>E. I. Levitina</u>	35	40
Investigation of a Suspended Layer of Mobile Foam in Sieve-Plate Equipment. <u>I. P. Mukhlenov</u>	40	45
Theory of Absorption Complicated by an Equilibrium Chemical Reaction in the Liquid Phase. <u>I. G. Plit.</u>	49	54
Desorption of Solvents From Activated Carbon by Means of Inert Gases. <u>N. D. Gorchakov and I. I. Pogodin.</u>	55	60
Equilibrium Potentials of Calcium Oxide - Carbon Electrodes. <u>M. V. Smirnov, S. F. Pal'guev, Iu. N. Krasnov and L. A. Liapina</u>	60	66
Electrolytic Deposition of Lead-Indium Alloy. <u>M. A. Shluger, A. I. Lipin and P. P. Tel'nykh.</u>	65	71
Electrolytic Deposition of Palladium From Solutions Containing Caustic Alkali. <u>V. V. Ostroumov</u>	70	77
Corrosion of Steel by Hydrochloric Acid in the Spheroidal State. <u>Kh. L. Tseitlin and S. M. Babitskaia</u>	76	84
Study of Binary Systems of Sulfuryl Chloride with Chlorinated Hydrocarbons. <u>V. M. Vdovenko and T. V. Kovaleva</u>	81	89
Action of Oxidizing Agents on Humic Substances of the Water from the River Dnepr. <u>M. A. Shevchenko.</u>	95	105
Production of Rapidly-Drying Coatings Based on Polyester Resins from Semidrying Oils and Butyl Orthotitanate. <u>V. S. Kiselev and T. A. Ermolaeva</u>	100	111

CONTENTS (continued)

	PAGE	RUSS. PAGE
Cast Unsaturated Polyester Resins Hardening in the Cold. <u>R. K. Gavurina, P. A. Medvedeva and Sh. G. Ianovskaia</u>	106	116
Azo Dyes From Aminocarbaniide and its Substitution Products. <u>V. N. Kliuev, L. A. Dogadkina, S. N. Solodushenkov and A. A. Spryskov</u>	113	124
The Molecular Weight of Flax Pectins. <u>M. A. Sobolev and A. A. Krasivskaia</u>	119	129
Brief Communications		
Reaction of Indium With Arsenate Ions. <u>A. A. Shokol and A. D. Pakhomova</u>	124	135
Sorption of Nitrogen Oxides by Solid Sorbents. <u>S. N. Ganz</u>	128	138
Thermal Decomposition of Middle-Temperature Coal Pitch. <u>A. N. Chistiakov</u>	131	140
Catalytic Method for the Synthesis of Vinyl Esters. <u>N. S. Kozlov and S. Ia. Chumakov</u>	134	143
Condensation of Xylenols (with Formaldehyde) in Presence of an Acid Catalyst. <u>N. V. Shorygina and G. I. Kurochkina</u>	136	144
The Effects of Some Impurities in Melamine on its Condensation with Formaldehyde. <u>L. M. Pesin, V. N. Kotrelev, A. E. Zarubitskii and F. E. Segalevich</u>	139	146
Book Reviews		
I. I. Revzin. <i>Plastics in Medicine</i> . State Medical Press, Moscow, 1957.	142	149
D. A. Epshtein. <i>Fundamentals of Chemical Technology</i> . Academy of Pedagogical Sciences Press, Moscow, 1957	144	150
N. I. Putokhin. <i>Organic Chemistry</i> . State Agricultural Literature Press, Moscow, 1956	146	151

VLADIMIR VIL'GEL'MOVICH STENDER

(On his 60th birthday, and on the completion of 36 years of scientific and teaching activity)

August 6, 1957 marked the 60th birthday and the completion of 36 years of scientific and teaching activity of Corresponding Member of the Academy of the Kazakh Soviet Socialist Republic, Professor and Doctor of Technical Sciences, Vladimir Vil'gel'movich Stender.

Stender is a scientist of wide scientific outlook. He possesses great creative energy and initiative in work on scientific problems related to the development of the electrochemical and electrometallurgical industries of our country.

Stender's early scientific and teaching work was done in Leningrad. He was a pupil of one of the founders of electrochemical science in Russia, Professor Pavel Pavlovich Fedot'ev, and inherited from him the ability to combine his daily scientific and teaching activity with the solution of the most urgent problems of the electrochemical industry. While being head of the Chair of Technology of Electrochemical Industries in the Leningrad Institute of Chemical Technology, he was also the scientific head of the Laboratory of Chlorine and Electrochemistry in the State Institute of Applied Chemistry in Leningrad. At the same time he took active part in the planning and construction of electrochemical plants.

During this period he carried out a number of investigations on the electrochemical production of chlorine (theory of the process, studies of the properties of diaphragms and electrodes), the electrolytic production of persulfates, perchlorates, chlorination of ethylene, etc. This period of Stender's activity culminated in the publication of the monograph entitled "The Electrolytic Production of Chlorine and Alkali," a major work of 80 signatures, which still remains a manual of technical electrochemistry.

Since 1939, Stender's scientific and teaching work has been carried out in Kazakhstan — a republic with a rapidly growing industry producing nonferrous, precious, and rare metals, with a demand for qualified workers and the need for research work on rational utilization of metallurgical raw materials. Stender's attention has been devoted to copper, zinc, lead, vanadium, chromium, manganese, and rare metals. He worked on plans for the utilization of the resources of the Altai and of Central and South Kazakhstan, and gave a series of lectures at sessions of the Academy of Sciences, Kazakh SSR. In his papers and addresses he has repeatedly dealt with questions of combined extraction of metals from multimetallic ores.

During his many years in Kazakhstan, Stender trained hundreds of engineers who are now working in non-ferrous metallurgy undertakings both in Kazakhstan and beyond its borders. He devotes much attention to the training of scientific workers, and his pupils include 3 doctors of science and several dozen graduates.

In addition to work in the fields of applied electrochemistry and electrometallurgy, V. V. Stender has carried out many theoretical investigations, which include research into the electrolytic production of chlorine and alkalis, and into the influence of various factors on the electrolytic production of zinc and other metals. V. V. Stender's studies on hydrogen overvoltage on a large number of metals are among the most thorough researches in this field. He was the first to suggest that the surface of an electrode should be regarded as a catalyst surface, and demonstrated this by a number of examples.

V. V. Stender has 150 published works, including two monographs, to his credit. He has patented 8 inventions and edited 11 books on theoretical and applied electrochemistry.

V. V. Stender is a talented organizer of the propagation of electrochemical knowledge. He organized the Chairs of Electrochemistry and Electrometallurgy in the Kazakh Institute of Mining and Metallurgy, the



V. V. Stender

Electrochemistry Laboratory in the Institute of Chemical Sciences of the Academy of Sciences, Kazakh SSR, the Chair of Chemistry in the Kemerovo Mining Institute, and the Chair of Technology of Electrochemical Industries in the Dnepropetrovsk Institute of Chemical Technology.

On his sixtieth birthday, the scientific community wishes him good health and creative success for the good of our socialist country.

G. Z. Kir'iakov, L. N. Sheludiakov and P. I. Zabotin

PRODUCTION OF PURE XENON

V. G. Fastovskii, A. E. Rovinskii and Iu. V. Petrovskii

The production of pure xenon is of considerable interest in relation to vacuum-tube technology and other branches of technical physics. The great development of the oxygen industry, with the production of krypton as a by-product, has made it possible to obtain considerable amounts of xenon, which is present in the air in very small amounts (0.000008% by volume). The presentation of a summary of the results of our experiments on the production of pure xenon is therefore appropriate and timely.

As is known, the production of pure xenon is preceded by a complex process for the extraction of krypton-xenon mixture [1], containing on the average 7-8% of xenon, from the air. This mixture can be most effectively separated by two methods - fractional distillation, and adsorption. Calculations and experimental data pertaining to these two separation methods are presented below.

Fractional distillation

It follows from experimental data on the saturated vapor pressures of krypton and xenon [2] that mixtures of these gases can be separated relatively easily and very efficiently by means of fractional distillation. A considerable separation effect can be achieved even by simple fractional evaporation, which in the ideal case is represented by the equation

$$\ln \frac{L_1}{L_2} = \int_{x_{L_1}}^{x_{L_2}} \frac{dx}{y-x}, \quad (1)$$

where L_1 and L_2 are the initial and final amounts of the mixture, and x_{L_1} and x_{L_2} are the compositions of the initial and final mixtures.

We calculated the course of fractional evaporation of a binary krypton-xenon mixture with initial composition 90% Kr and 10% Xe. The relationship

$$\frac{1}{y-x} = f(x),$$

was plotted graphically, and the area under the curve, bounded by the coordinates x_{L_1} and x_{L_2} , was then determined. The variations of the composition of the distillate with the amount of residual liquid, and the degree of extraction of xenon in relation to a given degree of purity, were determined. The total pressure was 1 atm absolute. The results of the calculations are plotted in Figs. 1 and 2. It is assumed that the system Kr-Xe is an ideal solution, which is approximately true. Figure 2 shows that in the course of equilibrium fractional evaporation, about 5% of xenon is lost during enrichment of the liquid to from 10 to 70% Xe; further enrichment of the liquid results in a sharp increase of xenon lost; this reaches 25% when a product containing 99% Xe is obtained. Since during fractional evaporation the conditions of phase equilibrium are not maintained, it is quite natural that the losses of xenon in fractional evaporation should be greater than calculated; i.e., the method can be recommended only for preliminary enrichment of the original mixture to 50-60% xenon.

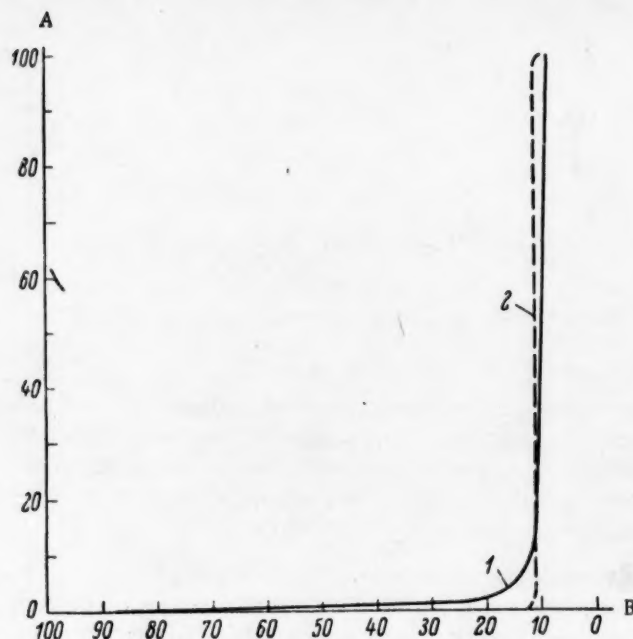


Fig. 1. Variation of distillate composition with the amount of residual liquid.

A) Content of xenon in vapor (%); B) amount of residual liquid (%).

Original mixture: 90% Kr and 10% Xe; $P = 1$ atm.

Curves: 1) Simple distillation; 2) rectification with a column equivalent to 5 theoretical plates, reflux ratio 0.5.

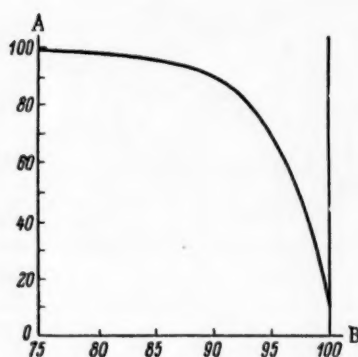


Fig. 2. The degree of extraction of xenon for a given degree of purity.

A) Content of Xe in residual liquid (molar %); B) degree of extraction of Xe (%).

and batch rectification of the mixture are given in the Table.

The apparatus used for certain experiments on the fractional evaporation of Kr-Xe mixtures is shown diagrammatically in Fig. 3. The purified mixture was passed from the bulb 1 to the glass column 2, contained in an unsilvered Dewar flask 3; liquid O_2 (or N_2) was put into the flask 3, and the vacuum jacket of the column 2 was filled with hydrogen to create thermal contact between the refrigerant and the condensing mixture.

The maximum yield of xenon can only be obtained by rectification of Kr-Xe mixture, which does not extend beyond the laboratory scale; thus, in an industrial oxygen unit producing 3600 cubic meters of O_2 per hour the daily output of Kr + Xe does not exceed 400 liters, so that ~700 cc of the liquefied mixture must be rectified daily. Batch rectification is suitable for this purpose. We therefore calculated batch-rectification data for a mixture containing 90% Kr and 10% Xe, over a column equivalent to 5 theoretical plates, at constant reflux ratio ($R = 0.5$) and variable distillate composition ($P = 1$ atm). The x - y diagram was plotted for the Kr-Xe mixture, from which the compositions of the distillate x_p and still residue x_s were determined, and the $\frac{1}{x_p - x_s} = f(x_s)$, were plotted. This curve

was graphically integrated to determine the relationship between the composition of the liquid in the still, x_s , and its residual amount L_2 , and the degrees of extraction of Xe were calculated. The rectification curve in Fig. 1 illustrates the sharp separation of the Kr-Xe mixture and the negligible losses of Xe with the Kr. Calculated data on the degree of extraction of Xe in fractional evaporation

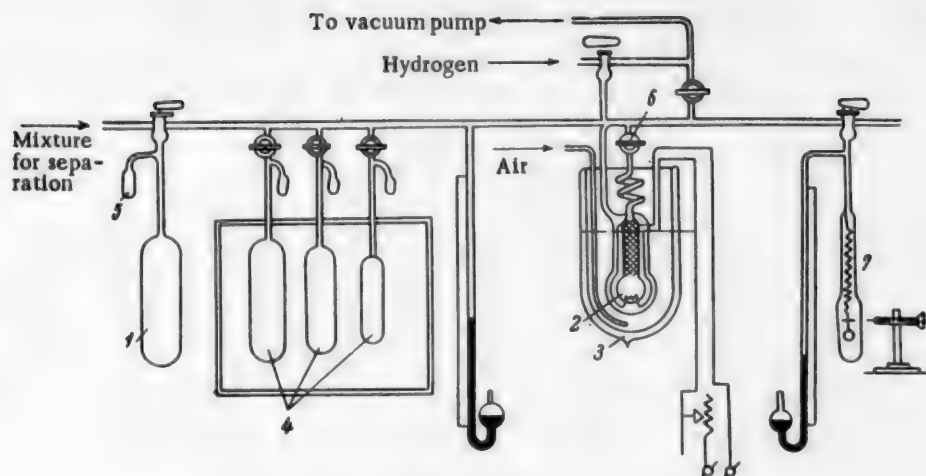


Fig. 3. Apparatus for fractional evaporation.
Explanations in text.

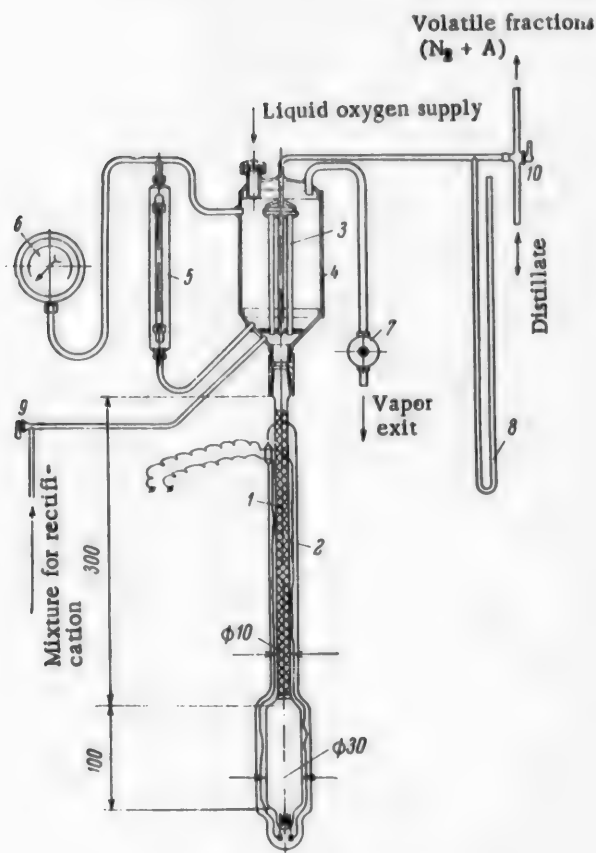


Fig. 4. Rectification column.
Explanations in text.

After the mixture had been transferred from the bulb 1 into the still of the column 2, hydrogen was pumped out of the vacuum jacket of the column, and the vessel 3 with the refrigerant was removed. The heater was switched on, the mixture melted, and the pressure in the column was maintained at 850-900 mm Hg during the

Concentration in residue (vol. %)	Degree of extraction of Xe (%)	
	by fractional evaporation	by rectification
90.0	91.0	100
96.0	84.0	100
99.0	76.2	97.2
99.6	—	92.6
99.9	—	85.3

subsequent evaporation of the liquefied mixture. The pressure in the column was regulated by the supply of heat to the still. The whole mixture was evaporated slowly, separate fractions being consecutively transferred to the series of bulbs 4, of known capacity.

At the end of the evaporation, the residual gas (xenon) in the column and connecting tubes was withdrawn into the side tube 5, immersed in a Dewar flask containing liquid nitrogen, and transferred to the bulb 4 in which the last fraction was collected. The tap 6 was then closed and the column 2 disconnected from the rest of the system. The gas pressure in each bulb was then determined, and the composition of each fraction was found by means of the gas balance 7.

Phase equilibrium between the escaping vapor and the residual liquid could only be attained to any extent when the evaporation was extremely slow; the degree of extraction was generally considerably below the calculated value. This may be illustrated by two examples: the degree of extraction in the formation of a product containing 81% Xe was 70.6%, while the calculated value was 92% (see Fig. 2); for a product containing 97-98% Xe the degree of extraction did not exceed 55-56%, whereas the calculated value is $\sim 80\%$.

Some experiments on the rectification of Kr-Xe mixtures were carried out. The rectification column is shown schematically in Fig. 4.

The column is made of molybdenum glass, and provided with a vacuum jacket 2. Over the column is a copper condenser 3, consisting of 12 tubes, 6 mm in diameter and 200 mm long, soldered in brass grids. The tubes are enclosed in a cylinder 4, 2.5 liters in capacity, made of sheet copper 2.5 mm thick, and tested under 20 atm excess pressure. The amount of refrigerant in the space between the condenser tubes is indicated by the level gage 5, while the pressure over the liquid is indicated by the manometer 6 and regulated by the valve 7. The pressure in the column is measured by the mercury manometer 8. The diameter of the column is 10 mm, and the height of the packing 300 mm. The packing consists of copper foil in the form of Raschig rings 2×2 mm. The volume of the still is ~ 75 cc. The gas is let in through the tap 9 and out through the three-way tap 10.

The connection between the metal condenser and the glass column is effected by a conical ground-glass joint packed with Mendeleev's grease. This form of connection was previously tested by measurements of leakage into the column after thorough evacuation by means of a vacuum pump, and proved to be quite effective.

The most convenient refrigerant for rectification of Kr-Xe mixtures is liquid methane; with excess pressure of 0.2-0.3 atm over the liquid methane the original mixture condenses and flows down the packing into the still. The electric heater of the still is then switched on, and the pressure over the methane regulated so as to maintain 180-200 mm excess pressure in the column. For 25-30 minutes the rectification proceeds with total reflux, and then the distillate (Kr) is collected in glass bulbs at a rate of 0.3-0.4 liter/minute.

The effectiveness of the separation can be clearly estimated from the pressure changes in the column - pure krypton distills over during the first stage and a constant pressure is maintained in the column, indicating that the composition of the distillate remains unchanged, with 0.4-0.6 atm excess pressure in the intertubular space over the liquid methane, at a given rate of heat supply to the still and a given rate of distillate removal. The pressure in the column then drops sharply, showing that most of the krypton has been distilled off; the pressure over the liquid methane is gradually raised by closing of the valve 7, and the last fraction (xenon) is distilled off at 18.5-19.0 atm excess pressure over the liquid methane.

Four fractions were collected during the distillation - the first three in gas holders, and the fourth in an evacuated glass cylinder. Data on two runs of the rectification column, which is now in systematic use for the production of pure xenon, are given below.

The total volume condensed was 33 liters. Four fractions were collected, 15, 10, 6.2, and 1.8 liters in volume. Xenon was not detected in the first two fractions; the third fraction contained 4.2% xenon, and the last, 96%. The yield was ~87%. In rectification of small quantities of gas, the holding power of the packing has a pronounced adverse effect on the separation. For example, in distillation of 68 liters of original mixture containing 6.5% Xe, five fractions were collected - no xenon was found in the first three fractions, total volume 52 liters, the fourth fraction (11.8 liters) contained 2.8% xenon, and the fifth (4.2 liters), 98.5%. The yield of xenon was 93%.

For rectification of larger quantities it is convenient, in order to decrease the still capacity, to feed the original mixture continuously into the column, with removal of pure krypton as the distillate, and to perform the last distillation stage under batch-rectification conditions, by analogy with the rectification of O_2 -Kr mixtures [3]. To obtain xenon of a high degree of purity it is recommended, with ~19 atm excess pressure in the intertube space of the condenser, to draw off an intermediate fraction of technical xenon (90-95%), the amount of which depends on the dimensions of the column; in this way it is possible to obtain xenon with a slight admixture of krypton as the final product; in our experiments, it was possible to obtain pure xenon after removal of 250-300 cc of gas (technical xenon). The individual fractions can be sent directly to the gas balance for density determinations.

Adsorption method for separation of krypton - xenon mixtures

In some cases it is more convenient to use an adsorption method for separation of Kr-Xe mixtures, by analogy with the technique used for separation of Ne-He mixtures [4]. Our method of adsorptive separation consists of two consecutive stages: 1) adsorption of the krypton-xenon mixture by a dynamic method to break-through of xenon; this stage involves the production of pure krypton and of an adsorbed phase rich in xenon; 2) fractional desorption effected by one method or another - partial evacuation of the adsorbed phase under isothermal conditions, fractional desorption with gradual zonal heating of the adsorption column, etc. Data are presented below on the adsorption and separation of Kr-Xe mixtures on Ag-2 activated carbon, for which adsorption isotherms of pure Kr and Xe were determined earlier [5].

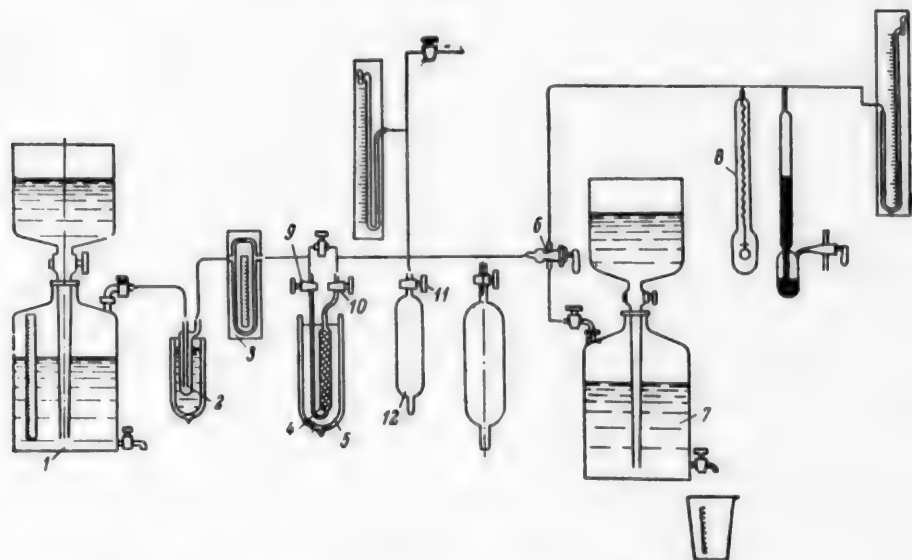


Fig. 5. Apparatus for investigation of adsorption of Kr-Xe mixtures. Explanations in text.

A diagram of the apparatus used for investigation of adsorption of Kr-Xe mixtures is shown in Fig. 5. The original mixture of given composition passed from the gas holder 1 through the vessel 2 for drying, and was then fed at a constant velocity through the rheometer 3 into the adsorber 4 cooled in the vessel 5. The unadsorbed gas passed through the tap 6 into the gas holder 7; samples of gas were taken at intervals in the gas balance 8.

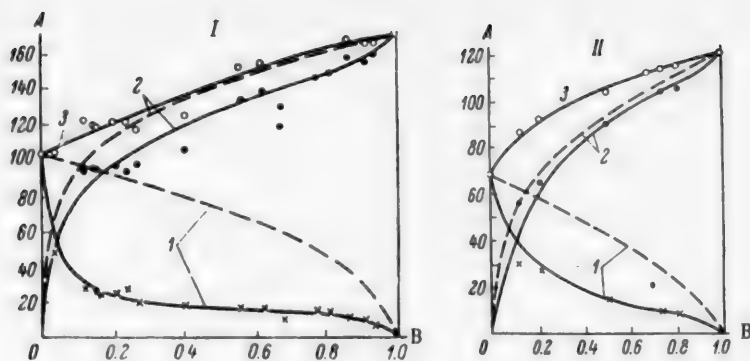


Fig. 6. Adsorption of krypton-xenon mixture at various temperatures. Pressure 1 atm.

A) Volume of adsorbed phase (normal cc/g); B) equilibrium content of Xe in the unadsorbed phase, y (mole fractions of Xe).

Curves: 1) Kr, 2) Xe, 3) Kr-Xe mixture. Temperature ($^{\circ}\text{K}$): 1) 193, 2) 233.

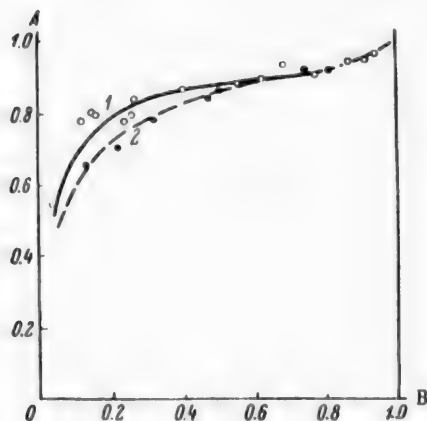


Fig. 7. Equilibrium curve for coexisting phases in the adsorption of krypton-xenon mixture.

A) Composition of adsorbed phase, x (mole fractions of Xe); B) composition of unadsorbed phase, y (mole fractions of Xe).

Temperature ($^{\circ}\text{K}$): 1) 193, 2) 233.

After complete saturation had been reached, as shown by the unchanged composition of the mixture after it passed through the adsorber, indicating a state of equilibrium between the adsorbed and unadsorbed phases, the taps 9 and 10 were closed, the system was evacuated again, and the gas from the adsorber was transferred into the cylinder 12 through taps 10 and 11; for complete extraction of the adsorbed phase, the end tube of the cylinder 12 was immersed in a vessel with liquid nitrogen, and the adsorber was heated. The volume of the adsorbed phase was determined from the pressure in the cylinder 12 and the adjoining tubes; the composition of this phase was determined by means of the gas balance 8.

The adsorption of krypton-xenon mixture from a stream of the gas was measured at 193 and 233 $^{\circ}\text{K}$. The results of determinations of the volume of the adsorbed phase are plotted in Fig. 6; the dash lines represent the adsorption isotherms of Kr and Xe plotted on the assumption of independent adsorption, determined only by the partial pressures of the components [5]. It is seen that in adsorption of the mixture the adsorption of each of the components is decreased; this is especially prominent in the case of krypton.*

Figure 7 represents the enrichment of the adsorbed phase with xenon; for example, at 193 $^{\circ}\text{K}$ a gas phase containing 20% Xe (y_0) corresponds, at saturation, to an adsorbed phase containing 79-80% Xe (x), i.e., a single saturation of the adsorbent already results in considerable enrichment. It is also seen that in the region $0.15 < y_0 < 0.85$ the composition of the adsorbed phase depends little on the composition of the original gaseous mixture, and is about $x = 0.85-0.87$. The temperature was not found to have any significant influence on the composition of the adsorbed phase in the two isotherms studied (193 and 233 $^{\circ}\text{K}$); there is some divergence between the values of x at low values of y .

*The thermodynamics of adsorption of this gaseous mixture requires special consideration.

The experiments on fractional desorption of the mixture were performed in the apparatus described (Fig. 5), but with a larger amount of adsorbent (17 g). It was found that the simplest and most effective method of desorption is by evacuation under isothermal conditions. The results of a typical experiment on isothermal desorption at 233°K are given below. At the end of adsorption the adsorber was disconnected and all the tubes were evacuated. Taps 10 and 11 were opened, and the adsorber was connected to the cylinder 12, the end tube of which was immersed in a Dewar flask containing liquid nitrogen. The pressure in the adsorber fell from 760 to 50-60 mm, and the evacuation of the adsorber was then stopped. The volume and composition of the gas in the cylinder 12 were determined. Vessel 5 with the refrigerant was then removed, and as the pressure rose in the adsorber the gas was passed into the gas balance for determination of the composition of the first fractions. In the original mixture $y_0 = 49.4\%$ Xe. The total amount of gas adsorbed was 1658 cc. 415 cc was pumped off, containing 62.8% Kr and 37.2% Xe. The loss of xenon with this fraction was ~11%. After this, initial warming of the adsorbent resulted in removal of ~80 cc of a fraction containing 94% Xe. The fractions subsequently desorbed (1160 cc) were almost pure xenon. The average composition of the adsorbed phase was 84% Xe. The total volume of the intermediate fractions was ~500 cc, or ~30% of the volume of the adsorbed phase. The degree of extraction of xenon was 0.84.

The results of experiments on fractional desorption without preliminary isothermal evacuation (by gradual increase of the temperature of the adsorbent on removal of the refrigerant) were less good — in two experiments the degree of extraction was 0.754 and 0.769.

SUMMARY

1. Adsorption of the mixture should be carried out by the dynamic method at 233-213°K. The degree of adsorption is 80-100 cc/g, depending on the composition of the original mixture; this determines the amount of adsorbent and adsorber dimensions required for a given rate of output.
2. A product containing 70-80% xenon can be obtained by complete single desorption of the adsorbed phase. To obtain pure xenon, it is convenient to use fractional desorption, with brief preliminary evacuation of the unadsorbed phase under isothermal conditions at about 223-233°K. This gives an acceptable degree of separation, with a degree of extraction of the order of 0.80-0.85.
3. The adsorption method for separation of Kr-Xe mixtures can be used without preliminary enrichment of the original mixture (93% Kr and 7% Xe). As the initial process of fractional evaporation of Kr-Xe mixtures does not involve any considerable loss of xenon (see above), in evaporation of the Kr-Xe mixture it is convenient to evaporate 60-65% of the gas, and pass the rest through an adsorber unit for preparation of pure xenon. The maximum amount of xenon obtainable from an oxygen unit yielding 3600 m³ of O₂ per hour is 30 liters/day. The amount of adsorbent required for extraction of this quantity of gas from Kr-Xe mixture does not exceed 450-500 g.
4. The suitability of the fractional distillation and adsorption methods for the extraction of pure xenon was demonstrated by calculation and experimentally. The rectification method gives higher degrees of extraction of xenon and more clear-cut separation, but it is somewhat more complicated.

LITERATURE CITED

- [1] V. G. Fastovskii, Krypton and Xenon (Gosenergoizdat, 1940).*
- [2] K. Peters, K. Weil, Z. phys. Chem. A, 180, 1 (1937); K. Clusius, L. Riccoboni, Z. phys. Chem. 38, 81 (1938); A. Michels, T. Wassenaar, Physica, 16, 3, 253 (1950); E. Justi, Phys. Z. 36, 571 (1935); J. Melhuizen, C. Grommellin, Physica, 4, 1, 1-4 (1937); W. Keesom, S. Mazur, J. Melhuizen, Physica, 2, 669 (1935).
- [3] V. G. Fastovskii and Iu. V. Petrovskii, J. Chem. Ind. 8 (1957).
- [4] V. G. Fastovskii and A. E. Rovinskii, J. Chem. Ind. 7, 201 (1953); 9, 345 (1953).
- [5] V. G. Fastovskii and A. E. Rovinskii, Oxygen, 4 (1952).

Received April 26, 1956

*In Russian.

EFFECT OF ADDITIONS OF CERTAIN CATIONS AND BUFFER SOLUTIONS ON THE REGENERATION OF ARSENICAL SODA LIQUORS*

N. I. Brodskaya, M. I. Gerber and S. S. Jordan

The Leningrad Scientific Research Institute of Petroleum Processing
and Production of Synthetic Liquid Fuel

The effects of certain metals ions and buffer solutions on the regeneration (oxidation) rate of arsenical soda liquors were studied in order to elucidate certain factors which may influence the rate of the process.

The method of investigation is described in the previous papers [1-3].

Effect of additions of certain cations on the regeneration of arsenical soda liquor. The effects of the cations Fe^{2+} , Mn^{2+} , Sn^{4+} , Cr^{3+} , Cu^{2+} , added as the sulfates or chlorides in concentrations of 10^{-3} - 10^{-5} mole/liter were investigated. The arsenical soda liquor contained 10.8 g of arsenic per liter (calculated as As_2O_3), 12.6 g/liter of Na_2CO_3 , and had pH 6.8. The results of the experiments are given in Table 1 and Figs. 1-3.

TABLE 1

Effect of Additions of Salts of Mn^{2+} , Fe^{2+} , Cu^{2+} , Sn^{4+} and Cr^{3+} on the Regeneration of Arsenical Soda Liquor

$$\frac{\text{g-atoms Na}}{\text{g-atoms As}} = 2.5$$

Added salt (10^{-4} mole/liter)	Start of sulfur liberation (min)	Amount of sulfur libera- ted (g/liter)	Amount of $\text{Na}_2\text{S}_2\text{O}_3$ formed, calc. as sulfur (g/liter)	Sum of ele- mental S and thiosulfate S (g/liter)	Sulfur liberated in elemental state (%)	Elemental S liberated, in g-atoms per g-atom As
—	6	2.006	1.098	3.104	66.4	1.26
FeSO_4	3	2.109	0.980	3.089	68.3	1.32
CuSO_4	3	1.940	0.984	2.924	66.3	1.21
MnCl_2	1	2.648	0.784	3.432	77.2	1.66
SnCl_2	2	0.784	0.894	1.677	46.7	0.50
$\text{KCr(SO}_4)_2$	2	1.654	1.274	2.928	56.5	1.06

The results of experiments with 10^{-4} mole/liter of the additions, the mean of the concentrations used, are given in Table 1.

The results show that additions of salts increase the regeneration rate during the initial period, accelerate the start of sulfur liberation, and in some cases increase the yield of sulfur. The best results are obtained with additions of Fe^{2+} and Mn^{2+} salts. The course of the curves in Figs. 1 and 2 shows clearly that the regeneration rate rises sharply in presence of Fe^{2+} and Mn^{2+} salts.

As was stated earlier [2, 3] the regeneration process is carried out in plant conditions in such a way as to obtain the maximum yield of elemental sulfur and lowest yield of thiosulfate. The influence of salt additions on the yields of sulfur and thiosulfate is clearly seen in Fig. 3. The dash line in the graph shows the amounts of

*Communication III on the oxidation of oxythioarsenates in aqueous solutions. This investigation was carried out under the guidance of V. V. Ipat'ev.

sulfur corresponding to S/As ratio (in gram-atoms) of unity, i.e., the amounts of sulfur in grams liberated by replacement of 1 atom of sulfur in Na_2HAsS_4 by oxygen.

The following conclusions may be drawn from these results: addition of Fe^{2+} and Mn^{2+} ions accelerates the regeneration process and results in earlier liberation of sulfur. The yield of sulfur is also increased in presence of Mn^{2+} . The formation of thiosulfate is almost independent of the presence of additives. Additions of Cr^{3+} and Sn^{2+} ions affect the regeneration process adversely, and decrease the yield of sulfur, while Cr^{3+} increases the amount of thiosulfate formed.

It was found in 5 consecutive absorption-regeneration cycles in presence of Fe^{2+} and Mn^{2+} salts that the effects of the additives persist during this number of cycles, and that in presence of Mn^{2+} ions the regeneration proceeds as far as liberation of arsenious sulfide. The explanation is that oxythioarsenates are less stable than thioarsenates.

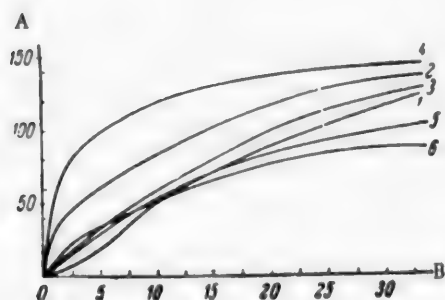


Fig. 1. Influence of salt additions on the regeneration of arsenical soda liquors.

A) Total oxygen absorbed (ml); B) time (minutes).

Additions: 1) without additions, 2) Fe^{2+} , 3) Cu^{2+} , 4) Mn^{2+} , 5) Cr^{3+} , 6) Sn^{2+} .

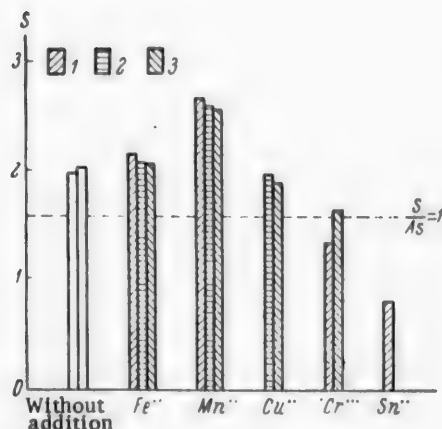


Fig. 3. Effect of salt additions on the yield of sulfur in the regeneration of arsenical soda liquor.

Contents of additives (in moles/liter): 1) 10^{-3} , 2) 10^{-4} , 3) 10^{-5} .

S) Sulfur content (g/liter).

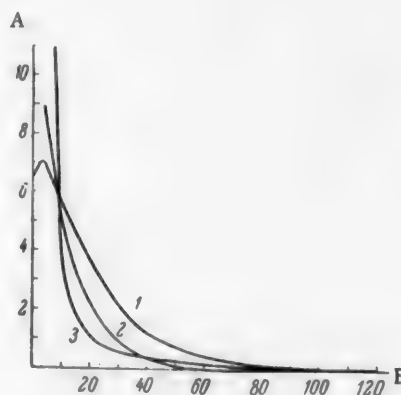


Fig. 2. Effect of additions of Fe^{2+} and Mn^{2+} salts on regeneration of arsenical soda liquor.

A) Rate of oxygen absorption (in ml/min), B) time (min).

Additions: 1) without addition, 2) Fe^{2+} , 3) Mn^{2+} .

Effect of additions of buffer solutions on the regeneration of arsenical soda liquor. In order to study the effect of hydrogen ion concentration on the regeneration of arsenical soda liquor, a series of experiments was carried out in which buffer solutions differing in pH were added to the liquor for regeneration. The buffer solutions were mixtures of KH_2PO_4 and NaOH in different proportions, at approximately 0.5 molar concentrations.

The liquors for regeneration were two arsenical soda solutions with Na/As atomic ratios of 2.5 and 3. The arsenic concentration was 10.8 g/liter, and the soda concentration 12.5 g/liter.

The results are given in Tables 2 and 3.

These experimental results indicate that addition of buffer solutions to the liquors has a strong influence on the regeneration process. The rate of side reactions is decreased sharply, almost to zero in some

TABLE 2

Effect of Buffer Solution on the Regeneration of Arsenical Soda Liquor with $\frac{Na}{As} = 3.0$

Amount of buffer solution added (%) ^a	Start of sulfur liberation (min)	pH of original solution	Amount of sulfur liberated (g/liter)	Amount of $Na_2S_2O_3$ formed, calc. as S (g/liter)	Sel + Sthio (g/liter)	Sulfur liberated in elemental state (%)	Elemental S liberated, in g-atoms per g-atom As
0	8	6.85	1.216	1.28	2.496	48.7	0.76
0	8	6.85	1.292	1.15	2.442	52.9	0.81
40 (pH = 6.8) . .	4	7.0	1.708	0.106	1.814	94.1	0.06
40 (pH = 6.8) . .	5	7.0	1.795	0.028	1.818	98.7	1.12
20 (pH = 6.6) . .	5	6.8	1.761	0.108	1.929	91.8	1.10
40 (pH = 6.0) . .	5	6.7	Arsenious sulfide precipitated				

^a The buffer solutions were added to the arsenical soda liquor in such a way that the arsenic concentration remained constant in all the experiments (the same applies to Tables 3, 4, 5, and 6).

TABLE 3

Effect of Buffer Solutions on the Regeneration of Arsenical Soda Liquor with $\frac{Na}{As} = 2.5$

Amount of buffer solution added (%)	pH value		Start of sulfur liberation (min)	Amount of sulfur liberated (g/liter)	Amount of $Na_2S_2O_3$ formed, calc. as S (g/liter)	Sel + Sthio (g/liter)	Sulfur liberated in elemental state (%)	Elemental S liberated, in g-atoms per g-atom As
	before experiment	after experiment						
0	6.8	8.25	6	1.778	1.11	2.888	61.6	0.93
0	6.8	7.95	5	2.000	0.877	2.877	69.5	1.03
20 (pH = 7.35) . .	7.0	8.6	6	2.224	0.402	2.626	84.7	1.14
40 (pH = 7.35) . .	7.0	8.35	6	2.552	0.126	2.678	95.3	1.30
40 (pH = 7.6) . .	7.3	8.45	5	2.560	0.010	2.570	99.6	1.32
40 (pH = 8.4) . .	7.45	8.9	4	2.259	0.450	2.709	83.4	1.15
40 (pH = 8.4) . .	7.45	8.3	4	2.030	0.500	2.530	80.2	1.04
40 (pH = 7.0) . .	6.8	7.9	5	Arsenious sulfide precipitated				

TABLE 4

Effect of Buffer Solutions on the Oxidation of Sodium Sulfide (0.11 N)

Amount of buffer solution added (%) and pH value	Total sulfur taken (g-atom/liter)	pH of original solution	Start of sulfur liberation (min)	Amount of elemental sulfur liberated (g-atom/liter)	Total sulfur found in soln. (g-atom/liter)	Amount of elemental sulfur liberated (g/liter)	Amount of $Na_2S_2O_3$ formed, calc. as S (g/liter)	Sel + Sthio (g/liter)	Amount of sulfur liberated in elemental state (%)
0	0.059*	< 11	—	0	0.059	0	1.133	1.133**	0
40 (pH = 6.6) . .	0.059	10.1	—	0	0.055	0	0.545	0.545	0
40 (pH = 5.8) . .	0.059	7.5	35	0.013	0.098	0.539	0.872	1.411	38.2
40 (pH = 5.3) . .	0.059	7.4	17	0.024	0.035	0.781	0.714	1.495	52.2
40 (pH = 4.4) . .	0.059	7.35	9	0.030	0.028	0.956	0.528	1.484	64.4

* Including HS^- , 0.055 g-ion/liter.

** Oxidation of all the sulfur available in the solution would give 1.888 g sulfur per liter, as elemental sulfur or thiosulfate.

cases. The yield of sulfur increases, and the S/As ratio rises accordingly. For each solution there is a definite initial pH at which the maximum amount of sulfur is liberated and the minimum amount of thiosulfate is formed. This value is pH = 7.0 for solutions with Na/As = 3.0, and pH = 7.3 for solutions with Na/As = 2.5.

Moreover, these results give an indication of the influence of the Na/As ratio on the quality of the liquor (its capacity for regeneration). It is evident that a liquor with Na/As = 3.0 gives a considerably lower yield of sulfur, and much more thiosulfate is formed in its regeneration without additives (see Column 6 in Tables 2 and 3). The addition of a buffer solution which lowers the pH below a certain value (below 6.8 for a liquor with Na/As = 3, and below 7.0 for a liquor with Na/As = 2.5) results in precipitation of arsenious sulfide during the regeneration.

Effect of buffer solutions on the oxidation of sodium sulfide. An industrial arsenical soda liquor may contain some sodium sulfide, the amounts being greater in solutions of higher free alkalinity.

According to available data, oxidation of sodium sulfide under the usual conditions gives sodium thiosulfate. It was of interest to find conditions in which oxidation of sodium sulfide would yield elemental sulfur. A series of experiments was carried out on the oxidation of sodium sulfide (0.11 N solution) by oxygen in presence of buffer solutions. The buffer solutions were added in order to increase the hydrogen ion concentrations in the solutions being oxidized. The oxidation was performed in a laboratory regenerator. The results are given in Table 4 and Fig. 4.

It follows from the results that when the solution pH is lowered to 7.5, sodium sulfide begins to be oxidized with liberation of elemental sulfur, and not only with formation of thiosulfate (as is the case at high pH values). The amount of liberated sulfur increases with decrease of pH. The amount of thiosulfate formed also decreases, i.e., more of the sulfur is liberated in the elemental state.

Effect of buffer solutions on the regeneration of arsenical soda liquors in presence of Na_2S . After it has been shown that at decreased solution pH sodium sulfide is oxidized with liberation of elemental sulfur, experiments were carried out on the regeneration of arsenical soda liquors in presence of sodium sulfide with the pH lowered by addition of buffer solutions. The results of these experiments are given in Table 5 and Fig. 5.

These results show that considerably more sulfur is liberated in presence of sodium sulfide from arsenical soda liquors at pH = 7. This is probably because oxidation of sodium sulfide (at this pH) gives elemental sulfur.

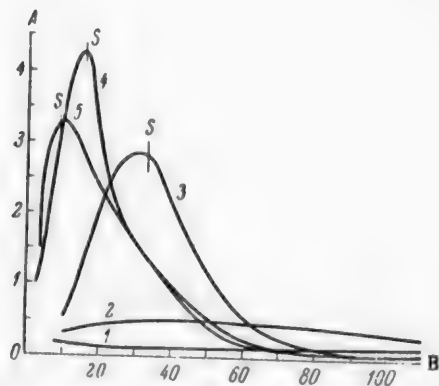


Fig. 4. Effect of buffer solutions on the oxidation of sodium sulfide.

A) Rate of oxygen absorption (ml/minute),

B) time (minutes).

- 1) 0.11 N Na_2S solution; 2) 0.11 N Na_2S +
+ buffer solution (pH = 10); 3) same (pH = 7.5);
- 4) same (pH = 7.4); 5) same (pH = 7.35).

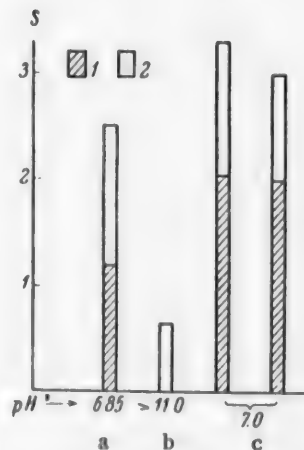


Fig. 5. Effect of buffer solutions on the regeneration of arsenical soda liquors in presence of Na_2S .

S) Sulfur content (g/liter).

- 1) Elemental sulfur, 2) thiosulfate sulfur.
- a) Without additive, b) with 0.11 N Na_2S
solution, c) with 0.11 N Na_2S solution +
+ buffer solution.

TABLE 5

Effect of Buffer Solutions on the Regeneration of Arsenical Soda Liquor in Presence of Na_2S (0.11 N)
 $\frac{\text{g-atoms Na}}{\text{g-atoms As}} = 3.0$

Amount of Na_2S solution added (%)	Amount of buffer solution added (%)	Start of sulfur liberation (min)	Amount of sulfur liberated (g/liter)	Amount of $\text{Na}_2\text{S}_2\text{O}_3$ formed, calc. as S (g/liter)	$\text{S}_{\text{el}} + \text{S}_{\text{thio}}$ (g/liter)	Amount of S liberated in elemental state (%)	Elemental S liberated, in g-atoms per g-atom As
0	0	2	1.216	1.28	2.5	48.6	0.63
20	0	—	0	0.62	0.62	0	—
20	20	3	2.016	1.25	3.27	61.6	1.05
20	20	3	1.974	1.01	2.98	65.2	1.03

TABLE 6

Effect of Buffer

$\frac{\text{g-atoms Na}}{\text{g-atoms As}}$	Added (%)	Start of sulfur liberation (min)	Amount of sulfur liberated (g/liter)	Amount of $\text{Na}_2\text{S}_2\text{O}_3$ formed, calc. as S (g/liter)	$\text{S}_{\text{el}} + \text{S}_{\text{thio}}$ (g/liter)	Amount of S liberated in elemental state (%)	Elemental S liberated, in g-atoms per g-atom As
8.0	$\text{Na}_2\text{As}_2\text{O}_4$						
	0	5	2.01	1.01	3.11	64.6	1.26
	5	6	1.56	0.79	2.35	66.4	0.97
	15	8	0.83	0.41	1.24	66.9	0.52
	25	18	0.61	0.28	0.89	68.5	0.38
	40	Not liberated	0	0.10	0.10	0	—
2.5	Sodium thioarsenate						
	0	4	2.20	1.00	3.20	68.8	1.14
	19	4	1.94	0.82	2.76	70.4	1.01
	40	12	2.53	1.18	3.71	68.2	1.32

Effect of additions of trivalent arsenic on the regeneration of arsenical soda liquor. In plant conditions, oxygen compounds of trivalent arsenic are periodically added to the liquor to replace arsenic compounds lost in the process. To determine the effect of additions of trivalent arsenic, experiments were carried out on the regeneration of arsenical soda liquor with added $\text{Na}_2\text{As}_2\text{O}_4$. The results, given in Table 6, show that additions of trivalent arsenic have a very adverse effect on the regeneration process, and decrease the amount of sulfur liberated. It is possible that addition of trivalent arsenic is followed by partial interaction between sodium oxyarsenite and thioarsenate according to the equation



The compound $\text{Na}_2\text{HAS}_2\text{O}_2$ formed in this reaction cannot be regenerated further. If trivalent arsenic is added to the liquor in the form of thio compounds, the regeneration proceeds without apparent change.

These results explain why it is necessary to saturate freshly prepared solutions of trivalent arsenic in sodium carbonate with hydrogen sulfide before these solutions are introduced into the cycle. This preliminary "ripening" of the solutions has come into use on purely empirical grounds in a number of plants, and has resulted in more stable operation of the purification units.

SUMMARY

1. Additions of Fe^{2+} and Mn^{2+} salts to the liquor for regeneration increases the regeneration rate and accelerates the start of sulfur liberation. In presence of Mn^{2+} ions the ratio of liberated sulfur to arsenic is considerably higher than unity, and arsenious sulfide is precipitated during repeated regeneration cycles.
2. Addition of Cu^{2+} , Cr^{3+} , Sn^{2+} ions does not improve but often worsens regeneration of the liquor.
3. By addition of buffer solutions, it is possible to find the optimum pH for each arsenical soda liquor at which side reactions are greatly reduced and the yield of sulfur increases.
4. When the pH of a sodium sulfide solution is decreased by addition of buffer solutions, the sulfide begins to be oxidized by oxygen with liberation of elemental sulfur. The amount of sulfur liberated increases with decrease of solution pH.
5. The presence of trivalent arsenic in the form of oxy compounds has an adverse effect on regeneration and lowers the sulfur yield. The presence of trivalent arsenic in the form of thio compounds has almost no influence on the regeneration process.

LITERATURE CITED

- [1] M. I. Gerber, V. P. Teodorovich, N. I. Brodskaya and V. V. Ipat'ev, J. Appl. Chem. 26, 657 (1953).
- [2] N. I. Brodskaya, M. I. Gerber and V. P. Teodorovich, J. Appl. Chem. 30, No. 10, 1510 (1957).*
- [3] N. I. Brodskaya, M. I. Gerber, V. P. Teodorovich and A. D. Shusharina, J. Appl. Chem. 30, No. 11, 1588 (1957).*

Received July 17, 1956

*Original Russian pagination. See C. B. Translation.

THE HARDENING OF MAGNESIUM OXYCHLORIDE CEMENTS

A. G. Bergman and I. P. Vyrodov

Magnesium oxychloride cement is made by the action of concentrated magnesium chloride solution on calcined magnesite.

There are two theories of the hardening of magnesium oxychloride cements. One group of scientists, including Berg and Ganelina [1], who studied magnesium oxychloride cements by the thermographic method, attribute their hardening to formation of hydrated magnesium oxychlorides, but the quantities and composition of these oxychlorides were not determined conclusively.

Another group of scientists, consisting of Baikov and his school, reduces the hardening of magnesium oxychloride cements to the hydration of magnesium oxide, with magnesium chloride playing only a subsidiary role in the hydration process.

Baikov's theory is supported by a number of experimental results [2], most of which are refuted on close critical examination.

If hardened magnesium oxychloride cement is powdered and washed with water, almost all its magnesium chloride is washed out. In a study of the equilibrium system $H_2O-MgCl_2-MgO$, Robinson and Waggeman [3] showed that when the magnesium chloride concentration is over 15%, the solid phase is an oxychloride of the composition $MgCl_2 \cdot 3Mg(OH)_2 \cdot 8H_2O$. With less than 15% of magnesium chloride, this compound is partially decomposed. Therefore when the powdered hardened cement is leached with water, the hydrated oxychloride is naturally hydrolyzed, finally yielding magnesium hydroxide containing a little magnesium chloride.

One of us showed, jointly with Sinani [4], that when dehydrated carnallite ($KCl \cdot MgCl_2$) is extracted with anhydrous alcohol it is separated into potassium chloride which is insoluble in alcohol, and anhydrous magnesium chloride, readily soluble in alcohol. Anhydrous carnallite is a substance with well-defined properties, more stable than the hydrated oxychloride, and melts without decomposition at 495° . Nevertheless, because of the different solubilities of its components in alcohol, it can be separated completely by alcohol extraction.

In another of Baikov's experiments, calcined magnesite was treated with excess concentrated solution of magnesium chloride. The filtered solution of magnesium chloride deposited a copious white precipitate after some time. After being washed on the filter with 95% alcohol, this precipitate contained only a few tenths of one per cent of chlorine. From this Baikov concluded that "... this precipitate, which was formerly believed to be magnesium oxychloride, is none other than magnesium hydroxide $Mg(OH)_2$ " [2]. It is quite evident that the oxychloride is decomposed when washed with 95% alcohol, and this experiment in no way disproves the formation of oxychlorides in concentrated solutions of magnesium chloride.

Baikov also held that the hardening process reduces to the slaking of magnesite, analogous to the slaking of lime. The value for the heat of hydration of magnesium oxide in the reaction $MgO + H_2O = Mg(OH)_2$, which is 5400 calories according to Berthelot, indicates that the heat effect of this reaction is considerable. It is probable that in the mixing of magnesium oxychloride cement the heat of hydration of magnesium oxide is augmented by the heat of formation of a hydrated oxychloride with the general formula $xMgCl_2 \cdot yMg(OH)_2 \cdot zH_2O$ or $xMgCl_2 \cdot yMgO \cdot zH_2O$. The handbook of thermal data on inorganic substances compiled by Britske, Kapustinskii, et al. [5] gives the following heats of formation (from the elements): $MgCl_2 \cdot MgO - 421.1$ kcal; $MgCl_2 \cdot MgO \cdot 6H_2O - 810.2$ kcal; $MgCl_2 \cdot MgO \cdot 16H_2O - 1507.9$ kcal; $MgO \cdot HCl$ (i.e., $MgOHCl$) - 194.1 kcal. The chemical processes in mixing of the cements involve formation of these compounds.

Baikov's assertion that hydrated magnesium oxide does not give rise to cement is not supported by our results; hydrated magnesium oxide dried at 100° gave, with 35% magnesium chloride solution taken in the proportions $\text{Mg}(\text{OH})_2 : \text{MgCl}_2 \cdot 6\text{H}_2\text{O} = 1 : 1$, a hardened cement with high mechanical strength after 5-7 hours. The more rapid setting of magnesium oxide with magnesium chloride solution is quite natural, as it is known that when magnesium oxide is mixed with hot magnesium chloride solution the hardening is very rapid.

When magnesium oxide is mixed with magnesium chloride solution, the first step is, of course, hydration of magnesium oxide, accompanied by evolution of heat; the heat evolved accelerates hardening, and therefore already hydrated magnesium oxide sets more slowly in magnesium chloride solution.

Baikov's statement [2] that "... the solubility of anhydrous magnesia is many times that of magnesium hydroxide; therefore a solution saturated with respect to anhydrous magnesia is supersaturated with respect to magnesium hydroxide" is puzzling. It is difficult to imagine that, with a relatively high heat of hydration, a solution of anhydrous magnesium oxide in water can exist if the hydration reaction is so vigorous. Therefore Baikov's assertion [2] that "... the physical aspect of the hardening of calcined magnesite is that the liquid (magnesium chloride solution) dissolves anhydrous magnesium oxide and deposits magnesium hydroxide - and therefore the process itself yields the hardened product in the form of a monolithic mass" is without foundation.

There is as yet no satisfactory scientific explanation for the induction period which precedes the vigorous reaction in which magnesium oxychloride cement hardens, and this period cannot be used as an argument to support any particular theory of hardening of magnesium oxychloride cement. The theory that hydrated oxychlorides are formed is also supported by crystallographic and x-ray data. Zhuraviev [6] stated very briefly that "... it follows from a comparison of x-ray patterns that all the $\text{Mg}(\text{OH})_2$ lines are present in their entirety in the x-ray diagram of $\text{MgO}-\text{MgCl}_2-\text{H}_2\text{O}$. The few additional lines most likely correspond to MgCl_2 ."

Our preliminary x-ray patterns show quite clearly that the patterns given by $\text{Mg}(\text{OH})_2$ and magnesium oxychloride cement differ appreciably.

The starting mixtures taken for the investigation had the composition $(65\% \text{H}_2\text{O} + 35\% \text{MgCl}_2) + n\% \text{MgO}$, where n was from 5% to 85%, in 5% steps. The starting materials were analytical-grade magnesium oxide made by the "Krasnyi Khimik" Leningrad Factory of Chemical Reagents, and $\text{MgCl}_2 \cdot 6\text{H}_2\text{O}$.

This relatively pure magnesium oxide was tested for the presence of a hydrate film which, according to Baikov, prevents the immediate hydration of magnesium oxide, and hence the liberation of heat. Our experiments did not confirm the existence of such a film, because both undehydrated magnesium oxide and the dehydrated oxide (heated at 800-900°) gave a heat effect 3.5 hours after being mixed with water.

Preliminary studies of the hardening of magnesium oxychloride cements showed that the time of initial set depends on the value of n , the time decreasing with increase of n . For example, with $n = 5\%$ the cement set in 8-10 hours, while cements with $n = 85\%$ set within 1.5 hours. It follows that the formation of cements with high magnesium oxide contents is much more rapid than the hydration of magnesium oxide, as hydration, as already stated, begins 3.5-4 hours after the magnesium oxide is mixed with water.

The x-ray investigations also fully justify the view that none of the specimens in the composition range studied contained magnesium hydroxide. The patterns were taken by means of a BSV-4 tube with a copper anode. The conditions were: $v = 35 \text{ kv}$, $I = 15 \text{ ma}$, exposure 18 to 20 hours.

The principal interplane spacings for magnesium oxychloride cements, magnesium oxide, and magnesium hydroxide are given in Table 1.

Comparison of x-ray patterns for specimens with different ratios of magnesium oxide to magnesium chloride (Figs. 1, 2) shows an abrupt structural change when the ratio of MgO to MgCl_2 is 3 : 1.

The x-ray patterns (Fig. 1) of cements with $n = 5$ to 40% show that these cements contain oxychloride. The top diagram represents the oxychloride corresponding to the composition $\text{MgO} + 3 (\text{MgCl}_2 \cdot 6\text{H}_2\text{O}) + 12\text{H}_2\text{O}$, which was prepared with the shortest possible washing of the mixture with cold water, removal of the water by suction, and drying at 100°. It can also be asserted that the cements containing 50 to 85% magnesium oxide likewise do not contain magnesium hydroxide (the x-ray patterns of magnesium oxide and magnesium hydroxide are given in Fig. 3).

TABLE 1

Interplane Spacings of Magnesium Oxychloride Cements, Magnesium Oxide, and Magnesium Hydroxide

Line intensities*	L (in mm)	θ°	$\sin \theta$	$\frac{d}{n}$ (in Å)	Line intensities*	L (in mm)	θ°	$\sin \theta$	$\frac{d}{n}$ (in Å)
MgO					Mixture with 50% MgO				
vs	137.1	21.4	0.366	2.101	s	21.5	10.55	0.186	3.36
vs	117.15	31.12	0.516	1.49	w	29.75	14.9	0.258	2.741
m	112.9	33.5	0.552	1.394	m	33.8	16.9	0.291	2.43
s	101.8	39.1	0.631	1.220	vs	37.1	18.5	0.318	2.21
m	86.15	46.93	0.730	1.054	vw	40.75	20.37	0.353	2.01
m	70.23	54.88	0.815	0.942	s	46.6	23.3	0.396	1.799
vs	52.3	63.95	0.897	0.900					
Mg(OH) ₂					Mixture with 60% MgO				
w	18.35	9.175	0.1585	4.80	s	21.6	10.8	0.186	3.80
vs	37.85	18.925	0.324	2.38	w	29.9	14.95	0.258	2.741
w	50.8	25.40	0.430	1.793	m	33.6	16.8	0.291	2.43
s	58.75	29.375	0.492	1.566	vs	37.3	18.65	0.32	2.21
w	62.15	31.075	0.516	1.492	vw	40.9	20.45	0.356	1.985
					s	46.45	23.22	0.394	1.785
Oxychloride					Mixture with 75% MgO				
vs	22	11	0.190	3.72	s	21.3	10.6	0.184	3.84
s	30.5	15.25	0.263	2.69	w	30.2	15.1	0.261	2.71
s	33.8	16.9	0.291	2.43	w	33.8	16.9	0.29	2.44
vs	37.2	18.6	0.320	2.21	vs	37.35	18.7	0.321	2.71
w	40.3	20.15	0.35	2.02	vw	40.8	20.8	0.371	1.895
m	45.0	22.5	0.383	1.847	s	46.45	23.22	0.394	1.795
Mixture with 50% MgO					Mixture with 85% MgO				
s	22.15	11.06	0.192	3.60	s	21.6	10.8	0.187	3.78
m	30.5	15.25	0.263	2.690	w	30	15	0.259	2.73
m	33.75	16.9	0.291	2.43	m	33.7	16.85	0.29	2.44
vs	37.35	18.7	0.321	2.21	vs	37.4	18.7	0.321	2.21
vw	40.3	20.15	0.35	2.02	vw	40.5	20.25	0.369	1.92
m	45	22.5	0.383	1.847	s	46.45	23.22	0.394	1.795
Mixture with 25% MgO					Mg(OH) ₂ : MgCl ₂ · 6H ₂ O = 1 : 1				
s	22.8	11.4	0.193	3.6	vs	22.7	11.4	0.193	3.6
m	30.1	15.05	0.258	2.741	s	30.0	15.0	0.258	2.741
m	34.0	17	0.291	2.43	vs	37.25	18.62	0.321	2.21
vs	37.5	18.75	0.321	1.895	m	46.1	23.05	0.391	1.984
vw	40.8	20.4	0.373	1.795	m	49.3	25.65	0.431	1.64
m	46.45	23.22	0.394	1.795					
Mixture with 40% MgO									
s	22.6	11.3	0.193	3.6					
m	29.8	14.9	0.258	2.741					
m	34.0	17	0.291	2.43					
vw	37.1	18.55	0.318	2.20					
vw	40.8	20.4	0.356	1.985					
m	46.0	23.0	0.390	1.814					

* The designations are: vs - very strong, s - strong, m - moderate, w - weak, vw - very weak.

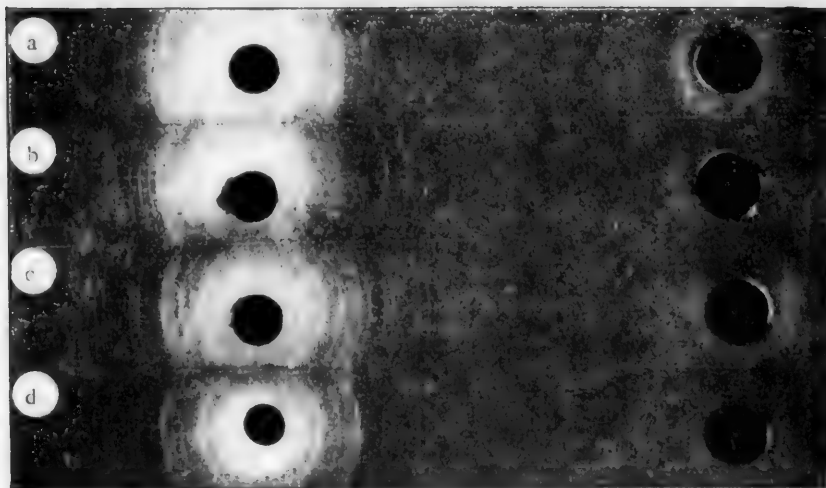


Fig. 1. x-Ray patterns of a) oxychloride; b, c, d) cements containing 5, 25, and 40% magnesium oxide respectively.

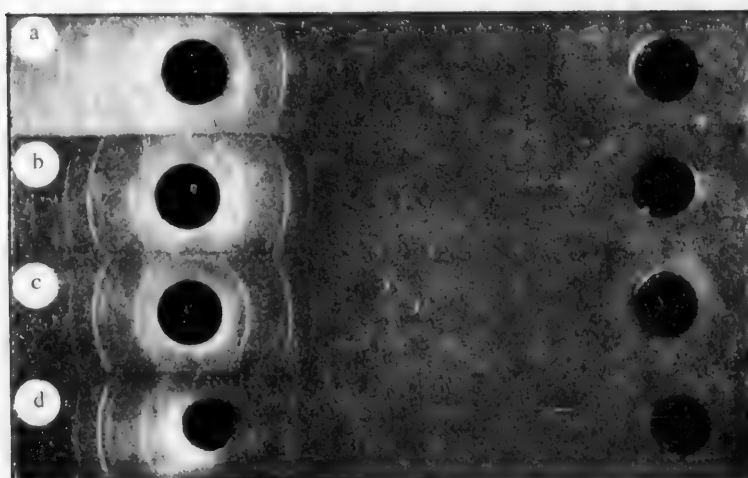


Fig. 2. x-Ray patterns of cements containing a) 50%, b) 60%, c) 75%, d) 85% magnesium oxide.

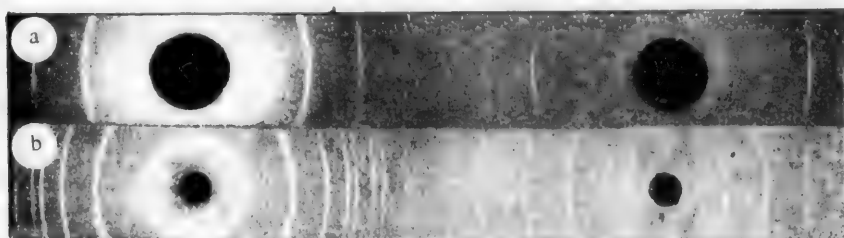


Fig. 3. x-Ray patterns of magnesium oxide (a) and magnesium hydroxide (b).



Fig. 4. x-Ray pattern of stonelike mass formed by addition of 35% magnesium chloride to magnesium hydroxide.



Fig. 5. x-Ray patterns of cement containing 50% magnesium oxide: a) 7 days, b) 28 days after mixing.

TABLE 2

Compressive Strength of Cement Specimens

Magnesium oxide content (%)	Compressive strength (in kg/cm ²) after		
	1 day	7 days	28 days
50	500	420	500
55	420	480	480
60	500	510	500
65	500	510	510

However, the presence of lines of the same intensity as in magnesium hydroxide, and with interplane spacings $\frac{d_1}{n} = 3.8$ Å, $\frac{d_2}{n} = 2.4$ Å, i.e., close to the interplane spacings of magnesium hydroxide ($\frac{d_1}{n} = 4.75$ Å, $\frac{d_2}{n} = 2.35$ Å), and therefore characteristic of magnesium hydroxide, suggests that growth of the magnesium hydroxide lattice occurs during setting of the cement, but does not go to completion. This is probably associated with the formation of a crystal structure which is geometrically analogous in one direction to the structure of magnesium hydroxide. This is a very attractive hypothesis, especially in view of the layer structure of magnesium hydroxide, which forms a hexagonal lattice. This would account for displacement of the lines corresponding to the interplane spacings $\frac{d_1}{n} = 4.75$ Å and $\frac{d_2}{n} = 2.35$ Å and the indices (001) and (101). Evidently, after the layer has been formed, partial replacement of OH^- ions by Cl^- ions in the layer itself begins. Completion of the layer results in a structure which no longer resembles the structure of magnesium hydroxide. The x-ray pattern of hardened cement formed by addition of 35% magnesium chloride solution to magnesium hydroxide (Fig. 4) does not contain the lines for magnesium hydroxide; this partly confirms our hypothesis.

This question can be finally settled by high-speed x-ray structure analysis or by the application of ionization methods to x-ray structure analysis.

It was then shown that both the mechanical and the chemical properties of the cements form during the setting process itself, and do not change during the subsequent 28 days. It follows from the data in Table 2 that the compressive strength remains unchanged for a month after preparation of the specimens.

It follows from Fig. 5 that no additional phases or structures arise in the cement during the month following preparation of the specimens, as both the positions and the numbers of the lines on the x-ray patterns remain unchanged.

SUMMARY

1. Sharp structural differences between magnesium hydroxide, magnesium oxychloride, and specimens of magnesium oxychloride cements were found by x-ray structure analyses of magnesium hydroxide, magnesium oxychloride, and cements obtained by the mixing of magnesium oxide with 35% magnesium chloride solution.

2. Specimens of magnesium oxychloride cements kept for different times (from 1 to 28 days) did not show any significant structural differences; this shows that equilibrium is reached rapidly during hardening of these cements.

3. The hardening of some magnesium oxychloride cements is much more rapid than the hydration of magnesium oxide.

4. Magnesium hydroxide mixed with 35% magnesium chloride solution hardens within 5-7 hours. The stonelike mass so formed does not contain magnesium hydroxide after 28 days.

The absence of lines corresponding to magnesium hydroxide in the x-ray pattern, and the fact that a mixture formed from magnesium hydroxide and 35% magnesium chloride solution hardens, refute Baikov's theory, according to which complexes are not formed in magnesium oxychloride cement, and the hardening process reduces to hydration of magnesium oxide.

5. The structure was found to change sharply at 3:1 ratio of magnesium chloride and magnesium oxide in the cement.

LITERATURE CITED

- [1] L. G. Berg and S. G. Ganellina, *Bull. Kazan Branch Acad. Sci. USSR, Chem. Ser.* 2 (1955).
- [2] A. A. Baikov, *Collected Works* 5, 49-70 (1948).*
- [3] Robinson and Waggeman, *J. Phys. chem.* 13, 673 (1909).
- [4] A. G. Bergman and S. S. Sinani, *Coll. Trans. State Inst. Appl. Chem.* 27, 102 (1937).*
- [5] E. V. Britske, A. F. Kapustinskiĭ, B. K. Veselovskii, L. M. Shamovskii, L. G. Chentsova and B. I. Anvaer, *Thermal Constants of Inorganic Substances* (Izd. AN SSSR, 1949).*
- [6] V. F. Zhuravlev, *Chemistry of Cements* (Goskhimizdat, 1952) p. 180.*

Received March 8, 1956

*In Russian.

CHROMIUM BORIDE AND ITS USE IN HARD FACING ALLOYS

I. I. Iskol'dskii and S. L. Cherkinskaia

All-Union Scientific Research Institute of Hard Alloys

Modifications of metal surfaces for increasing wear resistance are of great importance in modern technology.

Among the methods used for this purpose is deposition of hard substances on steel surfaces. The materials used for this purpose in the USSR are the powdered mixture "stalinit" [1], and T-590 electrodes [2]. Our object was to develop a facing alloy and electrodes with greater resistance to wear than stalinit and T-590 electrodes.

BKh boride facing mixture. In 1892 the first experiments were carried out on the preparation of the borides of nickel, iron, and cobalt by direct combination of the metals with boron [3]. Two years later Moissan prepared chromium boride, also by direct combination of the elements in the electric arc furnace. Since that time there have been many investigations of the preparation of borides [4].

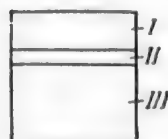


Fig. 1. Structure of surface layers formed from boride facing mixtures.

Specimens 1, 1a, 2, 2a, 3, 3a, 4, 4a (see Table 1).

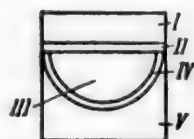


Fig. 2. Structure of surface layers formed from boride facing mixtures.

Specimens 5, 5a (see Table 1).

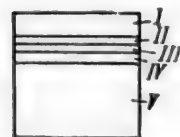


Fig. 3. Structure of surface layers formed from boride facing mixtures.

Specimens 6, 6a (see Table 1).

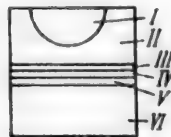


Fig. 4. Structure of surface layers formed from boride facing mixtures.

Specimens 7, 7a, 8, 8a, 9, 9a (see Table 1).

Our method for the preparation of chromium boride makes it possible to obtain chromium boride in large quantities. It is known that chromium boride reacts with iron powder to form a trimetallic compound. However, a certain proportion of the crystals of chromium boride remains unchanged on instantaneous contact of iron with chromium boride at a high temperature of the electric arc. We utilized this important property of chromium boride in preparation of the facing mixtures. The particle size of the iron powder used in our experiments was in the range 10-500 μ m.

Nine different mixtures with various contents of CrN and Fe (powder) were prepared in order to find a composition which gives the hardest and most wear-resistant coatings.

The structures of the layers formed from the boride facing mixtures are shown schematically in Figs. 1-4; the composition of the mixtures, and its influence on the hardness (Rockwell A scale), is given in Table 1.

The chromium boride used in the facing mixtures had the following composition (%):

C _{total}	Cr	B	Insoluble residue
0.35	80.93	17.48	1.2

TABLE 1

Effect of Composition of the Facing Mixture on the Hardness of the Layer Formed, and Characteristics of the Zones

Specimen No.	Composition of facing mixture (%)	Average hardness of layer 1 mm thick, Rockwell A scale	Zone characteristics (Fig. 1)
1 1a	} 90Fe + 10CrB	70.6	I) polyhedrons of solid solution bordered by eutectic; eutectic consists of chromium boride and solid solution, II) strip of unetched alloyed solid solution, III) steel structure (ferrite + pearlite)
		72.6	
2 2a	} 80Fe + 20CrB	78.5	I) austenite-martensite solid solution + network of eutectic of chromium boride and solid solution, II) strip of unetched alloyed solid solution, III) steel structure (ferrite, and pearlite at grain boundaries)
		78.0	
3 3a	} 70Fe + 30CrB	79.1	I) hypoeutectoid structure, consisting of dendrites of alloyed solid solution and eutectic, II) strip of unetched alloyed solid solution, III) steel structure
		82.1	
4 4a	} 60Fe + 40CrB	82.1	I) dendrites of alloyed solid solution and eutectic, II) strip of unetched alloyed solid solution, III) steel structure
		80.6	
5 5a	} 50Fe + 50CrB	81.7	I) excess crystals of chromium boride + laminar eutectic, II) eutectic of laminar type, of CrB crystals and alloyed solid solution, III) alloyed solid solution, IV) strip of unetched alloyed solid solution, V) steel structure
		82.0	
6 6a	} 40Fe + 60CrB	83.6	I) excess crystals of chromium boride + laminar eutectic, II) eutectic of laminar type, III) solid solution, IV) strip of unetched solid solution, V) steel structure
		82.8	
7 7a	} 30Fe + 70CrB	84.1	I) excess crystals of CrB + eutectic, II) numerous CrB crystals + eutectic, III) eutectic of laminar type, IV) iron-based solid solution, V) strip of unetched solid solution, VI) steel structure
		83.5	
8 8a	} 20Fe + 80CrB	83.3	I) excess crystals of chromium boride + eutectic, II) eutectic of laminar type, III) iron-based solid solution, IV) strip of unetched solid solution, V) steel structure
		83.8	
9 9a	} 10Fe + 90CrB	84.1	I) excess crystals of chromium boride + eutectic, II) eutectic of laminar type, III) iron-based solid solution, IV) strip of unetched alloyed solid solution, V) steel structure
		84.0	

Metallographic investigations confirmed that the composition of the mixture determines to a considerable extent the structure of the facing layer formed.

With 50% CrB and 50% Fe in the mixture, the structure of the facing layer begins to change sharply; an upper layer appears, saturated with crystals of chromium boride cemented together by the eutectic.

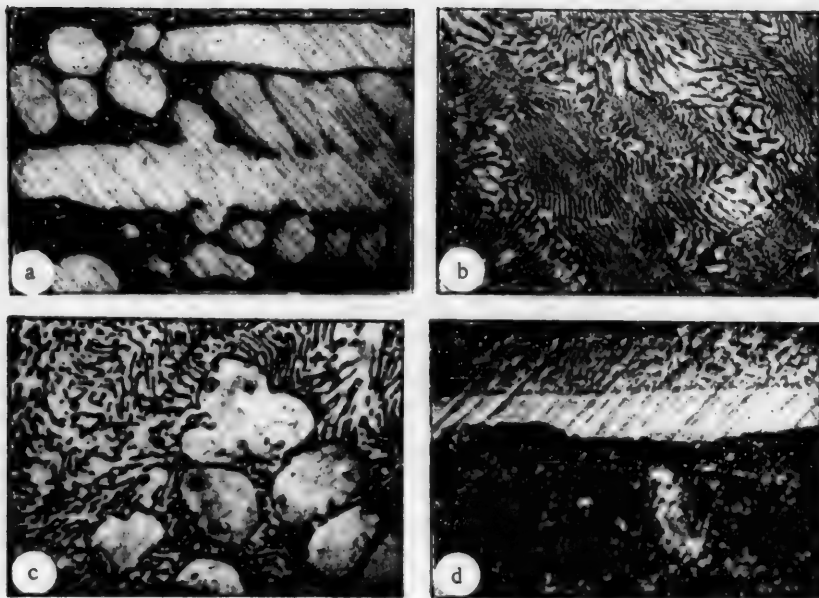


Fig. 5. Polished section of a boride facing layer.

a) Eutectic and crystals of chromium boride, b) lamellar eutectic, c) dendrites of solid solution, d) strip of alloyed solid solution and steel.

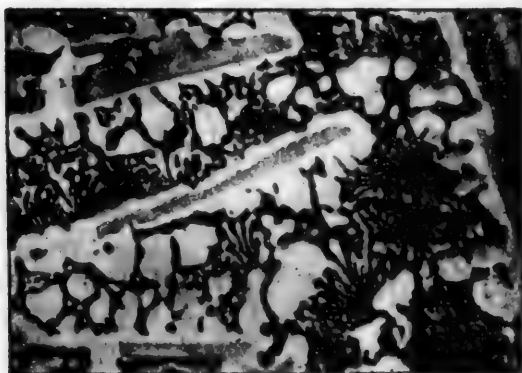


Fig. 6. "Splitting" of chromium boride crystals.

With up to 50% CrB in the mixture, the upper layer contains polyhedrons and dendrites of solid solution, cemented together by the eutectic.

Micrographs of a polished section of a layer of the mixture 50% CrB + 50% Fe (powder) fused on No. 3 steel are given below. It was found that it is preferable to apply the chromium boride mixed with iron powder (with strictly defined proportions of the components in the mixture) as pure chromium boride does not give a good coating. Moreover, if chromium boride is used alone, the layer formed is always of variable composition, as iron enters into the layer accidentally from the article being coated.

The structure of the coating layer, consisting of four zones, can generally vary; it depends on the surfacing conditions. Structures with only three zones may be found — one of the zones vanishes. Such vanishing zones are: 1) dendrites of solid solution + eutectic, or 2) eutectic as an independent layer. However, the wear resistance of the layer is determined by its first zone, which consists of crystals of chromium boride cemented together by the eutectic consisting of very fine crystals of chromium boride and a trimetallic compound of iron, boron, and chromium.

"Splitting" of CrB crystals is observed in the first layer of the boride facing. The micrograph of a polished section (Fig. 6) shows clearly that the CrB crystals are surrounded by a layer consisting of a compound of chromium boride and iron (this layer is colored yellow during etching), while the CrB crystals remain light colored.*

Microhardness values for the crystals, eutectic, and solid solution of the boride layer, determined by means of the PMT-3 instrument at 100 g load, are given below.

*The sections were studied by E. A. Shchetilina, R. V. Rybal'chenko, and N. P. Vasil'eva.

Microhardness (kg/mm²)

Pale crystals	1700
Yellow coating of crystals	1420
Eutectic	1023
Solid solution	520

BKh-2 electrodes for hard facing. Boride facing materials can be used in the form of BKh boride mixture or in the form of BKh-2 electrodes covered with a coating containing chromium boride.

The composition of the electrode coating was developed by us jointly with engineers of the Experimental Welding Plant of the Scientific Research Institute of the Ministry of Industrial Construction USSR, N. A. Tarkhanov and A. D. Rakhmanov. The amount of chromium boride in the coating is 50% of the amount of iron in the rod.

The coating on the rod had the following composition (%): chromium boride 80, mica powder 8, graphite 10, potash 2.

Comparative hardness tests were performed on facing layers applied on No. 3 steel from stalinit, boride facing mixture, and T-590 and BKh-2 electrodes (Table 2).

TABLE 2

Hardness of Facing Layers on Rockwell A Scale

Facing material	Single-layer coating of thickness (mm)		Two-layer coating, 5 mm thick
	1	2	
Stalinit	76.4	—	77.0
Boride facing mixture	85.5	—	85.4
T-590 electrode	78.3	79.3	79.8
BKh-2 electrode	83.5	81.7	82.4

It follows from Table 2 that in the case of boride coatings the hardness is not increased when thicker coatings are used. On the contrary, high hardness values are obtained for thin layers. This is explained by the effect of overheating on the structure of boride coatings. It is therefore recommended to apply boride coatings in a single layer. During the facing process not all the components of the mixtures or electrode coatings pass into the layer formed. Oxidation, evaporation, and mixing take place during the process, and this has a considerable influence on the chemical composition of the applied layer.

It must be noted that in determinations of the composition of the layers the coatings were applied not to steel, but to copper strip 30 mm thick, in order to avoid any possible mixing of the coating with iron from the molten surface of an iron block.

Analytical data on the composition of the facing layers formed (in %) are given below:

Facing material	B	Cr	Fe	Mn	C _{total}	Insoluble residue	Total
Boride facing mixture	7.65	35.0	57.5	—	0.12	0.10	100.3
BKh-2 electrode	9.40	29.07	60.84	—	1.10	0.15	100.5
	7.67	31.29	60.00	—	0.55	0.35	99.8

These results show that the layers formed from boride mixture and BKh-2 electrodes differ little in chemical composition. However, metallographic investigations showed that they differed in structure.

Metallographic data on the coating formed by means of BKh-2 electrodes are given in Table 3.

The following conclusions may be drawn from metallographic data on the two types of boride facings, i.e., applied from a boride mixture in the carbon arc, and applied by means of an electrode with a boride coating:

TABLE 3

Metallographic Data on Coatings from BKh-2 Electrodes

Zones	Details of zones	Size of zone (in $\mu\mu$)
I	Laminar eutectic and small amount of excess boride crystals. Most of the crystals 240-400 $\mu\mu$ in size	1000-3500
II	Laminar eutectic. Eutectic consists of iron-based alloyed solid solution and boride crystals	100-1000
III	Dendrites of iron-based solid solution and laminar eutectic	70-300
IV	Strip of unetched alloyed iron-based solid solution	15-20

1) zone I of the facing produced from the boride mixture contains excess of chromium boride crystals; 2) zone I of the BKh-2 facing contains a small quantity of crystals, with laminar eutectic predominant; 3) in zone I of the facing produced from the boride mixture of the crystals split when a microsection is oxidized in air at 450-500°; this is not found in zone I of the facings made from BKh-2 electrodes. The microhardness of crystals of the BKh-2 facing was found to be 1398 kg/mm² (load 100 g); in other words, these crystals differ in chemical composition from the crystals formed in the facings from boride mixture. No pale crystals remained in this case. The chromium boride had reacted completely with iron, with formation of a trimetallic compound. The effect of this on the wear resistance of the facing is discussed below (see Fig. 7).

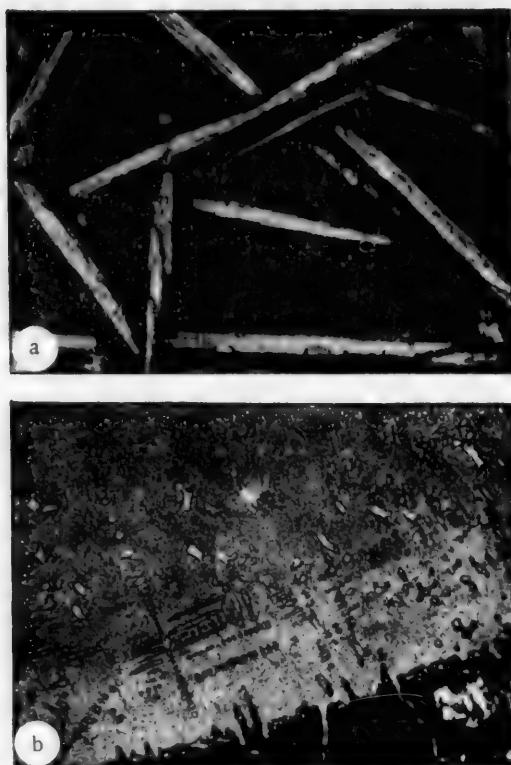


Fig. 7. Polished section of facing layer applied by means of BKh-2 electrodes.

a) Crystals of Cr-B-Fe ternary compound and eutectic, b) eutectic, dendrites of solid solution, strip of solid solution, steel.

This example demonstrates another important fact of scientific interest - the coating formed by application of powdered materials in the carbon arc differs from the coating formed by the use of coated steel electrodes.



Fig. 8. No. 3 steel faced with boride mixture.

The facing of one specimen is polished.

The chemical composition is the same in both cases (50% CrB + 50% Fe) but the structure of the coatings formed is different. This evidently depends on the rates of the processes taking place during the application, and on the temperature conditions. The theory of hard facing by the use of powders and electrodes is not sufficiently well understood as yet.

Some theoretical conclusions relating to the wear resistance of hard facing layers. The structure of facing layers formed from facing mixtures and electrodes differs from the structure of compact metals and powder alloys in consisting of several heterogeneous zones arranged in consecutive layers. The number of these zones depends on the composition of the mixture or electrode coating, and also on the current strength and voltage during the treatment (treatment conditions).

Our experimental investigations, lasting several years, led to certain theoretical conclusions which may be useful in relation to studies of hard facing alloys.

1. The wear resistance of the facing depends to a considerable extent on the structure of the first zone of the layer formed. The macrohardness of the layer is determined by the structure of the first zone, and is not a direct function of the wear resistance. In some cases harder layers are less wear-resistant than layers of lower hardness.

2. The microhardness of the crystals and eutectics determines the wear resistance of the facing, but it sometimes happens that the concentration of the crystals of the greatest microhardness is low. Therefore the wear resistance is influenced by the concentration (distribution) of the hard crystals in the surrounding eutectic layer.

3. Eutectics differing in hardness may be present in the facing layer, depending on the proportions of the components in the mixture; eutectics of the highest microhardness are the most wear-resistant.

4. The facing layer may contain the following components: crystals, eutectic, solid solution, trimetallic chemical compound.

5. The hard-facing process in the carbon arc differs from the process with the use of coated steel electrodes, as the rates of the processes and the heat conditions are different.

Application of boride materials. According to our experimental results, the boride facing mixture (50% CrB + 50% Fe) melts at $1470 \pm 30^\circ$. The boride mixture can be applied by means of alternating or direct current.

A layer of the boride mixture, 4-5 mm thick, is spread over the horizontal plane of the article to be faced, by means of a trowel. The facing equipment is then switched on, and a graphite electrode 6-10 mm in diameter and 150-300 mm long is moved toward the article. If alternating current is used, the current strength should be 200 amps, and the voltage 40 v.

The "facing factor" $\alpha = 6.9 \text{ g/amp} \cdot \text{hr}$ (Fig. 8).

In the direct-current process, the operation is carried out with direct polarity: (+) on the article, (-) on the electrode. Direct-current welding equipment - SMG-1, SMG-2, and SUG-26 motor-generators, or alternating-current STN-500, STE-22, and STE-34 welding transformers may be used. Alternating-current facing with the use of BKh-2 electrodes is carried out at 180-210 amps, the voltage fluctuating in the range 28-30 v. The "facing factor" is 7.5-7.7 g/amp-hr. Two-layer applications are not recommended, either with BKh-2 electrodes or with boride mixture. The porosity of the facings obtained from the boride electrodes and mixtures is from 1 to 2%.

Determination of the wear resistance of boride facings. The wear resistance of boride facings was tested under production conditions in brickwork presses. In the molding of raw bricks, the blades of the screw presses are subjected to abrasive wear. The blades were faced with different facing materials and their wear resistance was determined; the results were used to calculate the coefficient of wear resistance

$$K = \frac{a}{b},$$

where a is the number of tons of clay passed through the press with the blades coated by means of the boride mixture or BKh-2 electrodes, and b is the number of tons of clay passed through the press with the blades faced with stalinit or by means of T-590 electrodes.

The results of the production trials are given in Table 4.

TABLE 4

Comparative Data on Wear Resistance Under Production Conditions

Facing materials	Total number of machine-hours worked	Total amount of clay passed through press cylinder (tons)	Clay passed through (tons/machine-hour)	Relative wear-resistance coefficient K
Stalinit	129,6	2616,5	20,1	1
Boride facing mixture	336	7979,5	23,7	3,0
BKh-2 electrodes	218,5	5604,7	25,6	2,1
T-590 electrodes	155	3752,8	24,1	1,4

Boride facings were subsequently tested in other plants; the results confirmed the results obtained previously.

SUMMARY

1. Industrial trials carried out in different plants showed that the wear resistance of facings made from boride mixture is 2.5-3 times, and that of facings applied by means of BKh-2 electrodes is twice that of stalinit facings.

2. Crystals of a trimetallic compound of chromium boride and iron predominate in the facing layer formed from BKh-2 electrodes. If the boride mixture is used, crystals of chromium boride enclosed in a coating of the trimetallic compound are partially retained in the facing layer. This accounts for the higher wear resistance of the coatings formed from the boride mixture.

3. Economic calculations confirm that boride facing materials can replace the cheaper stalinit and T-590 electrodes, as the machine standstill time is reduced, the number of adjustments is decreased, and labor costs are lower.

LITERATURE CITED

- [1] V. S. Rakovskii and I. I. Kriukov, *Hard Facing Alloys* (Moscow, 1948) p. 37.*
- [2] G. D. Vol'pert, *Application of Wear-Resistant Facing Alloys* (Moscow, 1953) p. 32.*
- [3] H. Moissan, *Comptes Rend.*, 114, 392 (1892).
- [4] G. V. Samsonov and L. Ia. Markovskii, *Progr. Chem.* 25, 2, 190 (1956).

Received June 28, 1956

* In Russian.

PRODUCTION OF ALUMINUM AND CHROMIUM PHOSPHATE FILMS ON ALUMINUM AND ITS ALLOYS

I. V. Krotov, V. V. Grinina and N. A. Zapol'skaia

Since 1949, Spruance et al. [1] described a number of methods for the production of protective films on aluminum and its alloys, by the use of passivating mixtures of phosphoric, chromic, and hydrofluoric acids. In some variations of the processes, solutions of these acids are replaced totally or partially by solutions of their salts. Spruance also described an additional treatment with solutions of dichromates, chromic acid, or mixed chromic and phosphoric acid solutions, for improving the quality of the films formed on aluminum and its alloys.

The name "Alodine" was given to the coatings formed on aluminum and its alloys by this process.

The production of "Alodine" coatings on aluminum is described in considerable detail by Douty and Spruance [2].

In this paper a graph is given with the $F:CrO_3$ ratio plotted against the phosphoric acid content (in g/liter of solution). It is not stated what fluorides and chromates were used for making the solution. The graph in question is also somewhat indefinite because the absolute contents of fluoride and chromate in the solution are not given. Nevertheless, the diagram shows the approximate region of F, Cr, and H_3PO_4 concentrations in which stable films should be formed. The bath composition is adjusted by simple addition.

The optimum bath temperature is 38-54°; at higher temperatures the volatility of hydrogen fluoride greatly increases.

The coating may be applied to the metal by immersion, spraying, or brushing. The coating must be dried at a low temperature, after which it can be heated to the melting point of aluminum without appreciable change of protective properties.

According to these authors, an "Alodine" film covered with a single coat of paint is much more effective in protecting the aluminum against corrosion when sprayed with sodium chloride solution, than an anodic oxide film with three coats of paint. "Alodine" coatings are amorphous, hard, and nonporous. After low-temperature drying, the main components of the coating are presumed to be: $CrPO_4$ 50-55%; $AlPO_4$ 17-25%; H_2O 22-23%; traces (less than 0.5%) of the fluorides of aluminum, chromium, and calcium may also be present.

A very good account of the "Alodine" process has been given by Hess [3]. It is pointed out that the dimensions of parts made from aluminum and aluminum alloys are changed little as the result of treatment with "Alodine" solution. Pollack [4] reported that the coatings formed on aluminum and its alloys by the "Alodine" process are more effective in protecting the metal against corrosion than the films made by anodizing. Moreover, the "Alodine" process is considerably simpler and cheaper than anodizing. According to Pollack, "Alodine" coatings are fairly elastic, and allow of some deformation of the coated parts without risk of destruction of the film.

The purpose of the present investigation was to produce protective films on aluminum and its alloys by treatment with aqueous solutions of phosphoric acid with additions of potassium dichromate and sodium fluoride, to investigate the properties of these films, and to determine the possible mechanism of their formation.

For evaluation of the protective properties of the films, drops of a solution of the following composition were applied: concentrated hydrochloric acid 25 cc, potassium dichromate 3 g, water 75 cc. The protective effect of a film on aluminum or aluminum alloy is estimated by the time which elapses before a drop of this

solution applied to the surface turns green. This method is widely used in the aircraft industry for determination of the stability of anodic films. In addition to the accelerated drop tests, we tested the coated specimens of aluminum and alloys by periodic spraying with 3% sodium chloride solution, and by consecutive application of drops of 3% sodium chloride solution at the same point (each successive drop was applied when the preceding drop dried). In the latter case the resistance of the film is given by the number of drops applied consecutively at the given point before the appearance of the first signs of destruction of the film.

The influence of each of the components of the "Alodine" solution on the corrosion resistance of the film was tested by the accelerated drop test method. The optimum concentration of one component was found at constant concentrations of the other two components. This was repeated for each of the other two components. By this method of approximations, the optimum concentrations of all the components were determined. The optimum time of passivation was determined at 45° bath temperature for the optimum concentrations of the components.

The composition of the "Alodine" films formed on aluminum and its alloys was determined by the following procedure. The aluminum or alloy sample was powdered by means of a special device. The powder was then treated with the appropriate quantity of "Alodine" solution, with vigorous stirring; it may be assumed that the film formed on each grain of the metal has the same composition as the film on a plate of the metal. The amount of film substance (relative to the weight of the coated metal) is greatly increased if the "Alodine" film is formed on metal powder. This makes it possible to use ordinary chemical methods for analysis of the film.

The principal elements of the film can be easily determined by the usual methods of analysis if the exact content of the main metal in the powder after the "Alodine" treatment is known. This can be found by exact determination of the amount of hydrogen [5] liberated when a known weight of the passivated powder is dissolved in sulfuric acid.

For identification of individual chemical compounds present in the film, it is convenient to apply the method of thermographic analysis [6] to the metal powder after treatment with the passivating solution.

Since "Alodine" films are amorphous in structure, it follows from the literature that investigations of these films by x-ray and electron diffraction methods cannot be expected to give conclusive results.

The following procedure was generally used for the formation of "Alodine" films on specimens of aluminum and its alloys: 1) degreasing of the specimens by rubbing with cotton wool soaked in dichloroethane, and then in ethyl alcohol; 2) treatment for 3 minutes at 45° in an alkaline solution of the following composition: Na_3PO_4 50 g, NaOH 8 g, Na_2SiO_3 30 g, H_2O 1 liter; 3) thorough washing of the specimens in running water; 4) passivation in a solution of a given composition; 5) washing in running water; 6) additional treatment in chromic anhydride solution; 7) drying in air; 8) corrosion tests by the drop or other methods.

Determination of the optimum conditions for the formation of films on aluminum and its alloys. Specimens of A-1 soft aluminum, 60 × 15 × 0.8 mm in size, were used for one series of experiments. They were passivated at 45° in solutions differing in composition. In some of the experiments the bath composition was kept constant and the treatment time was varied. After the passivation the specimens were washed in running water, held for 10 minutes in 0.5% CrO_3 solution at room temperature, dried in air for 24 hours at the same temperature, and then subjected to drop tests for film resistance. The time during which the film remained resistant (until a green color appeared), denoted simply as "film resistance in minutes," is the average value of 6-12 individual determinations in each case. The resistance data for films made under different conditions on A-1 aluminum are plotted in Figs. 1-5. Examination of Figs. 1-5 shows that the following are the optimum conditions for the formation of films on A-1.

After degreasing and washing, the specimens are passivated in a solution of the following composition: NaF 2.4 g, $\text{K}_2\text{Cr}_2\text{O}_7$ 22.7 g, H_3PO_4 (sp. gr. 1.266) 303 cc, water 697 cc. Bath temperature 45°, passivation time 60 minutes. The passivated specimens are washed in running water and held for 10 minutes in 0.5% chromic anhydride solution. They are then taken out of this solution and dried in air for not less than 24 hours.

By the use of similar methods of pretreatment and selection of the passivation procedure, the conditions were found for the production of effective corrosion-resistant films on aluminum foil, clad DIATV alloy, clad D16 alloy, AMG and AMTs alloys (not clad), and Silumin alloy.

The pretreatment was the same for all these alloys. The alkaline solution used for degreasing was diluted 5-fold in the case of Silumin alloy. The passivating solutions differed for different alloys, but the variations in

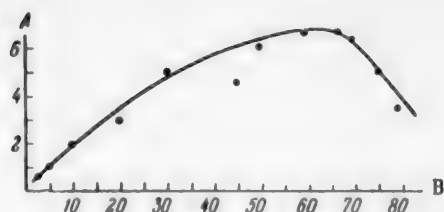


Fig. 1. Effect of passivation time on the resistance of films on A-1.

A) Film resistance (minutes), B) passivation time (minutes).

Bath composition: NaF 0.14 g, H_3PO_4 (sp. gr. 1.262) 18 cc, $K_2Cr_2O_7$ 2 g, H_2O 48 cc.

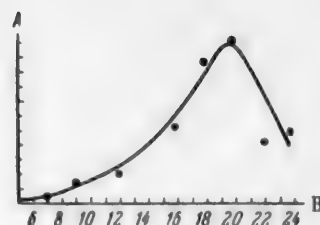


Fig. 2. Effect of H_3PO_4 content in solution on the resistance of films on A-1.

A) Film resistance (minutes), B) amount of H_3PO_4 (cc).

Bath composition: NaF 0.14 g, $K_2Cr_2O_7$ 2 g, total volume of H_3PO_4 (sp. gr. 1.262) and H_2O 66 cc.

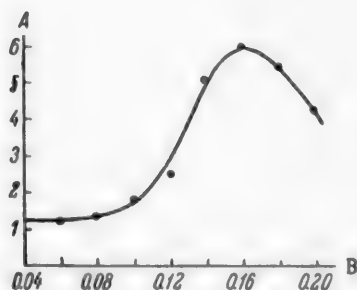


Fig. 3. Effect of amount of NaF in solution on the resistance of films on A-1.

A) Film resistance (minutes), B) amount of NaF (g).

Bath composition: NaF variable, $K_2Cr_2O_7$ 2 g, H_3PO_4 (sp. gr. 1.266) 20 cc, H_2O 48 cc.

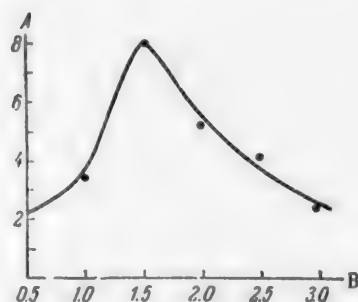


Fig. 4. Effect of amount of $K_2Cr_2O_7$ in solution on the resistance of films on A-1.

A) Film resistance (minutes), B) amount of $K_2Cr_2O_7$ (g).

Bath composition: NaF 0.16 g, $K_2Cr_2O_7$, variable, H_3PO_4 (sp. gr. 1.266) 20 cc, H_2O 46 cc.

the contents of the individual components were slight: H_3PO_4 (sp. gr. 1.262) 212-303 cc, $K_2Cr_2O_7$ 22.7-30.3 g, NaF 1.8-2.4 g, water 788-697 cc.

A procedure for regeneration of the passivating solutions used with DIATV clad alloy and AMG and AMTs alloys was worked out. When 4 alloy specimens have been treated in 66cc of solution, 4 more specimens can be treated after addition of 0.2 g of NaF, films of good protective properties being obtained. The effectiveness of the bath can be restored three times by additions of 0.2 g of sodium fluoride each time.

Tests of film resistance by the successive application of drops of 3% sodium chloride solution. The resistance of the films on the specimens of aluminum or aluminum alloys was found in terms of the number of drops of 3% sodium chloride solution applied successively until the film showed the first signs of breakdown and the metal under the film showed signs of corrosion; the results are given below:

Alloy	Resistance of specimen degreased with dichloroethane and rubbed with alcohol (not passivated)	Resistance of degreased and passivated specimen
DI6 alloy, clad	14	102
AMG alloy, plain	14	41
AMTs alloy, plain	43	184
DIATV alloy, clad	41	257

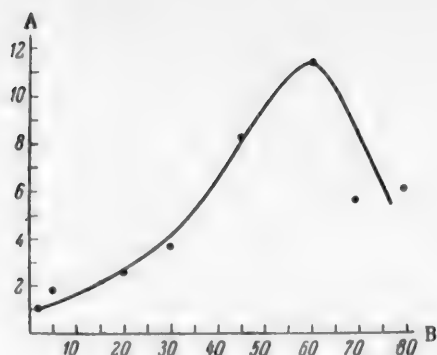


Fig. 5. Effect of treatment time on the resistance of films on A-1.

A) Film resistance (minutes), B) treatment time (minutes).

Bath composition: NaF 0.16 g, $K_2Cr_2O_7$ 1.5 g, H_3PO_4 (sp. gr. 1.266) 20 cc, H_2O 46 cc.

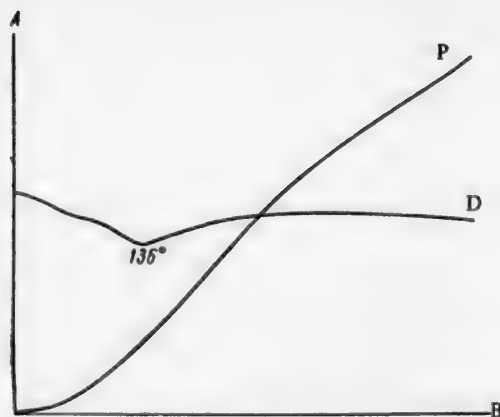


Fig. 6. Thermogram of passivated AMG alloy powder.

A) Temperature, B) time.

The tests by the method of consecutive application of drops of 3% NaCl solution were of different duration for different specimens (from 2.5 to 12 months).

Determination of film composition. Aluminum or aluminum alloys, in powder form, were treated in solutions of phosphoric acid with additions of potassium dichromate and sodium fluoride. These powders did not require preliminary degreasing. The bath contents were stirred continuously during passivation of the metal powders. At the end of the treatment the solution was decanted off, the powder was washed three times with ordinary water, with stirring, and then held for 10 minutes in 0.5% chromic anhydride solution. This solution was then decanted off, the powder dried with filter paper, dried for a long time in air, and finally dried to constant weight in a weighing bottle over calcium chloride. The powders were dark green in color.

The differential heating curve in Fig. 6 does not reveal any pronounced transitions in the film on the grains of AMG alloy during heating up to about 600°. The very weak minimum observed on this curve at 136° indicates that up to 136° the film loses the small amount of moisture present in it. Thermograms of passivated powders of technical A-1 aluminum and AMTsAM alloy are similar in appearance.

The weight of the passivated AMG alloy powder was 4.4136 g before and 4.3303 g after the thermographic analysis. The metal contents of the AMG alloy powder (determined from the volume of hydrogen liberated by the powder in sulfuric acid solution) were equivalent to the following contents of aluminum: before passivation 99.77%, after passivation 90.40%, and after passivation and thermographic analysis, 92.41%. The powder contained 1.26% chromium and 1.4% phosphorus after the thermographic analysis. From these results it was calculated that the film on AMG alloy contains 1.2 g of water per 3.561 g $CrPO_4$ and 2.551 g $AlPO_4$. Hence the composition of the film (in %) is: $CrPO_4$ 48.7, $AlPO_4$ 34.89, H_2O 16.24. The water in the film is evidently not constitutional but merely adsorbed, as the thermogram indicates that it is given off at low temperatures.

Analogous calculations gave the following compositions for the passivating films (in %): on technical aluminum, $CrPO_4$ 43.89, $AlPO_4$ 36.98, H_2O 19.12; on AMTsAM alloy, $CrPO_4$ 49.45, $AlPO_4$ 28.47, H_2O 22.05.

Possible mechanism of the process

When aluminum or an aluminum alloy is immersed in phosphoric acid containing potassium dichromate and sodium fluoride, it is highly probable that a hydrated film of aluminum oxide is present on the surface or is newly formed on active regions of the surface; it is possible that the newly formed film is more complex in composition and contains both hydrated aluminum oxide and hydrated chromium oxide.

The hydrogen fluoride present in the solution activates the metal surface and causes pores to form in the film of hydrated aluminum oxide: $Al_2O_3 \cdot nH_2O + 12 HF = 2AlF_3 \cdot 3HF + (n + 3)H_2O$. $AlF_3 \cdot 3HF$ can enter into an

exchange reaction with the sodium salts in solution, forming a precipitate of $\text{AlF}_3 \cdot 3\text{NaF}$ and the acid of the sodium salt which took part in the reaction. Pore formation in the film of hydrated oxide on the metal surface is a prerequisite for the occurrence of an electrochemical process between portions of the film acting as cathodes, and regions of film-free metal acting as anodes.

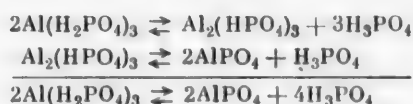
As the solution contains a high concentration of hydrogen ions, the following processes take place at the cathodes (regions of electronically conducting film):



with formation of trivalent chromium ions (in presence of fluoride ions in the solution [7]), leading to the appearance of CrPO_4 in solution.

CrPO_4 is almost entirely insoluble in water, and is present in the solution in the colloidal state. We found that the colloidal particles of artificially prepared CrPO_4 are positively charged.

The following process takes place at the anode: $\text{Al} + 3\text{H}_2\text{PO}_4^- - 3e = \text{Al}(\text{H}_2\text{PO}_4)_3$. $\text{Al}(\text{H}_2\text{PO}_4)_3$ is readily soluble in water. $\text{Al}(\text{H}_2\text{PO}_4)_3$ undergoes hydrolysis with formation of acid and normal phosphates of aluminum.



It may be assumed that $\text{Al}_2(\text{HPO}_4)_3$ although only slightly soluble, forms ordinary solutions in water, whereas AlPO_4 forms mainly colloidal solutions with positively charged particles; this was demonstrated experimentally for colloidal particles of artificially prepared AlPO_4 .

The colloidal particles of CrPO_4 and AlPO_4 , having considerable positive charges, are deposited on the anodic (active) regions of the metal. Subsequently, if initial crystallization centers have been formed from CrPO_4 and AlPO_4 , particles of CrPO_4 and AlPO_4 are deposited on them.

The processes described above can be repeated in the remaining pores, until finally an almost nonporous film is formed. Treatment with chromic acid solution (like treatment with phosphoric acid solution) probably converts the hydrated forms of aluminum oxide, formed during the washing with water and contained in the pores of the original film, into insoluble salts of the $\text{Al}_2(\text{CrO}_4)_3$ or AlPO_4 type.

Oxidation of the surface of aluminum or aluminum alloys may readily occur at the active regions by reaction with solutions containing oxidizing agents. Phosphoric acid solutions with additions of potassium dichromate and sodium fluoride contain a powerful oxidizing agent - chromic acid.

Attempts to form passivating films on aluminum by anodic or cathodic treatment in solutions of phosphoric acid with additions of potassium dichromate and sodium fluoride were not successful. Aluminum cathodes were quite unchanged in appearance, while aluminum anodes were merely etched.

Tests on the passivation of A-1 aluminum in contact with copper in this solution showed that a passivating film is not formed either on the copper or on the aluminum near the point of contact, up to 3-4 cm from the point of contact. At greater distances from the point of contact a film is formed, but of somewhat inferior quality, and it only acquired its normal protective properties at a distance of 8-10 cm from the point of contact with the copper. On the other hand, contact with magnesium has almost no influence on the properties of the passivating film formed on A-1 in this solution.

SUMMARY

It was found by thermographic and chemical analysis of passivated powders of aluminum and its alloys that the film consists of CrPO_4 , AlPO_4 and water; the percentage contents of each of these components in the film were determined.

LITERATURE CITED

- [1] F. P. Spruance and A. Douty, U. S. Patent 2438877 (1949); F. P. Spruance and J. H. Thirsk, U. S. Patent 2494908, (1950); F. P. Spruance, U. S. Patent 2494910, June 17, (1950); F. P. Spruance, U. S. Patent, 2563431, August 7 (1951); F. P. Spruance, U. S. Patent, 2568936, September 25 (1951); F. P. Spruance and N. J. Newart, U. S. Patent, 2678291, (1954).
- [2] A. Douty and F. P. Spruance, Proc. Am. Electrodepositors Soc. 36, 193-216 (1949).
- [3] C. Hess, Rev. Aluminium, 174, 44-50 (1951).
- [4] A. Pollack, Metall, 19-20, 434-436 (1951).
- [5] I. V. Krotov, J. Appl. Chem. 28, 1302-1307 (1955).
- [6] L. G. Berg, A. V. Nikolaev and E. Ia. Rode, Thermography (Izd. AN SSSR, 1944);*J. Phys. Chem. 28, 9, 1550-1554 (1954); Ann. Sector Phys.-Chem. Analysis 26, 304-312 (1955).
- [7] M. Mitskus, Author's Summary of Dissertation, Acad. Sci. Lithuanian SSR, Institute of Chemistry, Vilnius (1956). *

Received August 27, 1956

*In Russian.

NATURE OF THE OXIDE FILM FORMED ON IRON IN ALKALINE SOLUTIONS OF OXIDIZING AGENTS

E. I. Levitina

Iron readily becomes passive in hot concentrated alkali solutions containing potassium (or sodium) nitrate as oxidizing agent. A black protective oxide film is formed on the metal surface. This process is extensively used in practice for production of a decorative finish and for increasing the corrosion resistance of the metal.

Little was known until recently about the nature of the film and the mechanism of its formation.

The mechanism of film formation, and the composition of the film, were determined as the result of detailed studies of the passivation of iron in alkalis [1]. It was shown that the film consists of magnetic oxide of iron, and is formed by interaction of saltlike compounds of ferrous and ferric oxides in alkali, yielding the sparingly soluble magnetic oxide of iron. The reaction takes place in solution, in immediate proximity to the metal surface. It may be schematically represented as follows:



Not all the dissolved metal is used in the formation of the protective film. Some is lost in solution.

Since the film is formed by reactions in solution, its composition may be varied. If salts of the corresponding bi- or trivalent metals are added to the alkali solution, the formation of compounds of the spinel type, $\text{MeO} \cdot \text{Fe}_2\text{O}_3$ or $\text{FeO} \cdot \text{Me}_2\text{O}_3$, analogous to magnetic oxide of iron, may be expected.

The influence of salts of different metals on the passivation of iron in alkali is not clearly understood. There seem to have been no attempts to change the nature of the film formed.

The present paper contains the results of experiments on the influence of salts of various metals on the formation of protective films on iron in alkali solutions.

EXPERIMENTAL

Cylindrical specimens of low-carbon steel were used for the experiments. The surface area of each specimen was 30 cm^2 . The solution used for most of the experiments contained 810 g of caustic soda and 50 g of potassium nitrate per liter, at 130° (b. p. of the solution is 135°). The specimens were fixed in holders revolving at 30 r.p.m. in the solution.

Sulfates or oxides of various metals (cobalt, zinc, manganese, aluminum, chromium, etc.) were added to the alkali solution. The effects of the metal additions were judged by variations of the growth rate of the protective film. The weight (and thickness) of the film, and the total amount of metal oxidized, were determined from the change in weight of the specimens after removal of the film in 10% hydrochloric acid solution containing 0.05% gelatin. In some cases the influence of the added metal on the content of ferric iron in solution was studied. The participation of the added substance in the formation of the protective film was also investigated qualitatively.

Effect of addition of cobalt. Cobalt was added as the sulfate to the alkali solution. The alkali solution becomes intensely blue owing to formation of sodium cobaltite when cobalt sulfate is added to it. The solution is transparent and stable in time. The blue solution of bivalent cobalt in alkali is immediately decolorized in presence of such oxidizing agents as potassium or ammonium persulfate, hydrogen peroxide, or sodium peroxide.

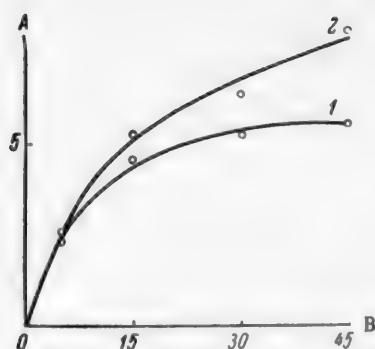


Fig. 1. Effect of addition of cobalt to the alkali solution on the weight of the film formed.
Solution contained 810 g NaOH and 50 g KNO_3 per liter; temperature 130° .
A) Weight of film (mg), B) time (minutes).
1) Alkali solution without addition, 2) with 2 g of cobalt per liter added.

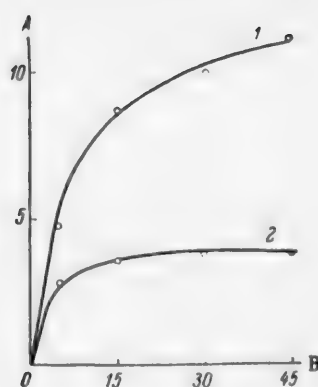


Fig. 2. Effect of addition of cobalt to the alkali solution on the amount of metal oxidized.
Experimental conditions as in Fig. 1.
A) Amount of metal oxidized (mg), B) time (minutes).
1) Solution without addition, 2) with 2 g of cobalt per liter added.

A black precipitate is formed, probably Co_3O_4 formed by the interaction of cobaltous and cobaltic oxide (similar to the formation of magnetic oxide of iron).

With an oxidizing agent such as potassium nitrite, the blue solution is decolorized only after several days. In this case a brown precipitate is deposited, probably Co_2O_3 , as the oxidation of the solution proceeds slowly. In presence of potassium nitrate, solutions of cobalt in alkali are stable indefinitely. A thin black film, probably Co_3O_4 or Co_2O_3 , is formed gradually on the surface of the solution. Therefore potassium nitrate, used as an oxidizing agent in oxide coating of steel, does not oxidize solutions of bivalent cobalt in alkali.

The growth of films on steel specimens in alkali solutions containing 2 g of cobalt per liter is represented by the curves in Figs. 1 and 2.

It is seen that addition of cobalt alters the course of the film growth. The weight of the film is somewhat greater, and the amount of metal oxidized is much less.

The appearance of the films formed is changed considerably on addition of cobalt. When 2 g of cobalt per liter is added to the alkali solution of b. p. 135° (containing 810 g of caustic soda and 50 g of potassium nitrate per liter), a film of an unusual yellow-blue color is formed on the metal surface, instead of the black film. After 30 minutes in the solution, the weight of this film was 6.3 mg and the weight of metal oxidized was 3.5 mg. This amount of oxidized metal is not enough for the formation of a film of magnetic oxide of iron (Fe_3O_4) formed in alkali solution with oxidizing agent but without additive. However, this amount of oxidized metal can give a film corresponding to the composition $\text{CoO} \cdot \text{Fe}_2\text{O}_3$, weighing 6.7 mg, i.e., close to the experimental result.

If the cobalt concentration is increased to 4 g/liter, black films with a gray-blue tinge are formed on the metal. In more highly concentrated alkali solutions, containing 930, 1065, and 1345 g of caustic soda per liter, the metal becomes coated with black homogeneous films, with a gradually increasing black deposit on the surface. These films differ considerably in properties from the films formed in solutions without added cobalt. For example, they dissolve very slowly in 10% hydrochloric acid, used for removal of films of magnetic oxide of iron. For a long time, measurable in hours, the films remain on the metal surface in the form of loose layers, readily removed mechanically, whereas films of magnetic oxide of iron of the same thickness dissolve completely in 30 seconds in the same acid solution. The color of the films changes during exposure to acid from bright red to yellow and then blue.

In relatively dilute alkali solutions thicker films are obtained in the presence than in the absence of cobalt.

Analysis showed that the cobalt enters into the protective film. Cobalt was detected in the acid solution used for removal of the oxide film by the color which it gives with an almost neutral solution containing potassium thiocyanate and acetone. This test for cobalt does not require separation of iron, which combines with the sodium pyrophosphate added to the solution. The solution becomes blue. The intensity of the color depends on the cobalt concentration.

The amount of ferric iron in the solution decreases on addition of cobalt salts to the alkali solution.

Cobalt therefore participates in the formation of the protective film. A reaction takes place between solutions of cobaltous oxide and ferric oxide in alkali. This is probably accompanied by the simultaneous formation of magnetic oxide of iron and of cobalt ferrite, the spinel $\text{CoO} \cdot \text{Fe}_2\text{O}_3$. One or the other of these processes predominates, according to the experimental conditions and the solubilities of the compounds.

Effect of addition of manganese. Manganese was added to the alkali solution in the form of the sulfate, corresponding to 5 and 10 g of the metal per 1 liter of solution. A considerable amount of a dark brown precipitate is formed on addition of manganese.

A black film, with bright interference colors and a small quantity of a loose black deposit, is formed on steel surface in a solution containing 810 g/liter of caustic soda (b. p. 135°) with 5 g/liter of manganese added. If the manganese content is increased to 10 g/liter, very thin protective films are formed, which give the metal only faint interference colors.

The growth of the protective films is illustrated by the experimental data plotted in Figs. 3 and 4. It is seen that the total amount of metal oxidized is very small in presence of manganese. In these experiments the specimens increased in weight after formation of the films, whereas in all other cases the weight decreased, some of the metal being dissolved. The weight of the film is much greater in presence of 5 g of manganese per liter than under the same conditions but without manganese. The weight of the film decreases sharply with increase of the manganese content to 10 g/liter. It is probable that the nature of the passivating film changes.

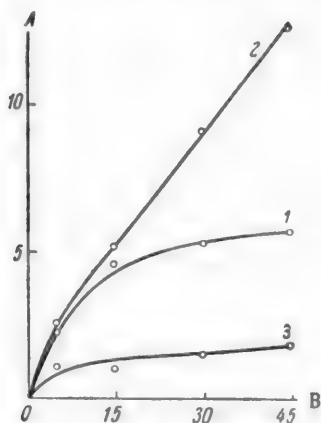


Fig. 3. Effect of additions of manganese to the alkali solution on the weight of the film formed.
Solution contained 810 g NaOH and 50 g KNO_3 per liter; temperature 130° .
A) Weight of film (mg), B) time (minutes).
Contents of manganese in the solution (g/liter): 1) 0, 2) 5, 3) 10.

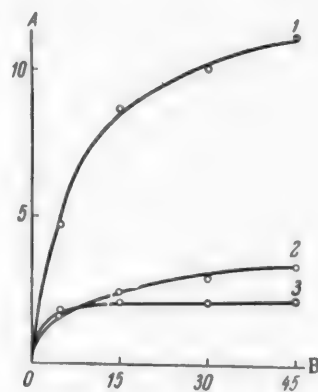


Fig. 4. Effect of additions of manganese to the alkali solution on the amount of metal oxidized.
Experimental conditions as in Fig. 3.
A) Amount of metal oxidized (mg), B) time (minutes).
Contents of manganese in the solution (g/liter): 1) 0, 2) 5, 3) 10.

Qualitative tests showed that the protective film contains a considerable amount of manganese. It is probable that when up to 5 g of manganese per liter is added, films of mixed composition with a predominant content of manganese oxides are formed.

With increase of the alkali concentration (solutions boiling at 140, 145, and 150°), black shiny films are formed on the metal, coated with a loose brown deposit. The amounts of metal oxidized and the film thickness are considerably less than in the corresponding solutions without manganese.

Effect of addition of zinc. Zinc was added to the alkali solution in the form of the sulfate, in amounts corresponding to 20 and 50 g of the metal per 1 liter of solution.

Additions of zinc only have an effect in relatively dilute solutions, containing 700 and 810 g of caustic soda per liter (b. p. 130 and 135°). In these solutions passivation takes place in presence of zinc: the thickness of the film formed and the amount of the metal oxidized decrease. In more highly concentrated alkali solutions zinc has no appreciable effects in amounts up to 50 g/liter.

The presence of zinc in the film was established by qualitative experiments. Therefore, in relatively dilute alkali solutions zinc takes part in film formation; it is probable that in addition to magnetic oxide of iron the compound $ZnO \cdot Fe_2O_3$ is formed, of lower solubility than magnetic oxide of iron.

The zinc and ferric ions in solution probably interact in this process.

Effect of addition of aluminum. Aluminum was introduced into the alkali solution in the form of the metal, 99.5% pure; 10, 20, and 50 g of the metal was added per liter of solution.

Addition of aluminum to the alkali solution results in a decrease of the film thickness and of the amount of metal oxidized.

Addition of aluminum to the alkali solution is probably equivalent to increase of the concentration of ferric iron, with a consequent decrease of the film thickness. The possibility of formation of a compound of the type $FeO \cdot Al_2O_3$ is not excluded.

Effect of addition of chromium. Chromium was introduced into the alkali solution in the form of chrome alum, in quantities corresponding to 2.5 and 10 g of the metal per liter of solution.

Effect of Salts of Different Metals on the Weight of the Film Formed and on the Total Amount of Metal Oxidized

Solution contained 810 g caustic soda and 50 g potassium nitrate per liter. Experiments were performed at 130°. The exposure time was 30 minutes. Specimen area 30 cm²

Additive in solution (g/liter)	Weight of film (g)	Amount of metal oxidized (g)
Without additive	0.0053	0.0092
2 Co	0.0063	0.0035
5 Mn	0.0091	0.0014
10 Mn	0.0030	0.0020
2 Cr	0.0057	0.0124
5 Cr	0.0080	0.0178
50 Zn	0.0038	0.0047
10 Al	0.0034	0.0067
50 Al	0.0028	0.0046

Addition of trivalent chromium colors the alkali solution yellow. The alkaline solutions of chromium formed at high temperatures (to a greater extent than the corresponding iron compounds) are unstable. When they are cooled, they first deposit a red-brown precipitate, probably consisting of mixed hydroxides of iron and chromium, or ferrous chromite $FeO \cdot Cr_2O_3$. The alkali solution always contains some ferric iron, as not all the dissolved metal is used in formation of the film. After some time green chromium hydroxide is precipitated until the solution becomes colorless.

The thickness of the film formed and the amount of metal oxidized increase with increasing chromium concentration in the alkali solution. It is possible that in this case the chromium binds the ferric iron present in the alkali solution, i.e., the hydroxides of iron and chromium are coprecipitated.

Chromium was detected qualitatively in the protective film. In this case the film is probably formed as the result of interaction of ferrous iron formed when

the metal dissolves with the trivalent chromium present in the solution.

Thus, the nature of the protective film formed can be varied by additions of salts of different metals to alkali solutions containing oxidizing agents. The course of the film growth also changes.

Data on the effects of additions of different metals to the alkali solutions on the film weight and on the amount of metal oxidized are given in the Table.

The weight of the film formed and the amount of metal oxidized are less in alkali solutions containing zinc or aluminum salts, and more in solutions containing manganese and chromium salts, than in solutions without additives. When cobalt is added, the weight of the film increases but the amount of metal oxidized decreases.

Additions of beryllium, cadmium or nickel salts to the alkali solution do not have any significant effect on the course of growth of the oxide film on iron in alkali solutions containing oxidizing agents. This is probably because these metals do not form saltlike compounds with alkalies.

When salts of copper or silver are added, the formation of a film of magnetic oxide of iron is accompanied by contact deposition of the metals. Moreover, silver removes ferric iron completely from the alkali solution, probably owing to formation of silver ferrites.

In conclusion, it is my duty to express my thanks to Professor A. G. Samartsev for his constant interest in this work.

SUMMARY

It is shown that films differing from magnetic oxide of iron can be obtained on iron in alkaline solutions of oxidizing agents; films containing oxides of cobalt, manganese, zinc, chromium, and aluminum, in addition to iron oxides, are formed.

LITERATURE CITED

- [1] A. G. Samartsev, Proc. Acad. Sci. USSR 25, 7, 234-238 (1942).

Received September 24, 1956

INVESTIGATION OF A SUSPENDED LAYER OF MOBILE FOAM IN SIEVE-PLATE EQUIPMENT

I. P. Mukhlenov

The Leningrad Technological Institute

Many workers who studied gas-liquid interaction on perforated and bubble-cap plates under bubbling conditions observed the formation of cellular foam [1-10]; some of them studied the effects of the process conditions on the height of the gas-liquid layer. However, these studies were not concerned with the operation of plates at high gas velocities in the open section of the apparatus, corresponding to the formation of a suspended layer of mobile foam [11, 12]. Therefore the results of the investigations cited above [1-10] cannot be used for the design of sieve-plate equipment operating in foam conditions (foam equipment) or for control of their operation. In our investigations, these results were mainly used for determination of the parameters the influence of which should be studied in foam layers.

The method and the results of our experiments on foam layers, carried out in most cases jointly with Pozin, Tumarkina, and Tarat, have been published in part [13-16].

Foam formation was studied under conditions similar to ours by Kuz'minykh et al. [17] and by Smirnov and U Tszin'-chen [18], parallel to our work.

In noting the breakdown of cellular foam at gas speeds of about 1 meter/second, which was also observed in our experiments [13-15], Kuz'minykh et al. state that "entirely different hydrodynamic conditions arise." These conditions evidently correspond to the formation of a suspended layer of liquid in the gas stream [11, 12]. When the hydrodynamic conditions are unfavorable for the formation of a mobile foam [11, 12], the suspended liquid layer is in the form of droplets, as was observed in a number of experiments by Kuz'minykh. Smirnov and U Tszin'-chen noted, for liquids not investigated by us, the same type of behavior in the transition from a bubbling to a foam regime as was found by us [13, 14]. They give the name of foam-emulsion regime to the foam regime. The effects of the principal process parameters - gas velocity and height of the original liquid layer - on the height of the foam layer were of the same character in their experiments as in ours [13].

As was stated in our earlier papers, the height of the foam layer on the grid determines the operating rate of the equipment and the tray efficiency, i.e., the ratio of the actual to the theoretically possible heat and mass transfer.

The purpose of the present investigation was generalization of experimental data in order to determine the influence of various parameters on the height of the foam layer and to derive the calculation formulas necessary for design and industrial operation of foam equipment.

The analysis of the experimental data was based on the criterial equation derived in the preceding paper [12]

$$H_{sp} = F_2 (Re_g, Re_l, We, \frac{v_g}{v_l}, \Gamma_1, \Gamma_2, \Gamma_3), \quad (1)$$

or

$$\frac{H}{h_0} = A \left(\frac{w_g \cdot D_e}{v_g} \right)^a \cdot \left(\frac{i}{v_l} \right)^b \cdot \left(\frac{\sigma}{\gamma_l h_0^2} \right)^c \cdot \left(\frac{v_g}{v_l} \right)^d \cdot \left(\frac{D_e}{h_0} \right)^e \cdot \left(\frac{m}{d_0} \right)^f \cdot \left(\frac{H_p \cdot b}{S_c} \right)^g, \quad (1a)$$

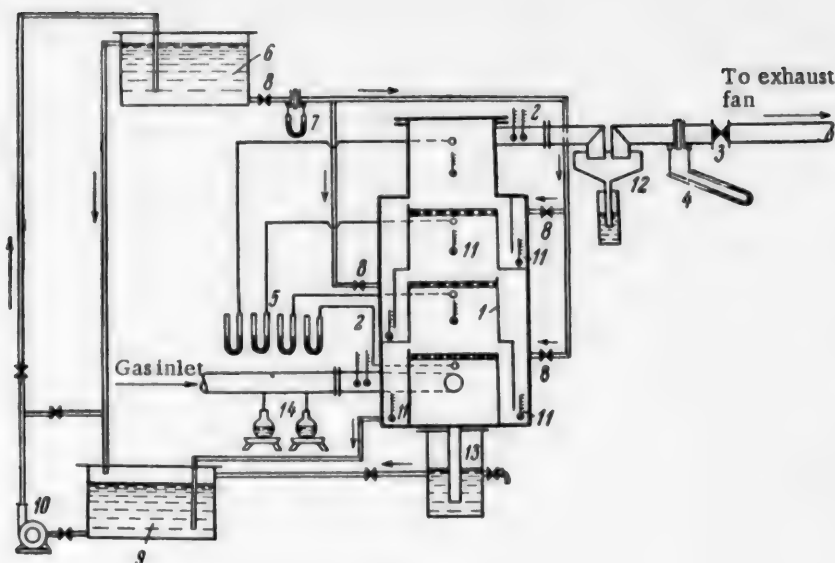


Fig. 1. Diagram of a three-tray foam apparatus.

1) Foam apparatus, 2) psychrometer, 3) slide valve for gas, 4) diaphragm with differential manometer, 5) manometers, 6) header tank, 7) flow meter, 8) liquid valves, 9) receiver tank, 10) pump, 11) thermometer, 12) spray trap, 13) overflow receiver, 14) vaporizers or gas sources.

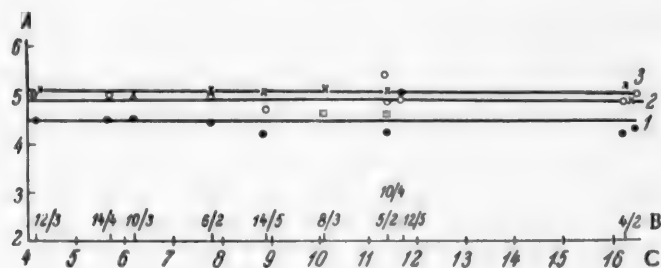


Fig. 2. Specific height of foam on grids with different orifice diameters d_0 and different orifice spacings m .

Noncirculating foam apparatus; air-20% NaCl solution; $h_0 = 0.02$ m.

A) Specific height of foam H/h_0 ; B) ratio m/d_0 ; C) open section S (%). Linear gas velocity w (in m/second): 1) 1.2, 2) 1.74, 3) 2.3.

which represents the functional relationship between the specific height of the foam layer and its determining parameters. The following notation is used:

$Re_g = \frac{w \cdot D_e}{\nu_g}$, the Reynolds criterion for the gas in the cross section of the apparatus; $Re_l = \frac{w_l \cdot h_0}{\nu_l}$, the Reynolds criterion for the liquid following along the grid; $We = \frac{\sigma}{\gamma_l h_0^2}$, the Weber criterion; $H_{sp} = \frac{H}{h_0}$, the specific height of the foam, equal to the ratio of foam volume to liquid volume; $\Gamma_1 = \frac{De}{h_0}$, a criterion representing the ratio of the height and length of the foam layer; $\Gamma_2 = \frac{m}{d_0}$, a criterion representing the open section of the grid; $\Gamma_3 = \frac{H_p \cdot b}{S_f}$, a criterion for overflow of the foam from the grid; A, a constant in

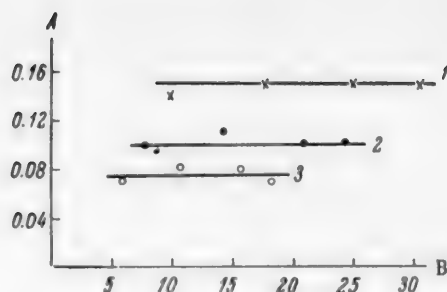


Fig. 3. Foam height at different gas velocities in the grid openings.

Three-tray circulating apparatus; air-water system; $l = 15 \text{ m}^3/\text{m} \cdot \text{hour}$; $h_f = 0$; grids: 12/4, 10/4, 8/4, 6/4.

A) Foam height (m), B) gas velocity in grid openings (m/second).

Gas velocity in apparatus (in m/second):

1) 2.5, 2) 2.0, 3) 1.5.

the equation; b , the width of the grid (in m), usually equal to the length of the overflow orifice b_f ; D_e , the equivalent diameter (in m); in the above expressions $D_e = 1.13 \text{ m}$; d_0 , the diameter of the orifice (in m); H , the height of the suspended liquid layer (mobile foam) (in m); H_p , the height of the foam layer above the center of the overflow orifice — the pressure head (in m); h_0 , the height of the original liquid layer from which the foam is formed on the grid (in m or mm); \bar{m} , the distance between the centers of the grid openings (in m); S_f , the area of the overflow orifice (in m^2); $w_{g,1}$, the linear velocity of the gas or liquid in the apparatus, with linear pulsations in the foam layer disregarded (in m/second); $\gamma_{g,1} = \rho g$, the specific gravity of the gas or liquid (in kg/m^3); $\nu_{g,1}$, the kinematic coefficient of viscosity of the gas or liquid (in m^2/second); σ , the coefficient of surface tension of the liquid at the gas interface (in kg/m).

Some of the experimental data in this paper are published for the first time. These experiments were also carried out in the equipment described in the earlier papers [11, 13, 16]. In illustration, Fig. 1 shows the design of a three-tray circulating foam apparatus used for most of the experiments on foam formation and on mass and heat transfer in mobile foam layers. It is clear from the diagram that the apparatus can operate with liquid feed not only to one tray, but to two or even three. Most of the experiments were performed with one tray in operation. Experiments were also performed with circulating single-tray units with grids of different types, fixed horizontally and at an angle to the flow of liquid. Several series of experiments were performed with noncirculating single-tray units, in which a definite amount of liquid was put on the grid, and during the course of the experiment enough liquid was added to compensate for the flow of liquid through the grid and entrainment in the gas in the form of vapor and spray.

In a study of the effects of the geometrical and physical parameters in Equation (1a) on the height of the foam layer it was found that, in foaming conditions and with equipment of sufficient size, the process is almost self-forming. The height of the mobile foam layer and its hydraulic resistance are almost independent of the geometrical dimensions, which many consider to be determining in bubbling conditions. A very important factor in model analysis of sieve equipment operating under foaming conditions is that, if loss of falling liquid is eliminated, foaming does not depend significantly on the diameter of the apparatus in the range 0.035 to 2.5 meters, on the distance h_g between the grids when $h_g > 400 \text{ mm} > H$, on the open section S of the grid in

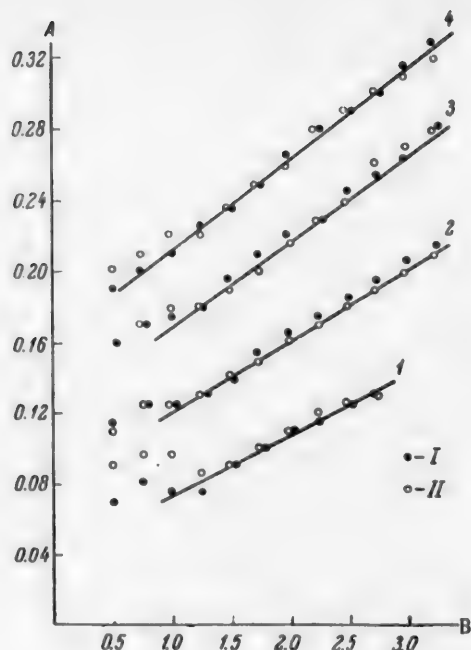


Fig. 4. Effect of gas velocity in the apparatus on the height of the foam layer.

Models of noncirculating apparatus; air-water system at 18° ; grids with $m/d_0 = 5/2$.

A) Foam height H (in m), B) gas velocity w_g in full section of the apparatus (in m/second).

Height of original liquid layer h_0 (in m): 1) 0.020, 2) 0.040, 3) 0.060, 4) 0.080.

Diameter of apparatus (in mm): I) 36, II) 86.

The straight lines represent calculated data.

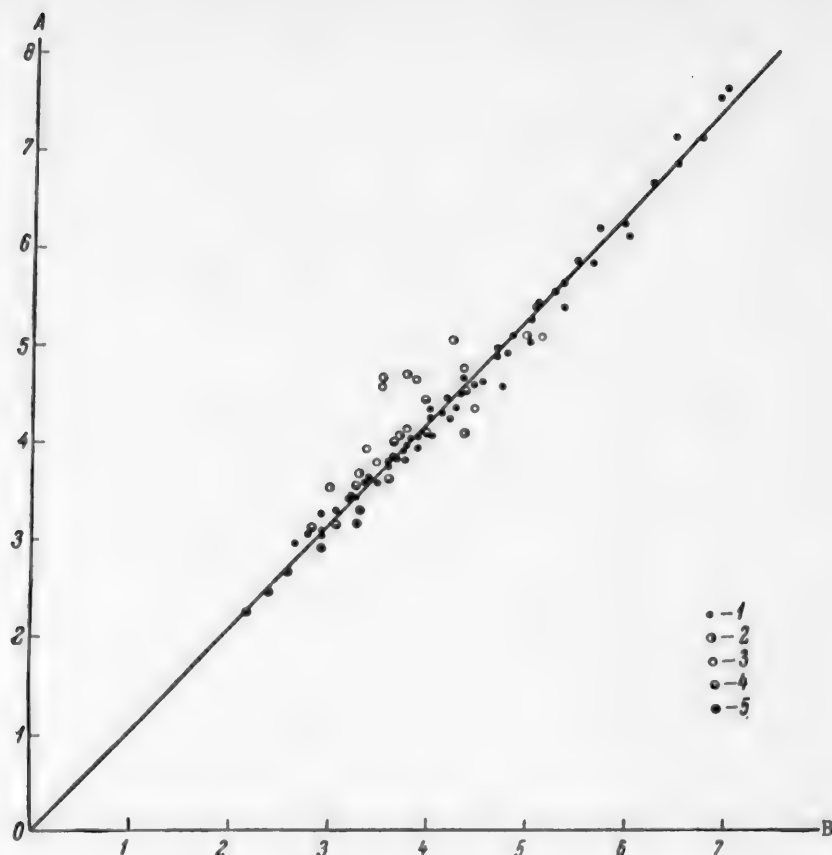


Fig. 5. Comparison of experimental and calculated values of the specific foam height in noncirculating equipment.

A) H/h_0 ratio (experimental data), B) the ratio $H/h_0 = A_1 \cdot Re^{0.5} \cdot We^{-1.3} \cdot N^{0.25} \cdot \Gamma^3$ (calculated).

1) Water, 2) filtration liquor from soda production, 3) solution of common salt, 4) glycerol solution, 5) sulfuric acid.

the range $S = 4-40\%$, or on the configuration and dimensions of the orifices within certain limits. The height of the foam layer on grids with round and slit openings is approximately the same. With round openings, the foam height H is approximately constant for opening diameters $d_0 = 3-8$ mm; this is illustrated by the experimental data in Fig. 2. With $d_0 < 3$ mm, H increases a little with decrease of d_0 .

Since

$$\frac{w}{w_0} = A \frac{d_0^3}{m^2}, \quad (2)$$

the fact that H is constant when \underline{m} and d_0 vary is equivalent to the fact that the foam height is independent of the gas velocity w_0 in the grid openings (Fig. 3). This is very important as it makes operation at low hydraulic resistances of the grid possible without adverse effects on the rate, whereas under bubbling conditions the operating rate of the equipment decreases with decrease of w_0 even if liquid is not lost by downflow.

It must be noted that the height of the foam may decrease greatly when the open section or orifice diameter are increased above a certain limit [11-13] owing to downflow of the liquid through the openings. It is this loss which limits the possibility of increasing the open section of the grid and the orifice diameter, and hence of decreasing the hydraulic resistance of the grid.

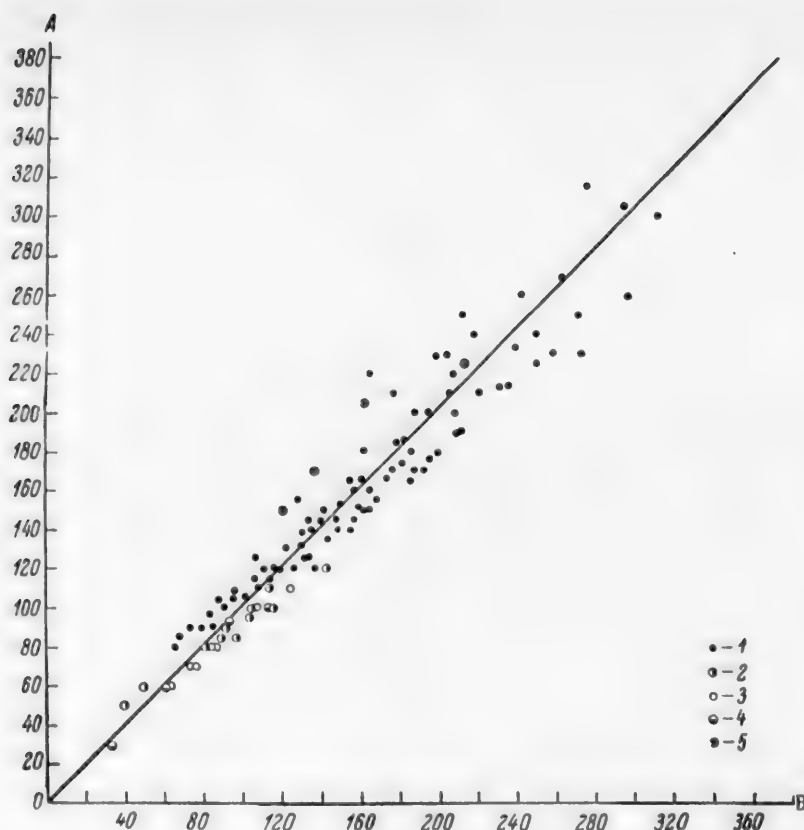


Fig. 6. Comparison of experimental and calculated values of foam height in circulating foam equipment.

A) Experimental values of $H \cdot 10^3$ (in m), B) calculated values of $H \cdot 10^3 = 6.2 \cdot 10^{-3}$.

$$\frac{h_i^{0.25} \cdot w_g^{0.5} \cdot H_p^{0.5}}{h_i^{0.3} \cdot v_e^{0.25} \cdot a_f^{1.3} \cdot 0.5} + h_f \quad (\text{in m}).$$

1) Water, 2) filtration liquor, 3) solution of common salt, 4) 75% sulfuric acid, 5) 98-100% sulfuric acid (Industrial plant).

The limits of existence of a suspended layer of mobile foam, and its height, are determined mainly by the gas velocity w_g in the apparatus, and the height h_0 of the liquid from which the foam is formed. This relationship is represented in Fig. 4 by an experimental graph which is typical for various gas-liquid systems on different grids. It follows from Fig. 4 that at gas velocities $w > 1.0-1.3$ m/second, corresponding to the foam regime, the relationship $H = f(w_g)$ is linear for all values of h_0 .

The departure from linearity in the regime of gas velocities $w_g < 1.0$ m/second, corresponding to bubbling and intermediate regimes [11, 12], can be attributed to the formation of cellular foam, which has low mobility (and is ineffective in relation to heat and mass transfer). With increase of gas velocity w_g above 1.0 m/second, the cellular foam is broken mechanically by the gas stream, and a suspended layer of finely divided mobile foam is formed [11, 12]. The gas content of the foam, bubble size, and turbulence increase with increasing w_g . Considerable spray loss begins at $w_g = 3$ m/second, while at $w_g > 3.5-4$ m/second it becomes difficult to recognize the boundary between the suspended layer and the stream of suspended liquid spray in the gas.

In addition to the effect of the gas velocity, Fig. 4 also illustrates the fact, noted above, that the height of the foam layer is independent of the diameter of the apparatus.

The influence of the gas velocity is represented in Equation (1) by Re_g ; h_0 enters into several criteria, and therefore its influence is considered after examination of the influence of other parameters. Suspended layers of liquid in gas, in the form of mobile foam, have a stable existence in water and electrolyte solutions, if h_0 is sufficiently large, in the range of Re_g from 80,000-100,000 to 260,000-280,000, according to the other conditions. The greater the height of the original liquid layer in the range h_0 from 5 to 100 mm, the wider is the range of gas velocities (and Re_g) in which a mobile foam exists. At $Re_g < 100,000$ transition begins from the mobile-foam regime to a bubbling regime. At $Re_g > 260,000$ the mobile-foam regime begins to pass into a flow of suspended spray in the gas.

The height of the foam layer H is proportional to the gas velocity w_g and the height of the original liquid layer h_0

$$H = \alpha w_g(h_0 + \beta) + \gamma h_0. \quad (3)$$

The coefficients α , β , and γ vary with the physical properties of the gas-liquid system, especially with the surface tension and viscosity of the liquids. These coefficients were determined empirically [13] for various conditions, i.e., calculation formulas of type (3) were derived for special cases. For example, Tarat derived the following equations for the air-water system at room temperature:

a) for h_0 from 8 to 60 mm:

$$H = 0.35 w_g (h_0 + 0.075) + 2h_0; \quad (3a)$$

b) for h_0 from 60 to 100 mm:

$$H = 0.1 w_g (h_0 + 0.42) + 2h_0, \quad (3b)$$

where H and h_0 are in meters, and w_g is in meters/second.

The physical properties of the liquid and gas have much less influence on the height of the gas-liquid layer under conditions of mobile foam than in the bubbling and intermediate regimes. They are represented in Equation (1) by the criteria Re_g , Re_l , We , ν_g/ν_l . It was found experimentally that within certain limits the specific gravity and viscosity of the gas have no significant influence on the foam height [11]. The height of the foam layer decreases rapidly with increase of the surface tension σ . The viscosity of the liquid ν_l has a dual effect on H . On the one hand, increase of ν_l increases friction between the liquid and the gas, which favors increase of H . In absence of friction, formation of a suspended layer due to the kinetic energy of the gas would be impossible. On the other hand, however, increase of the liquid viscosity hinders the stretching of its layers into very fine films of mobile foam. It was found by experiment that H decreases with increase of the viscosity of the liquid, i.e., the second aspect of the influence of ν_l prevails.

Experiments showed [11] that the chemical nature of the dissolved substance has no significant influence on foam formation: H remains approximately constant for solutions of salts; acids, and alkali of the same σ and ν_l .

The increase in the height of the layer of turbulent foam, produced by the action of surface-active substances, is a fraction of the increase produced in the height of cellular foam under bubbling conditions [13, 19, 20].

In the absorption of readily soluble gases in water and dilute solutions of the absorbed substances, the foam height is considerably less than in inert gas-water systems [13, 19]. The probable cause of this decrease of H is a change in the structure of the surface liquid layer which results in a decrease of its mechanical strength.

For calculation of the height of the foam layer in a given gas-liquid system, it is necessary to know the gas velocity and the height of the original layer of liquid. The gas velocity is easily measured, and is predetermined in equipment design. Determination of the height h_0 of the original liquid layer is more difficult. In noncirculating foam apparatus h_0 is calculated as the ratio of the volume of the liquid put in, to the cross section of the apparatus, with corrections for downflow of the liquid through the grid and entrainment with the gas. In circulating flow equipment the height h_0 of the original layer may depend on three parameters, namely: the height of the overflow weir h_f , the liquid rate l , and the foam pressure head H_p necessary to overcome the resistance

of the overflow orifice. This last factor [$h_0 = f(H_p)$] comes into operation when the cross section of the overflow orifice or pipe is inadequate for free overflow of the foam, and it is supported to an additional height. In equipment with external overflow, the height of the foam layer is then above the upper edge of the overflow orifice. These relationships have been considered in detail [11] for different types of apparatus under various conditions. Only the main principles relating to the influence of each of the parameters are discussed here.

The overflow weir supports a gas-liquid layer (foam in foam equipment), and not the liquid, as some workers assume. Therefore h_0 due to the weir is $\frac{1}{2}$ to $1/10$ of h_f (depending on w_g). A foam layer may be formed in absence of a weir, due to the liquid rate and support of the foam in the overflow orifice, or due to the liquid rate only if the foam flows freely from the grid, i.e., if it does not completely fill the overflow orifice. The height of the original layer due to the liquid rate, h_1 , is represented by the following empirical equation [13]:

$$h_1 = (3.15 - 0.005i) \sqrt[3]{i^2} \text{ mm}, \quad (4)$$

where the liquid rate i is in m^3 of liquid per hour per meter of the length of the overflow orifice (weir). The influence of i is represented in Equation (1) by Re_1 .

Support of the foam in the overflow orifice corresponds to accumulation of the liquid (and therefore increase of h_0) until the necessary pressure head H_p has been set up. For equipment with external overflow

$$H_p = H - h_f - 0.5a_f, \quad (5)$$

where a_f is the width (height) of the overflow orifice (in m).

For derivation of the calculation formulas, we analyzed [11] extensive experimental data by graphical methods and by statistical mathematics [21], and determined the coefficients and exponents of the criteria in Equation (1a). It proved possible to simplify the calculation formulas somewhat for various practical conditions.

- 1) For any gas-liquid system, both in noncirculating and in circulating equipment, with known h_0

$$\frac{H}{h_0} = A_1 \left(\frac{w_g \cdot D_e}{v_g} \right)^{0.5} \cdot \left(\frac{\sigma}{\gamma_1 \cdot h_0^2} \right)^{-1.3} \cdot \left(\frac{v_g}{v_1} \right)^{0.25} \cdot \left(\frac{D_e}{h_0} \right)^3, \quad (6)$$

where the coefficient

$$\begin{aligned} A_1 &= 2.83 \cdot 10^{-5} \cdot v_g^{0.25} \cdot \gamma_1^{-1.3} \\ \text{or} \\ H &= 4.35 \cdot 10^{-5} \frac{h_0^{0.6} \cdot w_g^{0.5}}{\sigma^{1.3} \cdot v_1^{0.25}} \text{ m} \end{aligned} \quad (6a)$$

For the system water-air at room temperature, and for other systems similar to it in physical properties, Equation (6a) assumes the simplified form:

$$H = 0.806 \cdot h_0^{0.6} \cdot w_g^{0.5}. \quad (6b)$$

- 2) For circulating equipment (if h_0 is not known)

$$H = A_2 \left(\frac{w_g \cdot D_e}{v_g} \right)^{0.5} \cdot \left(\frac{i}{v_1} \right)^{-0.25} \cdot \left(\frac{\sigma}{\gamma_1 \cdot h_1^2} \right)^{-1.3} \cdot \left(\frac{D_e}{h_1} \right)^{3.0} \cdot \left(\frac{H_p \cdot b}{S_f} \right)^{0.5} \cdot h_1 + h_f \text{ m} \quad (7)$$

where

$$A_2 = 3.62 \cdot 10^{-5} \cdot v_g^{0.5} \cdot \gamma_1^{-1.3}.$$

Equation (7) takes the following simplified forms:

a) for equipment with external overflow, with foam supported in the overflow orifice ($H > a_f + h_f$):

$$H = 6.2 \cdot 10^{-6} \frac{i^{0.25} \cdot w_g^{0.5} \cdot H_p^{0.5}}{h_l^{0.3} \cdot \sqrt{1}^{0.25} \cdot \sigma^{1.3} \cdot a_f^{0.5}} + h_f \text{ m}; \quad (7a)$$

b) for equipment with external overflow, with free overflow of foam ($H < a_f + h_f$):

$$H = 4.35 \cdot 10^{-8} \frac{h_l^{0.6} \cdot w_g^{0.5}}{\sigma^{1.3} \cdot \sqrt{1}^{0.25}} + h_f \text{ m}; \quad (7b)$$

c) for equipment with internal overflow:

$$H = 38.4 \cdot 10^{-12} \frac{i^{0.5} \cdot w_g}{h_l^{0.6} \cdot \sqrt{1}^{0.5} \cdot \sigma^{2.6} \cdot a_f} + h_f \text{ m}. \quad (7c)$$

These Equations (6,a,b, and 7,a,b,c) can be used for calculation of the suspended layer of mobile foam in sieve apparatus, without the need for experiments. The height of the foam determines the tray efficiency of the foam equipment in relation to mass or heat transfer.

Equations (6-7) can also be used for determination of the other values contained in them, with known H and under other defined conditions.

In the design of foam equipment, the unknown quantity in Equations (7) is usually h_f , as both a_f and H are determined previously from the coefficients of heat or mass transfer [11], w_g is fixed, ν and σ are found from tables, and h_l is calculated from Equation (4).

Comparison of calculated values of H with laboratory and plant experimental data, for noncirculating (Fig. 5) and circulating (Fig. 6) equipment showed that the agreement between the calculated and experimental values is quite acceptable for purposes of design calculations, over a wide range of conditions and for a great variety of gas-liquid systems. The calculated lines correspond to the average values of the experimental points.

SUMMARY

1. The height of the layer of mobile foam does not greatly depend on the geometrical parameters of the equipment over a wide range of conditions, i.e., the foaming process is almost self-forming. The height of the mobile foam is almost independent of the gas velocity in the grid openings if downflow of the liquid through the openings and spray entrainment are eliminated.
2. The limits of existence of a suspended layer of mobile foam, and its height, are mainly determined by the gas velocity in the apparatus and the height of the original liquid layer.
3. The physical properties of the liquid and gas have much less influence on the height of the gas-liquid layer under foam conditions than under the bubbling and intermediate regimes. The height of the foam decreases with increase of the surface tension and viscosity of the liquid.
4. Equations have been derived (5a, b - 7a, b, c) which can be used for calculation of the height of a suspended layer of mobile foam in sieve equipment without the need for experiments. The equations have been verified over a wide range of conditions.

LITERATURE CITED

- [1] V. N. Stabnikov, Chemical Machine Construction 6, 2, 14 (1937); 7, 1, 6 (1938); Trans. Voronezh Inst. Chem. Tech. 3-4, 177 and 197 (1939).
- [2] V. N. Stabnikov and S. E. Kharin, Theoretical Principles of the Distillation and Rectification of Alcohol (Food Industry Press, 1951).*

*In Russian.

- [3] E. Kirschbaum, Destillier-und Rektifiziertchnik, (Berlin, 1950).
- [4] K. N. Shabalin, Friction Between Gas and Liquid in Absorption Technology (Metallurgy Press, 1943).
- [5] N. M. Zhavoronkov and I. E. Furmer, Oxygen 5, 9 (1947).
- [6] J. A. Gerster, A. P. Colburn, W. E. Bonnet and T. W. Carmodi, Chem. Eng. Progr. 45, 12, 716 (1949).
- [7] L. S. Aksel'rod and G. M. Iusova, Oxygen 4, 1 (1950).
- [8] J. A. Gerster, W. E. Bonnet, J. Hess, Chem. Eng. Progr. 47, 10, 523; 12, 621 (1951).
- [9] M. B. Zelikin, J. Chem. Ind. 7, 215 (1953).
- [10] L. S. Aksel'rod and V. V. Dil'man, J. Chem. Ind. 1, 28 (1954).
- [11] I. P. Mukhlenov, Dissertation, the Lensoviet Technological Institute, Leningrad (1955).*
- [12] I. P. Mukhlenov, J. Appl. Chem. 30, 12, 1750 (1957).**
- [13] M. E. Pozin, I. P. Mukhlenov, E. S. Tumarkina and E. Ia. Tarat, The Foam Method for Treatment of Gases and Liquids (Goskhimizdat, 1955).
- [14] M. E. Pozin, I. P. Mukhlenova, E. S. Tumarkina and E. Ia. Tarat, J. Appl. Chem. 27, 1, 13 (1954).
- [15] M. E. Pozin, I. P. Mukhlenov and E. Ia. Tarat, J. Appl. Chem. 30, 1, 45 (1957).*
- [16] I. P. Mukhlenov and E. S. Tumarkina, J. Appl. Chem. 28, 2, 135; 4, 345 (1955).
- [17] I. N. Kuz'minykh et al., Trans. MKhTI, 18, 101 and 109 (1954); J. Appl. Chem. 4, 234 (1956).**
- [18] U Tszin'-chen, Author's summary of dissertation, Lensoviet Technol. Inst. Leningrad (1955).*
- [19] M. E. Pozin and E. S. Tumarkina, J. Appl. Chem. 27, 11, 1170 and 1180 (1954).
- [20] I. P. Mukhlenov and V. Ia. Demshin, J. Appl. Chem. 28, 1, 922 (1955).
- [21] K. P. Iakovlev, Mathematical Analysis of Experimental Data (GITTL, 1953).*

Received September 14, 1956

*In Russian.

**Original Russian pagination. See C. B. Translation.

THEORY OF ABSORPTION COMPLICATED BY AN EQUILIBRIUM CHEMICAL REACTION IN THE LIQUID PHASE

I. G. Pliit

The Dnepropetrovsk Institute of Chemical Technology

Theoretical investigations of the chemisorption process with reversible chemical reactions in the liquid phase were carried out a few years ago by Pozin [1] and Belopol'skii [2], the results being published almost simultaneously in this Journal.

Comparison of these publications shows that the mathematical interpretation of the physical nature of the process proposed by Belopol'skii is based on the assumption, improbable in general, that "... the main mass of the liquid is constantly at equilibrium with respect to the absorption reaction." On this assumption, his differential equation [2]

$$\frac{\partial^2 x}{\partial y^2} = \frac{K_c}{D_1} (x - x_e) \quad (1)$$

was integrated for the following boundary conditions:

$$\begin{aligned} y=0, \quad x &= x_l, \\ y=\delta_1, \quad x &= x_e, \end{aligned}$$

i.e., only for the case when the reaction zone in the absorption process is on the inner boundary of the liquid diffusion layer.

It is known, however, that the mechanism of chemisorption does not fit into any one scheme, and therefore the reaction zone does not always correspond to the above integration limits. Its position, as has been shown by Pozin, is determined in each particular case, on the one hand, by the rate constant K_r of the chemical reaction, and on the other, by the ratio of the diffusion coefficients of the gas in the liquid, D_1 , and in the chemically active part of the absorbent, D_2 . Figure 1 represents what is in our view a possible general scheme of the process for the conditions to which the differential Equation (1) corresponds. The concentration of the gas being absorbed varies in the limits of the gaseous diffusion layer δ_g from P to the equilibrium value P_1 . When the gas comes in contact with the liquid, a monomolecular layer at the interface is neutralized. After this, according to the relative values of K_r , D_1 , and D_2 , the reaction zone may remain on the surface, or move into the liquid diffusion layer δ_1 (as shown in Fig. 1) until a mobile equilibrium is established at which equivalent amounts of the absorbed gas and the chemically active part of the absorbent reached the reaction zone. In this case the reaction zone divides the diffusion layer into the neutralized part $\alpha \cdot \delta_1$ and the nonneutralized part $(1-\alpha)\delta_1$; the concentration of the dissolved gas in the neutralized part of the layer varies from x_1 at the phase boundary to the equilibrium concentration x_e in the reaction zone.

Let us consider the general solution of the problem. The differential Equation (1) is an inhomogeneous equation of the second order with a constant coefficient; putting $z = x - x_e$ and $\frac{K_c}{D_1} = R^2$, we have

$$\frac{\partial^2 z}{\partial y^2} = \frac{K_e}{D_1} \cdot z = R^2 \cdot z; \quad (2)$$

we seek a solution in the form of the function $z = A \cdot e^m$; by the condition (2)

$$A \cdot m^2 \cdot e^m = R^2 \cdot A \cdot e^m,$$

we find the characteristic equation $m^2 - R^2 = 0$, the roots of which are $m_1 = R$, and $m_2 = -R$, and consequently the general solution of differential Equation (2) is

$$z = A \cdot e^{R \cdot y} + B \cdot e^{-R \cdot y}.$$

Imposing the boundary conditions

$$y = 0, z = x_i - x_e,$$

$$y = a \cdot \delta_1 = \delta_0, z = 0,$$

on the general solution, we have:

$$A = \frac{(x_i - x_e) \cdot (e^{R \cdot \delta_0} - e^{-R \cdot \delta_0}) - (x_i - x_e) \cdot e^{R \cdot \delta_0}}{e^{R \cdot \delta_0} - e^{-R \cdot \delta_0}},$$

$$B = \frac{(x_i - x_e) \cdot e^{R \cdot \delta_0}}{e^{R \cdot \delta_0} - e^{-R \cdot \delta_0}},$$

$$z = \frac{(x_i - x_e) \cdot [e^{R \cdot (\delta_0 - y)} - e^{-R(\delta_0 - y)}]}{e^{R \cdot \delta_0} - e^{-R \cdot \delta_0}},$$

or

$$z = \frac{(x_i - x_e) \cdot Sh \cdot [R(\delta_0 - y)]}{Sh \cdot (R \cdot \delta_0)}$$

Substituting the value of z , we obtain an equation which represents the variation of the concentration of the dissolving gas in the neutralized part of the liquid diffusion layer:

$$x = x_e + \frac{(x_i - x_e) \cdot Sh \cdot [R(\delta_0 - y)]}{Sh \cdot (R \cdot \delta_0)}.$$

It will be remembered that the rate of absorption in the liquid film is equal to the diffusion current density at the interface

$$\frac{G}{F \cdot \tau} = -D_1 \frac{dx}{dy} \Big|_{y=0} \quad \text{or} \quad \frac{G}{F \cdot \tau} = \frac{R \cdot D_1}{th(R \cdot \delta_0)} (x_i - x_e). \quad (3)$$

Multiplying top and bottom of Equation (3) by δ_1 , we finally have

$$\begin{aligned} \frac{G}{F \cdot \tau} &= \frac{R \cdot \delta_1}{th(R \cdot \delta_0)} \cdot \frac{D_1}{\delta_1} (x_i - x_e) = \\ &= \frac{\delta_1 \cdot \sqrt{\frac{K_e}{D_1}}}{th\left(\frac{\delta_1}{\alpha \delta_1} \sqrt{\frac{K_e}{D_1}}\right)} \cdot \frac{D_1}{\delta_1} (x_i - x_e) = K_1 (x_i - x_e). \end{aligned} \quad (4)$$

The driving force in this kinetic equation is expressed as the concentration difference of the physically dissolved gas in the neutralized part of the film. The absorption coefficient is the product of two factors, one

2) The reaction zone is on the inner boundary of the film; $\alpha = 1$.

In this case the dimensionless parameter has its minimum value:

$$\beta_{\min} = \frac{\delta_1 \cdot \sqrt{\frac{K_e}{D_1}}}{th \left(\delta_1 \cdot \sqrt{\frac{K_e}{D_1}} \right)},$$

which depends only on the complex $\delta_1 \cdot \sqrt{\frac{K_e}{D_1}}$. The nature of this relationship is illustrated by the following values, found by analysis of the equation $\beta = \frac{a}{tha}$:

$a = \delta_1 \cdot \sqrt{\frac{K_e}{D_1}}$	0.01	0.04	0.08	0.10	0.15	0.18	0.2	0.3	0.4	0.5
β	1.00	1.00	1.00	1.00	1.00	1.00	1.01	1.02	1.05	1.08
$a = \delta_1 \cdot \sqrt{\frac{K_e}{D_1}}$	0.6	0.7	0.8	1.0	2	3	4	5	6	
β	1.11	1.15	1.20	1.3	2.05	3.00	4.00	5.00	6.00	

These values illustrate the existence of well-defined boundaries in the nature of the function β .

a) When $\delta_1 \sqrt{\frac{K_e}{D_1}} \leq 0.2$, the dimensionless parameter remains constant at almost all values of the term,

its value being unity. It follows that when the rate of chemical reaction is low or the diffusion film is thin, the absorption coefficient K_1 is equal to the coefficient for simple physical absorption, and the chemical reaction in the liquid phase has no significant influence on the rate of the process. The ordinary equation for simple physical absorption is suitable for calculations:

$$\frac{G}{F \cdot \tau} = \frac{x - x_e}{H/K_g - 1/K_1'}, \quad (6)$$

where $x = HP$ and H is the Henry constant.

b) In the range $\delta_1 \cdot \sqrt{\frac{K_e}{D_1}} = 0.2 - 2.0$, variations of the parameter β conform to a different characteristic law. In this range, known as the range of moderate reaction rates or moderate diffusion-film thicknesses, $\beta = 1.0-2.0$, and the process can be accelerated by nearly 100% as the result of chemical reaction; the numerical value of the dimensionless parameter is given by the equation

$$\beta = \frac{\delta_1 \cdot \sqrt{\frac{K_e}{D_1}}}{th \left(\delta_1 \cdot \sqrt{\frac{K_e}{D_1}} \right)},$$

and the rate of the process is

$$\frac{G}{F \cdot \tau} = \frac{x - x_e}{H/K_g + 1/\beta \cdot K_1'} \quad (7)$$

c) For values of $\delta_1 \cdot \sqrt{\frac{K_c}{D_1}} > 2.0$, which apparently corresponds to a high rate of reaction, the dimensionless parameter increases in proportion to the complex; this is represented in practice by the expression

$$\beta = \delta_1 \cdot \sqrt{\frac{K_c}{D_1}}.$$

The partial coefficient of absorption k_1 then becomes

$$K_1 = \beta \cdot K'_1 = \delta_1 \cdot \sqrt{\frac{K_c}{D_1}} \cdot \frac{D_1}{\delta_1} = \sqrt{K_c \cdot D_1},$$

and depends only on the chemical nature of the reacting substances. Combining this with the known partial equation for the gas film, we obtain the expression for the rate of the process

$$\frac{G}{F \cdot \tau} = \frac{x - x_e}{H/K_g + 1/\sqrt{K_c \cdot D_1}}.$$

3) The reaction zone is within the liquid diffusion layer, $1 > \alpha > 0$; in this case the rate of the process is given by the expression

$$\frac{G}{F \cdot \tau} = \frac{x - x_e}{H/K_g + 1/\beta \cdot K'_1},$$

here the dimensionless parameter is always greater than unity, and its value under constant conditions depends on α .

$$\beta = \frac{\delta_1 \cdot \sqrt{\frac{K_c}{D_1}}}{th\left(\alpha \delta_1 \cdot \sqrt{\frac{K_c}{D_1}}\right)}.$$

This dependence is illustrated by the

$\beta = \frac{a}{th(a)}$ curves in Fig. 2. It is seen that when $a = \delta_1 \cdot \sqrt{\frac{K_c}{D_1}} < 0.2$, β is almost independent of the absolute value of the complex, while at high values of a , β is independent of α .

On the other hand, since the position of the reaction zone depends on the ratio of D_1 to D_2 and on the corresponding concentration gradients across the film, the dimensionless parameter also depends on the concentration of the gas being absorbed and on the chemical capacity of the solution. This confirms, for the case in question, the peculiar feature of the scheme in that the absorption coefficient and therefore the rate of the process depends on the ratio of the concentrations of the reacting substances.

For kinetic calculations relating to the process, an equation is applicable in this case in which the driving force is represented as the difference of the solution capacities

$$\frac{G}{F \cdot \tau} = \frac{D_2}{(1 - \alpha) \cdot \delta_1} \cdot (c - c_0) = K_1 \cdot c.$$

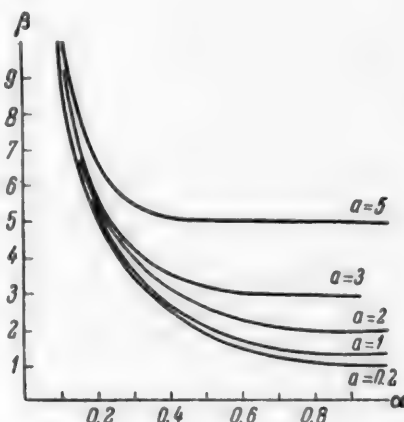


Fig. 2. Variation of the coefficient β with the parameter α , characterizing the position of the reaction zone.

In contrast to Equation (5), the absorption coefficient K_1 is determined in this case, under otherwise constant conditions, not only by the nature but also by the concentrations of the reactants.

Thus, the general solution of the differential equation confirms the existence of several chemisorption mechanisms, each of which corresponds to a definite range of the values of the complex $\delta_1 \sqrt{\frac{K_0}{D_1}}$ and of the coefficient α . There are five kinetic equations, each specific for one of these mechanisms.

This has been confirmed by the work of other investigators, and therefore Belopol'skii's conclusions must be regarded as particular cases.

LITERATURE CITED

- [1] M. E. Pozin, J. Appl. Chem. 19, 10-11 (1946); 19, 12 (1946).
- [2] A. P. Belopol'skii, J. Appl. Chem. 19, 10-11, 1181 (1946).

Received April 17, 1956

DESORPTION OF SOLVENTS FROM ACTIVATED CARBON BY MEANS OF INERT GASES *

N. D. Gorchakov and I. I. Pogodin

Laboratory of Sorption Technology, the Lenzoviet Technological Institute, Leningrad

A study of the desorption of ethyl alcohol and benzene from AR carbon by means of carbon dioxide and nitrogen was described in the preceding communications [1-3].

The present communication deals with the desorption of ethyl alcohol, ethyl ether - ethyl alcohol mixture, butyl alcohol, ethyl acetate, and gasoline from AR carbon by means of carbon dioxide.

EXPERIMENTAL

The procedure and equipment used for saturation were similar to those described for the experiments on the desorption of ethyl alcohol [2]. The earlier work on the desorption of ethyl alcohol showed that the most effective method of desorption is by operation of the apparatus on closed cycle. Therefore all the subsequent investigations of the desorption of solvents were carried out by this method only, without the use of a deep-cooling condenser.

AR carbon of the same grain size was used for the experiments. The length of the carbon layer was 100 cm, and the cross section 7 cm². The flow rate of the vapor-gas mixture was 2 liters/cm² · minute.

Breakthrough of the solvents was indicated by means of the electrical gas-analysis instrument designed by Sokolov and Gorchakov.

Effect of the temperature of the carbon on the degree of desorption of solvents. The desorption of solvents from carbon heated to various temperatures was studied with carbon dioxide circulated at 0.5 liter/cm² · minute, and with desorption time 10 minutes.

The data on the effects of the temperature of the carbon on the desorption of solvents are given in Table 1.

These results show that the temperature of the carbon has a great influence on desorption of solvents. For example, at 125° only 8.2% of the ether adsorbed by the carbon was desorbed; at 250° under the same conditions the desorption was 71.4%. The amount of ethyl ether condensed in the water-cooled condenser was 6.8% of the ether adsorbed by the carbon in the first case, and 69.0% in the second.

These results show that AR carbon has a high retentive capacity for ethyl ether.

The boiling point and refractive index of the condensate were close to the values for the original ether. Thus the boiling point of the original ether was 34.8-35°, $D_{20}^{20} = 1.3530$, and the boiling point of the desorbed condensate was 34.5-35.5°, $D_{20}^{20} = 1.3535$. No ethyl peroxide was detected in the condensate. The results therefore show that the optimum temperature of the carbon in desorption is 250°. The experimental results show that the desorption of alcohol-ether mixture also depends to a considerable extent on the temperature of the carbon. For example, 52.4% of the total amount of alcohol-ether mixture adsorbed by the carbon was desorbed when the carbon was heated to 150°, while at 250° 81.6% was desorbed. 51.9% of the alcohol-ether mixture was condensed in the water-cooled condenser in the first case, and 81.04% in the second. These experimental results suggest that the optimum temperature for desorption of alcohol-ether mixture is 250°. The composition of the alcohol-ether mixture (in %) was 88.95 alcohol and 11.05 ether at 150°, and 64.7 alcohol and 35.3 ether at 250°; i.e., with

*Communication V.

TABLE 1

Effect of Carbon Temperature on Desorption of Solvents

Temperature of carbon in desorption (°C)	Amount condensed (%)	Losses in system (%)	Amount desorbed (%)	Retained in carbon (%)	Temperature of carbon in desorption (°C)	Amount condensed (%)	Losses in system (%)	Amount desorbed (%)	Retained in carbon (%)
Desorption of ethyl ether					200	51.47	0.78	52.2	47.8
125	6.9	1.3	8.2	91.8	220	53.61	0.69	54.3	45.7
150	27.2	2.0	29.2	70.8	250	57.8	0.7	58.5	41.5
175	42.9	2.1	45.0	55.0	Desorption of ethyl acetate				
180	44.7	2.3	47.0	53.0	130	40.7	0.3	41.0	59.0
250	69.0	2.4	71.4	28.6	150	46.7	0.3	47.0	53.0
Desorption of alcohol-ether mixture					180	68.52	0.28	68.8	31.2
150	51.9	0.5	52.4	47.6	250	90.9	0.3	91.2	8.8
180	65.75	0.45	66.2	33.8	Desorption of gasoline				
250	81.04	0.56	81.6	18.4	150	26.95	0.35	27.3	72.7
Desorption of butyl alcohol					180	47.88	0.32	48.2	51.8
130	26.6	0.5	27.1	72.9	250	67.33	0.37	67.7	32.3
160	37.3	0.7	38.0	62.0	280	68.11	0.39	68.5	31.5
180	44.7	0.7	45.4	54.6					

TABLE 2

Effect of the Circulation Rate of Carbon Dioxide on the Desorption of Solvents from AR Carbon

Circulation rate of carbon dioxide (liters/cm ² ·min)	Amount condensed (%)	Losses in system (%)	Total amount desorbed (%)	Remained in carbon (%)	Circulation rate of carbon dioxide (liters/cm ² ·min)	Amount condensed (%)	Losses in system (%)	Total amount desorbed (%)	Remained in carbon (%)
Ethyl ether					1.0	78.1	0.8	78.9	21.1
0.25	70.0	1.3	71.3	28.7	1.5	78.2	1.0	79.2	20.8
0.5	69.0	2.4	71.4	28.6	Ethyl acetate				
1.0	68.6	3.2	71.8	28.2	0.25	88.77	0.23	89.0	11.0
Alcohol-ether mixture					0.5	90.9	0.3	91.2	8.8
0.25	81.2	0.3	81.5	18.5	1.0	90.7	0.8	91.50	8.5
0.5	81.04	0.56	81.6	18.4	Gasoline				
1.0	80.90	1.3	82.2	17.8	0.25	66.23	0.27	66.5	33.5
Butyl alcohol					0.5	67.33	0.37	67.7	32.3
0.5	57.8	0.7	58.5	41.5	1.0	76.40	0.8	77.2	22.8
					1.5	76.3	1.2	77.5	22.5

Increase of the carbon temperature the amount of ether in the mixture increases, and the relative alcohol content decreases. This shows that the retentive power of the carbon is considerably higher for ether than for alcohol. The temperature of the carbon has a great influence on the desorption of butyl alcohol. Thus, 27.1% of the alcohol adsorbed by the coal was desorbed at 130°, and 58.5% was desorbed at 250°. The degree of condensation of butyl alcohol in the condenser was very high; the values for the desorption and condensation almost coincided.

TABLE 3

Results of Experiments on Determination of the Optimum Desorption Time for Different Solvents

Desorption time (min)	Amount condensed (%)	Losses in system (%)	Total amount desorbed (%)	Remained in carbon (%)	Desorption time (min)	Amount condensed (%)	Losses in system (%)	Total amount desorbed (%)	Remained in carbon (%)
Ethyl ether					15	78.1	0.80	78.9	21.1
10	70.0	1.3	71.3	28.7	20	80.7	0.80	81.5	18.5
15	70.0	1.8	71.8	28.0	30	80.9	0.90	81.8	18.2
20	70.1	2.1	72.2	27.8	Ethyl acetate				
Alcohol - ether mixture					10	90.00	0.3	90.3	9.7
10	81.18	0.5	81.68	18.32	15	90.9	0.3	91.2	8.8
15	81.14	0.6	81.74	18.36	20	90.8	0.5	91.3	8.7
20	81.1	0.7	81.80	18.2	Gasoline				
Butyl alcohol					10	75.2	0.8	76.0	24.0
10	74.55	0.75	75.3	24.7	15	76.40	0.8	77.2	22.8
					20	76.37	0.93	77.3	22.7

TABLE 4

Results of Experiments on the Desorption of Solvents Under the Optimum Conditions

Amount condensed (%)	Losses in system (%)	Total amount desorbed (%)	Remained in carbon (%)	Operating cycle of carbon layer	Amount condensed (%)	Losses in system (%)	Total amount desorbed (%)	Remained in carbon (%)	Operating cycle of carbon layer
Ethyl ether					98.7	0.8	99.5	0.5	3
70.1	0.1	72.2	27.8	1	99.3	0.8	100.1	—	4
98.6	1.6	100.2	—	2	100.28	0.9	101.08	—	5
70.0	1.5	71.5	28.5	1	Ethyl acetate				
98.9	1.4	100.3	—	2	90.8	0.5	91.3	8.7	1
99.03	1.35	100.4	—	3	100.1	0.3	100.4	—	2
98.14	1.36	99.5	0.5	4	98.32	0.28	98.6	1.4	3
Alcohol-ether mixture					99.87	0.33	100.2	—	4
81.1	0.7	81.80	18.2	1	99.9	0.3	100.2	—	5
99.5	0.3	99.8	0.2	2	99.4	0.3	99.7	0.3	6
99.7	0.4	100.1	—	3	Gasoline				
99.4	0.3	99.7	0.3	4	76.37	0.93	77.3	22.7	1
100.1	0.3	100.4	—	5	98.5	0.8	99.3	0.7	2
Butyl alcohol					99.56	0.74	100.3	—	3
80.7	0.8	81.5	18.5	1	99.01	0.69	99.7	0.3	4
103.0	0.8	103.8	—	2	99.24	0.71	100.05	—	5

Of the temperatures studied, the greatest desorption of butyl alcohol took place at 250°.

Analysis of the condensate showed that the butyl alcohol did not undergo any chemical changes during desorption from carbon by means of carbon dioxide. The desorption of ethyl acetate from carbon increases

rapidly with increase of temperature. Thus, 41% of the ethyl acetate adsorbed by the carbon at saturation was desorbed at 130°, whereas at 250° 91.2% of the ethyl acetate was desorbed under the same conditions.

If the carbon temperature is increased further, up to 0.9% of aldehydes is formed in the desorbed ethyl acetate by the catalytic action of the carbon. Therefore 250° was chosen as the optimum temperature of the carbon in desorption.

The experiments show that the desorption of gasoline from carbon greatly depends on the temperature to which the carbon is heated. Thus, only 27.3% of the gasoline adsorbed by the carbon was desorbed at 150°, whereas the desorption of gasoline reached 67.7% at 250°. This indicates the higher retaining power of AR carbon for gasoline. Further increase of the carbon temperature to 280° results in greater desorption of gasoline. Therefore the optimum temperature of the carbon is 250°.

Effect of the circulation rate of carbon dioxide on the desorption of solvents from AR carbon. To study the effect of the circulation rate of carbon dioxide on the desorption of solvents from carbon, experiments were carried out at circulation rates of 0.25, 0.5, 1, and 1.5 liters/cm² · minute, with the carbon heated to 250°. The results of these experiments are given in Table 2. It follows from these results that the circulation rate of the carbon dioxide has very little influence on the total desorption of ether, alcohol-ether mixture, or ethyl acetate. For example, the total amount of ether desorbed at 0.25 liter/cm² · minute was 71.3% of the amount adsorbed by the carbon, and when the rate was increased to 1 liter/cm² · minute, the desorption was only 71.8%.

The optimum circulation rate of carbon dioxide for the desorption of these solvents was taken to be 0.25 liter/cm² · minute. Variations of the circulation rate of carbon dioxide have a great influence on the desorption of butyl alcohol. For example, 58.5% of the adsorbed butyl alcohol was desorbed at $v = 0.5$ liter/cm² · minute, and 78.9% at $v = 1.0$ liter/cm² · minute. Increase of the carbon dioxide rate above 1.0 liter/cm² · minute does not have as much effect on the desorption of butyl alcohol. These experimental results suggest that the optimum circulation rate of carbon dioxide in the desorption of butyl alcohol is 1.0 liter/cm² · minute.

It was found that increase of the circulation rate of carbon dioxide to 1.0 liter/cm² · minute has a strong influence on the desorption of gasoline from carbon. Increase of the rate above 1.0 liter/cm² · minute has very little effect. The greatest amount of gasoline is desorbed at carbon dioxide rate $v = 1.0$ liter/cm² · minutes.

To determine the optimum time of desorption of the solvents, experiments were carried out with carbon dioxide circulated for 10, 15, 20, and 30 minutes, at the optimum circulation rates of 0.25 and 1.0 liter/cm² · minute. The carbon was heated to 250° in all cases.

The results of these experiments are given in Table 3.

These results show that increase of the desorption time does not have any significant influence on the degree of desorption of ethyl alcohol, alcohol-ether mixture, or ethyl acetate. Therefore 10 minutes is taken as the optimum time of desorption. The results of experiments on the desorption of butyl alcohol show that the total amount desorbed increases considerably with the time of desorption. Thus, 75.3% of the butyl alcohol adsorbed on the carbon was desorbed in 10 minutes, and 74.5% was condensed; in 20 minutes 81.5% was desorbed and 80.7% condensed. The desorption of butyl alcohol increased little with increase of the desorption time to 30 minutes; the value was 81.8% of the amount adsorbed on the carbon. The optimum time for the desorption of butyl alcohol is therefore 20 minutes. The experimental results show that increase of the desorption time over the range studied has very little effect on the desorption of gasoline. Thus, 76% of the adsorbed benzene was desorbed in 10 minutes, 77.2% in 15 minutes, and 77.8% in 20 minutes. These results suggest that 15 minutes should be taken as the optimum time for the desorption of gasoline.

Investigation of the desorption of solvents under optimum conditions with continuous operation of the carbon layer. The sorption and desorption of solvents on AR carbon were studied under the optimum desorption conditions, i.e., carbon temperature 250°, desorption times 10, 15, and 20 minutes, and carbon dioxide rates 0.25 and 1.0 liter/cm² · minute, with continuous operation of the carbon layer, in which after the first desorption the carbon was again saturated with solvent vapor and the desorption was repeated. The experimental results are given in Table 4.

The results show that in repeated cycles of operation of the same carbon the total desorption of the solvents reaches 90-100% of the amounts adsorbed by the carbon in the repeated saturations.

From 98 to 100% of the solvents was condensed in the water-cooled condenser.

For ether, alcohol-ether mixture, and butyl alcohol, the gravimetric dynamic activity of the carbon decreased by 2-3% after the first cycle.

The dynamic activity of the carbon for ethyl acetate decreased in all subsequent cycles by 1-1.5% as compared with the first cycle.

It follows from the experimental data in Table 4 that in the first cycle the total amount of desorbed gasoline was 77.3%, and the residual amount in the carbon 22.7%, or 4% on the weight of the carbon.

In subsequent cycles with the same carbon the total gasoline desorbed was about 100% of the gasoline adsorbed during the subsequent saturations.

The amount of gasoline condensed in the condenser was 98-99%. The residual gasoline in the carbon was almost constant the whole time, the amount being equal to the amount after the 1st cycle. In the subsequent cycles the dynamic activity of the carbon decreased by 3-4% in comparison with the 1st cycle, i.e., the dynamic activity of the carbon fell from 21% to 17-18% in continuous operation.

SUMMARY

1. In studies of the desorption of ethyl ether, alcohol-ether mixture, butyl alcohol, gasoline, and ethyl acetate from AR carbon in carbon dioxide, with carbon temperatures from 125 to 280°, circulation rate of the inert gas from 0.25 to 1.5 liters/cm²·minute, and desorption time from 10 to 20 minutes it was found that the optimum temperature of the carbon for desorption is 250°.

2. The optimum circulation rate of carbon dioxide is 0.25 liter/cm²·minute in the desorption of ethyl ether, alcohol-ether mixture, and ethyl acetate, and 1.0 liter/cm²·minute in the desorption of gasoline and butyl alcohol.

3. The optimum desorption times are 10 minutes for ethyl ether, ethyl ether-alcohol mixture, and ethyl acetate; 20 minutes for butyl alcohol, and 15 minutes for gasoline.

4. In a study of the desorption of solvents in continuous operation of a 100-cm layer of carbon it was found that desorption with 100% recovery is possible, with only a slight decrease of the initial activity of the carbon.

LITERATURE CITED

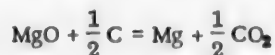
- [1] N. D. Gorchakov and I. I. Pogodin, J. Appl. Chem, 28, 7-8 (1945).
- [2] N. D. Gorchakov and I. I. Pogodin, J. Appl. Chem, 28, 9 (1945).
- [3] N. D. Gorchakov and S. Z. Vaniushina, J. Appl. Chem, 29, 1 (1946).

Received (for the second time) June 4, 1957

EQUILIBRIUM POTENTIALS OF CALCIUM OXIDE - CARBON ELECTRODES

M. V. Smirnov, S. F. Pal'guev, Iu. N. Krasnov and L. A. Liapina

Baimakov [1] states that in the electrolytic production of magnesium from chloride baths with the use of Dolgov's soluble anode the back e.m.f. is 1.7-1.8 v. This corresponds to the free-energy change of the reaction



at the temperature of electrolysis. Consequently, the cell



is an equilibrium galvanic cell.

The potentials of oxide-carbon electrodes in chloride melts are more negative than the potential of the chlorine electrode (carbon electrode in contact with pure chlorine in the melt). Thus, the potential of calcium oxide-carbon electrodes, consisting of an intimate mixture of calcium oxide and carbon, in fused chlorides is about 2 v on the negative side of the potential of the chlorine electrode. Therefore at equilibrium the pressure of the chlorine adsorbed on them should be negligibly small (of the order of 10^{-19} atmospheres for calcium oxide-carbon electrodes).

The potentials of oxide-carbon electrodes are most probably determined by the concentrations (activities) of the corresponding metals in the melts. To confirm this hypothesis, we determined the equilibrium potentials of calcium oxide-carbon electrodes in fused chlorides with different concentrations (activities) of calcium ions.

EXPERIMENTAL

Method for the measurement of equilibrium potentials of oxide-carbon electrodes

In determinations of the equilibrium potentials of oxide-carbon electrodes, special care must be taken to avoid access of chlorine to them. The oxide-carbon electrode in chloride melts must be reversible with respect both to metal ions and to chloride ions. This means that when the equilibrium value of the electrode potential has been reached, a strictly definite ratio must become established between the activity of the metal ions in the melt and the activity of the chlorine adsorbed on the electrode, represented by the equation

$$E_{\text{Me}}^0 + \frac{RT}{nF} \ln a_{\text{Me}^{n+}} = \text{const} + \frac{RT}{2F} \ln a_{\text{Cl}_2},$$

when the activity of chloride ions in the melt remains constant.

If chlorine reaches the oxide-carbon electrode for any reason, its potential will not be at its equilibrium value. In this case its value is determined by the activity of the chlorine adsorbed on the electrode, and this in turn depends on the ratio between the rate of access of chlorine to the electrode and the rate of its consumption in the chemical reaction of chlorination of the metal oxide. If chlorine enters continuously and at an approximately constant rate, the electrode potential may reach a definite value which changes little with time. However, this is not the value of the equilibrium potential, but a certain steady-state value above the equilibrium value.

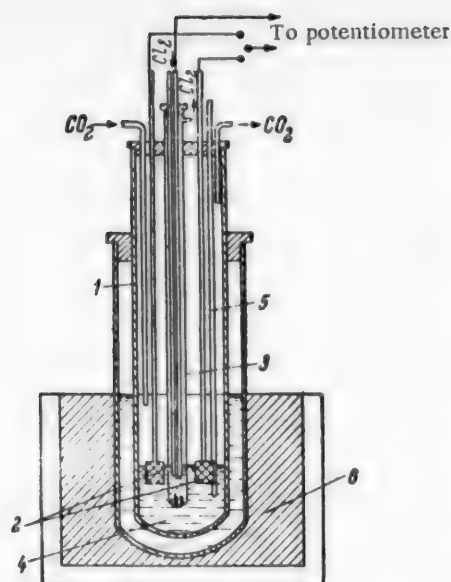


Fig. 1. Cell for measurement of equilibrium potentials of calcium oxide-carbon electrodes. 1) Quartz test tube, 2) oxide-carbon electrodes, 3) chlorine electrode, 4) fused electrolyte, 5) thermocouple, 6) thermostat.

If the concentration of calcium chloride was not high, the determinations could be carried out directly in the quartz test tube. At high concentrations of calcium chloride there was appreciable interaction between the quartz and the melt. The determinations of such melts were therefore carried out in alundum crucibles placed in the quartz test tube. The chlorine electrode was then contained in an alundum tube, the end of which was pressed against the bottom of the crucible and covered with oxide-carbon crumbs, and over this with finely divided alundum.

The electrolyte consisted of a mixture of the chlorides of sodium, potassium, and calcium. The determinations were carried out at different concentrations of calcium in the melt, a separate cell being used for each concentration. The concentration was varied in different experiments from 0.37 wt. % to pure fused calcium chloride. During the determinations, carbon dioxide carefully freed from moisture and oxygen was passed very slowly into the cell.

The oxide-carbon electrodes were prepared by a method described in one of our papers. The carbon source used was not sugar, but coal-tar pitch, as this completely eliminated the operations involved in treatment of the oxide with aqueous sugar solution. This was permissible, as calcium oxide is one of the most electronegative in the potential series of oxide-carbon electrodes in chloride melts.

The molar ratio of oxide to carbon in the electrodes was deliberately varied from the stoichiometric ratio required to combine the oxygen in the form of carbon dioxide, to a ten-fold excess of carbon, in order to determine whether this ratio has any influence on the electrode potential. From 2 to 5 electrodes with different molar ratios of oxide to carbon were placed in the cell simultaneously for the determinations.

The cell e.m.f. (the potential difference between the chlorine and the oxide-carbon electrodes) was measured by means of the PPTV-1 high-resistance potentiometer. The cell was contained in a thermostat heated in an electric furnace with automatic control of temperature, which was maintained constant at $800 \pm 2.5^\circ$ in all the experiments.

Special experiments were carried out in order to determine the role played by carbon dioxide in the electrode reaction which leads to establishment of the equilibrium potential. Two oxide-carbon electrodes made by the usual method were taken. They were heated for 5-8 hours at 800° under vacuum (a few tenths of

It is known [2] that chlorine dissolves in fused chlorides. Therefore it can penetrate to oxide-carbon electrodes even when the latter are not in contact with the gas space of the cell containing chlorine. The electrolyte acts as the carrier. For this reason it might be advisable to abandon the use of the chlorine electrode and to use, for example, a lead electrode as the reference electrode. However, it has been shown by us [3] and others that the chlorine electrode is the most suitable for accurate determinations. Its potential is stable in time, and reproducible to a few tenths of one mv.

It was shown by numerous experiments that chlorine dissolved in the melt is vigorously absorbed by crumbled mass made from calcium oxide-carbon electrodes. This material was used as a reliable diaphragm for preventing the penetration of chlorine into the section of the cell containing the oxide-carbon electrode.

A second possible source of error may be chlorine formed in the melt by decomposition of the latter by atmospheric oxygen which penetrates into the cell. Therefore the cell should be adequately air-tight.

The cell used for measurement of the equilibrium potentials of oxide-carbon electrodes is represented schematically in Fig. 1.

of a millimeter), and then kept for a long time in a current of argon-carbon dioxide mixture (the gases were thoroughly purified to remove traces of moisture and oxygen). One electrode was treated with a mixture containing 5.8 volume % of carbon dioxide, and the other with a mixture containing 8.2 volume % CO_2 . The electrodes were then quickly transferred into cells containing previously-prepared electrolyte (a fused equimolar mixture of sodium and potassium chlorides, containing 1% of calcium chloride by weight), and the same mixtures of argon and carbon dioxide were passed around them until the potentials became constant. Gas mixtures of different composition, with higher contents of carbon dioxide, were passed into the cells until the potentials became constant. These measurements were repeated with several gas mixtures in which the content of carbon dioxide was progressively increased. The temperature was kept constant at $800 \pm 2.5^\circ$ in all the experiments.

RESULTS AND DISCUSSION

The potentials of the oxide-carbon electrodes reached constant values rather slowly (during several hours) in all the experiments; this is seen in Fig. 2, which gives the results obtained in the determination of potentials of two electrodes greatly differing in their molar ratios of oxide to carbon.

The experiments showed that the molar ratios of oxide to carbon in the electrodes only have an influence while the potentials are becoming established, and have hardly any effect on the equilibrium values. It should be noted that the potentials of the oxide-carbon electrodes become established more slowly with decrease of temperature, and the individual characteristics of different electrodes are then more prominent. This is probably because of the different conditions in which the equilibrium ratios of the activities of the adsorbed chlorine and of the metal ions in the melt are reached on different electrodes. Moreover, equilibrium with respect to oxygen is established differently in these systems.

The results of determinations of the equilibrium potentials of calcium oxide-carbon electrodes in fused equimolar mixtures of sodium and potassium chlorides containing different amounts of calcium chloride are given in Fig. 3. The dash line in this diagram shows the variations of the cell e.m.f. which should occur if the melts behaved as ideal solutions, up to pure fused calcium chloride.

It is seen that the experimental and the ideal e.m.f. isotherms coincide when the calcium chloride concentration in the melt is below 16.5% by weight (when the mole fraction of calcium in the melt is less than 0.05). At higher concentrations the experimental isotherm deviates fairly sharply from the ideal; this shows that the activity coefficient of calcium chloride in the melt becomes greater than unity ($f_{\text{Ca}^{++}} \cdot f_{\text{Cl}^-}^2 > 1$).

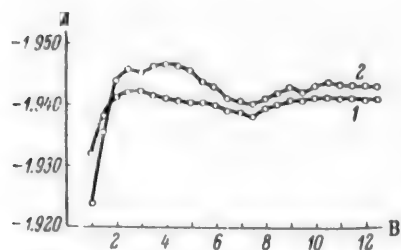


Fig. 2. Establishment of equilibrium potentials of calcium oxide-carbon electrodes in chloride melts (temperature 800° , calcium chloride concentration in melt 5% by weight). A) Electrode potential (v), B) time (hours). 1) Electrode with two-fold excess of carbon, 2) electrode with ten-fold excess of carbon.

In melts with low concentrations of calcium chloride the activity of chloride ions can be regarded as constant without any serious error, and the observed change in the cell e.m.f. must be attributed to changes in the potential of the oxide-carbon electrodes. The slope of the experimental isotherm is 0.106. This coincides

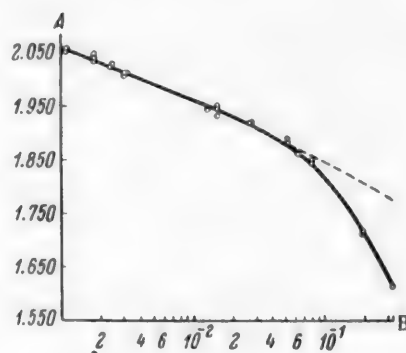


Fig. 3. Isotherm for the e.m.f. of a cell with chlorine and oxide-carbon electrodes in a melt containing sodium, potassium, and calcium chlorides at 800° . A) E. m.f. of cell with chlorine and oxide-carbon electrodes, B) mole fraction of calcium in melt.

with the theoretical value of the coefficient in the thermodynamic equation for the equilibrium potential of calcium oxide-carbon electrodes

$$E = E_0 + \frac{2.3RT}{2F} \log [Ca^{++}]_{\text{melt}},$$

where $\frac{2.3RT}{2F} = 0.106$ at 800° . Therefore at low concentrations of calcium chloride the melts behave like ideal solutions, and oxide-carbon electrodes like metallic electrodes.

The potentials of the oxide-carbon electrodes were unstable in pure fused calcium chloride. At first they reached constant values, and then fell fairly rapidly (the cell e.m.f. rose rapidly). When the surface layer was removed from the electrodes, which were not taken out of the melt, the potential returned to approximately the same value, 1.6 v on the negative side of the potential of the chlorine electrode. The probable cause of this instability of the potential of oxide-carbon electrodes in pure fused calcium chloride is the formation of oxy-chloride, which is insoluble in the melt and interrupts contact between the oxide-carbon mixture and the electrolyte.

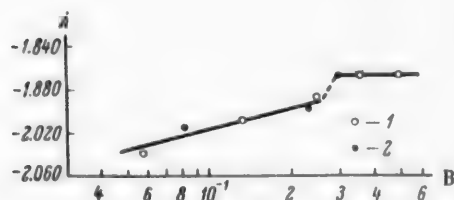


Fig. 4. Variation of the equilibrium potentials of calcium oxide-carbon electrodes with the partial pressure of carbon dioxide in the cell. A) Potential relative to the chlorine electrode, B) partial pressure of CO_2 (in atm). 1) First electrode, 2) second electrode.

The results of the experiments carried out to determine the role of carbon dioxide in the electrode reaction are given in Fig. 4 in the form of a graph, the potentials of the oxide-carbon electrodes being plotted against the partial pressure of carbon dioxide in the cell, in semi-logarithmic coordinates.

If the pressure of carbon dioxide in the cell does not exceed 0.25 atmosphere, the electrode potential is proportional to the logarithm of the pressure

$$E = \text{const} + 0.058 \log P_{CO_2}.$$

The coefficient of the logarithm is close to the theoretical value of $\frac{2.3RT}{4F}$ in the thermodynamic equation

$$E = E_0 + \frac{2.3RT}{4F} \log P_{CO_2},$$

which is 0.055 at 800° . Therefore the equilibrium potential of the calcium oxide-carbon electrode is determined by the electrode reaction

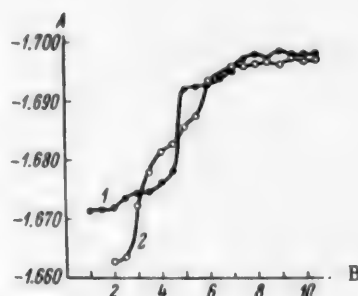


Fig. 5. Establishment of equilibrium potentials of oxide-carbon and mixed oxide-carbonate-carbon electrodes (temperature 800° , concentration of calcium chloride in melt 60% by weight). A) Electrode potential (v), B) time (hours). 1) Oxide-carbon electrode, 2) oxide-carbonate-carbon electrode.

When the partial pressure of carbon dioxide in the cell exceeded 0.25 atm, the e.m.f. isotherm increased abruptly, and the electrode potential ceased to vary with further increase of pressure. This is probably caused by interaction of calcium oxide with carbon dioxide, as the equilibrium pressure of carbon dioxide over the carbonate at 800° is 183 mm [4].

It was found in special experiments that calcium carbonate in presence of oxide does not determine the potential of the oxide-carbon electrode. The results of one such experiment are plotted in Fig. 5, which shows how the potentials of pure oxide-carbon and mixed oxide-carbonate-carbon electrodes reached equilibrium under identical conditions.

It is seen that the steady-state potentials of the two electrodes differed by about 2-3 mv.

SUMMARY

1. It is shown that the equilibrium potentials of oxide-carbon electrodes do not depend on the molar ratios of oxide and carbon present, but are determined by the molar concentration of Ca^{++} ions in the melt.

2. It is shown that fused mixtures of sodium potassium, and calcium chloride behave like ideal solutions when the concentration of calcium ions is below 5 molar %. At higher concentrations of calcium, the melts show fairly sharp deviations from ideality. The activity coefficient of calcium chloride in the melt becomes greater than unity.

3. It is shown that the pressure of carbon dioxide influences the equilibrium potentials of calcium oxide-carbon electrodes in accordance with the electrode reaction



if the pressure does not exceed the equilibrium dissociation pressure of calcium carbonate.

LITERATURE CITED

- [1] Iu. V. Baimakov, *Electrolysis in Metallurgy* (Metallurgy Press, 1944) 2, 203.*
- [2] H. Wartenberg, *Z. Elektroch.* 32, 331 (1926).
- [3] M. V. Smirnov, S. F. Pal'guev, and L. E. Ivanovskii, *J. Phys. Chem.* 29, 772 (1955).
- [4] *Chemist's Reference Book*, 3 (Goskhimizdat, Leningrad-Moscow, 1952).*

Received March 26, 1956

*In Russian.

ELECTROLYTIC DEPOSITION OF LEAD - INDIUM ALLOY

M. A. Shulger, A. I. Lipin and P. P. Tel'nykh

Thin layers of electrodeposited lead are extensively used for improvement of antifriction and running-in properties of some bearing alloys and other materials (such as bronzes). A coating of lead from several to some tens of microns thick, being soft, helps running-in and assists the surface to retain lubricants.

However, application of lead alone is not a completely efficient method for improvement of the anti-friction properties of rubbing surfaces. The reason is that lead coatings are strongly corroded in lubricating oils. In order to avoid corrosion of lead, the coatings used are not of pure lead but lead-indium alloy, made by the so-called "galvanothermic process" [1].

First, a layer of lead is deposited from the ordinary fluoborate electrolyte used for lead coating. About 4% of indium, calculated on the weight of lead, is then deposited from a sulfate electrolyte on the lead coating. The two-layer coating is then heat treated at a temperature close to the melting point of indium (150-155°). Indium then diffuses into the lead, and a lead-indium alloy is formed. The coating of Pb-In alloy has high resistance to corrosion, is harder than pure lead, and has better antifriction properties.

The galvanothermic process for production of lead-indium coatings gives an alloy of very irregular composition. The indium content on the surface of the coating is about 10-15%. The indium content decreases rapidly inside the deposit, in the direction of the basis metal.

Therefore it is the outer layer, with the highest indium content, which is largely responsible for the improved quality of the coatings applied to friction surfaces.

Because of the irregularity of the indium content, if the outer indium-rich layer is rubbed off, nicked, or scratched, the properties of the coatings are adversely affected. For example, it is known that corrosion occurs in many parts even after application of lead-indium coatings.

Therefore the most rational method of applying a lead-indium coating appears to be by electrolysis, with simultaneous deposition of lead and indium. This method should give an alloy uniform in composition and properties.

Several different electrolytes, including perchlorate and alkaline cyanide, can be used for deposition of lead-indium alloy [2].

We developed a method for electrodeposition of the alloy from fluoborate electrolytes. Solutions of this type are very reliable in use, and can be used for deposition both of lead and of indium.

EXPERIMENTAL

Method of investigation. The solutions were made from lead fluoborate electrolyte or fluoboric acid.

For preparation of the lead-coating electrolyte, hydrofluoboric acid was first prepared by the addition of boric acid to hydrofluoric acid in a vinyl-resin vessel. Lead oxide or lead carbonate was then added to the solution, and the volume was adjusted as required. Indium was dissolved in the electrolyte chemically or electrochemically.

In the chemical method, 1-2 ml of 30% H_2O_2 was added per gram of indium to be dissolved. When indium is dissolved in presence of hydrogen peroxide, heating accelerates the process and helps to remove excess H_2O_2 , which is harmful in electrolysis.

In the electrochemical method, an indium anode was dissolved in fluoborate electrolyte. The anode area was equal to the cathode area, 0.3 dm^2 . The electrolyte volume was 250 ml. The anode current density was 5 amps / dm^2 .

The experiments on electrodeposition of lead-indium alloy were performed at $18-20^\circ$ in a Plexiglas cell. The electrolyte volume in these experiments was 50 ml. The specimens were smoothly polished plates of stainless steel, 2 cm^2 in area. The deposits were applied on both sides of the plates, with anodes at each side 25-27 mm away. Indium and lead anodes were used. The anode operating times were 1:1.

The electrolysis was continued for a period of time, required to give coatings 10-12 microns thick. The deposits were removed from the cathodes after the electrolysis by means of a razor blade, and analyzed. Indium was determined in the alloy polarographically.

The usual polarization curves were used for the electrochemical investigation.

The cell was an H-shaped vessel containing the anode and the cathode. The cathode was a platinum plate 1 cm^2 in area.

The plate had a central opening, into which was sealed the tip of the contact tube. The reference electrode was a saturated calomel half cell. The strength of the current in the cell was measured by means of an M-15 milliammeter. The potential difference was measured by means of the PPTV-1 potentiometer. The null instrument was a highly sensitive galvanometer with a shadow pointer.

Before each experiment the cathode was coated with lead, indium, or an alloy of these metals, according to the electrolyte under investigation.

Composition of Electrolytes for Electrodeposition of Pb-In Alloy

Metal	Contents (in g/liter) in electrolytes			
	A	B	C	D
Lead	5	10	20	50
Indium	20	20	20	20

Effect of electrolysis conditions on the composition of the cathode deposit. The effects of current density and lead-indium ratio in the electrolyte on the composition of the cathode deposit were studied. Solutions the compositions of which are given in the Table were prepared in order to elucidate the influence of the In/Pb ratio on the composition of the cathode deposit.

In addition to lead and indium, each solution contained 10 g of free hydrofluoboric acid and 1.5 g of joiner's glue per liter.

With these solutions it was possible to study the influence of the In/Pb ratio in the electrolyte in the range 0.4 to 4. In addition to these four solutions, more highly concentrated solutions containing 75 to 140 g of Pb per liter were prepared.

Figure 1 shows that the composition of the cathode deposit varies greatly with variations of the In/Pb ratio in the electrolyte. The indium content of the deposit increases with increase of this ratio. The results show that large variations of the In/Pb ratio in the electrolyte lead to less pronounced variations of the composition of the cathode deposit. The indium content of the deposit decreases with increasing current density.

The results of a series of experiments on the influence of current density on the composition of the alloy deposited from a solution containing 95 g of lead and 15 g of indium per liter are plotted in Fig. 2. It is seen that the same relationship is found for this, more highly concentrated solution as for the more dilute electrolytes—the indium content of the deposit decreases with increasing current density. This decrease continues until the current density reaches about 1 amp/dm^2 , above which the indium content of the deposit remains almost constant. An explanation is that at high current densities equilibrium is probably established between the amounts of metal ion deposited on the cathode and diffusion toward it, these being the limiting amounts for the electrolyte of this composition [3].

Experiments were carried out in order to determine the effect of the free hydrofluoboric acid content on the composition of the cathode deposit. It was found that increase of the free hydrofluoboric acid from 10 to 40 g per liter decreases the indium content in the deposit by about 15%.

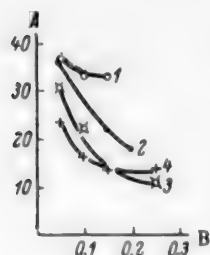


Fig. 1. Effect of In/Pb ratio in the electrolyte on the composition of the cathode deposit. A) In content (%), B) current density (amps/dm²). In/Pb ratio: 1) 4, 2) 2, 3) 1, 4) 0.4.

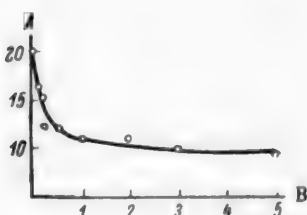


Fig. 2. Effect of current density on the composition of the cathode deposit from an electrolyte containing 95 g Pb and 15 g In per liter. A) In content (%), B) current density (amps/dm²).

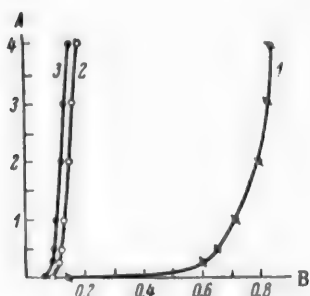


Fig. 3. Polarization curves for the deposition of indium, lead, and lead-indium alloy. Content of free HBF₄ 5 g/liter. A) Current density (amps/dm²), B) cathode potential (v). Contents of solutions (g/liter): 1) 10 In, 2) 100 Pb, 3) 100 Pb and 15 In.

It was found from the results of these experiments that for electrodeposition of an alloy containing about 10-12% of indium, which is necessary to ensure normal performance of certain friction parts, the following conditions should be used: electrolyte composition (g/liter): Pb 80-100, In 20-25, HBF₄ 10-20; electrolysis conditions: $D = 1-3$ amps/dm², $t = 18-25^\circ$.

Electrochemical investigation of the deposition of the alloy. To determine the principal causes of the simultaneous deposition of lead and indium, polarization curves were plotted for solutions containing indium only, lead only, and the two metals together. The results are given in Fig. 3.

It is seen that at zero current the potential of indium in the solution containing indium is very close to the potential of lead in the solution containing lead, so that their simultaneous deposition should be possible. However, with increase of current density the polarization in the indium solution is considerably greater, and the difference of the deposition potentials reaches about 0.6 v at $D_c = 1$ amp/dm², 0.65 v at $D_c = 2$ amps/dm², etc. This difference between the deposition potentials should mean that the simultaneous deposition of the two metals is difficult. Nevertheless, as the results of the experiments described earlier show, the alloy is deposited under these conditions. The curve for the deposition of the alloy is somewhat on the positive side of the curve for the deposition of lead.

The apparent contradiction between the results obtained in simultaneous deposition of lead and indium and the polarization curves can be explained as follows.

If simultaneous deposition of the metals occurs despite the considerable difference between the deposition potentials, and if the polarization curve for the deposition of the alloy lies on the positive side of the deposition curves of the individual metals, this means that some kind of depolarization factor is present. This may be formation of a solid solution, leading to easier simultaneous deposition of the metals.

It is known from the literature [4] that the system indium-lead has three one-phase regions along the concentration axis at room temperature: the α -phase with 0-13%, the γ -phase with 14-29%, and the β -phase with 32-100% Pb.

It is therefore likely that in the electrodeposition of indium a solid solution is formed consisting of the β -phase of the In-Pb system, as the β -phase exists over a fairly wide range of concentrations of the components.

The results of the electrochemical investigation account for the decrease of the proportion of indium in the alloy with increase of current density.

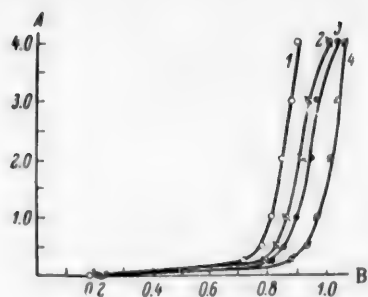


Fig. 4. Polarization curves for solutions with different contents of HBF_4 . In content 20 g/liter.

A) Current density (amps/ dm^2), B) cathode potential (v).

Contents of HBF_4 (g/liter): 1) 10, 2) 20, 3) 30, 4) 40.

considerable polarization in the deposition of indium, the difference between the deposition potentials of the metals increases rapidly. This makes the simultaneous deposition of indium and lead more difficult. The amount of indium in the electrolytic alloy decreases.

It follows from Fig. 3 that the cathode potential in the deposition of indium changes mainly up to $D_c = 1$ amp/ dm^2 . The content of indium in the electrolytic alloy decreases appreciably up to the same current density (Fig. 2).

Polarization curves for the deposition of indium from solutions containing 10, 20, 30, and 40 g HBF_4 per liter are given in Fig. 4. It is seen that increase of the HBF_4 content displaces the polarization curve for the deposition of indium in the negative direction. This naturally increases the difference between the deposition potentials of lead and indium, which is the reason for the decrease of the indium content of the cathode deposit.

Some properties of coatings from the electrolytic alloy

Anticorrosion properties. The corrosion tests were performed for 50 hours with the aid of the Pinkevich apparatus by the method of GOST 5162-49, with two intermediate weighings of the specimens. The specimen area was 0.15-0.18 dm^2 , and the coating thickness was 20-25 μ .

The specimens were tested for corrosion in MS-20 oil with intermittent immersion (15-16 times per minute) at 140-142°.

Two series of specimens were tested. The first consisted of specimens with the usual galvanothermic coatings and the second of specimens coated with the electrolytic alloy. The results of the experiments are given in Fig. 5.

It follows from these results that the corrosion resistance of the electrolytic alloy is approximately four times that of the galvanothermic alloy. The advantages of the electrolytic over the galvanothermic alloy may be attributed to the more ordered and denser structure of the former.

Structure and microhardness. The electrolytic lead-indium alloy is formed as a microcrystalline deposit. The packing of the crystals is closer than in electrolytic lead deposits.

The microhardness was tested by means of the PMT-3 instrument at 1 g load. As follows from Fig. 6, the microhardness first increases and then decreases with increase of current density. The maximum hardness corresponds to a current density of 2 amps/ dm^2 .

The coefficient of friction is an important characteristic of antifriction coatings; the coefficients of friction were therefore determined, a special apparatus for studies of the seizing of metals [5] being used.

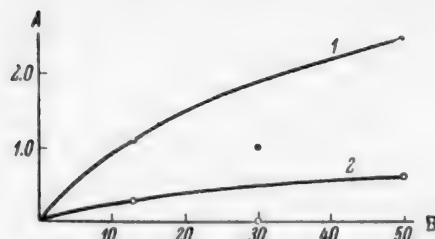


Fig. 5. Variation of weight loss of lead-indium alloys with duration of corrosion tests. A) Weight loss (g/m^2), B) duration of test (hours).

Alloys: 1) galvanothermic, 2) electrolytic.

It follows from Fig. 3 that at first, at low D_c , the potentials of In and Pb are fairly close together and therefore the simultaneous deposition of indium and lead is then easiest. With increase of D_c , in view of the con-

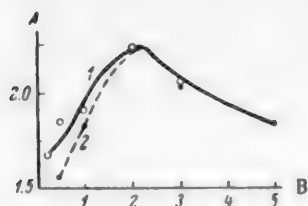


Fig. 6. Effect of current density on the microhardness of Pb-In alloys. Electrolyte composition (g/liter): Pb_{met} 95, In_{met} 15 and 20, HBF_4 free 5. A) Microhardness (kg/mm^2); B) current density D_c (amps/ dm^2). Indium contents of electrolyte (g/liter): 1) 25; 2) 20.



Fig. 7. Coefficients of friction of lead-indium coatings measured against 40 KhNMA steel. $P_{compression}$ 160 kg, $t = 150^\circ$, MS lubricant; A) coefficient of friction. Alloys: 1) Electrolytic, 2) electrolytic, heat-treated, 3) galvanothermic.

Three series of specimens were tested, with different coatings: galvanothermic alloy, electrolytic alloy, and electrolytic alloy subjected to the heat treatment used in the galvanothermic process.

This last coating was tested because it was expected that the properties of the alloy would be improved as the result of heat treatment.

The tests were carried out at loads of 30, 80, and 160 kg without lubricant, and at 160 kg and 150° with MS lubricant. The coefficients of friction were determined for direct and reverse pairs. The diagram in Fig. 7 represents the coefficients of friction of the different coatings tested against 40 KhNMA steel. In this and in all the other tests the best results were given by the electrolytic lead-indium alloy which had not been subjected to heat treatment: the coefficients of friction were the lowest for this alloy. The electrolytic alloy is least prone to seizing in friction against steel.

SUMMARY

It was found in a study of the electrodeposition of lead-indium alloy from fluoborate electrolytes that lead-indium alloy obtained by electrodeposition has better anticorrosion and antifriction properties than lead-indium coatings made by the galvanothermic process.

LITERATURE CITED

- [1] V. I. Lainer and N. T. Kudriavtsev, *Fundamentals of Electroplating*, 2 (Metallurgy Press, 1946).*
- [2] L. I. Kadaner, *Recent Advances in Electroplating* (The Gor'kii State University Press, Khar'kov, 1951) pp. 223-224.*
- [3] T. F. Frantsevich-Zabludovskaia et al., *J. Appl. Chem.* 27, 4, 413 (1954).
- [4] V. S. Kogan and B. Ia. Pines, *Proc. Acad. Sci. USSR* 87, 5, 771-773 (1952).
- [5] D. N. Garkunov and F. N. Naumov, *J. Machine Construction* 10 (1955).

Received June 22, 1956

*In Russian.

ELECTROLYTIC DEPOSITION OF PALLADIUM FROM SOLUTIONS CONTAINING CAUSTIC ALKALI

V. V. Ostroumov

There is almost no information in the literature on the electrolytic deposition of palladium from solutions containing caustic alkali. A brief mention of the possibility of formation of palladium coatings from such solutions was apparently made for the first time in 1933 [1].

The following typical electrolyte composition was recommended (in g/liter): caustic alkali 60, palladium chloride 0.5 (calculated as the metal).

The electrolyte is used at room temperature. The current efficiency with respect to the metal is 8-15% in the current-density range 3-7 ma/cm².

The simple composition and the low palladium content of the electrolyte seemed to be useful characteristics for the preparation of large-volume baths, especially if the deposition of thin layers of the metal is sufficient.

EXPERIMENTAL

The starting materials for the preparation of electrolytes in our experiments were solutions of palladium chloride and caustic potash, which were mixed in definite proportions.

For preparation of palladium chloride, the metal was dissolved in aqua regia, the solution being evaporated twice with hydrochloric acid.

It was found that the solutions must be mixed by a definite procedure. The palladium chloride solution must be added to the strong alkali solution, and not the other way round.

If palladium chloride solution is added to the alkali solution (with vigorous stirring), transparent, slightly yellow, fairly stable solutions are obtained. If the mixing procedure is reversed, deep red mixtures are formed, very similar to ferric hydroxide sols, unstable on keeping, and probably containing palladium in the form of the colloidal hydroxide. Not more than 3 g of palladium chloride per liter (calculated as the metal) can be added to a solution containing 200 g of alkali per liter, or 0.3 g of the metal per liter to a solution of 20 g of alkali per liter; otherwise the electrolytes are very unstable.

When the mixtures are heated, palladium hydroxide is always precipitated; therefore the electrolytes were investigated and used at room temperature only.

The nature of the solutions formed by the normal mixing procedure is still not clear, and was not studied further. It is possible that palladium compounds similar to zincates are formed.

A stock electrolyte containing 200 g KOH and 3 g Pd per liter was prepared for the experiments; the other solutions were prepared by dilution of this. Solid alkali was added to the electrolyte as necessary.

Electrolytes of the following compositions were tested:

Electrolyte No.	KOH content (g/liter)	Pd content (g/liter)
1	200	3
2	100	1.5
3	60-70	1.0
4	60	0.5
5	33.3	0.5
6	20	0.3

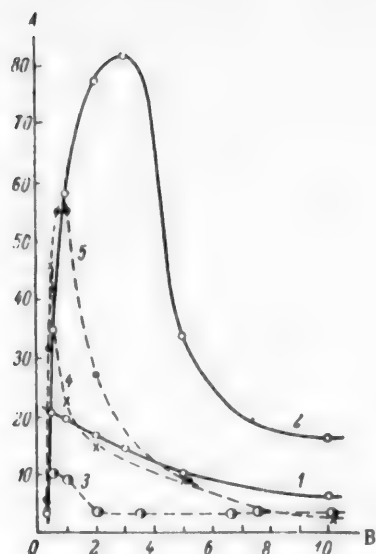


Fig. 1. Current efficiency with respect to palladium.
Electrolyte composition (in g/liter): 60 alkali, 0.5 palladium.
A) Current efficiency (%), B) current density (ma/cm^2).
State of electrolyte: 1) not stirred (brass cathode), 2) stirred (brass cathode), 3) not stirred (palladium cathode), 4) moderately stirred (palladium cathode), 5) vigorously stirred (palladium cathode).

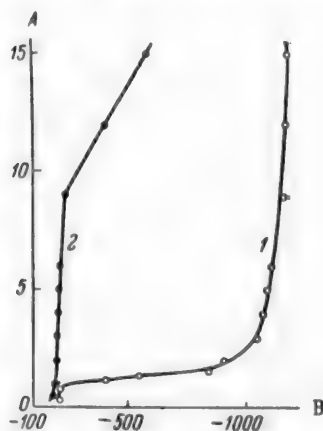


Fig. 3. Polarization of a brass cathode.
Composition of electrolyte No. 1 (g/liter): 200 alkali, 3.0 palladium.
A) Cathode current density (ma/cm^2), B) polarization (mv).
Curves: 1) electrolyte not stirred, 2) electrolyte stirred.



Fig. 2. Polarization of a palladium-plated cathode.
Electrolyte composition (g/liter): 60 alkali, 0.5 palladium.
A) Cathode current density (ma/cm^2), B) polarization (mv).
Curves: 1) electrolyte not stirred, 2) electrolyte stirred.

The electrolyte properties are greatly influenced by the concentrations of palladium and caustic alkali. The potassium chloride which is inevitably formed by the reaction between the starting substances has little effect. The stability of the electrolytes on keeping decreases somewhat with increasing concentration of potassium chloride.

The yield of the metal was determined on cathodes made from thin sheet brass, previously cleaned with fine emery paper. The quantity of electricity passed was measured by means of a copper coulometer.

The current efficiency was determined for solutions containing 60 g of caustic potash and 0.5 g of palladium per liter. The anode was palladium-plated. Experiments showed that platinum and palladium anodes are not soluble in alkaline palladium electrolytes.

The variations of the current efficiency with the current density and conditions of stirring of the electrolyte are plotted in Fig. 1.

In a solution at rest (Curve 1) the current efficiency varies from 6 to 20% with decrease of current density. The relatively low yield of the metal is due to the discharge of hydrogen ions. In fact, at all current densities above $0.5 \text{ ma}/\text{cm}^2$ hydrogen bubbles were seen at the cathode.

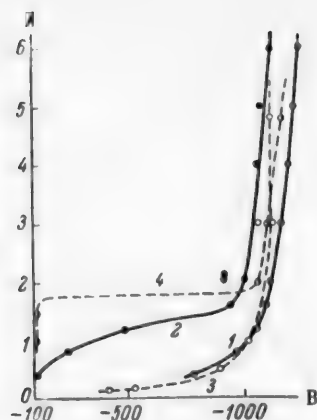


Fig. 4. Polarization of a brass cathode. Composition of electrolyte No. 6 (g/liter): 20 alkali, 0.3 palladium.

A) Cathode current density (ma/cm^2), B) polarization (mv).

Curves: 1) electrolyte not stirred, 2) electrolyte stirred.

After 10 minutes of electrolysis: 3) electrolyte not stirred, 4) electrolyte stirred.

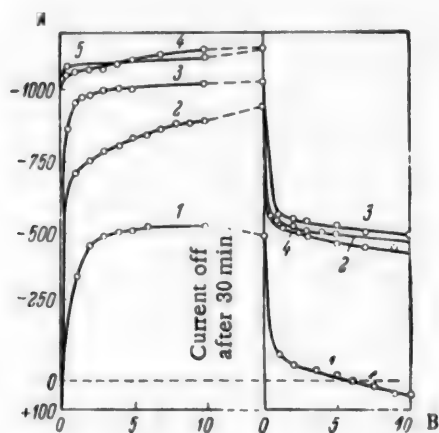


Fig. 6. Polarization and depolarization of a cathode in static electrolyte (33.3 g alkali and 0.5 g palladium per liter).

A) Polarization (mv), B) time (minutes). Current density (ma/cm^2): 1) 0.2, 2) 0.5, 3) 1.0, 4) 3, 5) 5.

In a stirred electrolyte (Curve 2 of the same graph) the efficiency increases at first (to 82%), and then decreases. The causes of the appearance of a maximum on the curve for the stirred electrolyte are probably as follows. In our experiments oxygen had access to the electrolyte, and was brought into

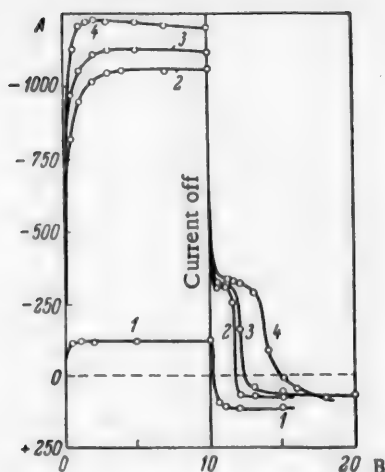


Fig. 5. Polarization and depolarization of a cathode in a stirred electrolyte (33.3 g alkali and 0.5 g palladium per liter).

A) Polarization (mv), B) time (minutes).

Current density (ma/cm^2): 1) 1-1.5, 2) 2, 3) 3, 4) 4.

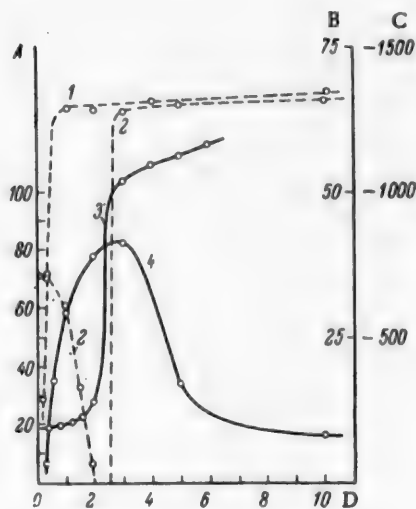


Fig. 7. Effects of current density on the reflecting power of the deposit (1,2), polarization (3), and current efficiency with respect to palladium (4).

Electrolyte composition (g/liter): 60 alkali, 0.5 palladium.

A) Current efficiency (%), B) reflecting power (%), C) polarization (mv), D) current density (ma/cm^2).

State of electrolyte: 1) not stirred, 2) stirred, 3) stirred, 4) not stirred.

vigorous contact with the cathode by the stirred liquid. The hydrogen liberated at the cathode together with the metal was oxidized to water, resulting in partial depolarization, and the yield of palladium at low current densities fell. The descending branch of the curve to the right of the maximum is the consequence of copious liberation of gaseous hydrogen, which is detected visually.

The nature of the current-efficiency curves changes if the cathodes are made of palladium plate and not of brass (Fig. 1, Curves 3, 4, and 5); no hydrogen bubbles were detected on such cathodes, even in stationary electrolytes, at the highest current densities used (10 amps/cm^2). The hydrogen formed dissolves in the massive palladium.

The current efficiency is changed little if the alkali concentration of the electrolyte is halved.

Cathodic polarization of palladium plate in a solution of 60 g KOH and 0.5 g Pd per liter at a low constant current density (0.2 ma/cm^2) results in a slow increase of the potential, which reaches its maximum value after one hour (730 mv relative to the standard hydrogen electrode). At higher current densities the final potentials are established much more rapidly.

Measurements of the potential at rising and falling current densities give higher values in the second case. This discrepancy is caused by saturation of the cathode with hydrogen, which is slowly lost into the surroundings during decrease of current density.

Polarization curves for a cathode made from palladium plate are given in Fig. 2. The values were measured with increasing current density, and are relative to the standard hydrogen electrode. Curves 1 and 2, for an electrolyte at rest and a stirred electrolyte respectively, coincide at current densities above 2 ma/cm^2 .

If the cathodes are made of bronze, brass, or nickel with polished surfaces, the polarization is generally higher; it is decreased sharply if the electrolyte is stirred.

Brass and bronze surfaces become appreciably dull in alkaline solutions in absence of current, and therefore the cathodes were covered by very thin protective layers of palladium before the determinations.

Polarization curves for electrolytes of the two extreme compositions (Solutions No. 1 and No. 6) are given in Figs. 3 and 4 (Curves 1 and 2). The polarization curves for the other electrolytes are intermediate between these.

The points on the curves were usually determined fairly quickly after the given current had been established (after 1-2 minutes) so that the original mirror surface of the cathode was not disturbed. The polarization values with increasing current densities are plotted in the graphs.

It should be noted that for static electrolytes a horizontal region on the polarization curve is found only for Electrolyte No. 1. On the other hand, for stirred electrolytes horizontal regions are found for all compositions; they appear at lower current densities if the palladium concentration in the solution is decreased.

A characteristic feature of these solutions is the strong influence of stirring on the polarization, showing that its variable part is concentrational in character.

The polarization curves become especially distinctive if steady values of the potentials are read off; this requires 10 minutes after the current has been switched on.

An example of this type of determination, for an electrolyte with 33.3 g of alkali and 0.5 g of palladium per liter, is given in Fig. 4 (Curves 3 and 4).

In the case of the stirred electrolyte (Curve 4) there is a region of current values up to 2 ma/cm^2 where only the solid phase is liberated; above 2 ma/cm^2 gaseous hydrogen is evolved in addition to the solid phase.

To determine the causes of the abrupt increase of polarization as the current density value 2 ma/cm^2 is approached, observations were made of the decrease of the cathode potential after cessation of electrolysis. It was found that in a stirred electrolyte the electrode potential does not decrease steadily, but shows a halt if the palladium layer on the cathode was formed at current densities 2 ma/cm^2 and over (Fig. 5). In a static electrolyte similar halts are found with layers formed at current densities 0.5 ma/cm^2 and over, and they are of considerable duration (Fig. 6). This course of the decrease of the potential indicates that the cathode deposit contains a new phase, consisting of palladium and hydrogen, which decomposes slowly after the current is switched off.

This phase breaks down more rapidly in a stirred than in a static electrolyte. The probable reason for the difference in the breakdown rates is that hydrogen must be removed from the deposit, and this takes place more rapidly in a stirred electrolyte, owing to more intensive exchange of oxygen and hydrogen between the liquid and the electrode.

Similar effects could be observed with a previously deposited layer of palladium after polarization in 3% caustic alkali solution, i.e., in absence of palladium ions.

For practical utilization of these electrolytes, it is useful to know the conditions in which bright layers of metal are deposited.

In an electrolyte containing 60 g of alkali and 0.5 g of palladium per liter, without mechanical stirring, bright deposits of palladium are formed over a wide range of current densities (Curve 1, Fig. 7). If the electrolyte is stirred, there are three current-density regions in which deposits with different properties are formed (Curve 2, Fig. 7). Electrolysis of current density 0.4-2.0 ma/cm² for 4 minutes gives spotty, dull deposits; in the range 2-3 ma/cm² black (loose) deposits are formed in the same time, while between 3 and 10 ma/cm² bright layers with a high reflective power are deposited.

The transition from black to bright deposits is fairly sharp - within a range of 0.5 ma/cm². The formation of black deposits is accompanied by liberation of gaseous hydrogen.

Conditions for the Formation of Bright Palladium Deposits, 0.1-0.2 μ Thick

Electrolyte composition (g/liter)		Current density (ma/cm ²)		Duration of electrolysis (min)
KOH	Pd	without stirring	with stirring	
60-70	1	5-10	—	10-15
60	0.5	2-10	5-10	10-20
30	0.5	2-5	5	10-20
20	0.3	2-5	—	15-40

Bright palladium deposits with 67% reflecting power can be obtained from alkaline electrolytes of different compositions under different electrolysis conditions (see Table).

Copper and brass articles should be coated with a thin electrolytic layer of nickel deposited from ordinary baths. It is not necessary to protect the palladium anode by a diaphragm.

DISCUSSION OF RESULTS

According to the polarization curve (Curve 3, Fig. 7) for an electrolyte containing 60 g of alkali and 0.5 g of palladium per liter, the limiting current density is about 2.5 ma/cm². At lower current densities only a single solid phase is liberated at the cathode. This is probably the α -phase, well-known from studies of equilibrium in the system gaseous hydrogen - palladium.

At the current density corresponding to the limiting value, the catholyte layer becomes impoverished of metal ions; this, as is known, disturbs crystallization of the metal and leads to the formation of loose black deposits on the cathode.

For many metals, further increase of the current density would merely loosen the deposit further owing to liberation of gaseous hydrogen.

The situation is different in the electrolytic deposition of palladium.

In the limiting-current region a considerable proportion of the electricity is transported through the catholyte layer by hydrogen ions; these are discharged to yield hydrogen atoms, which are involved equally

with palladium atoms in the formation of the β -phase lattice at the cathode. Conditions for the formation of a compact deposit are again present, and a bright layer of metal appears on the cathode (Curve 1, Fig. 7). If any excess hydrogen is formed, it leaves the cathode in gaseous form without disturbing the compact structure of the deposit.

The current efficiency should decrease appreciably from the instant at which intensified discharge of hydrogen ions begins, i.e., when the limiting current is reached; this is found to be the case (Curve 4, Fig. 7).

The β -phase can be formed only at a potential beyond the region of limiting current; this follows from the data in Figs. 5 and 6. It is seen that there are halts in the course of the decrease of potential during depolarization. These halts are evidently the consequences of decomposition of the β -phase:



which takes place slowly, as is generally characteristic of solid-state transformations. At potentials below values corresponding to the limiting-current region, the β -phase is not formed at the cathode, and therefore these halts do not occur.

In conclusion, it must be noted that the possibility of deposition of the α -phase at the cathode at current densities below the limiting current value requires confirmation. An equally justified assumption is that the pure metal is deposited in the current-density range, and that the α - and β -phases are formed simultaneously, when hydrogen ions begin to discharge at the cathode in quantities sufficient for formation of these phases, after the limiting current density has been reached. However, on this hypothesis it is difficult to account for the above-mentioned low value of the current efficiency in the 0.3-2.5 ma/cm² region of current densities.

SUMMARY

1. Conditions for the preparation of palladium electrolytes containing caustic alkali, stable on keeping, have been found.
2. Electrolysis conditions have been found for the formation of bright mirror layers of palladium on massive metal supports.
3. It is suggested that the solid β -phase is formed at the cathode at current densities above the limiting current. When electrolysis ceases, the β -phase decomposes into the α -phase and hydrogen, and then into the metal and hydrogen.
4. It is shown that after the limiting current density has been reached, loose black deposits are formed over a narrow range of current densities. Further increase of current density again leads to formation of compact and bright palladium deposits.

LITERATURE CITED

- [1] W. Pfannhauser, *Galvanotechnik*, 1,878 (1941).

Received June 19, 1956

CORROSION OF STEEL BY HYDROCHLORIC ACID IN THE SPHEROIDAL STATE

Kh. L. Tseitlin and S. M. Babitskaia

The K. E. Voroshilov Institute of Organic Intermediates and Dyes

Hydrochloric acid is very corrosive to metals. However, at temperatures above the dew point it is converted into the vapor-gas mixture $\text{HCl-H}_2\text{O}$ which has a different action from that of the original acid; above 150° the corrosion of iron alloys is hardly noticeable in this case [1].

It was of interest to determine the resistance of metals to hydrochloric acid in the spheroidal state, when the drops of the acid (spheroids) are separated from the heated surface by a heat-insulating layer of $\text{HCl-H}_2\text{O}$ vapor-gas mixture. The gap between the drop and the surface increases with increasing temperature of the solid body [2]. In technology, drops of liquid often fall on strongly-heated metals. This occurs, for example, in the action of sprays of corrosive solutions on hot metallic surfaces in the chemical and other industries. The number of such examples is increasing owing to the increase in the number of processes carried out at high temperatures. The literature contains no quantitative data on the corrosion of metals by liquids in the spheroidal state. Qualitative observations are very scanty.

Poggendorff [3] did not observe any corrosion in an incandescent platinum crucible used for studying the spheroidal state of sulfuric acid, although concentrated sulfuric acid attacks platinum at 250° . Berger [4] assumed that there was total absence of contact between spheroids and incandescent surfaces, on the grounds that spheroids do not interact with the walls of the vessel, and attributed all chemical attack on the material to the reaction of the layer of vapor between the spheroids and the bottom of the vessel.

Gezekhus [5] carried out experiments in platinum, silver, copper, and brass crucibles, and showed that spheroids in their normal state do not come in contact with the heated surface. For confirmation of this, drops of aqueous copper sulfate solution were put into incandescent platinum or silver vessels, and iron rods were plunged into the spheroids formed. The copper formed by contact deposition covered the rod, but the tip in contact with the metal was unaffected; this proved that the spheroid was not in contact with the metal surface.

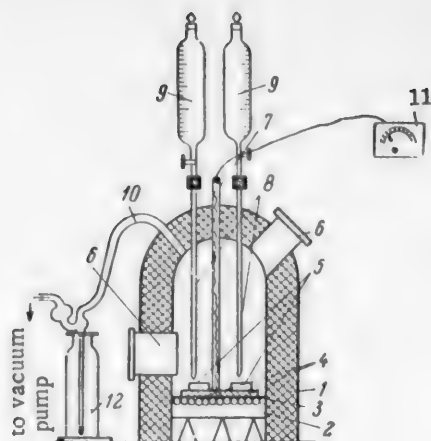
Pletneva and Rebinder [6], who studied the conditions of spheroid formation on a stainless steel plate with a spherical depression, showed that different liquids assume the spheroidal state at different temperatures which depend on the boiling points of the liquids; water becomes spheroidal at $225-250^\circ$, benzene at 175° , isoamyl alcohol at 230° etc. Surface-active substances have an appreciable influence on the spheroids.

Data on the corrosion of steel by hydrochloric acid in the spheroidal state are presented in this paper.

EXPERIMENTAL

Method. The Figure shows the unit used for the corrosion tests; this consists of the apparatus itself, measuring funnels, and a system for drawing off the $\text{HCl-H}_2\text{O}$ vapor-gas mixture.

The apparatus is enclosed in a steel case with double walls (the diameter of the internal case is 16 cm, and of the external, 22 cm), with a heat-insulating layer 3 cm thick between them. The case, made of ordinary carbon steel (for experiments up to $300-400^\circ$) or of stainless 1Kh18N9T steel (for temperature above 400°) is provided with two openings for quartz dropping tubes for addition of the reagents, an opening for a quartz socket for temperature measurement, and sight glasses (made of "Pyrex" glass or mica). For continuous observations of the process, artificial light must be provided inside the apparatus; this was done by means of an electric lamp



Apparatus for corrosion tests.

1) Case, 2) ceramic plate, 3) heating coil, 4) metals under test, 5) quartz rings, 6) sight glasses, 7) quartz socket for thermocouple, 8) quartz dropping tubes, 9) glass measuring funnels, 10) side tube for removal of gases, 11) galvanometer, 12) trap with alkali solution.

The temperature of the metal plates was measured by means of a thermometer (up to 300°) or a thermocouple (above 300°) inserted into the quartz socket fixed at the boundary between the two plates under test. The experiments were performed under slightly reduced pressure (5-10 mm water column) in order to ensure removal of HCl-H₂O vapor-gas mixture from the system.

The apparatus was not sufficiently air-tight, and the experiments were performed in presence of air drawn through the system by means of a pump. Polished and etched steel plates, 80 × 50 × 5 mm, were tested simultaneously. The specimens were measured with a micrometer before the experiments, dried in ether, and weighed on an analytical balance. After the tests the hot specimens (at about 200°) were washed with large amounts of water, and then boiled for 40 minutes in 20% alkali solution with excess zinc dust to remove corrosion products. The specimens were then again washed in water, then in alcohol, dried in ether, and weighed. The corrosion rate was estimated from the change in weight (in g/m²·hour).

If the corrosion is calculated only for the zone of action of the drops, confined by the quartz retaining ring, the corrosion rate is trebled (as compared with tabulated data), as the area of the whole plate is treble the area over which the drop can move. However, the corrosion was uniform in most cases, suggesting that it is caused mainly by HCl-H₂O vapor-gas mixture, and the corrosion should therefore be calculated for the whole specimen surface. If local attack took place, the pit depth was measured. For comparison with hydrochloric acid, the action of distilled water in the spheroidal state on the heated metals was determined in parallel experiments.

The specimens were tested mechanically and metallographically before and after the experiments. The following steels were tested: carbon steel (No. 3), chrome-nickel (1Kh18N9T), and chrome (EI-496, containing 0.1% carbon and 12% chromium). Pure hydrochloric acid was used for the experiments.

The results of the experiments are summarized in Tables 1 and 2. It was found that at 200° the spheroidal state often breaks down, and hydrochloric acid causes strong local corrosion of carbon steel (the pit depth reaches 900 mm/year). At 300-400° steel has satisfactory resistance to 30% hydrochloric acid in the spheroidal state (the corrosion rate is 1.5 g/m²·hour), while at 500° the attack on the metal is considerable, reaching 25-30 g/m²·hour. The duration of the test, up to 100 hours, has no significant influence on the corrosion rate of carbon steel. Up to 400° the concentration of hydrochloric acid (5 to 30%) has no appreciable influence on the resistance of the steel; at 500° a decrease of the concentration of hydrochloric acid from 30 to 5% decreases the corrosion rate.

with a reflector. The case is held over an electric hot plate (15 cm in diameter) used for heating the metals.

Two test specimens were laid simultaneously on quartz supports (rods 0.5 cm in diameter and 10 cm long, slightly flattened on one side for better stability) with the ends of the dropping tubes over their centers.

To retain the drops of hydrochloric acid on the test specimens, cylindrical quartz retaining rings (4 cm in diameter, 1.5 cm high) were placed on the specimens, the reagent being dropped in the center. The feed system consists of graduated glass funnels each 250 ml in capacity, with their ends joined by means of rubber tubing to quartz dropping tubes passing through rubber bungs in the openings of the case.

The system for drawing off the HCl-H₂O vapor-gas mixture and hydrochloric acid mist consists of a water-jet pump, flasks containing alkali solution, and a steel side tube (0.5 cm in diameter) for drawing off the gases, at the top of the case. The liquid was carefully dropped from the measuring funnels onto the metal plates previously heated to the required temperature in such a way that drops of liquid were always present on the surface. The rate of dropping was regulated by hand, by means of a well-greased ground-glass tap.

TABLE 1

Corrosion of Steels by Water and Hydrochloric Acid in the Spheroidal State

Temp. of metal (°C)	Reagent	Duration of test (hours)	Feed rate of reagent (ml/hour)	Loss of weight of specimens (g/m ² hour)		Type of corrosion	
				polished	etched		
Carbon steel							
200	H ₂ O 20% HCl	10	17	0.16	0.07	Uniform corrosion Local corrosion, reaching 900 mm/year at point of contact of the drops	
			14	0.30	0.77		
300	H ₂ O	10	38	0.02	0.07	Uniform corrosion	
		100	25	0.02	—		
	5% HCl	10	29	1.18	1.25		
		100	34	0.27	0.21		
	20% HCl	10	25	1.23	1.09		
		100	28	0.23	—		
400	30% HCl	10	27	1.27	1.57		
		100	25	0.08	0.08		
	H ₂ O	10	28	0.01	0.05		
		100	37	2.07	1.31		
	5% HCl	10	32	1.69	1.52		
		100	34	0.31	0.15		
500	20% HCl	10	27	4.76	3.82		
		100	40	0.15	0.72		
	H ₂ O	10	41	1.86	1.32		
		100	44	6.15	5.80		
	5% HCl	10	38	—	12.11		
		100	42	27.10	16.80		
500	30% HCl	10	40	17.86	12.86		
		100	40	17.86	12.86		
1Kh18N9T							
200	H ₂ O 20% HCl	10	15	0.02	0.01	Uniform corrosion Local corrosion, reaching 900 mm/year at point of contact of the drops	
		100	16	0.72	0.92		
500	H ₂ O	10	40	0.06	0.05	Uniform corrosion	
		100	43	0.01	0.01		
	5% HCl	10	42	0.15	0.34		
		100	40	0.19	0.42		
	20% HCl	10	42	0.23	0.62		
		100	39	0.49	—		
500	20% HCl	10	39	1.31	0.28		
		100	41	2.27	0.59		
EI-496 steel							
500	H ₂ O	10	37	0.18	0.22		Uniform corrosion
		100	38	0.02	0.07		
	5% HCl	10	40	0.05	0.56		
		100	41	0.16	0.67		
	20% HCl	10	39	0.83	0.22		
		100	37	0.26	0.07		

TABLE 2

Effects of Phenol and Chlorobenzene on the Corrosion of Steels by 20% Hydrochloric Acid in the Spheroidal State
(Duration of tests 10 hours)*

Temperature of metal (°C)	Corrosion of steels (g/m ² · hour)				Type of corrosion	
	in 20% HCl		in 20% HCl + 0.5% phenol + 0.01% chlorobenzene			
	polished specimens	etched specimens	polished specimens	etched specimens		
Carbon steel						
300	1.23	1.09	1.00	1.25	Uniform corrosion	
400	1.69	1.52	2.31	1.93		
500	27.10	16.80	7.44	5.10		
1Kh18N9T steel						
500	0.23	0.62	0.41	0.33		
EI-496 steel						
500	0.16	0.67	0.13	0.42		

* Resinification of the organic substances was not observed during the tests.

Distilled water, used in comparative tests, has little action on steel heated to 200-400° (the corrosion rate is 0.1 g/m² · hour); if the temperature is raised to 500° the corrosion rate increases to 0.8 g/m² · hour. The corrosion rate of carbon steel by hydrochloric acid is 900 times the rate of corrosion by water (at 200°), 15 times at 300°, and 23 times at 500°. Hot (80°) 20% hydrochloric acid is 800 to 1000 times as corrosive as the same acid in the spheroidal state in its effect on carbon steel.

The surface treatment (polishing or etching in our experiments) has no significant influence on the corrosion of steel by hydrochloric acid and water in the spheroidal state. During relatively short tests (100 hours), water and hydrochloric acid in the spheroidal state do not change the structure or the mechanical properties of carbon steel heated to 300-500°.

The results of experiments on the action of hydrochloric acid in the spheroidal state on stainless steels show that at 500° the behavior of 1Kh18N9T chrome-nickel steel is similar to that of EI-496 chrome steel. As in the case of carbon steel, at 200° the spheroidal state often breaks down and hydrochloric acid causes strong local corrosion of the steels (the maximum pitting depth reaches 900 mm/year). Stainless steels heated to 500° are fairly resistant to 5-20% hydrochloric acid in the spheroidal state (the corrosion rate is less than 1 g/m² · hour); the corrosion of carbon steel under these conditions is considerable.

The duration of the test, up to 100 hours, and variations of the hydrochloric acid concentration between 5 and 20%, do not have any significant influence on the corrosion rates of stainless steels.

As in the case of carbon steel, hydrochloric acid has a stronger effect than distilled water on heated stainless steels (the corrosion rate is 12 times as high at 500° in 20% hydrochloric acid).

20% hydrochloric acid at 100° corrodes 1Kh18N9T steel at 2000 times the rate of the same acid in the spheroidal state at 500°. The surface treatment (polishing or etching) has no appreciable influence on the corrosion of stainless steels by hydrochloric acid or water in the spheroidal state.

In relatively short tests (100 hours) water or hydrochloric acid in the spheroidal state do not alter the mechanical properties and structure of stainless steels (no intercrystalline corrosion was detected).

In several experiments phenol (0.5%) and chlorobenzene (0.01%) were added to the hydrochloric acid. It was found that at 300-500° these additions do not have any significant influence on the corrosion of steels by 20% hydrochloric acid in the spheroidal state (Table 2).

The following effects were observed in the experiments with hydrochloric acid:

- 1) breakdown of the spheroidal state (local flooding of the surface) results in a rapid acceleration of corrosion; thus, at 400° in a test lasting 10 hours two floodings of about 5 minutes total duration increased the corrosion of carbon steel from 0.31 (with the acid in the spheroidal state) to 19 g/m²·hour, i.e., the rate was increased 63-fold;
- 2) the spheroids formed evaporate slowly, and are in continuous motion; if the steel is not corroded, the spheroids are transparent and colorless; if the steel is attacked, the corrosion products color the spheroids yellow;
- 3) all the quartz parts of the apparatus are colored red; if the corrosion is considerable, the transparent quartz becomes opaque and black; the reddish black deposit of metal oxides can only be removed from the quartz surface mechanically – by means of emery cloth; the quartz is found to have lost much of its transparency;
- 4) the surface of the case made of carbon steel, and especially of 1Kh18N9T stainless steel, corroded very little after 500 hours of exposure to HCl–H₂O vapor–gas mixture, in agreement with literature reports on the slight corrosion of iron alloys under these conditions [1];
- 5) drops of hydrochloric acid jumped over the quartz retaining ring and came in contact with the incandescent heater spiral; however, these drops did not have any significant effect on the spiral, and therefore it was possible to place the test specimens directly on the ceramic plates of the electric heater on top of quartz supports. In many cases the Nichrome heater spirals, 0.6 mm thick, remained in service for hundreds of hours, and became unserviceable only if the experiments were interrupted, when the system cooled and HCl–H₂O vapor–gas mixture condensed to form droplets of acid.

SUMMARY

1. The spheroidal state of hydrochloric acid often breaks down at 200°. Steels heated to 200° have high resistance to water but undergo strong local corrosion under the action of hydrochloric acid.

2. Carbon steel heated to 300–400°, and 1Kh18N9T and EI-496 stainless steels heated to 500°, have high resistance to water, and satisfactory resistance to hydrochloric acid in the spheroidal state.

It follows that iron alloys may be used for equipment intended for processes in which hydrochloric acid acts in the spheroidal state. But the equipment must be so designed that breakdown of the spheroidal state is completely impossible.

The maximum operating temperature is 400° for carbon steel, and 500° for 1Kh18N9T and EI-496 stainless steels. To reduce the risk of breakdown of the spheroidal state of hydrochloric acid, the temperature of the metal surface must not be below 300°.

LITERATURE CITED

- [1] Kh. L. Tseitlin, J. Appl. Chem. 21, 1, 35 (1948).
- [2] O. D. Khvol'son, Course of Physics, 3 (State Press, 1923) p. 515.*
- [3] Poggendorff, Pogg. Ann. 52, 538 (1841).
- [4] Berger, Pogg. Ann. 119, 594 (1863); 147, 472 (1872).
- [5] N. A. Gezekhus, J. Russ. Phys.-Chem. Soc. 8 (physics section), 9, 311 (1876).
- [6] N. A. Pletneva and P. A. Rebinder, J. Phys. Chem. 20, 9, 961 (1946); 973 (1946).

Received July 11, 1956

*In Russian.

STUDY OF BINARY SYSTEMS OF SULFURYL CHLORIDE WITH CHLORINATED HYDROCARBONS

V. M. Vdovenko and T. V. Kovaleva

The purpose of this work was a physicochemical study of sulfonyl chloride and its mixtures with certain chlorinated hydrocarbons. The total and partial vapor pressures of binary systems of sulfonyl chloride with the following components were studied at various temperatures: carbon tetrachloride, dichloroethane, tetrachloroethane, and hexachloroethane; the compositions of the gas phases in relation to the liquid phase composition were also studied.

The principal properties of sulfonyl chloride and the above-named components are given in Table 1 [1].

All the solvents used are chlorinated hydrocarbons, and are therefore similar chemically. However, they differ considerably among each other in physical properties. Some are liquids of high volatility (carbon tetrachloride), others have low volatility (tetrachloroethane), or are solids (hexachloroethane).

TABLE 1

Principal Properties of the Components of the Binary Systems

Substances	Molecular weight	Temperature (°C)		Density d_4^{20}	Viscosity at 20° (in absolute units)	Surface tension at 20° (in absolute units)
		of boiling	of melting			
Sulfonyl chloride	135.0	69.3	-54	1.6943	0.00754	29.6
Carbon tetrachloride	153.84	76.9	-22.6	1.595	0.00998	25.7
Dichloroethane	98.97	83.7	-35.3	1.256	0.00834	33.1
Tetrachloroethane	167.86	146.3	-36	1.6220	0.01745	35.5
Hexachloroethane	236.8	—	187	2.09	—	—

The viscosities and surface tensions of the liquid solvents and sulfonyl chloride do not differ greatly among each other. It is therefore likely that the molecular interaction in all these substances is to a certain degree similar.

Accordingly, the property-composition diagrams for the binary systems sulfonyl chloride-solvent should be simple in character. If the mixing of these substances is not accompanied by appreciable heat effects, there are good grounds for expecting that solutions of sulfonyl chloride should have properties similar to the properties of ideal solutions. This can be confirmed by investigations of the vapor pressures of these solutions, mixtures of sulfonyl chloride with the above-named chlorinated hydrocarbons.

EXPERIMENTAL

Swietoslowski's method [2] was used for the determinations of vapor pressures of sulfonyl chloride and its mixtures.

The apparatus consists of the following parts: the ebullioscope a, the condenser b, the trap c, the manometer d, the buffer vessel e, and a vacuum pump (Fig. 1).

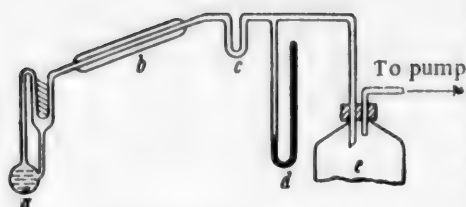


Fig. 1. Apparatus for vapor-pressure determinations.
Explanations in text.

The most important part is the ebullioscope (Fig. 2). Its principle of operation is as follows: the vessel A is filled with the liquid to the line aa, and the liquid is brought to the boil. The vapor formed displaces some of the liquid through the tube 1 and the tube C onto the glass test tube B, which contains mercury and a thermometer. The vapor then enters the condenser D, is condensed, and flows back into the vessel A. A platinum wire is sealed in the bottom of the vessel to ensure uniform boiling. The tube E is fitted with a ground-glass stopper, and is used for filling the ebullioscope.

The vapor pressure is measured as follows.

After the ebullioscope has been filled with the liquid, the vacuum pump is switched on and the system is evacuated to a definite degree. The pump is then switched off and the bottom of the ebullioscope is warmed by a spirit flame. After some time the liquid begins to boil uniformly and the thermometer readings become constant.

The boiling point, and the manometer reading in millimeters of mercury, are then recorded. After the first readings have been taken the heating is stopped and air is carefully admitted into the system to a definite pressure. The stopcock is then closed and the procedure described above is repeated. The manometer readings are corrected for the glass scale and temperature.

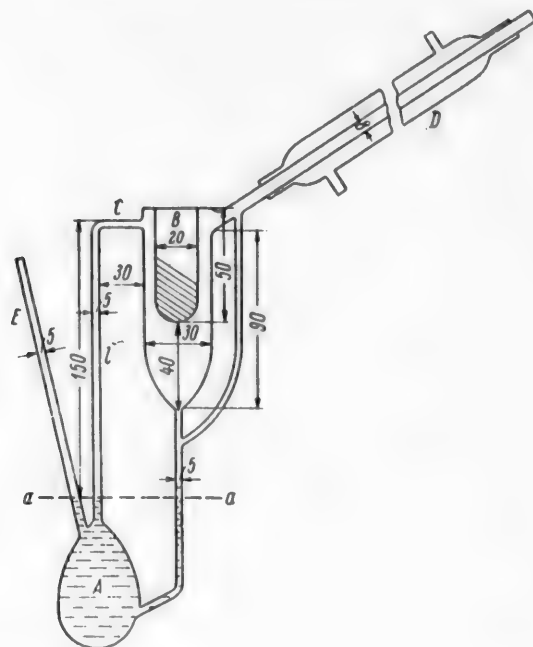


Fig. 2. Ebullioscope.
Explanations in text.

To test the apparatus, the vapor pressures of chemically pure sulfuryl chloride and carbon tetrachloride were determined. The results were in complete agreement with the data obtained by Trautz [3] and Young [4] for these substances (Table 2).

The effects of pressure on the boiling points of sulfuryl chloride and carbon tetrachloride are shown in Fig. 3.

The system sulfuryl chloride + carbon tetrachloride. The method described above was used to measure the total vapor pressures of binary mixtures of chemically pure sulfuryl chloride and carbon tetrachloride, of the following compositions (wt. %): 90 SO_2Cl_2 + 10 CCl_4 ; 70 SO_2Cl_2 + 30 CCl_4 ; 50 SO_2Cl_2 + 50 CCl_4 .

TABLE 2

Variations of the Vapor Pressure of Pure Sulfuryl Chloride with the Temperature

t (°C)	P (mm Hg)	T (°K)	$\frac{1}{T} \cdot 10^3$	log P
0	40.9	27.3	366	1.6117
11.5	69.1	284.5	351.5	1.8995
18.0	95.2	291	344.0	1.9786
26.0	149.1	299.0	334.0	2.1796
34.9	217.0	308.0	325.0	2.3365
38.0	242.0	311.0	321.6	2.3838
42.9	300.0	315.9	316.6	2.4771
46.1	341.0	319.1	313.0	2.5327
52.6	426.0	325.6	307.0	2.6294
55.4	470.0	328.4	304.5	2.6721
57.7	512.0	330.7	302.4	2.7093
60.0	556.0	333.1	300.2	2.7051
62.9	614.0	335.9	297.7	2.7882
64.9	656.0	337.9	295.9	2.8169
66.9	701.0	340.0	294.1	2.8457
69.5	767.0	342.6	291.9	2.8848

TABLE 3

Variations of the Vapor Pressures of Mixtures of Sulfuryl Chloride with Tetrachloroethane and Dichloroethane with the Temperature

t (°C)	P (mm Hg)	T (°K)	$\frac{1}{T} \cdot 10^3$	log P	t (°C)	P (mm Hg)	T (°K)	$\frac{1}{T} \cdot 10^3$	log P
80% SO ₂ Cl ₂ + 20% C ₂ H ₂ Cl ₄ *					30% SO ₂ Cl ₂ + 70% C ₂ H ₂ Cl ₄ *				
27.8	130.2	301.0	332.2	2.11461	59.2	199.9	332.4	300.8	2.30081
32.5	159.8	305.7	327.1	2.20358	63.3	233.6	336.5	297.2	2.34947
40.8	224.2	314.0	318.5	2.35064	68.3	269.3	341.5	293.7	2.42862
49.3	311.3	322.5	310.1	2.49318	72.9	314.7	346.1	288.9	2.49790
53.9	365.6	327.1	305.7	2.56301	77.2	366.2	350.4	285.4	2.56372
59.3	414.1	332.3	300.9	2.61711	80.8	402.3	354.0	282.5	2.60455
62.7	499.1	335.9	297.7	2.69819	84.3	450.7	357.5	279.7	2.65389
63.9	609.2	342.1	292.3	2.78476	88.4	512.5	361.6	276.5	2.70969
72.1	674.5	345.3	289.6	2.82898	91.9	570.5	365.1	273.9	2.75626
75.6	753.5	348.8	286.7	2.87708	97.7	670.7	370.9	269.9	2.82653
					102.3	758.3	375.5	266.3	2.87984
50% SO ₂ Cl ₂ + 50% C ₂ H ₂ Cl ₄ *					100% C ₂ H ₂ Cl ₄ *				
33.4	109.3	306.4	325.3	2.0386	66.0	47.3	339.2	294.8	1.67943
40.1	143.2	313.1	319.3	2.1559	74.9	70.8	348.1	287.3	1.85003
46.1	182.0	319.1	313.4	2.2601	81.4	101.4	354.0	280.0	2.00664
51.5	220.1	324.5	308.1	2.3426	88.6	123.3	361.8	276.4	2.0909
56.5	267.6	329.5	303.5	2.4275	94.1	152.3	367.3	272.3	2.18270
60.7	313.0	333.7	299.7	2.4955	102.0	200.4	375.2	266.5	2.30190
65.7	370.6	338.7	295.2	2.5689	110.1	266.7	383.3	260.9	2.42602
69.7	423.5	342.7	291.8	2.6268	116.6	328.5	389.8	256.5	2.5165
73.2	475.1	346.2	288.8	2.6763	123.3	409.5	396.5	252.2	2.61225
77.9	552.5	350.9	284.9	2.7423	128.7	486.9	401.9	248.8	2.68744
81.0	606.0	354.0	282.5	2.7825	137.0	623.7	410.2	243.8	2.79498
86.0	706.9	359.0	278.5	2.8494	143.8	761.7	417.0	239.8	2.88178

* Percentages by weight.

The results obtained for the mixture 50% SO₂Cl₂ + 50% CCl₄ are shown graphically in Fig. 3.

It follows from the results that additions of 10 to 50 wt. % of carbon tetrachloride to sulfuryl chloride do not lower the total vapor pressure of the mixtures (Fig. 3).

It is interesting to note that the vapor-pressure curve of pure carbon tetrachloride lies considerably below the vapor-pressure curve of pure sulfuryl chloride, and the latter almost coincides with the vapor-pressure curves

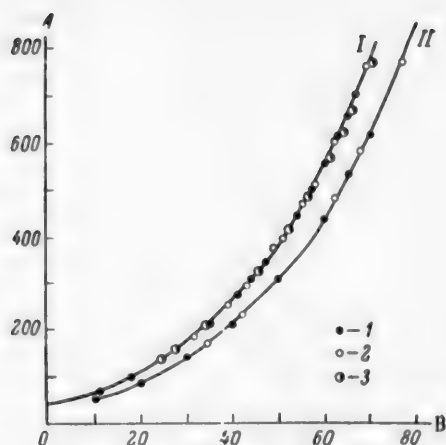


Fig. 3. Effect of pressure on the boiling points of sulfuryl chloride and carbon tetrachloride.

A) Pressure (mm Hg), B) temperature (°C).

Curves: I) SO_2Cl_2 , II) CCl_4 .

1) Data of Trautz for SO_2Cl_2 and Young for CCl_4 .

2) our data for SO_2Cl_2 and CCl_4 , 3) our data for the system 50% SO_2Cl_2 + 50% CCl_4 .

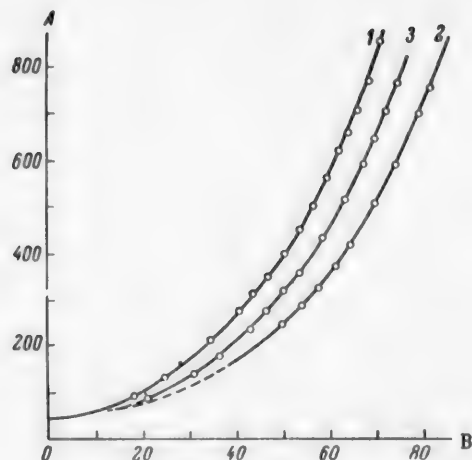


Fig. 4. Effect of pressure on the boiling points of sulfuryl chloride (1), dichloroethane (2), and their 1:1 mixture (3).

A) Pressure (mm Hg), B) boiling point (°C).

of its binary mixtures with carbon tetrachloride containing from 10 to 50 wt. % of the latter (Fig. 3).

The system sulfuryl chloride + dichloroethane.

Binary mixtures consisting of chemically pure sul-

furyl chloride and dichloroethane of the following compositions (in wt. %) were investigated: 90 SO_2Cl_2 + 10 $\text{C}_2\text{H}_4\text{Cl}_2$; 70 SO_2Cl_2 + 30 $\text{C}_2\text{H}_4\text{Cl}_2$; 50 SO_2Cl_2 + 50 $\text{C}_2\text{H}_4\text{Cl}_2$; 100 $\text{C}_2\text{H}_4\text{Cl}_2$.

The results of the determinations are given in Fig. 4.

It follows from these results that additions of 10 to 50 wt. % of dichloroethane to sulfuryl chloride lower not only the partial vapor pressure of sulfuryl chloride, but the total vapor pressure of the mixture.

In fact, if we consider the mixture consisting of 50% sulfuryl chloride and 50% dichloroethane, we see that at 25° the total vapor pressure is lowered from 144 to 107 mm Hg, i.e., by about 25%. At 40° the vapor pressure is lowered from 265 to 211 mm, which is a lowering of the total vapor pressure by about 20%. The same is found at higher temperatures.

The boiling point of the 50% mixture at 760 mm (75.5°) is 6.1° higher than the boiling point of pure sulfuryl chloride (69.4°).

The system sulfuryl chloride-tetrachloroethane. Binary mixtures consisting of chemically pure sulfuryl chloride and tetrachloroethane of the following composition (in wt. %) were studied: 80 SO_2Cl_2 + 20 $\text{C}_2\text{H}_2\text{Cl}_4$; 50 SO_2Cl_2 + 50 $\text{C}_2\text{H}_2\text{Cl}_4$; 30 SO_2Cl_2 + 70 $\text{C}_2\text{H}_2\text{Cl}_4$; 100 $\text{C}_2\text{H}_2\text{Cl}_4$.

The results of the vapor-pressure determinations are given in Table 3.

The results (Fig. 5) show that addition of tetrachloroethane to sulfuryl chloride produces a considerable lowering of the total vapor pressure of the mixture.

Let us consider the system consisting of 50% SO_2Cl_2 + 50% $\text{C}_2\text{H}_2\text{Cl}_4$. At 40° the total vapor pressure is lowered from 265 to 143 mm, which corresponds to a 45% lowering of the total vapor pressure, whereas in the case of dichloroethane the corresponding lowering was only 20%. The same is found at higher temperatures. The boiling point of a 50% mixture at 760 mm (88.5°) is 19.1° higher than the boiling point of pure sulfuryl chloride (69.4°), whereas in the case of dichloroethane the difference of boiling points was 6.1°. These results are significant for our purpose, and we shall therefore consider the physicochemical properties of this system in detail.

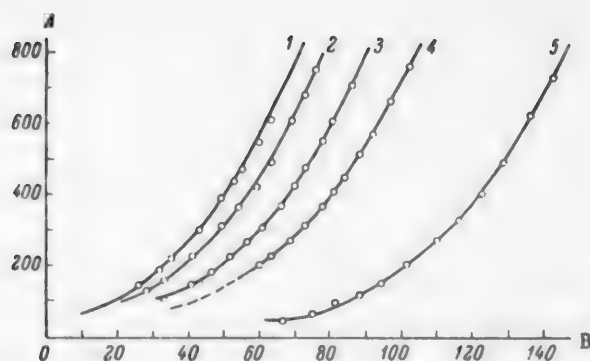


Fig. 5. Effect of pressure on the boiling points of sulfuryl chloride, tetrachloroethane, and their mixtures.

A) Pressure (mm Hg), B) boiling point ($^{\circ}\text{C}$).

Curves: 1) SO_2Cl_2 , 2) 80% SO_2Cl_2 + 20% $\text{C}_2\text{H}_2\text{Cl}_4$, 3) 50% SO_2Cl_2 + 50% $\text{C}_2\text{H}_2\text{Cl}_4$, 4) 30% SO_2Cl_2 + 70% $\text{C}_2\text{H}_2\text{Cl}_4$.

5) 100% $\text{C}_2\text{H}_2\text{Cl}_4$.

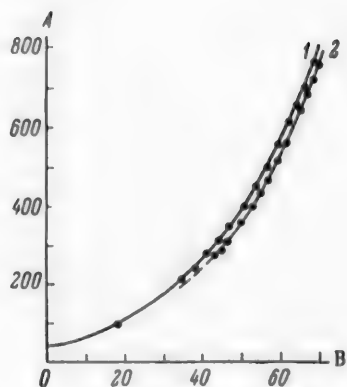


Fig. 6. Effect of pressure on the boiling points of sulfuryl chloride and its mixture with hexachloroethane.

A) Pressure (mm Hg), B) boiling point ($^{\circ}\text{C}$).

Curves: 1) SO_2Cl_2 , 2) 80% SO_2Cl_2 + 20% C_2Cl_6 .

The system sulfuryl chloride-hexachloroethane. As the effect of tetrachloroethane as a solvent lowering the vapor pressure was greater than that of dichloroethane, it was expected that hexachloroethane, which is more highly chlorinated and has a higher boiling point (185°) should form even less volatile mixtures.

It was found, however, that the solubility of solid hexachloroethane in sulfuryl chloride at room temperature (15°) is restricted to about 20%. Therefore binary mixtures of chemically pure sulfuryl chloride and hexachloroethane of the following compositions (in wt. %) were investigated: 91 SO_2Cl_2 + 9 C_2Cl_6 , 80 SO_2Cl_2 + 20 C_2Cl_6 .

The results of the determinations are given in Fig. 6.

Examination of the results shows that our expectations were not fulfilled. Addition of 20% hexachloroethane lowers the total vapor pressure of the mixture much less than the same addition of tetrachloroethane.

DISCUSSION OF RESULTS

First we consider the system sulfuryl chloride-tetrachloroethane. It is necessary to find the partial vapor pressures of the individual components of mixtures of different compositions at various temperatures, and to determine the compositions of the gas phase corresponding to different liquid-phase compositions. Data on the total vapor pressure of a mixture give an idea of the tendency of the mixture to evaporate. Data on the partial vapor pressures and vapor compositions indicate what is being evaporated from the mixtures, and in what proportions (under equilibrium conditions). Such data can be found by calculation only if the given system obeys Raoult's law at least approximately, i.e., if it forms solutions close to ideal in behavior.

Earlier it was stated that it was likely that these solutions are close to ideal. The question can be finally settled by consideration of the vapor-pressure data now available. For this it is necessary to plot the vapor pressure-composition isotherm. The method used for determinations of vapor pressure cannot be used to measure small vapor pressures. Therefore we do not have data necessary for plotting the isotherms in the $0-40^{\circ}$ range with which we are concerned.

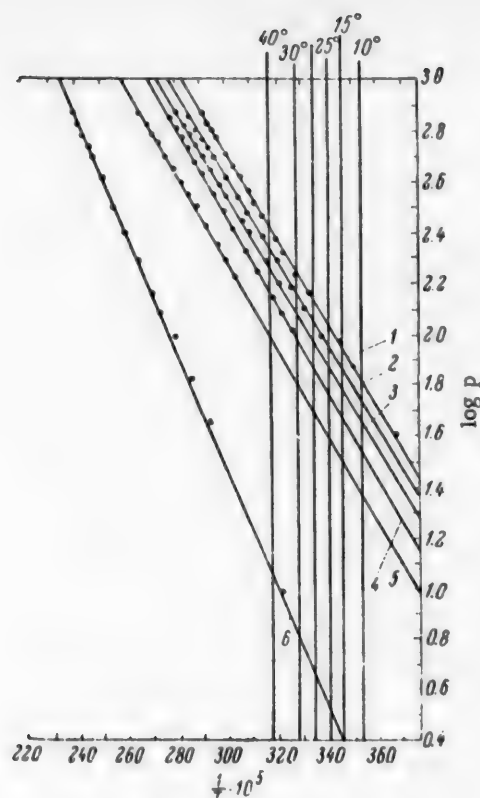


Fig. 7. Effect of temperature on the vapor pressures of mixtures of sulfuryl chloride with tetrachloroethane and dichloroethane.

Composition of $\text{SO}_2\text{Cl}_2 + \text{C}_2\text{H}_4\text{Cl}_2$ mixtures (in wt. %):

1) 100 + 0, 2) 50 + 50, 3) 0 + 100.

Composition of $\text{SO}_2\text{Cl}_2 + \text{C}_2\text{H}_2\text{Cl}_4$ mixtures (in wt. %):

4) 50 + 50, 5) 30 + 70, 6) 0 + 100.

represented by straight lines, in harmony with the Clausius-Clapeyron equation.

Figure 7 could therefore be used for fairly reliable extrapolation to 10, 20, 25, 30, and 40°. Further extrapolation to lower temperatures is also possible, but it is naturally less reliable. The corresponding data are given in Table 4 (P is in mm Hg and the composition in wt. %).

The results are plotted in the form of isotherms in Fig. 8.

Figure 8 shows that the isotherms for the total vapor pressure deviate only slightly from linearity, i.e., the system approximately conforms to Raoult's law. This makes it possible to make simple calculations of the partial pressures of the components.

Since tetrachloroethane has a low vapor pressure in comparison with sulfuryl chloride, it is highly probable that the plot of the partial vapor pressure P_B of tetrachloroethane is linear. If so, the partial vapor pressure P_A of sulfuryl chloride can readily be found from the difference between the total vapor pressure of the mixture and the partial pressure of tetrachloroethane vapor.

$$P_A = P - P_B.$$

The partial pressures calculated by this method are plotted in the form of isotherms in Fig. 9; it is seen that the partial pressure of sulfuryl chloride increases rapidly with increasing mole fraction of sulfuryl chloride in the mixture.

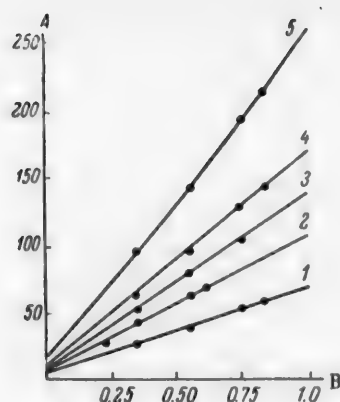


Fig. 8. Isotherms for the variation of the total vapor pressure of the system $\text{SO}_2\text{Cl}_2 + \text{C}_2\text{H}_2\text{Cl}_4$ with the mole fraction of SO_2Cl_2 .

A) Pressure (mm Hg), B) mole fraction of SO_2Cl_2 .

Temperature (°C): 1) 10, 2) 20, 3) 25, 4) 30, 5) 40.

To obtain vapor-pressure data for the mixtures in this temperature range, extrapolation is necessary; this is quite permissible in this case. Calculation diagrams were plotted for this purpose.

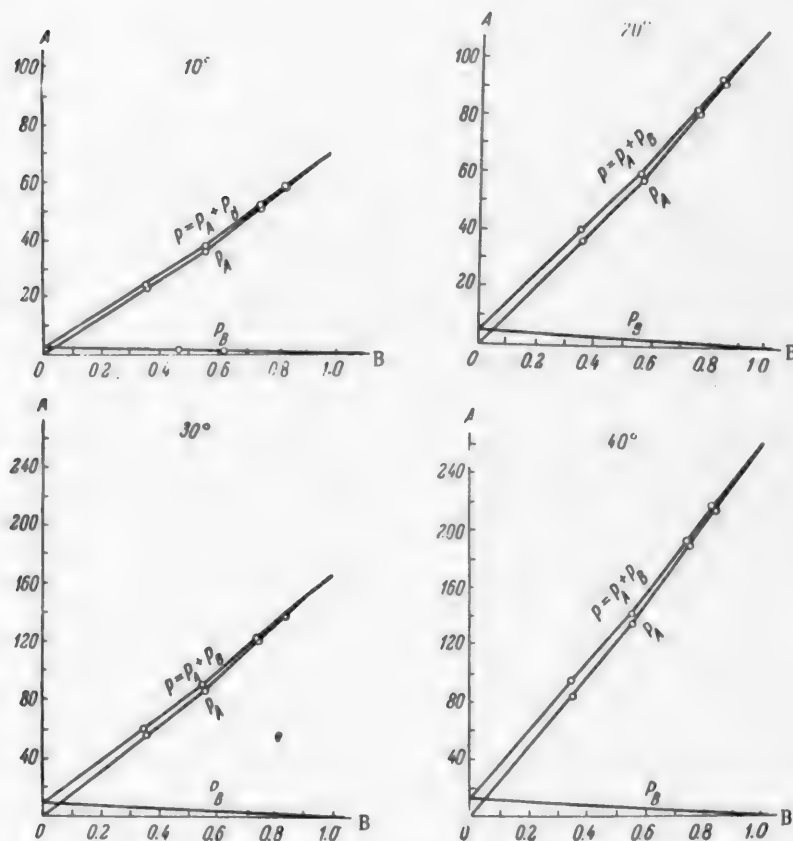
The experimental data in Tables 2 and 3 were used to calculate values of $1/T \cdot 10^{-5}$ (where T is the absolute temperature on the Kelvin scale); these were plotted against the logarithms of the pressures in Fig. 7. The corresponding data are given in Table 3.

In the narrow temperature range under consideration the relationship between $\log P$ and $1/T \cdot 10^{-5}$ is

TABLE 4

Variation of Vapor Pressure of the Mixtures with Temperature

Temperature (°C)	100% C_2H_5Cl		30% SO_2Cl_2 + +70% C_2H_5Cl		50% SO_2Cl_2 + +50% C_2H_5Cl		70% SO_2Cl_2 + +30% C_2H_5Cl		80% SO_2Cl_2 + +20% C_2H_5Cl		100% SO_2Cl_2	
	Mole fraction of SO_2Cl_2 0.000		Mole fraction of SO_2Cl_2 0.346		Mole fraction of SO_2Cl_2 0.553		Mole fraction of SO_2Cl_2 0.744		Mole fraction of SO_2Cl_2 0.833		Mole fraction of SO_2Cl_2 1.00	
	log P	P	log P	P	log P	P	log P	P	log P	P	log P	P
10	0.400	2.51	1.395	24.8	1.570	37.2	1.710	51.3	1.765	58.2	1.836	68
20	0.661	4.58	1.605	40.3	1.780	60.3	1.915	82.2	1.967	92.7	2.045	111
25	0.790	6.17	1.709	51.2	1.880	75.9	2.013	103	2.065	116	2.145	140
30	0.905	8.04	1.797	62.7	1.970	93.4	2.102	126	2.155	143	2.235	172
40	1.140	18.8	1.980	95.5	2.155	143.0	2.285	193	2.335	216	2.423	265

Fig. 9. Isotherms for the total vapor pressure of the system $SO_2Cl_2 + C_2H_4Cl_4$ as a function of the mole fraction of SO_2Cl_2 .A) Pressure (in mm Hg), B) mole fraction of SO_2Cl_2 .

For example, the total vapor pressure of the system containing 50% (molar) of sulfuryl chloride and 50% (molar) of tetrachloroethane is 55 mm Hg at 20°; of this, the partial pressure of tetrachloroethane vapor is 2.5 mm, and the partial pressure of sulfuryl chloride vapor under these conditions is 52.5 mm.

It is very useful to know the composition of the gas phase corresponding to a liquid mixture of a particular composition, at a given temperature.

The composition of the vapor phase is calculated from the equation

$$N_{\text{SO}_2\text{Cl}_2} = \frac{P_{\text{SO}_2\text{Cl}_2}}{P}$$

where $N_{\text{SO}_2\text{Cl}_2}$ is the mole fraction of SO_2Cl_2 in the vapor of the binary mixture, P is the total vapor pressure of the mixture, and $P_{\text{SO}_2\text{Cl}_2}$ is the partial pressure of SO_2Cl_2 vapor (in mm Hg).

The values of P for different temperatures and compositions, taken from Fig. 7, are given in Table 5; Table 5 was used to plot the graphs in Fig. 10.

The calculated values of $N_{\text{SO}_2\text{Cl}_2}$ for mixtures of different compositions were used to plot liquid-vapor composition isotherms (in mole fractions). The same relationship, but expressed in weight percentages, is given in Table 6.

TABLE 5

Variation of Vapor Composition with the Composition of the Liquid Phase

$\gamma_{\text{SO}_2\text{Cl}_2}^*$	P	$P_{\text{SO}_2\text{Cl}_2}$	$N_{\text{SO}_2\text{Cl}_2}$	$\gamma_{\text{SO}_2\text{Cl}_2}^*$	P	$P_{\text{SO}_2\text{Cl}_2}$	$N_{\text{SO}_2\text{Cl}_2}$
Temperature 40°				Temperature 20°			
1.00	265	265	1.00	1.00	111	111	1.00
1.833	216	214	0.993	0.833	92.7	92.1	0.992
0.744	193	189	0.982	0.744	83.2	81.2	0.988
0.553	143	136	0.951	0.553	60.3	58.0	0.961
0.348	95.5	85.8	0.897	0.348	40.3	36.5	0.904
0.200	60.8	48.5	0.800	0.200	24.7	20.7	0.836
0.10	37.0	23.5	0.640	0.100	14.5	10.3	0.711
Temperature 30°				Temperature 10°			
1.00	172	172	1.00	1.00	68.6	68.6	1.00
0.833	143	141.5	0.99	0.833	58.2	57.7	0.998
0.744	126	124	0.983	0.744	51.3	50.3	0.983
0.553	93.4	89.4	0.974	0.553	37.2	36.0	0.968
0.348	68.7	56.7	0.904	0.348	24.8	23.0	0.928
0.000	0.00	8.04	0.000	0.200	15.0	13.0	0.867
				0.100	8.6	6.4	0.744
				0.00	2.51	0.00	0.00

* $\gamma_{\text{SO}_2\text{Cl}_2}$ is the mole fraction of SO_2Cl_2 in the liquid.

TABLE 6

Variation of Vapor Composition with the Composition of the Liquid Phase

SO_2Cl_2 (in wt. %)	$\gamma_{\text{SO}_2\text{Cl}_2}$	10°		20°		40°	
		$N_{\text{SO}_2\text{Cl}_2}$	SO_2Cl_2 (in wt. %)	$N_{\text{SO}_2\text{Cl}_2}$	SO_2Cl_2 (in wt. %)	$N_{\text{SO}_2\text{Cl}_2}$	SO_2Cl_2 (in wt. %)
70	0.833	0.993	99.1	0.993	99.1	1.991	93.3
60	0.744	0.990	98.5	0.987	98.0	0.908	97.5
50	0.563	0.970	96.5	0.965	95.7	0.950	94.0
30	0.348	0.930	91.5	0.905	88.5	0.890	86.5
20	0.240	0.885	86.0	0.855	82.5	0.835	80.0
15	0.165	0.855	82.5	0.825	79.0	0.795	75.5
10	0.126	0.785	74.0	0.750	70.6	0.710	66.5
5	0.060	0.595	54.0	0.520	48.5	0.460	40.5

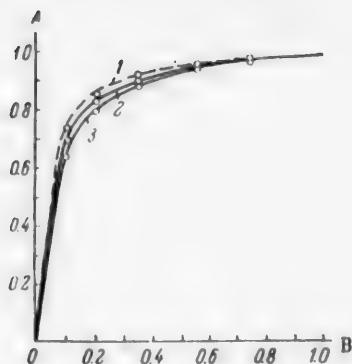


Fig. 10. Variation of vapor composition with composition of the liquid phase (in mole fractions).
A) Mole fraction of SO_2Cl_2 in vapor,
B) mole fraction of SO_2Cl_2 in liquid.
Temperature ($^{\circ}\text{C}$): 1) 10, 2) 20, 3) 40.

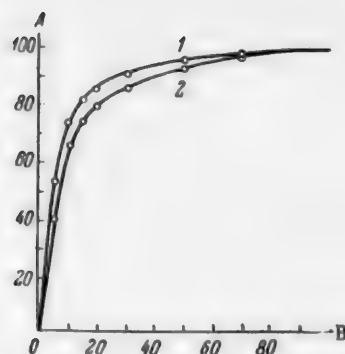


Fig. 11. Variation of vapor composition with composition of the liquid phase (in wt. %).
A) Content of SO_2Cl_2 in vapor (in wt. %), B) content of SO_2Cl_2 in liquid phase (in wt. %). Temperature ($^{\circ}\text{C}$): 1) 10, 2) 40.

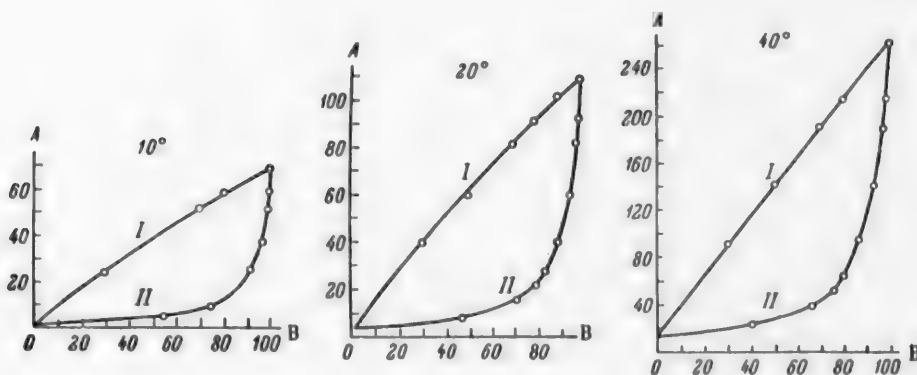


Fig. 12. Variations of total vapor pressure of the system SO_2Cl_2 - $\text{C}_2\text{H}_2\text{Cl}_4$ with the compositions of the liquid and vapor phases at constant temperature.
A) Pressure (in mm Hg), B) SO_2Cl_2 content (in wt. %). Curves: I) liquid, II) vapor.

It follows from the isotherms in Fig. 11 that the composition of the vapor phase of sulfuryl chloride-tetrachloroethane mixtures depends little on the temperature, and that the content of sulfuryl chloride is much higher in the vapor than in the liquid phase. When the liquid phase contains between 20 and 100 wt. % of sulfuryl chloride, the vapor consists almost entirely of sulfuryl chloride.

When the liquid phase contains 50 wt. % of sulfuryl chloride, the vapor at the same temperature contains 96%.

However, a somewhat different situation may arise in the course of evaporation of mixtures, as the mixture will become enriched (especially at the surface) with the less volatile tetrachloroethane as the more volatile sulfuryl chloride evaporates. Because of this, the amount of sulfuryl chloride evaporated may be decreased with its decreasing concentration.

Graphs showing simultaneously the variations of the total vapor pressure of mixtures with the composition of both the liquid and the vapor phases at constant temperature are useful for indicating variations of the composition of a mixture in the course of evaporation.

Figure 12 shows graphs of this type for 10, 20, and 40°. In these diagrams the Curves I are of the same type as in Fig. 8, but the weight percentages are not mole fractions of SO_2Cl_2 and are taken along the abscissa axis. Curves II represent the total vapor pressure as a function of the percentage composition of the vapor phase. These calculations were made with the aid of auxiliary Table 6 and Fig. 13, used for conversion of compositions given in mole fractions into weight percentages and vice versa.

Similar calculations were performed for the system consisting of 50% sulfuryl chloride and 50% dichloroethane.

Figure 7 shows the logarithms of the vapor pressure plotted against $\frac{1}{T} \cdot 10^{-5}$ for the mixture of 50% SO_2Cl_2 + 50% $\text{C}_2\text{H}_4\text{Cl}_2$ and for pure dichloroethane; the plots are linear, in accordance with the Clausius-Clapeyron equation.

It is interesting to note that the lines for the mixtures 50% SO_2Cl_2 + 50% $\text{C}_2\text{H}_4\text{Cl}_2$ and 80% SO_2Cl_2 + 20% $\text{C}_2\text{H}_4\text{Cl}_2$ exactly coincides. The extreme points of these two lines, corresponding to temperatures close to 0°, fit well on the straight lines, so that log P for this temperature can be found by direct interpolation from the following data:

P	t	T	$\frac{1}{T} \cdot 10^5$	log P
Dichloroethane				
204.7	45.2	318.4	314.1	2.3114
246.6	50.02	323.2	309.4	2.3920
285.5	54.27	327.5	305.3	2.4556
325.4	57.82	331.0	302.1	2.5124
369.3	61.54	334.7	298.7	2.5671
415.7	64.79	338.0	295.8	2.6187
497.1	70.07	343.3	291.8	2.6965
584.88	74.96	348.0	287.1	2.7670
664.2	78.89	352.1	284.0	2.8223
747.0	82.00	355.7	281.1	2.8733
50 SO_2Cl_2 + 50 dichloroethane (in wt. %)				
90.65	21.0	294.2	339.9	2.0579
144.38	31.0	304.2	328.7	2.1596
181.78	36.4	309.6	324.9	2.2596
232.53	43.5	316.7	315.7	2.3664
273.03	46.4	319.6	312.8	2.4362
316.03	50.4	323.6	309.0	2.4997
357.27	53.9	327.1	305.7	2.5531
429.37	59.00	332.2	301.0	2.6329
512.2	64.00	337.2	296.5	2.7095
588.35	68.05	341.25	293.0	2.7697
639.75	70.5	343.7	290.9	2.8060
698.5	73.05	346.25	288.8	2.8444
758.4	75.5	348.8	286.7	2.8807

Figure 14 gives isotherms for the total vapor pressure of the system SO_2Cl_2 + $\text{C}_2\text{H}_4\text{Cl}_2$ and the partial vapor pressures of sulfuryl chloride and dichloroethane at 40°. They are all almost linear. Therefore this system conforms closely to Raoult's law at all concentrations.

The isothermal values of partial vapor pressure of sulfuryl chloride were obtained by multiplication of the total vapor pressure by the mole fraction of sulfuryl chloride in the vapor, which was calculated from the formula for ideal mixtures.

$$N_{\text{SO}_2\text{Cl}_2} = \frac{\alpha \cdot \gamma_{\text{SO}_2\text{Cl}_2}}{1 + (\alpha - 1) \gamma_{\text{SO}_2\text{Cl}_2}},$$

where $N_{\text{SO}_2\text{Cl}_2}$ is the mole fraction of sulfuryl chloride in the vapor, $\alpha = \frac{P_{\text{SO}_2\text{Cl}_2}^0}{P_{\text{C}_2\text{H}_4\text{Cl}_2}^0}$ is the relative volatility of sulfuryl chloride at the given temperature, $P_{\text{SO}_2\text{Cl}_2}^0$ and $P_{\text{C}_2\text{H}_4\text{Cl}_2}^0$ are the saturated vapor pressures of pure sulfuryl

chloride and dichloroethane at the given temperature, and $\gamma_{\text{SO}_2\text{Cl}_2}$ is the mole fraction of sulfuryl chloride in the liquid phase.

TABLE 7

Data for Calculation of Partial Pressures of SO_2Cl_2 Vapor in the System Sulfuryl Chloride + Dichloroethane

Temperature (°C)	Content of SO_2Cl_2 in liquid phase (in wt. %)	Mole fraction of SO_2Cl_2			Total vapor pressure of mixture (experimental)	Partial vapor pressure of SO_2Cl_2 (cal- culated)
		in liquid phase	in vapor (calculated)	in vapor (experimental)		
15	100	1.0	1.0	—	86.3	—
	80	0.743	0.810	—	—	—
	70	0.630	0.724	—	—	—
	50	0.422	0.529	0.559	—	—
	30	0.239	0.327	—	—	—
40	100	1.0	1.0	—	264.0	—
	80	0.743	0.820	—	244.8	201.9
	70	0.630	0.727	—	231.1	168.0
	50	0.422	0.533	—	210.7	112.3
	30	0.239	0.529	—	—	—

The corresponding calculation data are given in Table 7. The partial vapor pressures of dichloroethane were found by difference between the total vapor pressure and the partial vapor pressure of sulfuryl chloride.

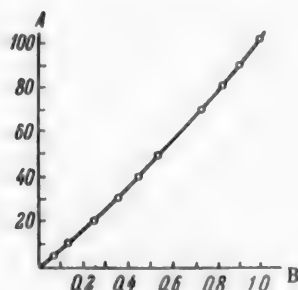


Fig. 13. Graph for conversion of compositions given in mole fractions into weight percentages.

A) Content of SO_2Cl_2 (wt. %), B) content of SO_2Cl_2 (mole fractions).

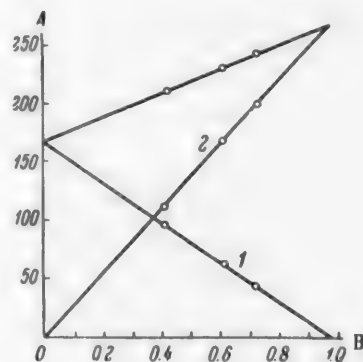


Fig. 14. Total vapor pressure isotherms for the system $\text{SO}_2\text{Cl}_2 + \text{C}_2\text{H}_4\text{Cl}_2$ at 40° , and partial vapor pressures of sulfuryl chloride (2) and dichloroethane (1).

A) Pressure (mm Hg), B) mole fraction of SO_2Cl_2 .

Figure 14 shows that the calculated partial pressures fit almost exactly on straight lines, in harmony with the almost linear course of the total vapor-pressure isotherm.

For the system containing 50% of sulfuryl chloride ($\gamma_{\text{SO}_2\text{Cl}_2} = 0.422$) and 50% of dichloroethane the total vapor pressure of the mixture at 40° is 211 mm, the partial pressure of sulfuryl chloride is 112 mm, and the partial pressure of dichloroethane is 99 mm. Therefore the relative content of sulfuryl chloride in the vapor phase is lower in its mixtures with dichloroethane than in its mixtures with tetrachloroethane. It must be remembered, however, that the total vapor pressure of a 50% mixture of sulfuryl chloride with dichloroethane at 40° is about 75-80% of the vapor pressure of sulfuryl chloride. Therefore it is to be expected that the complete evaporation

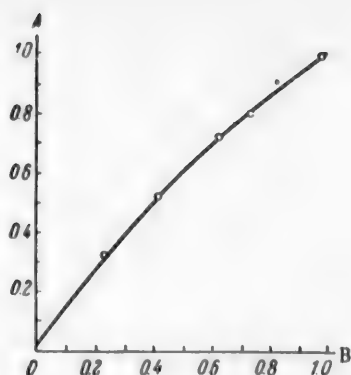


Fig. 15. Variation of vapor composition with composition of the liquid phase for the system $\text{SO}_2\text{Cl}_2\text{-C}_2\text{H}_4\text{Cl}_2$ at 15 and 40°. A) Mole fraction of SO_2Cl_2 vapor phase, B) mole fraction of SO_2Cl_2 in liquid phase.

In view of the great importance of data on the vapor-phase compositions of mixtures of sulfuryl chloride with various solvents, it was necessary to verify the degree to which the calculated data on vapor-phase compositions agree with the experimental values. The calculations were therefore checked experimentally for several mixtures.

Apparatus for determination of vapor compositions was assembled for this purpose. A diagram of the apparatus is given in Fig. 16.

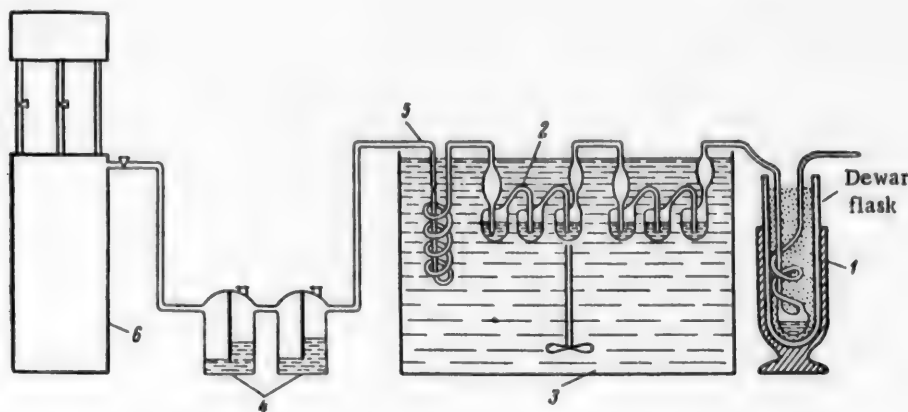


Fig. 16. Apparatus for determination of vapor composition. Explanations in text.

The apparatus consists of the following parts: receiver 1 for condensation of the vapor, immersed in a Dewar flask with freezing mixture (-20°); two sets of potash bulbs 2, in series, immersed in a water thermostat 3; traps 4 for drying the air; glass spiral 5; and gas holder 6.

The apparatus operates as follows. Both sets of potash bulbs are filled with the liquid to be investigated, and then connected to the receiver. Dry air is passed at a definite rate through the bulbs immersed in the water thermostat; the air first enters the glass spiral immersed in the water thermostat where it is heated to the required temperature. The air becomes saturated with vapor in the bulbs, the saturated vapor passed into the receiver, and is condensed there.

The duration of the experiment was such that enough liquid was collected in the receiver for analysis (about 0.5-0.8 g). The sulfuryl chloride content was determined by the method used for pure sulfuryl chloride.

The results of the check analyses are given in Table 8.

TABLE 8
Results of Analyses

Composition of mixture (in wt. %)	Wt. taken for deter- mination of SO_2Cl_2 (in g.)	SO_2 found (wt. %)	Wt. taken for determi- nation of SO_2Cl_2 (in g.)	SO_2Cl_2 found (wt. %)
Sulfuryl chloride 100	0.6250 0.6461 0.6720	2.89 2.87 2.99	0.6997 0.6796 0.6155	95.05 95.29 95.56
Sulfuryl chloride + + dichloroethane 50	0.6385 0.6242	1.45 1.42	1.2357 1.4109	48.52 48.15
Sulfuryl chloride + di- chloroethane 50.37	1.8387 1.5492	0.96 0.90	2.0794 1.8795	48.03 48.08
Sulfuryl chloride + di- chloroethane 50.74	1.5230 1.1597 1.3440	1.09 1.09 1.02	1.3155 1.2163 1.2687	49.09 49.10 48.42

Table 8 shows that the contents of sulfuryl chloride found in the mixtures are somewhat higher than the analytical data. The reason for this discrepancy was not studied, and requires special investigation, although these analytical errors are of no practical significance for our purposes.

In view of the particular interest which attaches to the system $\text{SO}_2\text{Cl}_2 + \text{C}_2\text{H}_4\text{Cl}_2$, the calculated vapor-composition data for a mixture of 50% sulfuryl chloride and 50% tetrachloroethane were verified first.

The calculated and experimentally determined contents of sulfuryl chloride in the vapor are given in Table 9.

For a mixture of 15% SO_2Cl_2 and 85% tetrachloroethane at 40°, the calculated content of sulfuryl chloride in the vapor is 75.5%, and the amount found experimentally is 73.2%.

These results show that the calculated and experimental values are in fairly good agreement.

TABLE 9
Calculated and Experimental Contents of SO_2Cl_2 in Vapor

Temperature (°C)	Calculated		Experimentally found SO_2Cl_2 content in vapor (wt. %)	
	mole fraction of SO_2Cl_2 in vapor	content of SO_2Cl_2 in vapor (wt. %)	in individual experiments	average
10	0.968	96.3	96.6 94.0 95.2	96.6
40	0.951	94.0		94.6

The existing discrepancies between the calculated and experimental values are probably caused by errors in the analytical determination of sulfuryl chloride in the mixtures.

A check of the calculated values for the composition of the vapor of a mixture of 50% dichloroethane and 50% sulfuryl chloride at 15° gave satisfactory results (Table 8).

The calculated mole fraction of sulfuryl chloride in the vapor was 0.53 (60.59 wt. %). The experimental value was 0.56.

Despite some inaccuracy in the analytical data, the calculated data on the vapor composition are largely in agreement with the experimental data.

SUMMARY

1. Liquid-vapor equilibria were studied in binary systems consisting of sulfuryl chloride and each of the following solvents: carbon tetrachloride, dichloroethane, tetrachloroethane, and hexachloroethane; the temperature-total vapor pressure relationships were determined for different compositions in these systems; the total and partial vapor pressures as functions of the liquid and vapor composition at various temperatures were calculated; vapor-liquid composition curves for these systems were plotted; the calculated vapor-phase compositions were verified experimentally, and it was shown that the experimental values are in satisfactory agreement with the calculated data.

2. It is shown that sulfuryl chloride and the solvents studied form solutions which are nearly ideal, i.e., the partial pressure of sulfuryl chloride vapor may be represented by the equation (by Raoult's law)

$$P_1 = P_1^0 \cdot \gamma_1,$$

where P_1 is the partial pressure of sulfuryl chloride vapor, P_1^0 is the vapor pressure of pure sulfuryl chloride, and γ_1 is its mole fraction in solution.

It follows from this equation that in the solutions studied the partial pressure of sulfuryl chloride vapor depends only on its mole fraction and not on the nature of the second component (solvent). The influence of all the solvents studied on sulfuryl chloride is almost the same in this respect. Differences in the action of different solvents consist only of differences in their partial vapor pressures, and hence of total vapor pressures of the solutions.

3. It was found that the greatest lowering of the total vapor pressure on addition of a second component to sulfuryl chloride is found in the system sulfuryl chloride-tetrachloroethane.

The authors express their deep gratitude to S. A. Shchukarev, B. P. Nikol'skii, and Ia. V. Durdin for their interest and valuable advice.

LITERATURE CITED

- [1] Chemist's Reference Book, 2 (Goskhimizdat, 1951).*
- [2] W. Swietoslowski, *Rocznik Chemie*, 9 (1929).
- [3] M. Trautz, *Z. Electroch.*, 14, 271 and 534 (1908).
- [4] S. Young, *J. Chem. Soc.*, 59, 911 (1891).

Received June 15, 1956

*In Russian.

ACTION OF OXIDIZING AGENTS ON HUMIC SUBSTANCES OF THE WATER FROM THE RIVER DNEPR

M. A. Shevchenko

The color of the water in the river Dnepr is caused by the presence of humic substances which are removed by treatment with coagulants. This process is based on the adsorption of the coloring matter on aluminum hydroxide floc. The residual color of the purified water is due to the equilibrium concentration of the colored organic substances remaining in the water after the adsorption. In recent years [1] there have been reports of the possibility of the use of an oxidation method of decolorization, based on destruction of the organic substances which color the water. However, further studies were required before final conclusions concerning the practicability of this method could be drawn, as the investigations cited did not include experiments in which seasonal variations of the properties of the organic impurities in water were taken into account.

Determinations of the oxidizability of water show that considerable amounts of organic substances remain in Dnepr water after coagulation treatment. It was shown in our preliminary investigations that these substances are faintly colored or colorless, and are compounds of low molecular weight and low degree of oxidation; this accounts for their poor adsorption on the coagulant floc. The ratio between the colored and colorless substances in the water varies according to the time of the year. This fact should influence the behavior of the humic substances in the treatment of water by oxidizing agents.

We therefore investigated the influence of a number of oxidizing agents (chlorine, ozone, oxygen) on the color of Dnepr water at different times of the year.

EXPERIMENTAL

In the experiments on chlorination of Dnepr water, chlorine water was added to the samples in amounts from 5 to 100 mg of chlorine per liter. The contact time was varied from 5 minutes to 72 hours. The color and residual chlorine contents of the samples were determined after the treatment.

The ozonation experiments were performed in a glass column ($d = 30$ cm, $h = 100$ cm) connected to an ozonizer. The ozone-air mixture from the ozonizer was passed through an absorber containing 2 N NaOH solution to remove nitrogen oxides before entry into the water. The volume rate of the ozone-air mixture was 0.88 liter/minute. The ozone concentration of the mixture was 0.1-0.15% (by volume). The volume of the treated sample was 100 ml. The same column was used for studying the oxidation of humus substances by atmospheric oxygen. The air was fed at 1.63 liters/minute. The experiments showed that when oxidizing agents act on the organic substances present in the water, two processes take place: the color of the faintly-colored substances increases, and the color of the highly-colored substances decreases. Therefore the total effect of the oxidation is determined by the relative proportions of these groups of substances, their degree of oxidation, and the concentration of the oxidizing agent added. The variations of the color of water, taken during the winter, in the course of chlorination are plotted in Fig. 1.

It is seen that chlorination resulted in a sharp intensification of the color of the water during the first hour, and later the color decreased, reaching the color of the original water after about two days of contact between the chlorine and the water.

The existence of two stages of the process, occurring at different rates, is clearly shown by Fig. 2, where the time in hours is taken along the abscissa axis and $\log \frac{a}{a-x}$ (where a is the initial color of the water, and x is the change in the color during time t) is taken along the ordinate axis.

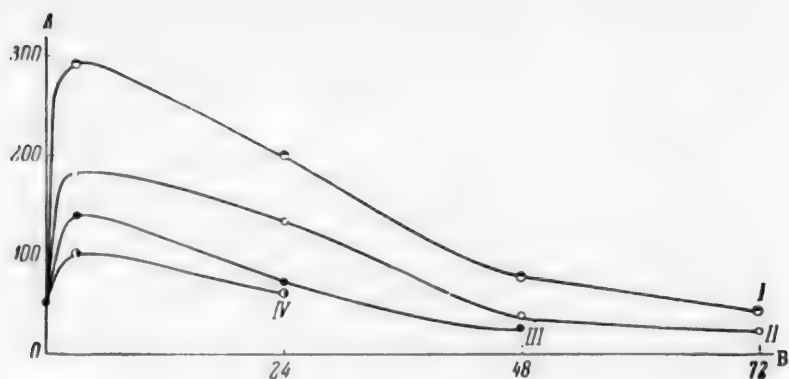


Fig. 1. Increase of the color of Dnepr water during chlorination in winter.
A) Color (degrees), B) time (hours).
Chlorine added (in mg/liter): I) 20, II) 50, III) 80, IV) 100.

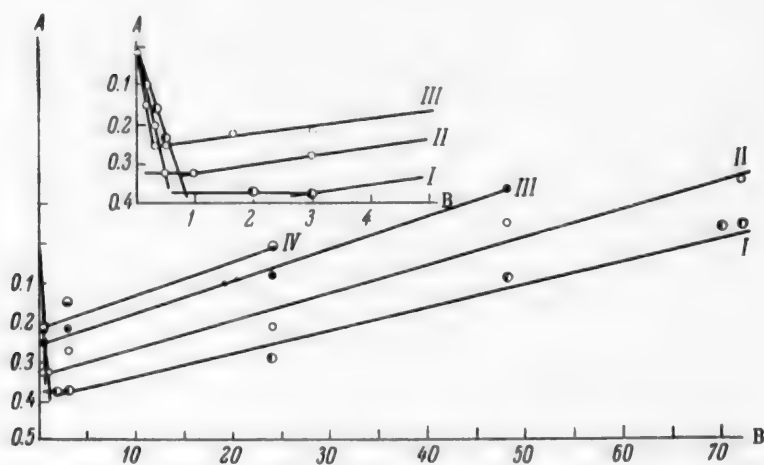


Fig. 2. Oxidation of humic substances by chlorine, accompanied by increase of color. A) Values of $\log a/a-x$, B) time (hours).
Chlorine added (in mg/liter): I) 20, II) 50, III) 80, IV) 100.

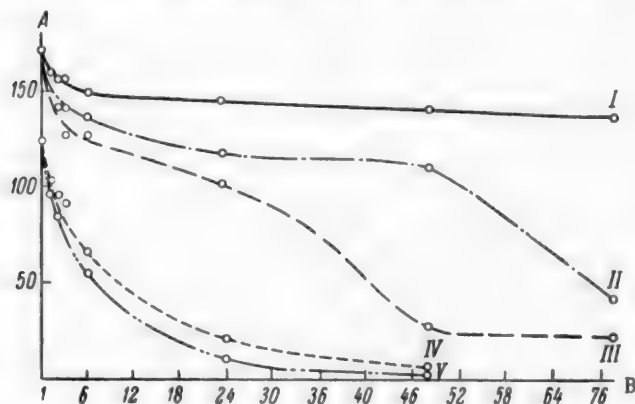


Fig. 3. Decrease of the color of Dnepr water during chlorination.
A) Residual color (in degrees), B) time (hours).
Chlorine added (in mg/liter): I) 5, II) 25, III) 40, V) 80, IV) 100.

At the first stage, the rate of oxidation of weakly-colored and colorless organic substances with formation of deeply-colored compounds exceeds the decomposition rate of the colored substances present in the water. Therefore the color of the water increases at first. The rate of this process increases with increasing chlorine content.

The second stage mainly consists of the decomposition of the highly-colored compounds formed, at a constant rate.

Figure 3 shows the variations of the color of water sampled during winter, in the course of chlorination, when the color of the water decreased under the action of the oxidizing agent. It is seen that with 5 mg of chlorine per liter there was a slight and smooth decrease of the color over the entire period of investigation. With 25 mg of chlorine per liter the curve was smooth for 46 hours, and the color then decreased sharply. With 40 mg of chlorine per liter the smooth region was shorter, and with 100 mg per liter it was entirely absent.

These results are plotted in semilogarithmic coordinates in Fig. 4; it is seen that in this case the oxidation of organic substances consists of three stages. The first corresponds to predominant breakdown of easily-oxidized organic substances; in the second stage the rate of oxidation of the weakly-colored and colorless humus substances and the breakdown rate of highly-colored humus substances are approximately equal, and this region on the curve is therefore parallel to the abscissa axis.

The third stage mainly corresponds to oxidation of highly-colored humic substances. This stage is absent with small amounts of chlorine (5 mg/liter). With increase of the chlorine concentration the second stage shortens, and the rates of the reactions taking place at this stage increase. These graphs suggest that the decolorization of water under the action of chlorine can be represented by an equation for a first-order reaction. Weakly-colored and colorless humic substances play the main role in the increase of the color of water on chlorination. When water was chlorinated after treatment with coagulants, when the highly-colored organic substances were removed, there was a sharp increase in the color of the water. The final color of the water was 4-6 times as deep, and even more, as the initial. The more highly oxidized highly-colored compounds were readily removed by a second coagulation, and were broken down on additional chlorination. It is significant that the degree of chlorine absorption with time remained almost unchanged with increase of the color. The sharp increase of the color was in all probability caused by reaction initiated by the action of chlorine. Similar results were found in the ozonation of water during the same period. Ozone treatment of water samples after coagulation resulted in a very considerable increase of color. For example, there were instances in which the color of the water rose from 10 to 40° on the dichromate-cobalt scale after 5 minutes of ozonation; subsequent ozonation led to a decrease of the color. This increase in the color of water on treatment with oxidizing agents is observed in the winter only, when oxidation of organic substances in reservoirs is retarded owing to the low temperature and inadequate access of oxygen. When such water is treated, the weakly colored compounds present in the water are oxidized, with the above-mentioned increase of color. During the other seasons of the year this process takes place in the reservoir itself.

Therefore chlorination of the water during the flood period, in summer, fall, and the first half of winter led to a sharp decrease of color both before and after coagulation (Fig. 5). Experiments showed (see Table) that during this period the chlorination absorption of the colored organic compounds removed by coagulation, and the consumption of chlorine for their decolorization, are very much less than the corresponding values for the group of weakly-colored compounds. For example, 3.3 mg of chlorine per liter was required to decrease the color by 1 degree in the chlorination of weakly-colored organic substances remaining in the water after coagulation, whereas 0.2 g of chlorine per liter was required to produce the same decrease in the color of the group of highly-colored compounds adsorbed on the coagulant floc.

Determinations of the oxidizability of the water after chlorination showed that ~30% of the compounds present in the water is completely decomposed. The change of oxidizability on chlorination of water after coagulation was considerably less (~10%). Therefore the oxidation of the weakly-colored compounds is not complete and the oxidation products remain in solution.

Experiments showed that ozonation of water during these periods is also accompanied by decreases of color and oxidizability (Fig. 6).

As in chlorination, the change of color on ozonation after coagulation was slight.

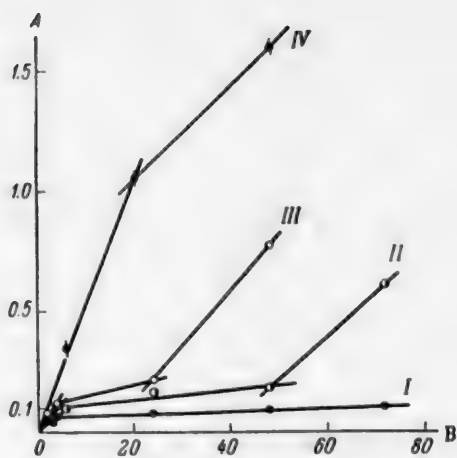


Fig. 4. Oxidation of humic substances by chlorine, accompanied by decrease of color.

A) Values of $\log \frac{a}{a-x}$, B) time (hours),

Chlorine added (in mg/liter): I) 5, II) 25, III) 40, IV) 100.

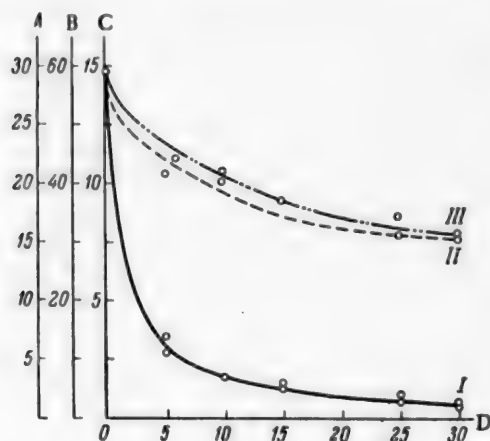


Fig. 6. Ozonation of Dnepr water during the flood period, in the summer, and in the fall.

A) Dichromate oxidizability III (mg O_2 per liter), B) color I (degrees), C) permanganate oxidizability II (mg O_2 per liter), D) time (minutes).

the order of reaction showed that oxidation of humus substances by ozone conforms to a second-order reaction equation.

During certain periods of the year it is possible to decrease the color of the water by aeration (Fig. 7).

Comparison of the oxidizing agents tested showed that the degree of decolorization of the water depends on the oxidation potential of the system. Change of temperature from 6 to 40° had almost no effect on the decolorization; in aeration, however, increase of the temperature to 20° resulted in a considerable decrease of color, while on further increase of the temperature to 40° the color increased and exceeded the initial value by about 10%. The reason for this course of the curve is intensive oxidation of weakly-colored humic substances

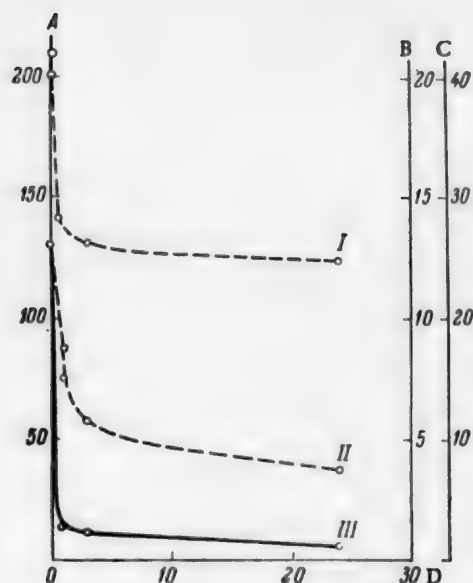


Fig. 5. Chlorination of Dnepr water during the flood period, in summer, and in the fall.

A) Color III (degrees), B) oxidizability I (in mg O_2 per liter), C) chlorine concentration II (in mg/liter), D) time (minutes).

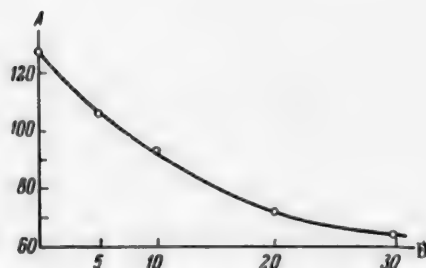


Fig. 7. Variation of the color of Dnepr water during aeration.

A) Color (degrees), B) time (minutes).

In these experiments the oxidizability of the water decreased by 50%, but total oxidation of the humic substances to CO_2 did not occur. No variations of the oxidizability with time after ozonation were observed in the samples tested. Determination of

Chlorine Absorption of Different Groups of Organic Compounds Coloring Dnepr Water

Group	Oxidizability by permanganate (mg/liter)	Chlorine absorption (mg/liter)	Color		Chlorine absorption relative to mg O ₂ per liter	Chlorine absorption per 1° of color
			before chlorination	after chlorination		
Original water	19.6	36.73	149	109	1.87	0.92
Weakly-colored compounds	9.6	36.17	32	21	3.77	3.3
Highly-colored compounds	10.0	0.56	117	88	0.06	0.2

at higher temperatures. When oxidizing agents with higher oxidation potentials were used, this effect was not found, as the highly-colored compounds formed were destroyed by them.

This investigation showed that the effects produced by oxidizing agents (chlorine, ozone, oxygen) on humic substances which color Dnepr water depend on the properties of the substances present in the water, and are very greatly influenced by the season of sampling.

It was found that the humic substances which color the water can be divided into two groups: highly-colored compounds of a high degree of oxidation, readily adsorbed on aluminum or ferric hydroxide floc, and easily decomposed by chlorine with formation of carbon dioxide or of weakly-colored and colorless compounds; and a group of weakly-colored compounds of a low degree of oxidation, slightly adsorbed on hydroxide floc, and requiring large amounts of oxidizing agents for decolorization. The relative proportions of these groups vary during the year, and this is reflected in the course of the decolorization process.

The results of this investigation confirm that oxidation is a promising method for decolorization of Dnepr water.

The process conditions, amounts of reagents, and contact time would depend on the nature of the humic substances present in the water. An increase in the content of weakly-colored compounds of a low degree of oxidation would require larger doses of the reagents, or the use of oxidizing agents with higher oxidation potentials.

SUMMARY

1. The seasonal variations of the color of Dnepr water under the action of oxidizing agents were studied, and it was found that the organic substances which color Dnepr water contain two groups of substances, which differ from each other in color, degree of oxidation, and behavior toward adsorbents and oxidizing agents.

2. It is shown that the decolorization of water by the action of oxidizing agents depends on the relative proportions of these groups of compounds and the oxidation potential of the system.

LITERATURE CITED

[1] L. A. Kul'skii, Technology of Disinfection of Potable Water (1946); D. Mints, T. K. Sidenko, Z. S. Vashchenko, V. P. Krishtul, and L. N. Paskutskaia, Sanitary Technology, Coll. Trans. K. D. Pamfilov Acad. Communist Economy (1954).

Received October 9, 1956

PRODUCTION OF RAPIDLY DRYING COATINGS BASED ON POLYESTER RESINS FROM SEMIDRYING OILS AND BUTYL ORTHOTITANATE*

V. S. Kiselev and T. A. Ermolaeva

It was reported in earlier papers [1-3] that butyl orthotitanate reacts with mono- and diglycerides of vegetable oils, and with fatty acids of vegetable oils, with formation of products having film-forming properties.

The purpose of the present investigation was the production of quick-drying coatings based on polyester resins from semidrying oils and butyl orthotitanate.

The materials chosen for the study were polyester resins of medium fatty-acid content, based on sunflower and cottonseed oils.

EXPERIMENTAL

Two polyester resins were used, made according to the following recipe (in %): sunflower or cottonseed oil 52.2, glycerol 17.4, phthalic anhydride 30.4.

Coatings based on the polyester resin containing sunflower oil were slightly tacky after cold drying, even after several days.

Films made from the polyester resin with cottonseed oil did not dry at all at room temperature, and remained slightly tacky after hot drying (160-170° for 2 hours).

Addition of butyl orthotitanate to polyester resin varnishes shortened the film-drying time considerably.

As Table 1 shows, the influence of butyl orthotitanate is particularly prominent in the drying of films made from polyester resin with cottonseed oil.

A varnish which formed films which could be dried only at high temperatures (160-170°), quickly formed films at room temperature if butyl orthotitanate was added.

Determination of the reaction mechanism. It was found that the films dry more slowly in dry air.

A film of polyester resin containing 50% butyl orthotitanate (on the weight of the original resin), which dried in 10-15 minutes under normal conditions of exposure to room air, remained appreciably tacky after 5 hours when kept in a desiccator with dry air.

A film kept in a desiccator with dry air for 24 hours still retained slight tack.

It follows from these experiments that atmospheric moisture causes partial hydrolysis and polycondensation of the butyl orthotitanate added to the polyester resin, and aids more complete drying of the film.

To determine the nature of the processes which cause rapid drying of films of polyester resins with added butyl orthotitanate, cold, and hot-dried films were analyzed for bromine numbers by the McIlhiney method [4], for titanium content by oxidation with nitric acid followed by ignition [5], for hydroxyl group content by the Verley and Bölsing method [6], and for butoxyl group content by a somewhat-modified Zeisel method [7].

The results of the analyses are given in Table 2.

*Communication IV in the series on the preparation of titanium-containing film formers and coatings based on them.

TABLE 1

Effect of the Amount of Butyl Orthotitanate Added on the Drying Time of Films

Resin taken	Amount of butyl orthotitanate added (% on the original resin)	Amount of white spirit (% on the original resin)	Drying time at room temperature (tack-free)	Complete drying time (free from tack) at room temperature
Polyester resin No. 1 with sunflower oil	—	170	24 hr	Slightly tacky for several weeks
	2	150	2 hr	48 hr
	5	150	2 hr	24 hr
	10	150	30 min	2 hr
	20	150	10-15 min	1 hr
	30	120	5-10 min	15-20 min
Polyester resin with cottonseed oil, 52% fatty acids	—	130	Does not dry	Does not dry
	10	130	1-2 hr	24 hr
	20	130	1 hr	12 hr
	30	130	15 min	1-2 hr
	40	130	15 min	1 hr
	50	130	5 min	15-20 min
	75	130	5 min	10-15 min
	90	130	4-5 min	10-12 min
	100	130	3-4 min	8-10 min

TABLE 2

Analysis of Films Obtained from Polyester Resins with Added Butyl Orthotitanate

Resin	Amount of butyl orthotitanate added (% on the original resin)	Drying temperature (°C)	Drying time (hours)	Titanium content (%)	Bromine number (% bromine added)	Butoxyl group content (%)	Hydroxyl number (mg KOH)
Polyester resin with sunflower oil (original resin)	—	—	—	—	44.5	—	102.3
Film from polyester resin with sunflower oil	—	160-170	1.5	—	33.5	—	113.2
Film from polyester resin with sunflower oil, with addition of butyl orthotitanate	10	160	1.5	2.84	36.13	13.64	100.9
	20	160	1.5	3.15	38.0	16.3	113.8
	10	18-20	24	2.08	43.63	15.96	62.0
	20	18-20	24	3.0	39.61	16.94	54.25
Polyester resin with cottonseed oil (original resin)	—	—	—	—	38.83	—	98.3
Film from polyester resin with cottonseed oil	—	160	1.5	—	30.5	—	114.6
Film from polyester resin with cottonseed oil, with addition of butyl orthotitanate	10	160	1.5	1.4	33.5	11.2	87.56

TABLE 3

Analyses of the Products Obtained After Extraction of the Films in the Soxhlet Apparatus

Extraction No.	Substance taken	Fractions after extraction	Amount of fraction as % of the original film taken	Hydroxyl number (mg KOH)	Saponification number (mg KOH)	Titanium content (%)	Butoxyl group content (%)	Molecular weight, cryoscopically in benzene
—	Polyester resin with cottonseed oil	—	—	98.3	321.0	—	—	—
1	Film from polyester resin. Dried for 2 hours at 170°, extracted for 12 hours	Resin extracted in benzene	33.63	163.2	380.7	0	0	984
2	Film from polyester resin with addition of 20% butyl orthotitanate. Dried for 2 hours at 160-170°, extracted for 12 hours	Residue after extraction	66.37	124.6	423.0	0	0	—
		Resin extracted in benzene	28.8	—	322.1	0.406	10.3	2022
		Residue after extraction	71.2	95.3	350.0	3.57	17.0	—

TABLE 4

Mechanical Properties of Films Obtained from Polyester Resins with Added Butyl Orthotitanate

Resin used	Amount of butyl orthotitanate added (% on the original resin)	Amount of white spirit added (% on the original resin)	Cold-dried films			Films dried at 160-170° for 2 hours		
			Hardness, by NILK* pendulum test	Elasticity, NILK* scale (mm)	Impact strength, kg/cm	Hardness, by NILK* pendulum test	Elasticity, NILK* scale (mm)	Impact strength, kg/cm
Polyester resin with sunflower oil	—	130	Does not dry			1	1	50
	5	115	1.25	1	50	1.75	1	50
	10	115	1.5	1	50	4	1	50
	20	115	2.25	1	50	4.5	1	50
	30	115	3	1	50	4.5	1	50
	40	140	4.5	1	50	5.5	1	50
Polyester resin with cottonseed oil	0	—	Does not dry			0.75	1	50
	10	115	1.25	1	50	2.75	1	50
	20	115	1.75	1	50	3.75	1	50
	30	115	2.5	1	50	4.75	1	50
	40	115	3	1	50	4.5	1	50
	50	130	3.5	1	50	5.0	1	50
	75	130	4.75	1	50	6.75	1	50
	90	130	5	1	50	7.0	10	50
	100	130	5.75	10	50	7.25	20	50

* Scientific Research Institute for Varnishes and Paints.

It follows from these results that in the formation of films by cold drying, the double bonds of the polyester resin take almost no part in the processes leading to quick hardening of the films, as the bromine numbers do not decrease.

It was possible that film formation occurs exclusively by polycondensation of butyl orthotitanate under the action of atmospheric moisture, while the polyester resin acts merely as a plasticizer and therefore does not undergo extensive changes.

To test this hypothesis, cold- and hot-dried films were extracted in a Soxhlet apparatus.

It follows from the data in Table 3 that the amount of benzene-soluble resin decreases with increase of the amount of butyl orthotitanate added.

When a hot-dried film (dried at 160-170° for 2 hours) of polyester resin with 20% butyl orthotitanate was extracted with benzene for 12 hours, 28.83% of the total film weight was dissolved.

Analysis of the resin extracted in benzene (Table 3) showed that it contains small amounts of titanium and butoxyl groups. This shows that butyl orthotitanate reacts with the polyester resin during hot drying, with formation of products of different molecular weight.

Although its titanium content was low, the molecular weight of the benzene-soluble resin was about 2000, whereas the resin extracted from a similar film of polyester resin without added butyl orthotitanate had molecular weight 984, and represented a considerable proportion of the total weight of the film. The residue insoluble in benzene contained 3.57% titanium, and probably had a much higher molecular weight, which could not be determined as it proved impossible to find a suitable solvent. The large amount of insoluble residue indicates that most of the polyester resin reacts with butyl orthotitanate during hot drying, with formation of a hard insoluble film.

The results of these investigations show that the main reactions leading to the rapid drying of films of polyester resins modified with sunflower or cottonseed oils are condensation reactions of the free hydroxyl and carboxyl groups of the polyester resin with the butoxyl groups of butyl orthotitanate, and hydrolysis and condensation of butyl orthotitanate in presence of atmospheric moisture. The presence of the polyester resin retards hydrolysis and condensation of butyl orthotitanate, and the reaction products of butyl orthotitanate and polyester resin confer good adhesion and elasticity to the film.

Determinations of the mechanical properties of coatings based on polyester resins with added butyl orthotitanate. The principal mechanical characteristics: hardness, elasticity, and impact strength [8] were determined in cold- and hot-dried films made from polyester resin with added butyl orthotitanate.

The results of the tests on polyester resin films with added butyl orthotitanate, given in Table 4, show that addition of butyl orthotitanate to polyester resins considerably improves the mechanical properties of coatings made from them.

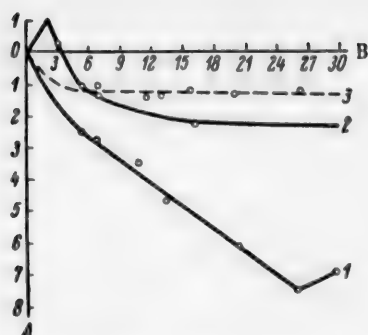
Addition of butyl orthotitanate to polyester resins not only shortens the drying time of the films, but increases the hardness considerably.

Cold- and hot-dried films have good adhesion and elasticity, and have an impact strength of 50 kg/cm. Increase of the amount of added butyl orthotitanate shortens the drying time and increases film hardness.

If a large amount (90-100% on the weight of the original resin) of butyl orthotitanate is added, the films are very hard but have decreased elasticity, because of the high content of titanium in the films (11.2%).

Tests of film resistance to water and chemical reagents. Tests in which the films were exposed to the prolonged action of water (for 1 month) showed that films made from polyester resin modified with cottonseed oil with addition of 20% butyl orthotitanate, dried cold or hot, show considerably lower weight losses (1.1-2.2%) than hot-dried films made from the original polyester resin (7.6%) (see Figures).

The weight loss of polyester films with additions of 20% butyl orthotitanate, especially if dried at 160-170° for 2 hours, changes little during the test, whereas the weight loss of a hot-dried film (170°, 2 hours) of the original resin increased continuously.



Loss of weight of the films.

A) Loss of weight (%), B) time (hours).

1) Hot-dried film from original polyester resin; 2) cold-dried film from the same resin with 20% butyl orthotitanate added; 3) hot-dried film from polyester resin with 20% butyl orthotitanate added.

The lower contents of the water-soluble fraction in polyester films containing butyl orthotitanate as compared with films of the original resin may be attributed to a decrease in the number of free reactive groups and to an increase of the molecular weight of the products formed during drying of the films.

Cold- and hot-dried films containing butyl orthotitanate had good resistance to 10% sulfuric acid solution: no significant changes were found in the films after 2600 hours of exposure.

SUMMARY

1. The main processes occurring in the drying of butyl orthotitanate are partial hydrolysis and polycondensation, accompanied by loss of butoxyl groups and formation of insoluble products.

2. When butyl orthotitanate reacts with compounds containing hydroxyl groups, such as mono- and diglycerides of vegetable oils or incompletely esterified glycol phthalate and glycol maleate, transesterification takes place. The products formed have film-forming properties.

3. Butyl orthotitanate reacts with fatty acids of vegetable oils to give film formers. When butyl orthotitanate reacts with oleic acid, formation of titanium salts is accompanied by esterification of oleic acid with liberation of butyl alcohol. At the same time, hydrolysis and condensation of titanium compounds takes place, leading to formation of polymeric products which can be isolated by molecular distillation.

4. Varnishes made from polyester resins of moderate fatty-acid content made with sunflower and cottonseed oils, films of which can be dried completely only by the action of heat, after addition of butyl orthotitanate give coatings which dry quickly either in the cold or on heating.

5. The principal reactions causing the rapid drying of the films are condensation reactions between the free hydroxyl or carboxyl groups of the polyester resin and the butoxyl groups of butyl orthotitanate. In presence of atmospheric moisture, butyl orthotitanate also undergoes partial hydrolysis and condensation.

6. Coatings based on polyester resins of moderate fatty-acid content, modified with sunflower or cottonseed oil, with additions of butyl orthotitanate, are a new type of coating in which the valuable properties of polyester resins - good adhesion and elasticity - are combined with a high rate of drying and hardness characteristic of butyl orthotitanate films.

LITERATURE CITED

- [1] V. S. Kiselev and T. A. Ermolaeva, *J. Appl. Chem.* 29, 2, 288 (1956).*
- [2] V. S. Kiselev and T. A. Ermolaeva, *J. Appl. Chem.* 29, 3, 432 (1956).*
- [3] V. S. Kiselev and T. A. Ermolaeva, *J. Appl. Chem.* 30, 12, 1810 (1957).*
- [4] H. Meyer, *Analysis and Structure Determination of Organic Compounds* (Russian translation) (ONTI, Khar'kov-Kiev, 1935).
- [5] R. I. Speer, *J. Org. Ch.* 14, 655 (1949).
- [6] V. S. Kiselev, *Practical Manual of Film-Former Technology* (State Sci.-Tech. Press, Chem. Lit., Moscow-Leningrad, 1948).*

*Original Russian pagination. See C. B. Translation.

**In Russian.

[7] S. A. Kaptorovich and O. P. Alegina, Bull. Exchange of Experience in the Varnish and Paint Industry, 4 (Goskhimizdat, 1953).•

[8] S. V. Iakubovich, Testing of Lacquer and Paint Materials and Coatings, 9 (Sci.-Tech. Press Chem. Lit., Moscow - Leningrad, 1952).•

Received May 12, 1956

• In Russian.

CAST UNSATURATED POLYESTER RESINS HARDENING IN THE COLD

R. K. Gavurina, P. A. Medvedeva and Sh. G. Ianovskaia

Synthesis conditions of unsaturated polyester resins are described mainly in patents and reviews [1-4]. The number of original research papers published on the subject is small, and most of these have appeared very recently. The range of problems touched upon in these papers is fairly wide.

In one of the earlier investigations, Ushakov and Mitsengendler [5] studied the products of copolymerization of glycol maleate with vinyl acetate.

Nichols and Bliss [6] studied exothermic curves for cold-hardening resins. Parker and Moffett [7] studied the physical properties of unsaturated polyesters in relation to their composition. Cass and Burnett [11] investigated the inhibition of polyesters.

The experimental part of the present investigation was devoted to the synthesis of cast unsaturated polyester compositions and study of their hardening conditions.

EXPERIMENTAL

Various unsaturated polyesters, such as polyethylene glycol maleate - phthalates, - adipates, - sebacates, etc. were synthesized. Styrene was used as the monomer in all the experiments. Most of the investigations were performed on polyethylene glycol maleate - phthalates and adipates.

The polycondensation was carried out at 190-200° in a continuous stream of inert gas (CO_2 or N_2).

The course of the polycondensation process was evaluated by variations of the acid number. The linear polyesters formed were copolymerized with styrene. Various additives: inhibitors, catalysts, or accelerators, were added as required to the reaction mixtures.

The inhibitor used in all the experiments was hydroquinone; the catalysts were benzoyl peroxide and 1-hydroxy-1'-hydroperoxy-biscyclohexyl peroxide, henceforth described as cyclohexyl hydroperoxide. The accelerators were dimethylaniline and Accelerator B (containing cobalt naphthenate). The copolymerization (hardening) was carried out at elevated and room temperatures in glass or metal molds. The molds were coated with insulating films of polyvinyl alcohol or organosilicon compounds. The course of the hardening process was followed by means of exothermic curves.

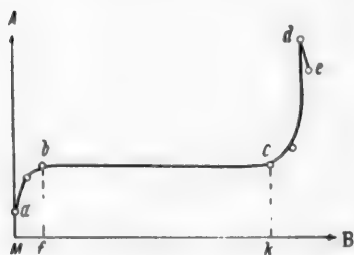


Fig. 1. Exothermic curve.
A) Temperature ($^{\circ}\text{C}$), B) time.

A typical exothermic curve is shown in Fig. 1.

The section fk was recorded as the gelation time, as in practice the mixture became immobile at the instant k , while the point d was recorded as the exothermic peak.

Two main characteristics were determined in the hardened samples: heat resistance, and content of gel fraction. The heat resistance was determined by means of an instrument operating on the principle of the Vicat apparatus, but not identical with it (area of needle tip 0.1 mm^2 , load 5 kg/mm^2 , depth of immersion 0.5 mm).

TABLE 1

Effect of Additions of Dimethylaniline

Additions (% on the resin)				Gelation time at 64° (min.)	Exother- mic peak (°C)	Heat resist- ance (°C)	Soluble fraction (%)
benzoyl peroxide	cyclo- hexyl hy- droper- oxide	hydro- quinone	di- methyl- aniline				
1.0	—	—	—	8	163	97	13.8
1.0	—	—	0.01	instantaneous at 20°	—	—	—
1.0	—	—	—	9	153	94	14.4
1.0	—	—	0.01	instantaneous at 20°	—	—	—
1.0	—	0.02	—	60	149	155	12.6
1.0	—	0.02	0.01	10	160	155	12.6
1.0	—	0.02	—	35	165	163	14.0
1.0	—	0.02	0.02	10	170	178	14.2
1.0	—	0.02	0.03	5	170	—	13.9
—	0.5	—	—	13	70	48	20.2
—	0.5	—	0.01	13	75	43	21.1
—	0.5	—	—	17	63	38	20.6
—	0.5	—	0.01	13	63	38	20.8
—	0.5	0.02	—	35	64	37	21.5
—	0.5	0.02	0.01	44	69	39	—
—	1.0	0.02	—	40	63	57	18.4
—	1.0	0.02	0.01	47	67	57	18.4

TABLE 2

Effect of Additions of Accelerator B

Additions (% on the resin)				Gelation time at 64° (min.)	Exother- mic peak (°C)	Heat resist- ance (°C)	Soluble fraction (%)
benzoyl peroxide	cyclo- hexyl hy- droper- oxide	hydro- quinone	dimethyl- aniline				
—	0.5	—	—	16	75	46	17.8
—	0.5	—	0.02	8	118	98	12.1
—	0.5	0.02	—	37	63	48	18.7
—	0.5	0.02	0.02	30	101	97	12.9
—	0.5	—	—	17	63	38	20.6
—	0.5	—	0.02	10	131	38	13.8
—	0.5	0.02	—	35	64	37	21.5
—	0.5	0.02	0.02	35	96	101	15.1
—	0.5	—	—	13	70	48	20.2
—	0.5	—	0.02	6	95	90	14.3
—	1.0	0.02	—	40	74	57	16.6
—	1.0	0.02	0.02	12	166	125	12.6
—	1.0	—	—	12	63	—	—
—	1.0	—	0.02	5	143	—	—
—	1.0	0.02	—	27	75	—	—
—	1.0	0.02	0.02	16	151	—	—
1.0	—	—	—	8	163	97	13.8
1.0	—	—	0.02	9	163	91	13.5
1.0	—	—	—	9	153	94	14.4
1.0	—	—	0.02	8	158	103	13.6
1.0	—	0.02	—	63	154	—	—
1.0	—	0.02	0.02	140	139	—	—
1.0	—	0.02	—	35	165	100	14.0
1.0	—	0.02	0.3	120	160	120	13.6

TABLE 3

Influence of Accelerators on Mixtures Without Catalysts

Additions (% on the resin)				Gelation time (min)	Exother- mic peak (°C)	Heat resist- ance (°C)	Soluble fraction (%)
benzoyl peroxide	cyclo- hexyl hydro- peroxide	dimethyl- aniline	Accele- rator B				
Mixtures without inhibitor							
—	—	—	—	140	64	55	18.7
—	0.5	—	—	17	68	88	20.6
1.0	—	—	—	9	153	94	14.4
—	—	0.01	—	68	64	57	19.2
—	—	—	0.02	60	64	48	22.6
—	—	—	—	120	64	55	—
—	—	0.02	—	20	64	52	—
—	—	—	0.02	45	64	62	—
Mixtures with inhibitor							
—	—	—	—	13500	—	—	—
1.0	—	—	—	60	—	—	—
—	1.0	—	—	40	—	—	—
—	—	0.02	—	5400	—	—	—
—	—	—	0.02	16800	—	—	—

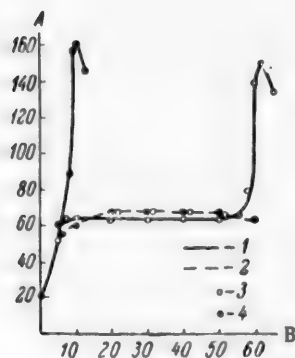


Fig. 2. Effect of dimethylaniline accelerator on the course of the exothermic curves. Hardening at 64°.

A) Temperature (°C), B) time (minutes).

1) BP catalyst, 2) CHP catalyst, 3) without accelerator, 4) with accelerator.

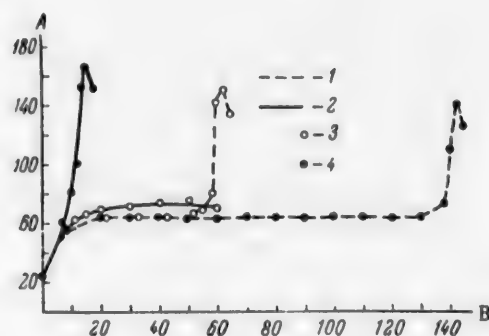


Fig. 3. Effect of Accelerator B on the course of the exothermic curves. Hardening at 64°.

A) Temperature (°C), B) time (minutes).

1) BP catalyst, 2) CHP catalyst, 3) without accelerator, 4) with accelerator.

These tests for heat resistance were used only for comparison of the specimens during the investigation. The final technical characteristics of the compositions were determined after additional tests under standard conditions (see Table on p. 111).

The gel fraction was determined by extraction with acetone in the Soxhlet apparatus.

The investigations began with selection of conditions in which the hardening process could be carried out in the cold. Cold hardening of cast resins decreases the risk of crack formation. Hardening at room temperatures is usually effected by addition of accelerators. The mechanism by which the accelerators act is not yet fully understood. Some views on the action of different accelerators have been put forward [9, 10]. In practice, the accelerator is usually chosen by purely empirical methods. It is pointed out in the literature [1, 6, 11] that each

accelerator is selective in its action, and must be chosen in a "pair" with a catalyst. The recommended systems include: a) benzoyl peroxide (BP) with tertiary amines, b) cyclohexyl hydroperoxide (CHP) with driers, and c) methyl ethyl ketone peroxide with driers.

It is also reported that benzoyl peroxide can be used in conjunction with cobalt or manganese naphthenate [2].

In the choice of the catalyst and accelerator it is necessary to take into account the action of the inhibitor added to prevent spontaneous gelation of the polyester mixtures during storage.

In the first stage of the investigations an experimental study was carried out of the action of the two above-named accelerators, dimethylaniline and Accelerator B, each used in conjunction both with a "paired" and a "nonpaired" catalyst. Mixtures with and without hydroquinone were investigated. In this series of experiments the exothermic curves were determined at 64°.

The specimens used for determinations of the gel fraction and heat resistance were subjected to additional heating for 8 hours at 64° after the hardening. The results are given in Tables 1 and 2. The exothermic curves obtained in certain experiments are given in Figs. 2 and 3 as examples.

The results of the experiments confirmed that the accelerators are selective in their action: dimethylaniline is an active accelerator of the copolymerization process catalyzed by benzoyl peroxide, while Accelerator B works well in conjunction with cyclohexyl hydroperoxide. This effect is observed for systems both with and without inhibitors. However, the effects of each of the two accelerators in conjunction with its "paired" catalyst were different under the conditions studied.

Addition of dimethylaniline to mixtures catalyzed by benzoyl peroxide resulted in a noticeable shortening of the induction period, whereas the exothermic peak, the gel-fraction content, and heat resistance remain unchanged.

When Accelerator B is used in conjunction with cyclohexyl hydroperoxide, not only is the time of gelation shortened, but the exothermic peak, heat resistance, and gel-fraction content are all higher.

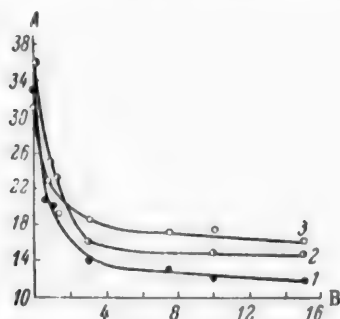


Fig. 4. Effects of accelerators on increase of the gel-fraction content.

A) Contents of soluble fraction (%),
B) time (hours).

Curves: 1) with dimethylaniline,
2) with Accelerator B, 3) without
accelerator.

The "paired" accelerator, dimethylaniline, gives a somewhat more pronounced effect; Curve 1 lies below the others. The instant of gel formation corresponded to 64-72% of the gel fraction in all cases.

In addition to the quantitative determinations of the gel fraction, the extractable fractions of the products were analyzed. The acid and ester numbers were determined. The ester numbers were high in all cases, exceeding the acid numbers considerably (about 10-fold). This shows that the extractable portion consists mainly of polyester.

The action of the two accelerators also differs in "nonpaired" systems. Dimethylaniline has almost no action on systems catalyzed by cyclohexyl hydroperoxide, whereas Accelerator B in conjunction with benzoyl peroxide only shows such behavior in systems without inhibitor. In mixtures containing hydroquinone the process is retarded considerably, but the properties of the hardened products remain almost unchanged. The effects of the accelerators are clearly seen in Figs. 2 and 3.

It was also desirable to test the effects of accelerators on the increase of the gel-fraction content from the start of gelation and during subsequent heating. Experiments for this purpose were performed with one of the catalysts, benzoyl peroxide, used in conjunction both with its "paired" accelerator, dimethylaniline, and the "nonpaired" Accelerator B. The results are plotted in Fig. 4. The instant of gel formation is taken as the zero point in these curves. The gelation time was 1 hour 43 minutes for the sample without accelerator, 34 minutes with dimethylaniline, and 3 hours 5 minutes with Accelerator B.

Despite the considerable difference in the length of the induction period, the increase of the gel-fraction content is changed little by addition of either the "paired" or the "nonpaired" accelerator. The

For determination of the role of accelerators in the copolymerization process, their effects on mixtures without initiators were also studied. Mixtures with and without hydroquinone were used. The results are summarized in Table 3. The exothermic curves were determined at 64°. It follows from Table 3 that in presence of atmospheric oxygen both the accelerators are capable in themselves (without catalyst) of accelerating the hardening of mixtures without inhibitors. This is probably due to the formation of peroxide compounds of polyester under the action of atmospheric oxygen. The acceleration effect is quite pronounced – the gelation time is shortened to a fraction of its former value. For comparison, Table 3 contains data on the same mixtures catalyzed by benzoyl peroxide and cyclohexyl hydroperoxide, taken in the usual amounts (0.5-1.0%). The acceleration effected by dimethylaniline in systems without inhibitors is quite comparable to the acceleration produced on addition of typical catalysts – benzoyl peroxide and cyclohexyl hydroperoxide.

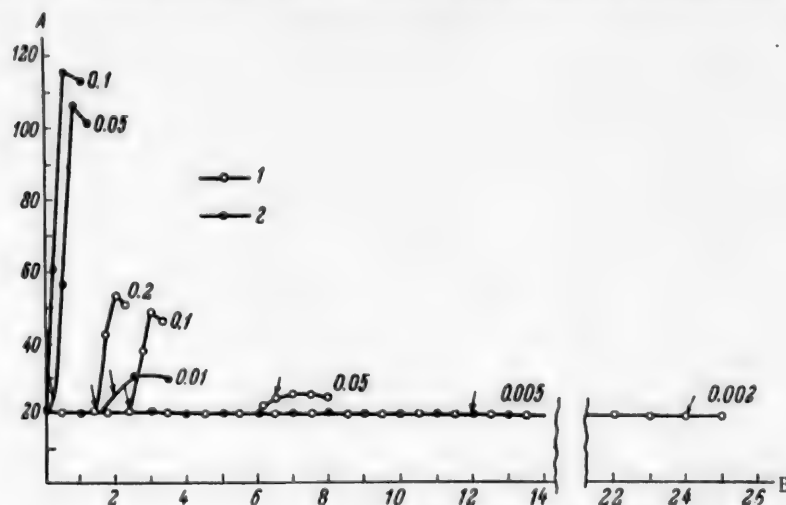


Fig. 5. Effect of the amount of accelerator on the course of the exothermic curves. Hardening at 20°.

A) Temperature (°C), B) time (hours).

1) 0.5% CHP, 0.02% hydroquinone, Accelerator B; 2) 1.0% BP, 0.02% hydroquinone, dimethylaniline.

Arrows indicate the instant of gel formation, the numbers on the curves represent the % contents of accelerator.

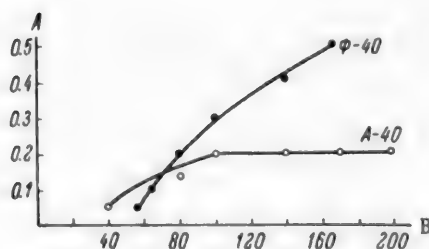


Fig. 6. Effect of temperature on deformation (under load).

A) Depth of penetration of needle (mm),

B) temperature (°C).

For systems with inhibitor, a shortening of the induction period (approximately 2.5-fold) occurs only on addition of dimethylaniline, and the acceleration effect is not comparable with that produced by catalysts. The results of experiments on the action of accelerators on systems without catalysts are of some theoretical interest. For a practical solution of the problem, experiments were continued with catalyzed mixtures.

The next stage of the work was a detailed study of the conditions for cold hardening.

Cold-hardening compositions were studied with both the catalysts in conjunction with "paired" accelerators. Two systems were therefore investigated: 1) benzoyl peroxide and dimethylaniline, 2) cyclohexyl hydroperoxide and Accelerator B.

In both cases the problem was essentially to choose the proportions of catalyst, accelerator, and inhibitor which would make it possible to carry out the copolymerization at room temperatures within technically acceptable times, with the production of specimens free from defects.

The principal method for regulation of the hardening process was variation of the amount of accelerator.

The influence of this factor in both the systems studied is illustrated in Fig. 5.

Cold hardening took place both with benzoyl peroxide in conjunction with dimethylaniline, and with cyclohexyl hydroperoxide in conjunction with Accelerator B.

The hardening time can be varied over very wide limits (from 12 hours to 25 minutes, and from 64 hours to 1.5 hours respectively) by variations of the amount of accelerator.

It should be noted that the course of hardening differs somewhat with the two catalysts.

With benzoyl peroxide (together with dimethylaniline), short hardening cycles yield specimens with defects (cracks), whereas with long cycles the hardening is not uniform through the mass of the resin, and a relatively large layer of viscofluid, tacky resin remains on top.

Considerably better results were obtained by the use of cyclohexyl hydroperoxide in conjunction with Accelerator B.

TABLE 4

Properties of Hardened Filled Compositions

	A-40	F-40
Density (g/cc)	1.7	1.7
Static bend strength (kg/cm ²)	750	820
Compressive strength (kg/cm ²)	1200	1500
Specific impact viscosity (kg · cm/cm ²)	7-10	5-6
Heat resistance, Martens test (°C)	50	73
Heat resistance, Vicat test (°C)	280	150
Water absorption at 20° (%)		
after 24 hours	0.09	0.03
after 6 days	0.25	0.11
after 30 days	0.60	0.32
Water absorption at 95 ± 3% relative humidity (%)		
after 24 hours	0.09	0.03
after 6 days	0.27	0.10
after 30 days	0.63	0.30
Dielectric strength (kv/mm) (alternating current, smooth increase of voltage)		20-25
tan δ at 50 c.p.s., at t = 20°.	0.02-0.03	0.015-0.018
t = 80°	0.06-0.15	0.06 - 0.07
tan δ at 10 ⁶ c.p.s., at t = 20°	0.018	0.013

Uniformly-hardening castings free from defects (over 1 kg in weight) were obtained by suitable choice of formulations. The materials are optically active; apart from their other fields of application, they can be used, as demonstrated by trials performed at the Polzunov Central Institute of Boilers and Turbines, for optical studies of stress (photoelasticity).

Thin films were also hardened in the cold. For this, wax or other substances were added to protect the compositions against the inhibiting action of atmospheric oxygen.

The final stage of the work was a study of "filled" compositions.

The fillers used were kaolin, mica, quartz powder, chalk, talc, and magnesium oxide.

The nature of the filler influences both the hardening conditions and the properties of the products. The main differences are in the viscosities of the mixtures, the duration of the induction period, and the moisture resistance of the products. Addition of fillers lowers the exothermic peak, increases the heat resistance, and decreases the specific impact viscosity in all cases.

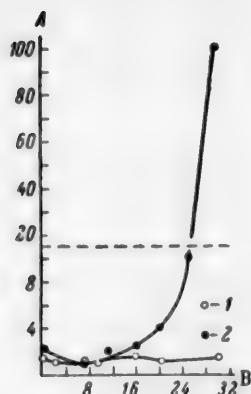


Fig. 7. Effect of time of exposure to water on $\tan \delta$.
Temperature 15-20°; (measurements at $U = 1$ kv, $f = 50$ c.p.s.)
A) $\tan \delta$ (%), B) time (days).
1) F-40 resin, 2) A-40 resin.

As a result of all these investigations, several formulations were worked out for cold-hardening cast unsaturated polyester resins with and without fillers.

The technical characteristics of two of the filled compositions are given in Table 4.

Both compositions have good frost resistance (especially A-40); for example, specimens in the form of copper pipes ($d = 32$ mm, $h = 400$ mm) coated with a layer of the material 2-3 mm thick withstand cooling to -70° without crack formation and without change of electrical properties.

In addition, Fig. 6 shows the effect of temperature on the deformation under load (5 kg/mm^2).

It is seen in Fig. 6 that the two compositions differ in their behavior on heating. Deformation of A-40 begins at a lower temperature, but the curve is flatter, and above 80° the deformation is less than that of F-40.

The two grades also differ considerably in their water resistance; this is seen clearly in Fig. 7, which shows the variations of $\tan \delta$ under prolonged action of water.

Various specimens, including castings containing metallic reinforcements, were made from A-40 and F-40 compositions.

The materials have good adhesion to the reinforcement (copper, aluminum, steel, etc.) and give solid castings without peeling, bubbles, or other defects. The weights of the specimens reached 10 kg, including about 4 kg of metallic parts in the castings.

LITERATURE CITED

- [1] H. Barron, *Rubber Age and Synthetics*, 4, 162 (1953).
- [2] C. P. Vale, *Brit. Plastics*, 26, 292, 327 (1953).
- [3] Z. A. Rogovin (ed.), *Advances in Polymer Chemistry and Technology*, 1 (1955) p. 151.*
- [4] E. M. Evans, *Brit. Plastics*, 27, 3, 100 (1954).
- [5] S. N. Ushakov and S. P. Mitsengendler, *J. Appl. Chem.* 22, 12, 1261 (1947).
- [6] E. S. Nichols and C. H. Bliss, *Modern Plastics*, 29, 9, 124 (1952).
- [7] E. E. Parker and E. W. Moffett, *Ind. Eng. Chem.* 46, 8, 1615 (1954).
- [8] W. E. Cass and R. E. Burnett, *Ind. Eng. Chem.* 46, 8, 1619 (1954).
- [9] C. E. H. Bawn, *Discussions Faraday Soc.* 14, 181 (1953).
- [10] M. Imoto, T. Otsu and K. Kimura, *J. Polymer Sci.* XV, 80, 475 (1955).
- [11] B. Berndtsson and L. Turunen, *Kunststoffe*, 44, 10, 430 (1954).
- [12] T. E. Bockstahler, G. E. Forsyth and I. I. Gouza, *Ind. Eng. Chem.* 46, 8, 1639 (1954).

Received April 12, 1956

*In Russian.

AZO DYES FROM AMINOCARBANILIDE AND ITS SUBSTITUTION PRODUCTS*

V. N. Kluev, L. A. Dogadkina, S. N. Solodushenkov
and A. A. Spryskov

The Ivanovo Institute of Chemical Technology

A common defect of most azo dyes is their low fastness to light and weather. Exceptions to this include certain bisazo dyes, generally made by treatment of p-aminoazo dyes with phosgene, which have high fastness to light. Phosgenated dyes may be regarded as derivatives of 4,4'-diaminocarbaniilide with the general formula



At present, 4,4'-diaminocarbaniilides have been studied little and are therefore not readily available. This partly explains why dyes of this type are made almost exclusively by phosgenation of monoazo dyes, and have not been made directly on the fiber by the cold-dyeing method. Recently Bumistrov and two of the present authors [1] proposed the use of substituted 4,4'-diaminocarbaniilides as azoamines for the cold dyeing of cotton fabrics.

In the present investigation, all the previously-synthesized [2] substituted, 4,4'-diamino- and 4-mono-aminocarbaniilides were tested as azoamines for cold dyeing of cotton fabrics.

EXPERIMENTAL

For the dyeing tests with the substituted aminocarbaniilides, Azotols A, OT, OA, and PA at concentrations of 5 and 10 g/liter were used. The concentration of the azoamine was 5 g/liter in all the dyeings. The fabrics used were calico and mercerized satin. The alkaline Azotol solutions were made according to the recipes in the Coloristic Manual [3]. After immersion in the Azotol solution, the fabric was squeezed out to contain its own weight of solution and dried in an oven at 80-85°, stretched on a frame. For preparation of the diazo solution, 50% excess of hydrochloric acid was used, while the excess of sodium nitrite was not over 5% of the calculated quantity.

The fabric impregnated with the alkaline Azotol solution was immersed for 20 seconds at room temperature in the diazo solution neutralized with sodium bicarbonate, exposed to air for 5 minutes, washed in cold water, soap solution (5 g of 70% soap and 3 g of sodium carbonate per liter) at 70° for 3 minutes, hot water, and cold water again. The specimens were dried in air and ironed moist from the reverse side.

The fastness tests were carried out according to the specifications of All-Union Standard 10085-39. The light and weather fastness tests were performed on specimens dyed with the use of all four Azotols at both concentrations, and the tests for fastness to wet treatments and rubbing, only on specimens dyed with the use of Azotol A at 10 g/liter. Specimens which had a fastness of 1 to light and weather were generally not subjected to further tests. For the light and weathering tests the specimens were sewn into openings in a cloth stretched on the test frame. The fastness was assessed on a 5-point scale.

* Communication IV in the series on the synthesis and applications of carbanilide derivatives.

TABLE 1

Light and Weather Fastness Tests on Dyeings with Azoamines from Substituted Carbanilides

Serial No.	Structure of azoamine, and diazo-tization and coupling characteristics	Azotol		Fastness to light and weather	Color of dyeing
		mark	concentration (g/liter)		
1	$\text{H}_2\text{N}-\text{C}_6\text{H}_3(\text{Cl})-\text{NH} \cdot \text{CO} \cdot \text{HN}-\text{C}_6\text{H}_3(\text{Cl})-\text{NH}_2$ Hydrochloride soluble in water, readily diazotized. Yellow diazo solution transparent and stable	A	5	1	Bordeaux
		A	10	1	
		OT	5	1	
		OT	10	1	
		OA	5	1	
		OA	10	2-3	
		PA	5	1	
		PA	10	3	
2	$\text{H}_2\text{N}-\text{C}_6\text{H}_3(\text{Cl})-\text{NH} \cdot \text{CO} \cdot \text{HN}-\text{C}_6\text{H}_3(\text{Cl})-\text{NH}_2$ Hydrochloride not easily soluble in water; diazotized in suspension	A	5	1-2	Garnet
		A	10	2-3	
		OT	5	1-2	
		OT	10	3	
		OA	5	2	
		OA	10	3-4	
		PA	5	2	
		PA	10	3-4	
3	$\text{H}_2\text{N}-\text{C}_6\text{H}_2(\text{Cl})_2-\text{NH} \cdot \text{CO} \cdot \text{HN}-\text{C}_6\text{H}_2(\text{Cl})_2-\text{NH}_2$ Hydrochloride not easily soluble in water; diazotized in suspension. Diazo solution filtered before coupling	A	5	1	Red
		A	10	1	
		OA	5	1	
		OA	10	1	
		PA	5	1	
		PA	10	1	
4	$\text{H}_2\text{N}-\text{C}_6\text{H}_2(\text{Cl})_2-\text{NH} \cdot \text{CO} \cdot \text{HN}-\text{C}_6\text{H}_2(\text{Cl})_2-\text{NH}_2$ Hydrochloride not easily soluble in water; diazotized in suspension. Diazo solution filtered before coupling	A	5	1	Red
		A	10	1	
		OA	5	1	
		OA	10	1	
		PA	5	1	
		PA	10	1	
5	$\text{H}_2\text{N}-\text{C}_6\text{H}_3(\text{Cl})(\text{CH}_3)-\text{NH} \cdot \text{CO} \cdot \text{HN}-\text{C}_6\text{H}_3(\text{Cl})(\text{CH}_3)-\text{NH}_2$ Hydrochloride not easily soluble in water, but readily diazotized in suspension. Diazo solution clear and stable	A	5	1	Garnet
		A	10	1	
		OT	5	1	
		OT	10	2	
		OA	5	2-3	
		OA	10	3	
		PA	5	2-3	
		PA	10	3	
6	$\text{H}_2\text{N}-\text{C}_6\text{H}_3(\text{Cl})(\text{OCH}_3)-\text{NH} \cdot \text{CO} \cdot \text{HN}-\text{C}_6\text{H}_3(\text{Cl})(\text{OCH}_3)-\text{NH}_2$ Hydrochloride fairly readily soluble and easily diazotized. Transparent and stable diazo solution, greenish in color	A	5	2	Navy blue
		A	10	3	
		OT	5	3	
		OT	10	3	
		OA	5	2-3	
		OA	10	3-4	
		PA	5	3-4	
		PA	10	4	
7	$\text{H}_2\text{N}-\text{C}_6\text{H}_3(\text{Cl})(\text{OCH}_3)-\text{NH} \cdot \text{CO} \cdot \text{HN}-\text{C}_6\text{H}_3(\text{Cl})(\text{OCH}_3)-\text{NH}_2$ Hydrochloride soluble in water and readily diazotized. Diazo solution yellow	A	5	1	Violet
		A	10	1	
		OA	5	1	
		OA	10	1	
		PA	5	1	
		PA	10	1	

TABLE 1 (continued)

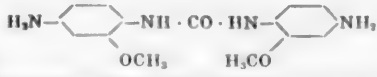





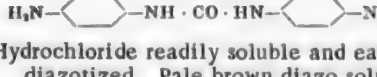
Serial No.	Structure of azoamine, and diazotization and coupling characteristics	Azotol		Fastness to light and weather	Color of dyeing
		mark	concentration (g/liter)		
8	 <p>Hydrochloride readily soluble in water and easily diazotized. Bright green diazo solution transparent and stable</p>	A	5	1	Navy blue
		A	10	2-3	
		OT	5	1-2	
		OT	10	3	
		OA	5	2	
		OA	10	3	
		PA	5	2-3	
9	 <p>Hydrochloride soluble in water and easily diazotized. Dark green diazo solution</p>	A	10	1-2	Blue-violet
		OA	10	2-3	
		PA	10	3	
10	 <p>Hydrochloride readily soluble and easily diazotized. Yellow diazo solution transparent and stable</p>	A	5	2	Navy blue
		A	10	3	
		OT	5	2	
		OT	10	3	
		OA	5	3	
		OA	10	3-4	
		PA	5	3	
11	 <p>Hydrochloride readily soluble and easily diazotized. Yellow diazo solution transparent and stable</p>	A	5	1-2	Light blue
		A	10	2-3	
		OT	5	3-4	
		OT	10	3-4	
		OA	5	3	
		OA	10	3-4	
		PA	5	2	
12	 <p>Hydrochloride sparingly soluble, but diazotized satisfactorily</p>	A	5	1	Light blue
		A	10	1	
		OA	5	1	
		OA	10	1	
13	 <p>Hydrochloride readily soluble and easily diazotized. Yellow diazo solution transparent and stable</p>	A	5	4	Light blue
		A	10	4	
		OT	5	4	
		OT	10	4	
		OA	5	4	
		OA	10	4	
		PA	5	4	
14	 <p>Hydrochloride readily soluble and easily diazotized. Pale brown diazo solution stable</p>	A	5	1	Garnet-violet
		A	10	1	
		OT	5	1	
		OT	10	2	
		OA	5	1	
		OA	10	2-3	
		PA	5	2	
		PA	10	2-3	

TABLE 1 (continued)

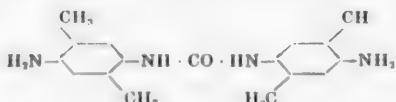
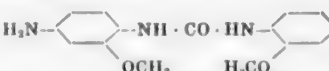
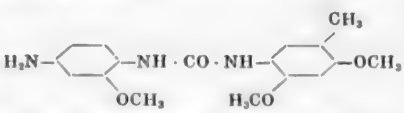
Serial No.	Structure of azoamine, and diazotization and coupling characteristics	Azotol		Fastness to light and weather	Color of dyeing
		mark	concentration (g/liter)		
15	 <p>Hydrochloride readily soluble and easily diazotized. Yellow diazo solution transparent and stable</p>	A	5	1	Garnet
		A	10	1	
		OA	5	1	
		OA	10	1	
16	 <p>Hydrochloride soluble. Dark green precipitate formed rapidly from bright green diazo solution</p>	A	5	1	Violet
		A	10	1	
		OT	5	1	
		OT	10	1	
		OA	5	1-2	
		OA	10	2	
17	 <p>Hydrochloride sparingly soluble, diazotization slow. Diazo solution with green precipitate</p>	A	5	2	Violet
		A	10	2	
		OT	5	1	
		OT	10	1-2	
		OA	5	2	
		OA	10	3	
		PA	5	2-3	
		PA	10	3-4	

TABLE 2

Fastness Tests on Dyeings from Azoamines from Substituted Carbanilides and Azotol A (10 g/liter)

Number of compound in Table 1	Name	Fastness to				
		soaping at		perspiration	rubbing	
		100°	40°		dry	wet
1	4,4'-Diamino-2,2'-dichlorocarbanilide	5/3	5/3-4	5/5	2	1
2	4,4'-Diamino-3,3'-dichlorocarbanilide	5/3	5/5	5/5	4	2
5	4,4'-Diamino-2,2'-dimethyl-5,5'-dichlorocarbanilide	5/3	5/5	5/5	3	1
6	4,4'-Diamino-2,2'-dimethoxy-5,5'-dichlorocarbanilide	4/3	5/5	5/5	4	1-2
8	4,4'-Diamino-2,2'-dimethoxycarbanilide		5/5	5/5	2-3	1
10	4,4'-Diamino-2,2'-dimethoxy-5,5'-dimethylcarbanilide	5/3	5/5	5/5	4	1
11	4,4'-Diamino-2,2',5,5'-tetramethoxycarbanilide	4-5/3	5/5	5/5	2-3	1
12	4,4'-Diamino-2,2'-diethoxy-5,5'-dimethylcarbanilide	3/2	4-5/4-5	4-5/4-5	2	1
13	4,4'-Diamino-2,2',5,5'-tetraethoxycarbanilide	4-5/4	5/5	5/5	3-4	1
14	4,4'-Diaminocarbanilide	5/3	5/3-4	5/5	3	1
15	4,4'-Diamino-2,2',5,5'-tetramethylcarbanilide	3/3	3/4	5/3-4	2	1
16	4-Amino-2,2'-dimethoxycarbanilide	3/3	5/4-5	5/4-5	3	1
17	4-Amino-2,2',4-trimethoxy-5'-methylcarbanilide	2/3-2	5/4	5/4	3	2

The results of the tests, summarized in Tables 1 and 2, show that the fastness to light and weather was almost always lowest in dyeings with Azotol A, highest with Azotol PA, and intermediate with Azotols OT and OA.

The fastness was the same with all four Azotols only if the dyeings had either very low or very high fastness.

If the average fastness of dyeings with Azotol A to light and weather is taken as 100, the average fastness of dyeings with Azotols OT, OA, and PA are 110, 126, and 142 respectively. Therefore the adoption of Azotols OT, OA, and especially PA, in dyeing practice should provide the industry with a considerable increase in the number of fast dyes obtained from the same azoamines.

The simplest of the azoamines studied, 4,4'-diaminocarbanilide, gives dyeings of relatively low fastness to light and weather; introduction of various substituents into its molecules modifies the properties and color of the dye formed.

Despite the common view that chlorine deepens dye hue, introduction of chlorine atoms into the molecule of 4,4'-diaminocarbanilide lightens the hue of the dyeings and lowers their fastness to light and weather. The exception is 4,4'-diamino-3,3'-dichlorocarbanilide, the fastness of which to all treatments is 1 point higher than that of 4,4'-diaminocarbanilide.

In all the cases studied, introduction of two or four methoxyl groups deepens the hue of the dyeings to dark or light blue and raises their fastness to light and weather without lowering the fastness to wet treatments. Introduction of four ethoxyl groups into the 4,4'-diaminocarbanilide molecule in the 2,2',5,5' positions has a particularly strong deepening effect on the hue (to light blue) and increases the fastness of the dyeings to light and weather. In this case the fastness of the dyeings to light and weather is 4 points with all the Azotols, with high fastness to other treatments, apart from wet rubbing.

In the two examples given, the simultaneous introduction of two chlorine atoms and two methoxyl groups deepens the hue of the dyeings. The dyeings obtained with 4,4'-diamino-2,2'-dimethoxy-5,5'-dichlorocarbanilide are faster, and those with 4,4'-diamino-5,5'-dimethoxy-2,2'-dichlorocarbanilide are less fast to the action of light and weather than dyeings obtained with 4,4'-diaminocarbanilide. In a corresponding comparison of 4,4'-diamino-2,2'-dimethoxycarbanilide and 4,4'-diamino-3,3'-dimethoxycarbanilide, introduction of chlorine somewhat lightens the color of the dyeings in both cases, raises the fastness to light and weather in the former case, and lowers it in the latter.

The simultaneous introduction of two chlorine atoms in the 5,5'-positions and two methyl groups in the 2,2'-positions lightens the hue of the dyeings without appreciable change of fastness.

The simultaneous introduction of two methyl groups in the 5,5'-positions and two alkoxy groups in the 2,2'-positions deepens the hue of the dyeings. However, dyeings obtained from 4,4'-diamino-2,2'-dimethoxy-5,5'-dimethylcarbanilide have high fastness, and dyeings from 4,4'-diamino-2,2'-diethoxy-5,5'-dimethylcarbanilide have lower fastness than those from 4,4'-diaminocarbanilide.

The monoaminocarbanilides of asymmetric structure studied gave dyeings which differed little in color and fastness from those obtained with 4,4'-diaminocarbanilide.

The results of these tests are not final, as the dyeings were carried out under the same conditions with all the amines, without their peculiarities being taken into account. Since 4,4'-diaminocarbanilides are derivatives of a class of compounds not yet used for this purpose, it may be possible to find new optimum conditions of dyeings for them, both in the diazotization stage and in the coupling stage.

SUMMARY

1. It was found that substituted 4,4'-diaminocarbanilides (with certain exceptions) can be diazotized to form soluble bisdazo compounds, stable at room temperature, which couple with Azotols at a satisfactory rate.
2. The azoamines tested give a range of colors from red to blue with Azotol A. Among the derivatives of 4,4'-diaminocarbanilide several have been found which couple with Azotols to give dyeings of deep shades and of fairly high fastness to light, weather, water, and soap solution.

LITERATURE CITED

- [1] S. N. Solodushenkov, S. I. Burmistrov, and V. N. Kliuev, Authors' Certif. 89798 (1950).
- [2] V. N. Kliuev, S. N. Solodushenkov, and A. A. Spryskov, J. Appl. Chem. 30, No. 11, 1672 (1957).*
- [3] Coloristic Manual, 2nd edition (Moscow, 1941) pp. 171-175.**

Received June 9, 1956

*Original Russian pagination. See C. B. Translation.

**In Russian.

THE MOLECULAR WEIGHT OF FLAX PECTINS

M. A. Sobolev and A. A. Krasivskaia

The Kostroma Textile Institute

According to the modern views on high polymers, which include pectic substances, the properties of a high polymer are determined by the size of the macromolecule, i.e., the molecular weight, the chemical structure of the molecule, and the physical structure of the macro specimen. The variations in the molecular size of a given substance, which determine the so-called polydispersity of the polymer, are no less important.

There have been few determinations of the molecular weight of the pectic substances of flax and other bast-fiber plants; studies of the pectins in beet, fruits, and vegetables have been far more common, owing to the demands of the food industry.

Ehrlich [1] gave about 1400 for the molecular weight of pectic acid; this agrees fairly closely with his formula for pectic acid, $C_{40}H_{60}O_{36}$. Similar results were obtained by Gaponenkov [2] for the pectic acid in sugar beet. Schneider [3] made use of the fact that esters are more convenient for molecular weight determinations, as they are easy to purify, and determined the molecular weight of nitropectin; he found that each galacturonic residue acquires two nitro groups on treatment with nitric acid; the "dinitropectin" so prepared was soluble in acetone. The molecular weight of this nitropectin, determined by the osmotic method, was 50,000-100,000 for nitropectin obtained by direct nitration of beet pulp, 30,000-50,000 for a preparation extracted in hot water, and 20,000-40,000 for nitrated pectic acid. Shorygin reports that according to Schneider's experiments the molecular weight of apple and lemon pectins, extracted by hot water, reaches 220,000-280,000. Values of 3,000-30,000 have been given for pectic acid from flax [5]. Sosnovskii [6] gives values of the order of 100,000-300,000 (osmometric) and 25,000-50,000 (by the ultracentrifuge) for the molecular weight of apple pectin.

Similar values for the molecular weights of pectins are usually given in more recent papers. Thus, it is stated in the survey by Solms et al. [7] that pectin preparations have molecular weights in the range of 10,000-200,000. Garrick [8] gives 64,000 for the molecular weight of flax pectins.

The industrial production of fibers from flax, which must be widely developed during the Sixth Five-Year Plan, requires extensive studies of the substances which accompany cellulose, and in particular, of pectic substances and of their properties.

Since the pectins of the flax stem have different functions from the pectins of fruits, vegetables, and roots, we consider that data on the properties of fruit and root pectins cannot be extended to stem pectins of bast-fiber plants. Moreover, the pectins in different regions and tissues of the stem should differ, and the data on the total pectin contents, given in the literature, cannot provide a scientific basis for chemical methods for the extraction and subsequent processing of the fibers.

Our purpose was to determine differences in the degree of polymerization of pectins in various tissues of the flax stem — in the bast, in the cortical tissues, and in the technical fibers. The bast was made by hand for this purpose, and was free from visible traces of scutch; cortical tissue was obtained in the form of dust by careful rubbing of bast dried at 30-40°; the fibers (dew-retted and water-retted) were combed to remove traces of scutch. The pectins were converted into nitropectins by nitration of the isolated pectins and also by direct nitration of the pectin-containing materials. The solubility, degree of esterification (from the nitrogen content), and the molecular weight (by the viscosimetric method) of the nitropectins were determined. The methoxyl group contents and gelating power of the pectins were also determined.

EXPERIMENTAL

The pectins were extracted by means of 1% ammonium citrate solution, and isolated from solution by 70% ethyl alcohol. The filtered pectins were washed and dried to the air-dry state. Nitropectins were prepared by treatment a) with nitric acid (sp. gr. 1.51) and b) with nitric acid in presence of metaphosphoric acid.

a) A weighed sample of dry pectin, 1 g in weight, previously ground to a powder, was treated with 100 ml of fuming nitric acid (sp. gr. 1.51) for 1.5 hours with frequent stirring. The whole mass was then poured into 1 liter of distilled water, and the precipitated nitropectins were filtered through paper, washed with water until free from nitric acid, and dried in a vacuum drier at 65° for 6 hours.

The nitropectin was a pale yellow powder, readily soluble in pyridine and caustic alkali solutions, and partially soluble in acetone. The nitrogen content of bast nitropectin was 5.52 to 5.62%, and of the cortical nitropectin, 6.90 to 7.30%. Attempts to increase the percentage of nitrogen and to obtain a product completely soluble in acetone by prolonging the nitration did not give the desired results; moreover, prolonged nitration caused degradation of the nitropectin, as indicated by the decrease of the specific viscosity of the nitropectin solution (Table 1). Therefore the nitration time in the subsequent experiments did not exceed 1.5 hours.

TABLE 1

Effect of Nitration Time on the Specific Viscosity of Bast Nitropectin in 10% NaOH Solution

Nitration time (hours)	Specific viscosity
1.5	0.0677
	0.0801
	0.0731
3	0.0541
	0.0539
8	0.0274
	0.0276

b) A sample weighing 1 g was treated with 100 ml of nitric acid (sp. gr. 1.51) and 30 g of metaphosphoric acid for 1.5 hours at 10°. The nitropectin was a pale yellow powder, readily soluble in pyridine and caustic alkalies, and partially soluble in acetone. The nitrogen content of bast nitropectin was 7.07 to 7.32%, and of the nitropectin from cortical tissue, 7.20 to 7.40%. Therefore nitration in presence of metaphosphoric acid is preferable.

It was reported by Schneider [3] that direct nitration of vegetable material gave nitropectins of higher molecular weight than nitration of isolated pectin; we therefore nitrated flax pectins by both methods. However, direct nitration of tissues containing pectins gave products with low nitrogen contents (average of 6.37% for the bast, and 5.11% for the cortical tissue), darker in color, and of worse solubility.

To determine the degree of esterification, nitrogen was determined in the products by means of the nitrometer. If pectin molecules are assumed to be chains of galacturonic residues, about 75% methylated, then the average molecular weight of such a residue, containing two nitro groups as the result of nitration, is 276.5, and each residue containing 10.10% N. Our preparations contained much less nitrogen; bast nitropectin contained from 7.07 to 7.36%, cortical nitropectin from 7.3 to 7.4%, and fiber nitropectin from 6.18 to 6.77%.

After evaporation of the solvent (acetone), flax nitropectins gave transparent colorless films, similar to films of the corresponding cellulose esters.

The molecular weights of the nitropectins were determined from the specific viscosities of the solutions [9]. The calculations were performed by means of Staudinger's formula $\eta_{sp}/C = K_m M$, where $K_m = 6.3 \cdot 10^{-4}$ [2].

Pyridine and 10% caustic soda were tested as solvents for the nitropectins. It is seen in Tables 2 and 3 that the molecular weights of the nitropectins determined in the two solvents do not agree.

Because of the discrepancies in the molecular weights found by the use of different solvents, it was necessary to investigate the effect of concentration on the specific and reduced viscosity (Figs. 1 and 2).

It was found that in caustic soda solution there is no direct relationship between concentration and specific viscosity. If the concentration is doubled, the specific viscosity is almost unchanged; a 10-fold increase of the concentration changes the viscosity only slightly. This suggests that when nitropectins are dissolved in 10% NaOH solution the macromolecules undergo degradation.

TABLE 2

Specific Viscosity and Molecular Weight of Nitropectins in 10% NaOH Solution

Material studied	Concentration (%)	Specific viscosity	Molecular weight
Cortical nitropectin	0.1	0.0464	20820
		0.0476	20920
Bast nitropectin	0.1	0.0541	23780
		0.0541	23780
		0.0678	29720
		0.0801	35080
Fiber nitropectin	0.1	0.0321	14080
		0.0357	15650
		0.0303	13300

TABLE 3

Specific Viscosity and Molecular Weight of Nitropectins in Pyridine Solution

Material studied	Concentration (%)	Specific viscosity	Molecular weight
Cortical nitropectin	0.005	0.392	124500
		0.430	136600
		0.380	120600
		0.372	118100
Bast nitropectin	0.005	0.386	122600
		0.439	139400
		0.458	145400
		0.446	141600
Fiber nitropectin	0.005	0.077	24440
		0.065	20640
		0.087	27620
		0.090	28570

TABLE 4

Specific Viscosities of Solutions of Different Samples of Bast Nitropectin in Pyridine, of Different Concentrations

Concentration (base-molar)	Specific viscosity	Molecular weight	Concentration (base-molar)	Specific viscosity	Molecular weight
0.005	0.313	99.130	0.005	0.485	157.500
	0.313	99.130		0.453	143.800
	0.330	104.700		0.439	139.400
	0.330	104.700		0.406	128.900
0.05	2.970	94.520	0.05	6.370	202200
	2.980	94.610		6.400	203200
	2.870	91.110		6.350	201650
	3.040	96.510			

TABLE 5

Molecular Weights and Degrees of Polymerization of Nitropectins from Different Parts of the Stem, at a Concentration of 0.005 Base Moles per Liter

Material	Specific viscosity	Molecular weight	Degree of polymerization	Material	Specific viscosity	Molecular weight	Degree of polymerization
Nitropectin from cortical tissue	0.392	124500	444	Nitropectin from water retted fibers	0.077	24440	87
	0.430	136600	487		0.106	33650	120
	0.430	136600	437		0.107	33970	121
	0.372	118100	421		0.065	20640	74
	0.380	120600	431		0.061	19360	69
	0.370	117400	419		0.060	19050	68
Nitropectin from bast	0.439	139400	497	Nitropectin from dew retted fibers	0.100	31750	113
	0.453	143800	513		0.048	15240	54
	0.435	157500	562		0.066	20950	74
	0.406	128900	460		0.072	22860	81
	0.697	221300	790		0.087	27620	99
	0.671	213000	760		0.104	33010	117

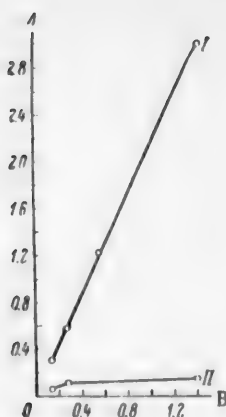


Fig. 1. Variations of the specific viscosity of solutions of flax bast nitropectin in pyridine (I) and 10% NaOH (II) with the concentration. A) Specific viscosity η_{sp} , B) concentration C (%).

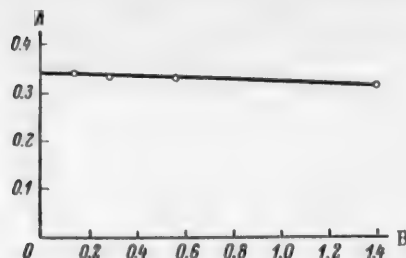


Fig. 2. Variation of reduced viscosity of flax bast nitropectin solution in pyridine with concentration.

A) $\log \eta_{sp}/C$, B) concentration C (%).

The use of caustic soda solutions was therefore abandoned, and pyridine was used as solvent in the subsequent experiments. When the concentration of a solution of nitropectin in pyridine was doubled, the specific viscosity was also doubled; even a 10-fold increase of concentration produced a corresponding change of viscosity (Table 4).

The small deviations in Table 4 may be ascribed not so much to the lack of a linear relationship between vis-

cosity and molecular weight, as to the fact that in some cases sols are not present at these concentrations.

A concentration of 0.005 mole/liter gives the most concordant viscosity values; this concentration was therefore used in all subsequent comparisons of the molecular weights of pectins from different tissues of the flax stem. The results of these determinations are given in Table 5.

It follows from the data in Table 5 that bast pectins have the highest molecular weight, and therefore the highest degree of polymerization (496-790); the degree of polymerization of bast pectins is somewhat lower (421-485), and that of fiber pectins is lowest of all (54-121).

The methoxyl group contents of the same specimens were also determined. According to Ehrlich, the pectins of the flax stem as a whole contain 3.8% methoxyl groups. Our preliminary data suggest that bast pectins have a considerably higher methoxyl content than pectins isolated from the fibers. Average methoxyl contents of the bast and fibers (in %) are given below:

In bast	In fibers
5.03	1.88
2.04	0.82

It was also found that pectins from the bast of the flax stem have a high tendency to gelation, but pectins from the fibers did not form gels under the same conditions. This confirms the known observation that a high molecular weight and presence of methoxyl groups favors gelation of pectins.

SUMMARY

1. In the course of determinations of the molecular weight of flax pectins from the specific viscosity of nitropectin solutions it was found that the best solvent for nitropectins is pyridine, with solutions containing 0.005 base moles per liter
2. It is shown that pectins contained in different parts of the flax stem differ considerably in molecular weight; bast pectins were found to have molecular weight from 128,900 to 221,300, and fiber pectins from 15,240 to 33,070.
3. Pectins extracted from different tissues of the flax stem differ in their methoxyl contents; the methoxyl content of bast is considerably higher than of other tissues. Pectins from the bast of the flax stem had the highest gelating power.

LITERATURE CITED

- [1] F. Ehrlich and F. Schubert, *Biochemisch Z.* 169, 13-66 (1926).
- [2] T. K. Gaponenkov, *J. Gen. Chem.* 7, 14 (1937).
- [3] G. G. Schneider, *Ber.* 69, 2530-2537 (1936).
- [4] P. P. Shorygin, *Carbohydrate Chemistry* (1938) p. 308.
- [5] Z. A. Rogovin and N. N. Shorygina, *Chemistry of Cellulose and Associated Substances* (State Chemical Press, 1953) p. 545.*
- [6] A. L. Rapoport and L. D. Sosnovskii, *Technology of Confectionery Production* (Food Industry Press, 1951) p. 213.*
- [7] H. Deüel, I. Solms and H. Altermatt, *Vierteljahrschrift der Naturforschenden Gesellschaft in Zürich*, 2, 51 (1953).
- [8] P. Garrick, *Chemical products*, XI, 411 (1954).
- [9] F. I. Sadov, N. M. Sokolova, et al. *Laboratory Manual of Chemical Technology of Fibrous Materials* (State Light-Industry Press, 1953) pp. 140-150.*

Received May 18, 1956

*In Russian.

BRIEF COMMUNICATIONS

REACTION OF INDIUM WITH ARSENATE IONS

A. A. Shokol and A. D. Pakhomova

Institute of General and Inorganic Chemistry, Academy of Sciences Ukrainian SSR

The literature contains a considerable number of papers dealing with the interaction of heavy-metal ions with arsenic acid [1-2]. There is almost no information on the formation of indium arsenate. A method for isolation of indium from Cottrell dust by means of sodium arsenate has been patented [3]. While the present investigation was in progress, a brief communication was published in which it was stated that when indium sulfate solution was hydrolyzed in presence of quinquevalent arsenic ions a precipitate was formed, consisting of a compound of the type $5\text{In}_2\text{O}_3 \cdot 3\text{As}_2\text{O}_5 \cdot x\text{H}_2\text{O}$ [4].

The available information on the behavior of indium in the presence of trivalent arsenic ions is contradictory [4, 5].

The purpose of the present investigation was a study of the reaction of indium with arsenic acid in the system indium sulfate-sodium arsenate-sulfuric acid. The original solutions were prepared as follows. To prepare indium sulfate, a weighed quantity of metallic indium was dissolved in sulfuric acid on heating, with addition of a little concentrated nitric acid. The solution was evaporated to dryness twice. The dry residue was cooled and dissolved in a small volume of water; the result was used for preparation of solutions of the required concentration. A solution containing quinquevalent arsenic was prepared from commercial disubstituted sodium arsenate, of "chemically pure" grade.

0.01 M solutions of indium sulfate and sodium arsenate were used for the experiments, the indium-arsenic ratio being varied from 1:1, 1:2, 1:4 to 2:1 and 4:1, the initial acidity of the mixtures corresponding to 25 g of sulfuric acid per liter. The acid was neutralized with caustic soda solution.

No precipitate was formed when the acidity was reduced from 25 to 1 g of sulfuric acid per liter by addition of 10% caustic soda solution. 0.1 and 0.01 N caustic soda solutions were used to reduce the acidity further to pH = 2.5 and 3.5. The pH of the solutions was determined by means of the glass electrode. The precipitates were separated off, washed with hot water, and analyzed. For this, the precipitate was dissolved in a small volume of hydrochloric acid (1:1) with warming; indium was then determined polarographically, and arsenic by the hypophosphite method.

The analytical data for the precipitates and solutions at pH = 3.5, with different indium-arsenic ratios, are given in Table 1.

These results show that at pH = 3.5 all the indium is present in the precipitate, while arsenic is precipitated in approximately equal amounts irrespective of variations of the indium-arsenic ratio. This shows that indium reacts chemically with arsenate ions in equimolar proportions. The absence of indium in solution when its concentration in the original solution is increased can be attributed to its precipitation as the hydroxide together with precipitation of the chemical compound of indium with arsenic acid.

According to literature data, indium hydroxide is precipitated at pH = 3-3.5 [6-9]. Our values for the pH at which indium hydroxide is precipitated from indium sulfate solutions (0.01-0.04 molar) were 3.1-3.2, which is close to the values reported by others (3-4% of indium remains in solution).

It was required to test whether indium reacts with arsenate ions at pH below 3, when indium hydroxide is not formed. It was found that when solutions of indium sulfate (pH = 2.15) and sodium arsenate (pH = 7.78) are mixed a white amorphous precipitate is formed. After separation of the precipitate, the pH of the solution was 2.2, in consequence of the reaction $\text{In}_2(\text{SO}_4)_3 + 2\text{Na}_2\text{HAsO}_4 = 2\text{InAsO}_4 + 2\text{Na}_2\text{SO}_4 + \text{H}_2\text{SO}_4$ (Table 2).

TABLE 1

Analytical Data on Precipitates and Solutions

Original solutions (in g)		In : As ratio	Contents						
indium arsenic			in precipitate				in solution		
			indium		arsenic		indium	arsenic	
			in g	in %	in g	in %			in g
0.0114	0.0075	1 : 1	Not determined		0.0063	84.0	Traces	0.0018	24.0
0.0114	0.0150	1 : 2	0.0112	98.2	0.0067	45.0		0.0074	49.4
0.0114	0.0300	1 : 4	0.0106	92.8	0.0070	23.3		0.0236	78.8
0.0228	0.0075	2 : 1	Not determined		0.0070	93.5		None	—
0.0456	0.0075	4 : 1	0.0450	98.8	0.0071	94.7		None	—

TABLE 2

Analytical Data on Precipitates and Solutions at Different pH

Original solutions (in g)		In : As ratio	Solution pH	Contents					
indium arsenic				in precipitate				in solution*	
				indium		arsenic		indium	
				in g	in %	in g	in %	in g	in %
0.0228	0.0150	1 : 1	2.18	0.0206	90.3	0.0121	80.6	0.0025	10.9
0.0114	0.0150	1 : 2	2.22	0.0108	96.3	0.0084	56.0	0.0005	4.4

* Arsenic was not determined in the solutions.

TABLE 3

Results of Experiments

Original solution (g)		In : As ratio	Contents					
indium	arsenic		in precipitate				in solution*	
			indium		arsenic		indium	
			in g	in %	in g	in %	in g	in %
0.0114	0.0075	1 : 1	0.0042	36.8	0.0025	33.3	0.0078	68.4
0.0114	0.0150	1 : 2	0.0045	39.5	0.0053	35.4	0.0075	67.0
0.0114	0.0300	1 : 4	0.0050	43.7	0.0070	23.3	0.0065	57.0
0.0228	0.0075	2 : 1	0.0033	16.7	0.0037	49.3	0.0201	83.0
0.0456	0.0075	4 : 1	0.0036	7.9	0.0041	54.8	0.0402	88.0

* Arsenic was not determined in the solutions.

These data show that indium is precipitated in presence of arsenic at pH = 2.2.

The values found for the pH of precipitation of indium in presence of quinquevalent arsenic ions agree with literature data [4].

For determination of the composition of the compound formed at pH = 2.2, it was isolated in the pure state by the mixing of 0.01 M solutions of indium sulfate and disubstituted sodium arsenate (In : As = 1 : 2). The white amorphous precipitate was filtered off, washed thoroughly with hot water to negative reactions for SO_4^{2-} and

AsO₄³⁻ ions, dried at 110° to constant weight, and analyzed. A weighed sample of the dry substance was dissolved in cold 1:1 hydrochloric acid. Indium was determined polarographically, and arsenic by the hypophosphite method. Water was determined by drying at 150, 300, and 600°. Water is removed in 2 hours at 300-310°. Water was also determined by the liberation of acetylene when a weighed sample of the salt was heated to 200° with calcium carbide. The acetylene liberated was found from the weight of copper acetylide precipitated by it [10].

Found %: Indium 42.36; arsenic 27.28; water 6.51. InAsO₄·H₂O Calculated %: Indium 42.24; arsenic 27.57; water 6.65.

It follows from the analytical data that in the conditions studied (pH of medium = 2.2), indium ortho-arsenate of the composition InAsO₄·H₂O is formed.

As is known, indium is isolated from industrial liquors containing various impurities (including arsenic) by means of metallic zinc [11], zinc amalgam [12], or zinc oxide [13-14]. It was therefore desired to study the behavior of indium in presence of arsenate ions in the neutralization of sulfuric acid solutions by an aqueous suspension of zinc oxide. The experimental conditions were as described above.

In contrast to neutralization by caustic soda, when zinc oxide is used indium is partially precipitated when 1 g of free acid per liter (pH ≈ 2) is left in solution. The results are given in Table 3.

These results show that the amount of indium in the precipitate varies only slightly with changes of the indium-arsenic ratio, whereas the arsenic content varies 1.5 to 2.5-fold. It is probable that the formation of the compound of indium with arsenate ions is accompanied either by adsorption of arsenic or zinc oxide, or by chemical reaction of zinc oxide with arsenic acid.

In this connection, and also for comparison with the results in Table 1, it was of interest to study the behavior of indium and arsenic in the neutralization of solutions by aqueous suspensions of zinc oxide to pH = 2.5-3.5.

The results of these experiments are given in Table 4.

TABLE 4

Analytical Data on Precipitates and Solutions at Different pH

Original solutions (In g)		In:As ratio	pH value	Contents							
Indium	arsenic			in precipitate				in solution			
				indium		arsenic		indium		arsenic	
				In g	In %	In g	In %	In g	In %	In g	In %
0.0114	0.0075	1:1	2.5	0.0088	77.2	0.0071	94.6	0.0025	21.9	Not determined	
0.0114	0.0075		3.5	0.0111	97.4	0.0072	96.0	Nil		Nil	
0.0114	0.0150	1:2	2.5	0.0085	74.5	0.0110	73.5	0.0024	21.1	0.0037	24.6
0.0114	0.0150		3.5	0.0110	96.5	0.0145	96.6	Nil		Nil	
0.0114	0.0300	1:4	2.5	0.0090	79.0	0.0245	81.5	0.0023	20.1	0.0045	15.0
0.0114	0.0300		3.5	0.0112	98.2	0.0293	97.6	Nil		Nil	
0.0228	0.0075	2:1	2.5	0.0110	48.2	0.0071	94.7	Not determined		Traces	
0.0228	0.0075		3.5	0.0211	92.5	0.0074	98.6	0.0014	6.1	Nil	
0.0456	0.0075	4:1	2.5	0.0112	24.5	0.0074	98.6	0.0337	73.9	Nil	
0.0456	0.0075		3.5	0.0440	96.5	0.0074	98.6	0.0020	4.4	Nil	

The results in Table 4 show that when the solutions are neutralized by aqueous suspensions of zinc oxide to pH = 2.5, indium is not completely precipitated, as might have been expected by analogy with the results in Table 2; over 20% of the indium remains in solution. Zinc was found in the precipitate together with indium and arsenic. From the amounts of indium, zinc, and arsenic found by analysis it was calculated that the

precipitate consists of a mixture of indium and zinc arsenates. The absence of arsenic in solution at pH = 3.5, even when taken in 4-fold excess, also shows that it reacts with zinc. For determination of the composition of the compound formed, the precipitate formed by the interaction of 0.01 M solutions of zinc sulfate (pH = 6.4) and disubstituted sodium arsenate (pH = 7.8) was analyzed. The pH of the mixture was 5.5. The following results were obtained:

Found %: Zinc 41.2; arsenic 32.0. $Zn_2(AsO_4)_2$. Calculated %: Zinc 41.4; arsenic 31.6.

Therefore when sulfuric acid solutions containing indium and arsenic are neutralized by zinc oxide to pH 2.5-3.5, the formation of indium arsenate is accompanied by partial formation of sparingly soluble zinc arsenate [16, 15] according to the equation:



The formation of zinc arsenate at pH = 2.5-3.5 is evidently the consequence of local increases of the hydroxyl-ion concentration on addition of aqueous suspensions of zinc oxide.

SUMMARY

It was found in a study of the reaction of indium with arsenate ions in the neutralization of sulfuric acid solutions containing indium and arsenic that indium orthoarsenate is formed at pH = 2.2 on neutralization of the solutions with caustic soda; if the solutions are neutralized with aqueous suspensions of zinc oxide, zinc orthoarsenate is formed in addition to indium orthoarsenate.

LITERATURE CITED

- [1] J. W. Mellor, A Comprehensive Treatise on Inorganic and Theoretical Chemistry, 9, 149-185 (1933).
- [2] Gmelins Handbuch der anorg. Chemie, Arsen, 17, 343-351 (1952).
- [3] Chem. Abs. 46, 11086 (1952).
- [4] D. M. Chizhikov, N. A. Gurovich and G. M. Denisova, J. Appl. Chem. 29, 5, 798 (1956).*
- [5] A. T. Nizhnik, Ukrain. Chem. J. 22, 4, 441 (1956).
- [6] E. M. Hattox and T. de Vries, J. Am. Chem. Soc. 58, 2126 (1936).
- [7] T. Müller, J. Am. Chem. Soc. 63, 2625 (1941).
- [8] B. N. Ivanov-Emin and E. A. Ostroumov, J. Gen. Chem. 14, 777 (1944).
- [9] B. V. Gromov, Non-Ferrous Metals 3, 29 (1948).
- [10] W. Boller, Ch. Zeit. 50, 537 (1926).
- [11] A. T. Nizhnik, Soviet Author's Certif. No. 68440, January 23 (1941).
- [12] A. K. Babko, G. P. Polishchuk and A. I. Volkova, Mem. Inst. Chem. Acad. Sci. Ukrainian SSR 7, 505 (1941).
- [13] A. N. Zelikman, G. B. Samsonov and O. E. Krein, Metallurgy of the Rare Metals (Metallurgy Press, 1954).**
- [14] G. A. Meerson and A. N. Zelikman, Metallurgy of the Rare Metals (Metallurgy Press, 1955).**
- [15] Chemist's Reference Book, 2 (State Chem. Tech. Press, 1951).**
- [16] J. W. Mellor, A Comprehensive Treatise on Inorganic and Theoretical Chemistry, 9, 197 (1933).

Received December 18, 1956

*Original Russian pagination. See C. B. Translation.

**In Russian.

SORPTION OF NITROGEN OXIDES BY SOLID SORBENTS*

S. N. Ganz

The Dnepropetrovsk Institute of Chemical Technology

There are still no satisfactory methods for sorption of nitrogen oxides at low concentrations (below 0.3-0.25%) under industrial conditions. In view of the rapid development of the nitric and sulfuric acid industries, and of the production of nitrogen fertilizers and other nitrogenous substances, it has become necessary to develop efficient methods for the sorption of low concentrations of nitrogen oxides in order to improve working conditions from the viewpoint of industrial hygiene, and to decrease losses of nitric acid.

The liquid sorbents used in industry can be used to absorb nitrogen oxides down to 0.15-0.3%. Adsorption should be used for more complete removal. The most rational procedure in the development of an efficient method of adsorption and the choice of a stable sorbent for sorption of nitrogen oxides is a combination of adsorption methods for concentrated gases with adsorption for gases at low concentrations.

Despite numerous investigations [1-5], solid sorbents are not used industrially for sorption of nitrogen oxides. The explanation is that a stable and effective sorbent has not yet been found, and no adequately economical and technically efficient method for adsorption of nitrogen oxides at low concentrations, especially from moist gases, has yet been developed.

In a search for the most efficient and stable sorbent, we studied the sorptive capacity of activated carbon, aluminosilicate, silica gel, manganese dioxide, copper oxide, hopcalite (60% MnO_2 + 40% CuO), and coke toward gas from an industrial nitric acid unit, and determined the desorption conditions for these sorbents.

EXPERIMENTAL**

The experiments were performed in the experimental unit of the nitric acid plant. The nitrous waste gas was drawn through a trap filled with glass wool (to trap droplets of liquid nitric acid) and then passed through sorption vessels filled with a given sorbent. The sorbent grains were all of similar size,*** and were supported on a layer of glass beads. The amount of gas drawn through was measured by means of flow meters.

After the adsorption, the gas was passed into the atmosphere by means of an exhauster. The concentrations of nitrogen oxides at the entry and exit were determined by the evacuated-bulb method, and the degree of oxidation of NO was determined iodometrically. The temperature fluctuated in the range of 18-20° during the experiments. The exhauster drew gas through the system at constant volume rates of 1000 or 2000 $\text{m}^3/\text{m}^3 \cdot \text{hour}$, the corresponding linear gas velocities being 0.024 and 0.048 meter/second.

The relative adsorptive capacities of the above-named sorbents and their desorbability in repeated adsorption and desorption cycles were studied in the first series of experiments. The physicochemical properties of the sorbents: mechanical strength, hardness, catalytic activity, desorption temperature, etc., were also studied for evaluation of their practical suitability.

The results were used to plot the interpolated curves in Fig. 1, which represent the sorptive capacities of the sorbents at a gas rate of 1000 $\text{m}^3/\text{m}^3 \cdot \text{hour}$, $t = 18-20^\circ$, and average concentration of $\text{NO} + \text{NO}_2$ in the gas 0.3%

*Communication I.

**M. A. Berlin took part in the experimental work.

***The sorbents were sifted through sieves of 3-4 mm mesh.

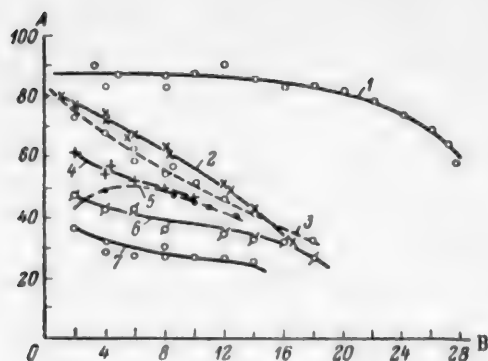


Fig. 1. Relative degree of adsorption of nitrogen oxides by granular sorbents as a function of time, with average concentration of $\text{NO} + \text{NO}_2 = 0.3\%$ and $t = 18-20^\circ$.

A) Degree of adsorption (%), B) time (hours). Sorbents: 1) active carbon, 2) aluminosilicate, 3) silica gel, 4) MnO_2 , 5) hopcalite at $w = 1000 \text{ m}^3/\text{m}^3 \cdot \text{hour}$, 6) CuO , 7) hopcalite at $w = 1600 \text{ m}^3/\text{m}^3 \cdot \text{hour}$.

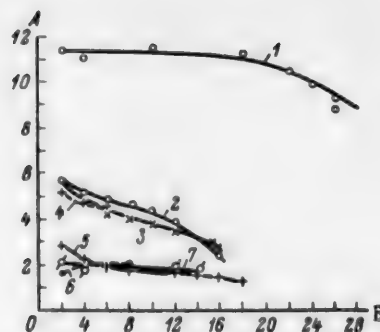


Fig. 2. Relative adsorptive capacity of granular sorbents with 0.3% of $\text{NO} + \text{NO}_2$ in the gas at $t = 18-20^\circ$.

A) Amount of nitrogen oxides adsorbed ($\ln \text{ cc/g}$), B) time (hours).

Sorbents: 1) active carbon, 2) aluminosilicate, 3) silica gel, 4) MnO_2 , 5) CuO , 6) hopcalite at $w = 1600 \text{ m}^3/\text{m}^3 \cdot \text{hour}$, 7) hopcalite at $w = 1000 \text{ m}^3/\text{m}^3 \cdot \text{hour}$.

($\text{NO} = 60\%$, $\text{NO}_2 = 40\%$). Figure 2 shows calculated data on the sorptive capacities of the sorbents, expressed in cc (reduced to normal conditions) of $\text{NO} + \text{NO}_2$ adsorbed per 1 g of sorbent.

The relative efficiencies of the sorbents are shown by the positions of the curves in Figs. 1 and 2.

These results show that active carbon has the highest adsorptive capacity. The curves for adsorption on aluminosilicate and silica gel lie below the curve for active carbon. All these three sorbents retain their adsorptive power for a long time, with a fairly high degree of sorption of nitrogen oxides.

The other sorbents — hopcalite, MnO_2 , CuO , and coke — have lower adsorptive capacities and, as subsequent experiments showed, are difficult to regenerate. The sorption of nitrogen oxides by hopcalite, MnO_2 , and CuO depends on chemical reactions of these substances with nitrogen oxides and with HNO_3 in the form of liquid drops [5]. Therefore these sorbents are probably unsuitable for practical use.

Experiments on the regeneration of activated carbon, aluminosilicate, and silica gel showed that these sorbents catalyze the oxidation of NO to a considerable extent, so that nitric acid is formed in their pores; removal of this acid presents considerable difficulties. Complete desorption of nitrogen oxides is possible only at temperatures of the order of $200-350^\circ$.

Desorption experiments with these sorbents showed that at temperatures above 300° carbon may ignite,** while at lower temperatures the adsorptive power of the adsorbent is not fully restored. Complete desorption of nitrogen oxides from silica gel and aluminosilicate is likewise not possible at temperatures below 300° . However, above 200° silica gel crumbles to a fine powder, which makes it difficult to use. The most stable sorbent under these conditions is aluminosilicate, which withstands regeneration temperatures of 500° and over (but not above 700°).

Moreover, aluminosilicate has the highest mechanical strength and hardness of these three sorbents; this is very important for prolonged use of the sorbent and for the operation of highly efficient adsorption methods (sorption in a fluidized layer, use of a moving bed of the sorbent, etc).

Although active carbon has the highest adsorptive power, because of its ease of oxidation under the given conditions and of its low mechanical strength it cannot be recommended for practical use. Similarly, silica gel

* The regeneration temperature (between 200 and 350°) depends on the nature of the sorbent.

** In presence of oxygen.

cannot be recommended for industrial use owing to its rapid powdering at high temperatures. Therefore the most suitable sorbent for sorption of nitrogen oxides is aluminosilicate, which has fairly high adsorptive power, high mechanical strength, and stability in high-temperature regeneration.

LITERATURE CITED

- [1] M. N. Merlis and O. D. Petrova, *J. Chem. Ind.* 5 (1935).
- [2] P. F. Cherepkov, *J. Chem. Ind.* 12 (1946).
- [3] V. N. Ruff, *J. Projection Construction Chem. Ind.* 8 (1935).
- [4] H. Curtis, *Fixed Nitrogen* (Russian translation) (ONTI Goskhimizdat, Moscow-Leningrad, 1934).
- [5] H. W. Webb, *Absorption of Nitrous Gases* (Russian Translation) (Supreme Council of the National Economy Ukrainian SSR, Khar'kov, 1931).

Received July 11, 1956

THERMAL DECOMPOSITION OF MIDDLE-TEMPERATURE COAL PITCH

A. N. Chistlakov

The thermal treatment of solid fuel without access of air yields tar in addition to coke or semicoke and gas; the yield and composition of the tar depend both on the nature of the original fuel and on the technological process conditions.

Tars are mixtures of individual compounds which have not yet been studied fully. Of the 10,000 compounds presumed to be present in high-temperature coal tar, only 282 have been established with certainty [1].

The fraction of tar which has been studied least is pitch – the residue from the distillation of coal tar up to 360°. The composition of all pitches obtained from high-temperature tars is the same in principle, and differs only in the relative proportions of the components; these consist mainly of polycyclic aromatic and heterocyclic compounds; only 55 have been identified so far, including 32 aromatic hydrocarbons and 23 heterocyclic compounds [2].

It may be noted that methylated aromatic hydrocarbons and compounds containing phenolic hydroxyl groups are found only in the fractions boiling between 350 and 400°.

Coal-tar pitch is widely used as a binder for briquetting in the electrode industry, for the production of electrode coke, and in building, etc.

In certain industries it is subjected to heating at various temperatures; it is then very important to know the behavior of the pitch and the yields and compositions of its decomposition products. This paper deals with an investigation of these problems.

EXPERIMENTAL

The experiments were performed with coal-tar pitch obtained from a tube still in one of the coke-oven plants; the characteristics of the pitch are given below:

Softening temperature (°C)	Content of "free" carbon (%)	Ash (%)	Elementary composition (% of the organic material)				
			C	H	N	S	(O by difference)
78	17.8	0.27	92.90	4.45	1.48	0.95	0.22

A diagram of the apparatus is given in Fig. 1.

30-50 g of pitch was put into the retort; the whole system was tested for air tightness, and the retort was then heated to a definite temperature at a rate of 3 degrees/minute; the experiments were performed at temperatures from 500 to 900°. The material balance in Table 1 shows that increase of temperature raises the yield of tar from 6.7% (at 500°) to 30.0% (at 900°) and of gas from 1.2 to 5.6 wt. % respectively; the yield of semicoke (coke) decreases.

Tar formation is most intensive at 700-800°.

The nature of the tar also changes appreciably; it becomes heavier (Table 2).

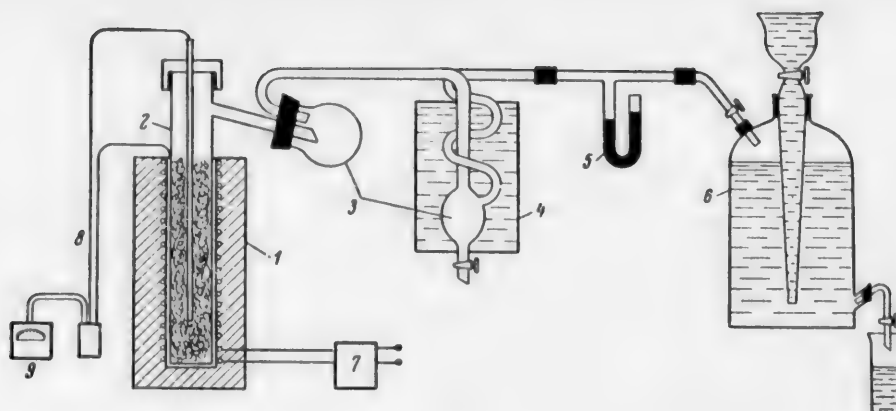


Fig. 1. Diagram of the apparatus.

1) Electric furnace, 2) retort, 3) tar receiver, 4) condenser, 5) manometer tube, 6) gas holder, 7) LATR-1 (transformer), 8) thermocouples, 9) millivoltmeter.

TABLE 1

Material Balance for the Thermal Decomposition of Pitch

Temperature of experiment (°C)	Orig.mat. pitch (g)	Yields					
		gas			tar		semicoke (coke) + losses
		density (in g/liter)	yield		in g	in %	in g
			in ml	in wt. %			in %
500	30	0.349	1050	1.23	2.0	6.67	27.6
600	30	0.300	2720	2.73	3.9	13.00	25.2
700	30	0.254	4880	4.12	5.6	18.70	23.1
800	30	0.212	7140	5.00	8.7	28.00	20.0
900	30	0.211	7970	5.60	9.0	30.00	19.3

TABLE 2

Characteristics of the Tar

Temperature of experiment (°C)	Elementary composition of tar (%)					Density d_4^{20}
	C	H	N	S	O (by difference)	
500	86.00	6.66	1.51	0.99	4.84	1.17
600	87.30	6.46	1.54	0.85	3.85	—
700	90.40	6.00	1.48	0.89	1.23	1.24
800	90.20	5.61	1.58	1.27	1.34	$d_{50}^{50} = 1.16$
900	91.65	5.59	1.68	0.86	0.22	$d_{50}^{50} = 1.17$

Variations in the composition of the gas with the heating temperature of the pitch are plotted in Fig. 2; the hydrogen content increases from 67 to 85%, and the carbon monoxide content increases somewhat; of the other components, the methane content decreases appreciably, from 27.2 to 10.3%.

Analyses of gas samples taken over definite ranges of temperature showed that the greatest changes in the contents of carbon dioxide and monoxide and methane take place between 400 and 700°; this shows that the

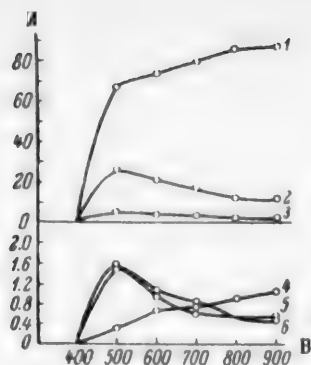


Fig. 2. Effect of coking temperature of middle-temperature pitch on the composition of the gas.

A) Composition of gas (vol. %), B) temperature ($^{\circ}C$).

Gases: 1) H_2 , 2) CH_4 , 3) N_2 , 4) CO , 5) $CO_2 + H_2S$, 6) $C_n H_m$.

oxygen-containing and methylated compounds in pitch are unstable at relatively low temperatures.

The sulfur content of the coke decreases with increase of the coking temperature of the peat, some of the sulfur compounds passing into the tar.

The behavior of pitch during heat treatment in absence of air shows some differences from the behavior of coal. This is seen primarily in the yields and properties of the tar; the probable explanation is that pitch, unlike coal, is a mixture of individual compounds.

LITERATURE CITED

- [1] O. Kruber, A. Raeithel and G. Grigolet, *Erdöl u. Kohle*, 9, 637 (1955).
- [2] H.-G. Franck, *Brennstoff-Chemie*, 1/2, 12 (1955); *Bitumen, Teere, Asphalte, Pech*, 2, 42 (1955).

Received July 7, 1956

CATALYTIC METHOD FOR THE SYNTHESIS OF VINYL ESTERS

N. S. Kozlov and S. Ia. Chumakov

The A. M. Gor'kii State University, Perm'

Vinyl esters have a great variety of technological uses: in the production of plastics, varnishes, synthetic fibers, etc. Because of their exceptional chemical reactivity, vinyl esters are also widely used in laboratory organic syntheses.

This accounts for the great deal of attention devoted in recent years to the synthesis and studies of the properties of vinyl esters. Despite the diversity of available methods for their preparation, the principal method used is catalytic vinylation of organic acids with acetylene. This reaction can be effected either in the liquid or in the vapor phase. In the former case, the organic acid, usually containing a mercury catalyst, is saturated with acetylene. In the latter case, organic-acid vapor is passed over a heated catalyst in a current of acetylene; zinc or cadmium salts of organic acids are recommended as catalysts.

The synthesis of vinyl esters is the subject of a number of reviews which give a clear picture of the field [1-4].

The present investigation consisted of a study of the catalytic synthesis of vinyl esters from organic acids and acetylene in the vapor phase. The effects of temperature and acetylene pressure on the ester yield were studied - questions which are not discussed in the literature.

The experiments on the synthesis of vinyl esters were performed in apparatus described by one of us earlier [5]. The catalyst used was zinc acetate supported on fireclay, and copper acetylide. For preparation of the copper acetylide, fireclay was impregnated with ammoniacal cuprous oxide solution; the product was treated with acetylene in a funnel and dried in a current of acetylene in the reaction tube. The fireclay contained about 1% of copper acetylide. This catalyst was safe to use. A portion of catalyst weighing about 30 g, with a volume of 45-50 ml, was taken for the experiments.

The experiments were performed as follows. After the reaction tube had been heated to the temperature of the experiment, acid was fed in from a header vessel at a rate of 10 drops per minute, and acetylene was then passed from a cylinder through a special valve, the necessary pressure of acetylene being maintained in the reactor throughout the experiment. With this procedure, although undiluted compressed acetylene was used, the acetylene became diluted in the reaction zone by vapors of the starting materials and reaction products, and the explosive properties of compressed acetylene under the action of heat were thereby diminished. 15-20 g of organic acid was generally taken for each experiment. The catalyzate was treated with sodium carbonate solution, and the vinyl ester formed was extracted in ether. The ether extract was dried, and the vinyl ester was distilled after evaporation of the solvent. The alkaline solution of salts formed after the catalyzate had been washed with sodium carbonate was acidified with sulfuric acid; the liberated fatty acids were distilled in steam. Unreacted fatty acids were determined in the distillate by titration. In the first experiments, the influence of acetylene pressure on the yield of vinyl acetate in the reaction of acetylene with acetic acid was studied; the reaction was performed at 210-220° in presence of zinc acetate on fireclay. The results are given below:

Acetylene pressure (atm)	1	5	10-12
Yield of vinyl acetate, on the acid taken (%)	9.3	34.9	53.1
Yield of vinyl acetate, on the acid reacted (%)	46.5	47.7	73.3

This shows the great effect of increase of the acetylene pressure in the reaction zone on the yield of vinyl acetate.

A special series of experiments were performed to determine the effect of temperature on the yield of vinyl acetate if the reaction is carried out under acetylene pressure of 10-12 atm. The results are given below:

Temperature (°C)	150	200	230	260	300
Yield of vinyl acetate, on the acid taken (%)	18.3	53.1	23.7	23.7	11.6
Yield of vinyl acetate, on the acid reacted (%)	70.2	73.6	29.6	29.6	2.0

It was found that the yield of vinyl ester decreases appreciably if the temperature is raised above 200°; high-boiling reaction products are formed. These products are probably formed as the result of chemical transformation of the vinyl ester.

A temperature of 200° and acetylene pressure of 10-12 atm are also the optimum conditions for the reaction of acetylene with acids in presence of copper acetylide. Therefore several fatty acids were vinylated under these conditions in presence of copper acetylide. The results are given in the Table.

Results of Experiments on the Vinylation of Fatty Acids

Acid	Yield of vinyl ester (%)	
	on acid taken	on acid reacted
Acetic acid	44.2	55.2
Propionic acid	59.3	70.1
N-Butyric acid	50.3	57.5
Isobutyric acid	48.1	60.3
Isovaleric acid	55.6	70.0

It is seen that the copper acetylide used was a highly active catalyst in the vinylation of fatty acids.

The vinyl esters obtained had the following constants:

Ester	Boiling point	d_4^{20}	n_D^{20}
Vinyl acetate	71-73	0.9346	1.3962
Vinyl propionate	91-92	0.9156	1.3980
Vinyl butyrate	112-114	0.9124	1.4065
Vinyl isobutyrate	103-104	0.9076	1.3991
Vinyl isovalerate	134-135	0.9060	1.4096

LITERATURE CITED

- [1] S. N. Ushakov and Iu. M. Fainshtein, *Plastics*, 1, 4 (1933); S. N. Ushakov, E. N. Rostovskii and I. A. Arbuzova, *J. Appl. Chem.*, 13, 1629 (1940); E. N. Rostovskii and A. I. Barinova, *J. Appl. Chem.*, 27, 1101 (1954).
- [2] J. Nieuwland and R. Vogt, *Chemistry of Acetylene* (Russian translation) (IL, 1947) p. 57.
- [3] *Monomers* (Russian translation) (IL, 1951) p. 57.
- [4] *Chemistry of Acetylene* (collected papers) (Russian translation) (IL, 1954) pp. 166, 204.
- [5] N. Kozlov, G. Fridman and V. Volchkova, *Trans. Inst. Chem. Acad. Sci. Belorussian SSR*, 3, 5 (1937).

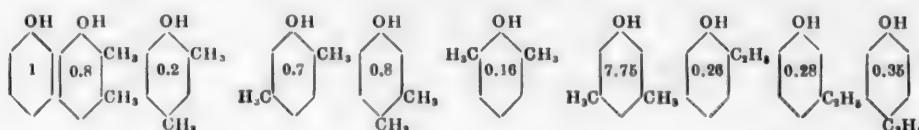
Received June 15, 1956

CONDENSATION OF XYLENOLS (WITH FORMALDEHYDE) IN PRESENCE OF AN ACID CATALYST*

N. V. Shorygina and G. I. Kurochkina

Technical xyenols are mixtures of six isomers with two substituent methyl groups in the nucleus, and three isomers with an ethyl group in the ortho, meta, and para positions respectively. According to the principles of classical organic chemistry, substituent groups, including the methylol group, occupy particular positions which depend on the directing effect of the groups present in the molecule.

It is known [1] that the reaction rates of different xylenol isomers with formaldehyde differ considerably. If the rate of reaction of phenol with formaldehyde is taken as unity, the rates of reaction of different xylenol isomers with formaldehyde are between 7.5 and 1/6:



These large differences between the reaction rates of different xylenol isomers with formaldehyde depend on the relative positions of the hydroxyl and methyl or ethyl groups. It is easily seen that when the directing influences of the hydroxyl and ethyl groups coincide (in *m*-ethylphenol), the rate of the reaction with formaldehyde increases, and is $2\frac{1}{2}$ times the reaction rate of the unsubstituted phenol. When the influences of the hydroxyl and two methyl groups coincide (3,5-xylenol), the rate of reaction with formaldehyde is 7.5 times as high.

When the directing influence of one methyl group coincides with the influence of the hydroxyl, while the directing influence of the other opposes the latter, the reaction rate of the isomer decreases and does not exceed 0.7-0.8 times the rate for phenol. Finally, if both the methyl groups of the xylenol oppose the directing influence of the hydroxyl, i.e., if they are in the ortho-ortho or in the ortho-para positions, the rate of reaction with formaldehyde falls to 0.16-0.3 times the rate for phenol.

Therefore a mixture of technical xylenols is a system containing molecules which react with formaldehyde at very different rates (3,5-xylenol reacts with formaldehyde at about 50 times the rate of 2,6-xylenol). It follows that if attempts are made to condense this mixture with formaldehyde under conditions suitable for condensation of phenol, a highly viscous, strongly structurized mass of the resite type is obtained, plasticized by the unchanged inactive isomers, instead of a more or less homogeneous resin.

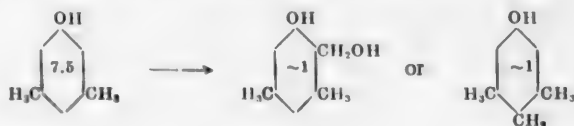
In industrial practice xylenols are used as additives (not over 40%) to crystalline phenol in the production of molding materials. Increase of the content of technical xylenols in the reaction mixture has an adverse effect on the hardening rate and the mechanical strength of the molding material.

By equalizing the rates of reaction of individual xylenol isomers with phenol, we obtained a novolak resin from technical xylenols without addition of crystalline phenol. The methods used for equalization of the reaction rates were: a) decrease of the reaction temperature at the first stage to 70°, b) stepwise addition of

*Communication I in the series on the synthesis of xylenol-formaldehyde resins.

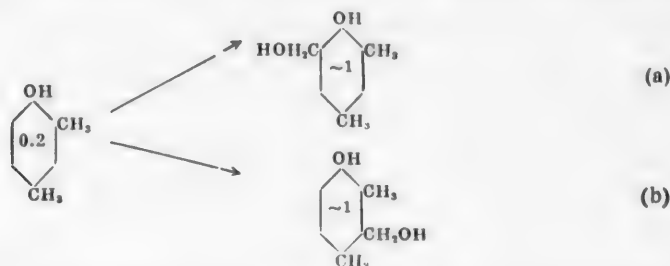
catalyst, c) partial neutralization of the acid catalyst before the start of dehydration of the finished resin.

At the first stage of the reaction, the reactivity of all the isomers is decreased by a shortage of acid (at pH about 3.5). If we assume that one methylol group enters the xylenol molecule, then the reactivity of the active isomers is decreased, and that of the less active isomers is increased.



In this case the new substituent hinders further substitution.

If the less active isomers react with formaldehyde, the compounds formed become more active:

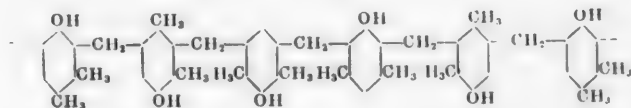


because the new substituent favors entry of further substituents. In case (a) the methylol group intensifies the directing influence of the methyl groups, and in case (b) its influence coincides with the directing influence of the hydroxyl.

After an hour, when the reaction has slowed down, a second portion of acid is added, the mixture is brought to the boil, and the condensation is continued for 1 hour more. Addition of the second portion of acid brings the pH of the medium to about 1, which favors the condensation of the least-active isomers with formaldehyde [2].

At the end of the condensation 40% NaOH is added to the reaction mixture, in a quantity sufficient to neutralize half the acid added, and the resin is dried under vacuum to a drop point of 120-135°. The yield of resin is 100% on the xylenol, and the hardening time is 50-90 seconds.

The chain molecule of the novolak resin made from xylenol has only one free position in each aromatic nucleus:



Naturally, hardening of such resins proceeds with difficulty, as the substituents in the molecules prevent mutual approach of the free positions in the chains. Moreover, as the reaction diagram shows, the formation of hydrogen bonds is hindered if isomers of different structure are condensed.

The hardening rate of xylenol-formaldehyde resins is somewhat lower than that of phenolic resins, and the mechanical strength of molded articles made from them is also lower. However, the difference is not large, and in a number of cases xylenol-formaldehyde resins may be recommended as partial or complete substitutes for phenolic resins.

For example, xylenol-formaldehyde resin may be used for production of a molding material containing 75% of xylenol and 25% of phenolic resins, which is undoubtedly more economic than the molding material now being produced from a mixture of 60% of phenol with 40% of xylenol.

Xylenol-formaldehyde novolaks are more suitable for use as binders for sand-resin molds in metal casting.

Trials of xylenol-formaldehyde resin as a substitute for bakelite powder in a number of foundries showed that molds and cores based on it have good smooth surfaces and adequate mechanical strength (tensile strength 35-40 kg/cm², as compared with up to 40-50 kg/cm² for bakelite powder).

SUMMARY

A condensation procedure and formulation is described for the production of novolak resins from technical xylenols without addition of crystalline phenol.

The xylenol-formaldehyde novolak resins can be used in the production of sand-resin mixtures for metal casting.

LITERATURE CITED

- [1] M. M. Sprung, J. Am. Chem. Soc. 63, 334 (1941).
- [2] H. Matsuo, J. Soc. Chem. Ind. Japan, 47, 466 (1944); H. F. Müller, J. Müller, Kunststoffe, 38, 221 (1948).

Received June 20, 1956

THE EFFECTS OF SOME IMPURITIES IN MELAMINE ON ITS CONDENSATION WITH FORMALDEHYDE

L. M. Pesin, V. N. Kotrelev, A. E. Zarubitskii and F. E. Segalevich

As is known, industrial melamine may contain certain impurities: dicyanodiamide, guanidine, ammeline, ammelide, and products of the deamination of melamine: melam, melem, melan, etc.

We studied the influence of alkali-soluble impurities (consisting mainly of ammeline and ammelide) on the course of condensation of melamine with formaldehyde.

A mixture of ammeline and ammelide, isolated by neutralization with hydrochloric acid of the mother liquor from the crystallization of melamine from a weakly alkaline medium, was added to chemically pure melamine, and the rate of condensation was determined by the following method. The standard and the test samples of melamine were ground in a porcelain mortar. 4 g of the powdered melamine was placed in a test tube 17-18 mm in diameter and 170-180 mm long. Formalin was then added, equivalent to 3 moles of formaldehyde per 1 mole of melamine. The formalin solution contained 36-37% formaldehyde by weight, with pH 7 established by the Michaelis method by means of 0.5 N NaOH solution. After the pH had been stabilized, the formalin solution was suitable for use for 6 hours.

The test tubes were provided with glass rods, fixed in a stand, and immersed in a water bath at 80-85°.

The depth of immersion of the tubes in water must be such that the reaction mixture in the tubes is at least 2 cm below the water level, and that the tubes are at least 2 cm from the bottom of the bath. The temperature of the water in the bath was maintained at 80-85° during the condensation.

The reaction mixtures in the tubes were periodically stirred by means of the glass rods. The water level in the bath was kept constant by additions of hot water to make up for evaporation.

The condensation times were recorded; condensation is complete when a drop of the resin on a glass plate becomes turbid on addition of a drop of water. Clouding of the drop of resin on the glass without addition of water, which occurs at the first stage of condensation owing to separation of primary products, was ignored.

The times of complete condensation in the control and test samples were recorded, and the retardation or acceleration of condensation relative to the control sample was calculated (the differences between parallel determinations did not exceed 5-6 minutes).

The influence of alkali-soluble impurities in melamine was first tested on 4 samples of the recrystallized commercial product, containing 98-99% of melamine (determined by the picrate method), which differed from each other mainly in their contents of ammeline and ammelide, which varied from 0.3 to 1.7% in these samples.

The alkali-soluble impurities in the melamine were determined by the following method. 15 g of melamine was dissolved in 500 ml of distilled water at 92-95°. 10 ml of 0.5 N alkali was added to the solution with stirring. The solution was cooled to 20°. The crystallized melamine was filtered on a Buchner funnel and washed 2-3 times with water (20 ml each time). The filtrate and washings were collected in a 700-750 ml flask, 2 drops of phenolphthalein were added, and 0.5 N hydrochloric acid solution was then added until the color disappeared, followed by 4 ml of 0.5 N hydrochloric acid in excess of the amount required for neutralization.

As the ammeline and ammelide which separate out are very difficult to filter, the contents of the flask were first poured into a cylinder to settle for 15-20 hours, and the supernatant liquid, followed by the sediment,

was then filtered through a No. 3 or No. 4 Schott filter. The residue was washed 2-3 times with water and dried in a drying oven at 100-105° to constant weight.

The following formula was used for the calculations:

$$x = \frac{a \cdot 100}{b}$$

where x is the content of alkali-soluble impurities (in %), a is the weight of alkali-soluble impurities (in g), and b is the weight of melamine (in g).

Comparative data on the condensation of these melamine samples and the control sample are given in Table 1.

TABLE 1

Condensation of Melamine Samples With Formaldehyde

No. of melamine sample	Content of alkali-soluble impurities (%)	Dissolving time (min)	Condensation time (min)	Acceleration of condensation relative to control sample (min)	Characteristics of condensation product	
					viscosity (centipoises)	polymerization time at 150° (sec)
Control	0	23	120	—	60	190
1	0.3	} Incomplete solution	63	57	57	122
2	0.8		33	87	87	100
3	1.2		27	93	} Resin coagulated {	80
4	1.7		22	98		80

It follows from Table 1 that as little as 0.32-0.8% of alkali-soluble organic impurities accelerates condensation appreciably; resin formation is considerably ahead of the solution process.

If over 1% of such impurities is present, the polycondensation is so rapid, even in test tubes, that the resin coagulates and is unsuitable for use in molding compositions. The samples contained, in addition to ammeline and ammelide, other impurities (up to 1%), which might also influence the course of condensation of melamine with formaldehyde; therefore, in order to verify the above findings, a series of experiments was carried out with chemically pure melamine to which various amounts of ammeline and ammelide extracted from Sample No. 4 were added.

The results of these experiments are summarized in Table 2.

The results in Table 2 show that additions of ammeline and ammelide actively catalyze condensation, which is completed even before the melamine is entirely dissolved in the formaldehyde. The resins formed has an excessively high polymerization rate, which makes it difficult to use in the production of high-quality molding materials.

TABLE 2

Effect of Additions of Ammeline and Ammelide on the Condensation of Melamine with Formaldehyde

Sample No.	Contents of ammeline + ammelide (%)	Dissolving time (min)	Condensation time (min)	Acceleration of condensation relative to control sample (min)	Characteristics of condensation product	
					viscosity (centipoises)	polymerization time at 150° (sec)
1	0	23	120	—	60	190
2	0.3	} Incomplete solution	63	57	57	152
3	0.5		42	78	72	105
4	0.9		33	87	80	80
5	1.2		27	93	} Resin coagulated {	80
6	1.5		25	95		70
7	1.8		21	99		60

It was next desired to determine how the removal of ammeline and ammelide from Samples No. 2 and No. 4 of commercial melamine, which did not condense normally (Table 1) would influence their condensation with formaldehyde; experiments showed that removal of these impurities from the two commercial samples of abnormally-condensing melamine yielded absolutely normal melamine, both samples of which condensed similarly.

SUMMARY

Organic alkali-soluble impurities in melamine, consisting mainly of ammeline and ammelide, have a harmful effect on the condensation of melamine with formaldehyde.

Received May 29, 1957

BOOK REVIEWS

I. I. Revzin. **PLASTICS IN MEDICINE.** State Medical Press, Moscow, 1957. Printing 14,000 copies.

Plastics are becoming more and more widely used in the most diverse fields of science and technology. It would be difficult to name any branch of industry in which these materials, with their range of different and technically advantageous properties, are not used.

I. I. Revzin's book "Plastics in Medicine," published by the state Medical Press in 1957, is devoted to one important aspect of the use of plastics — in the field of medical science.

The book under review is written in popular language and is intended for a wide circle of readers. However, not all the chapters are equally well written, and they are not all read with the same interest.

The first two chapters ("The achievements of organic chemistry" and "The age of plastics") are relatively weaker than the others. They deal rather briefly, almost in summary form, mainly with the principles of elementary organic chemistry (as the science which served as the foundation for the development of whole industries, including the plastics industry); the treatment of questions relating to the study and production of the special class of high-molecular compounds (polymers), and to the difficulties of plastics production, is equally weak.

Much more attention should have been devoted to this question, which is one of the most important and urgent problems of our time.

The omission of any classification of plastics, and in particular, of their subdivision into thermosetting and thermoplastic materials, in Chapter II (and, indeed, in the whole book) is methodologically wrong; so is the use, in Chapter III (pages 12 and 13), of even more complex and specific concepts ("polycondensation reaction," "polymerization resins," etc.), without any explanations, qualifications, or even a brief indication of their significance.

All these concepts and terms, which are difficult, especially in a popular presentation, must be neither avoided by silence, nor presented in the incomplete form as is done in this book. At the same time, the very rudiments of organic chemistry are explained in Chapter I.

Chapter III, which is the last (apart from the half-page conclusion), contains the main bulk of factual data on the use of plastics in medical practice: for false teeth and dental fillings, for eye prostheses, in traumatology and orthopedics, in plastic surgery, etc.

The amount of space devoted to the use of plastics for the production of medical instruments is unjustifiably small (only 1 page), although work in this direction, especially by means of pressure casting, is meeting with considerable success. The author discusses, with excessive detail, the history of dental prosthetics, while devoting little attention to certain other questions. Not enough is said about the actual plastics used in medicine — their properties are not described, the characteristics of individual types and grades are not given (in most cases the author confines himself to a list of trade names — and questions relating to the technology of the production of particular prostheses and of the necessary technological equipment are ignored altogether. For better clarity, such information should be given, if only in brief.

In addition to these omissions, certain other faults such as inaccuracies and contradictions in the text must be mentioned.

For example, on pages 9-10 the compound polyisobutylene is replaced by one of its trade names ("Oppanol"); this is, of course, incorrect.

The concept of "polymerization" is replaced by the ill-considered term "condensation" (page 10), which by no means conveys the specific nature of the phenomenon (and, moreover, is not sufficiently scientific).

On the same page, vinyl acetate is described as a type of plastics material, whereas in reality it is only a monomer. This page also contains the unfortunate statement; "all the hydrogen molecules are replaced by fluorine" (in Teflon - I.F.). It would be more correct to say that "in the molecule of Teflon (polytetrafluoroethylene) all the hydrogen atoms are replaced by fluorine atoms."

The author ought to know that cinnabar is the sulfide and not the oxide of mercury (page 17). There are misprints; one of the trade names of polyethylene (the German Lupolen) is given as Lopulen on page 13, and the word "plasticizer" is misspelled on page 9. The specific gravity of foam plastics is given as 0.2-0.3 in one instance (page 14), and as 0.15-0.2 in another (page 49) without any explanation (in fact, the value may be even lower, which the author should have taken into consideration.*

These are the main defects of the book. A point in its favor is the elegant presentation of the factual data from the historical aspect; it is true that this is excessively detailed in parts, with detriment to other and more useful material. Some of the statements are aptly illustrated by concrete examples from medical practice and by suitable photographs. The book is profusely illustrated, which makes the presentation more vivid.

It may be stated in conclusion that this book can be used as an introduction to the use of plastics in medicine, if the faults noted are taken into account.

I. G. Filatov

D. A. Epshtein. FUNDAMENTALS OF CHEMICAL TECHNOLOGY. Academy of Pedagogical Sciences Press, Moscow, 1957. 223 pp., 182 figs.

The development of polytechnic education in secondary schools confronts the teacher of chemistry with new problems. In the teaching of chemistry, the teacher must correlate theory with practice and acquaint his pupils with the fundamental principles of chemical industry. This means that the teacher must augment his knowledge of chemical technology. However, the existing technical literature is not intended for this purpose, and does not take into account questions of school teaching. The purpose of this book is to acquaint secondary-school teachers with the fundamentals of chemical technology.

The book consists of two parts. The first part deals with the basic concepts and laws of chemical technology: the subject of chemical technology, a review of its development, the main laws of chemical technology, the control of heterogeneous reactions, the techniques of catalytic reactions. The second part of the book is concerned with the technology of the most important inorganic chemical industries. It begins with a chapter on materials of construction. This is followed by chapters on water and on air, and then on the production of sulfur and sulfuric acid, nitrogen compounds, and phosphorus and potash fertilizers.

A brief historical sketch consists of an account of the development of the ideas of chemical technology from its foundations to the present day.

The principal concepts and laws of chemical technology are presented in the light of the author's own classification of chemical reactions in technology [see *Journal of Applied Chemistry* 19, No. 10-11, 1125 (1946); 24, No. 7, 770 (1951)]. The relationship which is established between the physicochemical principles and the technical execution of industrial processes enables the teacher to acquaint his pupils with the general methods and equipment of chemical industry with the aid of the most typical examples.

The chapters devoted to the control of different types of reactions reveal the importance of the basic chemical laws in the solution of technological problems. The reader is informed about methods of applying physicochemical laws in technology; in particular, the laws of chemical equilibrium, chemical kinetics, and catalysis. The author formulates the principles of industrial control of each type of reaction; these embody extensive experience and theory of chemical technology.

The consideration of general principles is very appropriately followed by information on materials which can be used for chemical equipment. The question of materials of construction is among the most important and difficult problems, as most processes in chemical technology are carried out at elevated temperatures, often under high pressures; corrosive substances are frequently handled in chemical plants, etc. The consideration of questions relating to the utilization of water and air prior to discussion of individual chemical processes is also justified.

The chapters dealing with individual branches of industry contain information on their history, development, present state, and future. These chapters are written so that they can be understood by readers who do not know the general principles of chemical technology. These chapters contain references to the first part of the book, assisting easier appreciation of general principles by study of individual industrial reactions. The whole book reveals a deep knowledge of chemical technology, a science to which the author has made many valuable contributions.

In our opinion, the book is also a very useful aid to teachers of chemistry and chemical technology in universities and technical colleges, and also to students who wish to acquaint themselves with the laws of chemical technology as a scientific discipline.

The book is well produced and printed. Some of the illustrations, however, are not reproduced clearly enough (for example, the micrographs on p. 147).

The reader will look forward to the continuation which is promised in the preface of the book — a book dealing with the technology of the most important organic industries considered in the light of the general laws of chemical technology.

A. P. Egorov

N. I. Putokhin. ORGANIC CHEMISTRY. State Agricultural Literature Press, Moscow, 1956, 334 pp. Printing 20,000.

There has long been a need for a text book of organic chemistry for use in agricultural colleges. It is to be expected that students of agricultural colleges welcome the publication, in late 1956, of N. I. Putokhin's text book "Organic Chemistry."

In addition to its considerable merits, the book contains a number of faults, which can be divided into three groups: methodological and methodical, inaccurate definitions and statements, errors and misprints.

There is no need to prove that all the disciplines studied in Soviet colleges should assist in the formation of a Marxist-Leninist outlook in the students. Chemistry contains a great wealth of material which must be utilized in the development of a dialectic-materialist understanding of natural phenomena in students. This is a task for the text book as well as for the teacher.

In the introduction of his book, N. I. Putokhin gives a correct outline of the struggle between the materialistic outlook and idealism in the development of organic chemistry in the 19th century, but nothing is said of the struggle against the idealistic theory of resonance. The law of the mutual influence of atoms in molecules, discovered by A. M. Butlerov and developed by V. V. Markovnikov, is an excellent illustration of the interrelationship and interdependence of natural phenomena. However, the author makes no mention of this either in the chapter on the influence of atoms and radicals, or in his discussion of a number of reactions in the light of this law. The law of the transition of quantity into quality is clearly reflected in the homologous series of organic compounds. However, the application of this law to isomeric organic compounds is not universally understood. The author should have mentioned this important law of Marxist dialectics in his consideration of the members of at least one homologous series of organic compounds.

In the discussions of the assimilation and dissimilation of carbohydrates in plants, of the properties of amino acids, and of ester formation and saponification, it should have been stressed that the action of the law of the unity and struggle of opposites is manifested here.

These comments are not to be taken to mean that a text book of organic chemistry must be turned into a text book of philosophy. However, if the author wants to correlate organic chemistry with the biochemistry and physiology of plants and animals, he should also correlate it with Marxist philosophy.

The composition of mineral oils, and the processes of cracking and aromatization of petroleum, can be understood more easily after consideration of the properties of the individual hydrocarbons present in different oils: alkanes, alkenes, cycloalkanes, and aromatic hydrocarbons. It would have been better to put the section on "Petroleum" after all the hydrocarbons, and not after the alkanes, as is done in this book.

The same applies to terpenes and essential oils. Essential oils contain alcohols, aldehydes, and ketones as well as hydrocarbons. It is not clear why the author discusses terpenes and essential oils in the section on hydrocarbons, and not in the place allotted to them by the accepted program.

Konovalov's reaction of the nitration of paraffins, and nitration in the vapor phase, are of great practical importance and are carried out on the industrial scale. Nevertheless, nothing is said in the book about the importance of Konovalov's reaction. Further, on p. 304 it is stated that "Aliphatic nitro compounds have no special practical importance."

It is known that in the halogenation of aromatic hydrocarbons halogen enters the nucleus under one of two conditions: either on halogenation in the cold, or with the use of catalysts such as iron salts. However, the author does not mention the use of catalysts for the halogenation of benzene homologs.

The bisulfite method for determination of aldehydes in natural mixtures is widely used in practice. Therefore the students should have been told about the reaction of sodium carbonate with the bisulfite compounds of aldehydes and ketones.

It is stated on p. 167 that "the Cannizzaro reaction or dismutation is characteristic of aromatic aldehydes; in the aliphatic series it proceeds readily only in the case of formaldehyde." However, V. E. Tishchenko showed that ester condensation under the action of aluminum alcoholate, and therefore dismutation, occurs with other aliphatic aldehydes. This reaction is therefore now known as the Cannizzaro-Tishchenko reaction. Strange enough, this is not mentioned in the book.

It is known that organic compounds with two hydroxyl groups attached to one carbon atom are unstable, and are converted into aldehydes or ketones. Students therefore may wonder why chloral hydrate ($\text{CCl}_3-\text{C}(\text{OH})_2\text{H}$) is a stable compound. They find no explanation in this book (p. 169).

Nor is anything said about the increase in the degree of dissociation of haloid-forming organic acids under the influence of halogen (p. 181).

It should have been explained why the Markovnikov rule is not obeyed in the reaction $\text{CH}_2=\text{CH}-\text{C}(=\text{O})\text{OH} + \text{HBr}$ (p. 187).

The question of the chemistry of carotenoids should have been discussed, at least in brief, in a text book of organic chemistry intended for agricultural colleges, especially as vitamin A, which is mentioned in the book, is formed from carotene.

The book contains incomplete or inaccurate statements; for example, it is stated on page 173: "A considerable amount of camphor is now made from pinene by the method developed by V. E. Tishchenko." The question naturally arises: what is this method?

On page 178 we read: "Acids with an odd number of carbon atoms melt at lower temperatures than acids with an even number of carbon atoms." According to this statement, formic acid ($\text{HC}(=\text{O})\text{OH}$) should melt at a lower temperature than butyric acid ($\text{CH}_3\text{CH}_2-\text{CH}_2-\text{C}(=\text{O})\text{OH}$). However, the melting point of formic acid is 8.25° , and that of butyric acid is -3.1° . Of course, the author meant neighboring members of the homologous series of acids. Nevertheless, a student may be confused by this statement.

There are many errors and misprints. It is stated on p. 223 that: "Hydroxy acids occur widely in nature: some are formed during fermentation of sugars (lactic and tartaric acids), others are found in fruits of plants (malic and citric acids)." Tartaric acid is not formed in sugar fermentation. On page 236 we have "Mesotartaric or D,L-acid." However, the D,L-acid is not mesotartaric but racemic acid. On page 240: "Pasteur showed that when sodium ammonium racemate is crystallized above 28° a mixture of crystals is formed, some of which are mirror images of the others." In reality, Pasteur showed that this occurs below and not above 28° . On page 272: "Fructose, in its turn, is converted into glucose and fructose" (?). It is known that esterification is a reversible reaction. It is not clear why the equations for such reactions are written with single arrows (pp. 190, 215, 226, 250). In the equation for the reaction of glutathione formation (p. 335), the formula for aspartic acid is written instead of the formula for glutamic acid. The formulas which are obtained for the reduced and oxidized forms of glutathione are therefore wrong (pp. 335-336).

The formula for the ketonic form of phloroglucinol is given incorrectly on p. 154.

Many of the chemical formulas of organic compounds contain misprints, which is inadmissible in any case, and especially in a book for students (pages 36, 53, 54, 67, 81, 84, 89, 246, 304, 313).

There is no doubt that elimination of these faults in a new edition of this book would make it still more valuable as a text book for agricultural students.

Ia. E. Ekster



SIGNIFICANCE OF ABBREVIATIONS MOST FREQUENTLY
ENCOUNTERED IN SOVIET PERIODICALS

FIAN	Phys. Inst. Acad. Sci. USSR.
GDI	Water Power Inst.
GITI	State Sci.-Tech. Press
GITTL	State Tech. and Theor. Lit. Press
GONTI	State United Sci.-Tech. Press
Gosenergoizdat	State Power Press
Goskhimizdat	State Chem. Press
GOST	All-Union State Standard
GTTI	State Tech. and Theor. Lit. Press
IL	Foreign Lit. Press
ISN (Izd. Sov. Nauk)	Soviet Science Press
Izd. AN SSSR	Acad. Sci. USSR Press
Izd. MGU	Moscow State Univ. Press
LEIIZhT	Leningrad Power Inst. of Railroad Engineering
LET	Leningrad Elec. Engr. School
LETI	Leningrad Electrotechnical Inst.
LETIIZhT	Leningrad Electrical Engineering Research Inst. of Railroad Engr.
Mashgiz	State Sci.-Tech. Press for Machine Construction Lit.
MEP	Ministry of Electrical Industry
MES	Ministry of Electrical Power Plants
MESEP	Ministry of Electrical Power Plants and the Electrical Industry
MGU	Moscow State Univ.
MKhTI	Moscow Inst. Chem. Tech.
MOPI	Moscow Regional Pedagogical Inst.
MSP	Ministry of Industrial Construction
NII ZVUKSZAPIOI	Scientific Research Inst. of Sound Recording
NIKFI	Sci. Inst. of Modern Motion Picture Photography
ONTI	United Sci.-Tech. Press
OTI	Division of Technical Information
OTN	Div. Tech. Sci.
Stroiizdat	Construction Press
TOE	Association of Power Engineers
TsKTI	Central Research Inst. for Boilers and Turbines
TsNIEL	Central Scientific Research Elec. Engr. Lab.
TsNIEL-MES	Central Scientific Research Elec. Engr. Lab.-Ministry of Electric Power Plants
TsVTI	Central Office of Economic Information
UF	Ural Branch
VIESKh	All-Union Inst. of Rural Elec. Power Stations
VNIIM	All-Union Scientific Research Inst. of Meteorology
VNIIZhDT	All-Union Scientific Research Inst. of Railroad Engineering
VTI	All-Union Thermotech. Inst.
VZEI	All-Union Power Correspondence Inst.

Note: Abbreviations not on this list and not explained in the translation have been transliterated, no further information about their significance being available to us. — Publisher.

THE UNIVERSITY OF CHICAGO
LIBRARY

THE UNIVERSITY OF CHICAGO
LIBRARY
1215 EAST 58TH STREET
CHICAGO, ILL. 60637
TEL: 773-936-5000
FAX: 773-936-5001
WWW.CHICAGO.EDU
LIBRARY@CHICAGO.EDU

U

THE UNIVERSITY OF CHICAGO
LIBRARY
1215 EAST 58TH STREET
CHICAGO, ILL. 60637
TEL: 773-936-5000
FAX: 773-936-5001
WWW.CHICAGO.EDU
LIBRARY@CHICAGO.EDU

Two volumes sponsored by

The Geochemical Society

and translated from Russian

PHYSICOCHEMICAL BASIS OF THE ANALYSIS OF THE PARAGENESIS OF MINERALS

by D.S. Korzhinskii

Member, Academy of Sciences, USSR

THIS ENTIRE WORK, based on the author's twenty years of investigative experience, has been written with a twofold purpose: a) To provide a complete text on the subject, heretofore unavailable; b) To supplement the comparatively sketchy training of most geologists in physical chemistry.

The main part of Academician Korzhinskii's volume is devoted to the presentation of different methods of analysis of dependence of mineralogical composition on: chemical composition, temperature, pressure and chemical potentials of the completely mobile components under conditions of chemical equilibrium—with emphasis laid on the use of projective geometry, so important for representing these relationships. To assure complete coverage of the subject, the author—in cooperation with the Geochemical Society—has personally edited and amplified this translation of his work. (Case-bound, 180 pp., illustrated, \$7.50)

ABRIDGED CONTENTS

Methods of determination of rare and dispersed elements in soils • General geochemical regularities in distribution of rare elements • Soil-forming rocks and soils of the East European Plain • Boron in soils • Fluorine, bromine and iodine in soils • Arsenic and selenium in soils • Lithium, rubidium and cesium in soils • Strontium and barium in soils • Rare earths and yttrium • Titanium and zirconium in soils • Vanadium, chromium, manganese, cobalt and nickel in soils • Copper, zinc and cadmium in soils • Lead and tin in soils • Molybdenum and tungsten • Radioactive elements in soils • Other dispersed elements in soils • Certain geochemical regularities in distribution of rare elements in soils

ABRIDGED CONTENTS

General conditions of equilibrium • Reversible (equilibrium) processes • Derivation of thermodynamic potentials for systems of different types • Representation of two-component compounds and projective transformation of a set of points • Three-component diagrams of composition and their projective transformations • Representation of multicomponent systems • Application of the phase rule to paragenetic analysis of minerals • Examples of paragenetic diagrams of minerals in multicomponent systems • Relation between composition and the magnitude of the chemical potentials of a component • Method of equipotential lines on the composition-paragenesis diagrams • Chemical potential surface in the three-component systems and its projection • Algebraic calculations of reactions in multicomponent systems by means of determinants • Systems with a negative number of degrees of freedom and general properties of multi-bundle diagrams

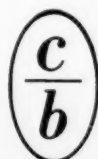
THE GEOCHEMISTRY OF RARE AND WIDELY SCATTERED CHEMICAL ELEMENTS IN SOILS

2nd Edition, Revised and Enlarged

by A.P. Vinogradov

IN THE LIGHT of new data from the laboratories of the V.I. Vernadskii Institute of Geochemistry and Analytical Chemistry, Academy of Sciences, USSR, the author has brought his work completely up to date—particularly with respect to the physicochemical properties of the individual rare elements, and to their occurrence and distribution in soils and rocks, as well as their role in the lives of plants, animals and humans. (236 pp., illustrated, \$9.50)

C.B. translations by bilingual scientists include all diagrammatic, tabular and photographic material integral with the text. Reproduction is by multilith process, from IBM "cold" type. Books are staplebound in durable paper covers, unless otherwise specified.



CONSULTANTS BUREAU, INC.

227 W. 17th St., NEW YORK 11, N. Y.

*What are the Russians doing in
my particular field? . . .*

*Is this information available
in translation?*

These pertinent questions which consistently confront technical librarians today, have pointed up the serious lack of a *standard source of reference* for translations of Soviet scientific information, and have led to the inauguration of a unique monthly service. . . .

Soviet Science and Technology

THIS HANDY MONTHLY GUIDE, available on an annual subscription basis, is specifically designed to furnish Western scientists with *English translations of the contents* of current Soviet journals being translated, cover to cover, on a *continuing basis* by Consultants Bureau, other firms and learned societies.

THROUGH SPECIAL ARRANGEMENT with the editors of these Soviet publications, expedited copies of the contents are made available, in translation, within two months after their release in Russia. Thus, each subscriber is constantly aware of the latest information available for translation in his specific field of scientific endeavor.

The format of SST is one which permits the reader instant access to all pertinent information:

- a) *Estimated date of publication in English* (when information is available from publisher)
- b) *Name and address of organization from which translation is available*
- c) *Yearly subscription prices*
- d) *Price of individual papers, or issues* (when sold separately)
- e) *A special section devoted exclusively to editorial material on the most up-to-date translating techniques*

The worldwide acceptance of SST in its few short months of existence (*first issue published in May, 1958*), has proved the urgent need for just such a service. And with the constant addition of new Russian journals-in-translation, each subscriber is assured of continuous, comprehensive and accurate information on the availability of the latest advances in SOVIET SCIENCE AND TECHNOLOGY.

ANNUAL SUBSCRIPTION

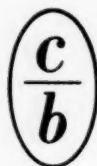
(includes 12 issues per year, which cover all calendar year issues of the original Russian journals)

1 copy.....	\$25.00 per copy
10-100 copies.....	18.00 per copy
100-500 copies.....	15.00 per copy
500 copies and over.....	11.50 per copy
<i>(500 copies includes, free of charge, your own special organizational cover)</i>	

AVAILABLE FOR A LIMITED TIME

One volume containing the contents for all 1957 issues of these journals, with the same information as in the 1958 SST...\$15.00

Write Consultants Bureau for free brochure on SST, and comprehensive catalogs of our current Russian translation-publishing program.



CONSULTANTS BUREAU, INC.

227 W. 17th St., NEW YORK 11, N. Y.

